

Studies of Poliovirus Virus Like Particle assembly in foreign expression systems

Thesis submitted for a PhD
School of Biological Sciences

Mai Uchida
March 2019

Declaration of original authorship

Declaration: I confirm that this is my own work and the use of all material from other sources has been properly and fully acknowledged

Mai Uchida

Abstract

Empty poliovirus particles, VLPs, consisting of capsid proteins VP0, VP1 and VP3, assemble into an icosahedral structure during normal poliovirus infection and represent a possible vaccine candidate. Similarly synthesis of capsid proteins in recombinant expression systems leads to VLP assembly and represents a potential infection free vaccine product. The poliovirus polyprotein P1 is cleaved by the virus encoded 3C or 3CD protease to derive the structural proteins. This work explored an expression cassette comprising the P1 precursor protein of poliovirus Mahoney (wildtype and thermostable variants), MEF-1 (wildtype) and Saukett (thermostable) and an adjusted 3C protease from enterovirus 71 to generate P1 cleaved polio proteins. Introduction of vectors containing the cassette into insect cells and yeast cells demonstrated successful P1 cleavage to molecules agreeing in size with polio VP0, VP3 and VP1. Sucrose velocity gradient analysis of recombinant poliovirus antigen from cell lysates indicated antigen in the fractions typical of wildtype virus particles and TEM imaging for the peak gradient fractions revealed empty poliovirus particles. The antigenicity of the empty particles was characterised to be H rather than N in most cases. Capsid stability improvements were studied by introducing mutations in the P1 coding region or by the addition of antiviral compounds. These modifications allowed continued P1 processing but the expression level was often modified confirming these modifications contribute to the entire capsid stability and consequently empty capsid yield. Novel modifications at the N-terminus of P1 led to higher levels of synthesis suggesting further engineering is yet possible.

Acknowledgement

I would like to show my gratitude to Professor Ian Jones for this PhD opportunity and guidance throughout my study.

I appreciate that my study was supported by University of Reading and Sanofi Pasteur without the funding, I could not start this PhD studentship.

I also would like to thank all the members of Polio empty capsid/VLP consortium, A Macadam, P Minor, H Fox, S Knowlson (National Institute for Biological Standards and Control) D Rowlands, N Stonehouse, C Nicol, O Adeyemi (University of Leeds), D Stuart, E Fry, L de Colibus, M Bahar, C Porta (University of Oxford), I Jones, G (J) Mulley, S Lyons (University of Reading), T Tuthill, J Newman (IAH Pirbright Institute), G Lomonossoff, J Marsian (John Innes Centre), J Hogle (Harvard University), E Ehrenfeld and J Almond. I specially appreciate analysis help from Helen Fox and Sarah Knowlson. I also would like to thank Silvia Loureiro and Sophie Jegouic at University of Reading for daily technical support.

Last but not the least, I would like to thank my family: husband Etienne, son Kai and 3 dogs for their patience and encouragement.

Table of Contents

Declaration of original authorship	2
Abstract	3
Acknowledgement	4
Table of Contents	5
List of Figures	10
List of Tables	15
List of Abbreviations	16
Chapter 1 Introduction	10
1.1 Overview	19
1.2 Poliovirus.....	20
1.2.1 History.....	21
1.2.2 Disease	22
1.2.3 Taxonomy	23
1.2.4 Genome	24
1.3 Replication cycle	28
1.3.1 Poliovirus attachment and entry	30
1.3.2 Viral RNA translation	32
1.3.3 RNA synthesis	34
1.3.4 Encapsidation of viral RNA.....	35
1.3.5 Exit of the viral particles.....	35
1.4 PV capsid	36
1.4.1 Capsid assembly	36
1.4.2 Capsid proteins	37
1.4.3 External capsid surface	39
1.4.4 Internal capsid surface.....	40
1.4.5 VP1 hydrophobic pocket.....	41

1.5	PV infection control	43
1.5.1	Current vaccines	44
1.5.2	PV eradication and its difficulties	45
1.5.3	Post-PV eradication world and vaccination	47
1.6	Thermal stability	48
1.6.1	Antipicornavirus compounds.....	50
1.6.2	Thermostable PV mutants	50
1.6.3	Capsid stabilising region	51
1.7	Recombinant VLP vaccines	53
1.8	Baculovirus expression system.....	55
1.8.1	Baculovirus	56
1.8.2	Baculovirus expression vector	58
1.8.3	Transfection	59
1.8.4	Post-translational modification.....	60
1.8.5	Purification of VLPs	60
1.8.6	Baculovirus expression system application for this project.....	61
1.9	Yeast expression system	62
1.9.1	Transformation of heterologous genes	63
1.9.2	Yeast cell selection markers	63
1.9.3	Transformation vectors for yeast cells	64
1.9.4	Promoters	64
1.9.5	Heterologous protein purification	65
1.10	Aims of the project.....	66
Chapter 2	Materials and General Methods.....	68
2.1	Materials.....	68
2.1.1	Chemical reagents, enzymes and columns	68
2.1.2	Specialised equipment.....	70
2.1.3	Vectors.....	71
2.1.4	Recombinant baculovirus strains	73
2.1.5	Recombinant yeasts	75

2.1.6	Cell lines	76
2.1.7	Antibodies	77
2.1.8	Buffers, solutions and media	78
2.1.9	Commercial Kits.....	82
2.2	Cloning.....	82
2.2.1	Construction of expression vector for insect cell expression system.....	82
2.2.2	Polymerase chain reaction (PCR)	86
2.3	Insect cell culture	87
2.3.1	Transfection and recombinant baculovirus production	87
2.3.2	Recombinant protein expression	87
2.3.3	Protein expression scale up.....	88
2.4	Yeast cell culture.....	88
2.4.1	Yeast cell transformation and its confirmation	89
2.4.2	PV VLP expression by <i>S. cerevisiae</i>	90
2.5	Purification of recombinant PV empty capsid	91
2.5.1	Cell lysis.....	91
2.5.2	Ultracentrifugation.....	91
2.6	SDS-PAGE and Western blot assay	93
2.6.1	Rapid analysis of VP expression in Yeast	94
2.7	Microscopy	95
2.7.1	Gated-Stimulated Emission Depletion (gSTED) microscopy.....	95
2.7.2	Transmission Electron Microscopy	96
2.8	N/H ELISA.....	96
Chapter 3	Capsid protein expression and assembly in insect cells.....	98
3.1	Introduction	98
3.1.1	VLP production in insect cells.....	98
3.1.2	Protease for P1 processing	100
3.2	The expression of viral proteins for PV1, PV2 and PV3	101
3.2.1	Construction of insect cell expression vector.....	101
3.2.2	Synthesis of VP0, VP3 and VP1 by 3C _{EV71}	101

3.2.3	Confirmation of P1 cleavage by the 3C _{EV71} protease	108
3.3	PV VLP assembly	111
3.3.1	Ultracentrifugation.....	111
3.3.2	gSTED imaging of VLPs and P1 in insect cells	113
3.3.3	TEM imaging.....	114
3.4	VLP yield optimisation.....	115
3.4.1	Cleavage efficiency enhancement in transfer vector	115
3.5	Discussion.....	119
Chapter 4	Poliovirus capsid protein expression and assembly in <i>Saccharomyces cerevisiae</i>	122
4.1	Introduction	122
4.2	Yeast expression system	123
4.2.1	RAY3A-D	124
4.2.2	pKT10	125
4.2.3	Yeast cell wall disruption	126
4.2.4	Expression vector cloning.....	127
4.2.5	Viral protein expression	128
4.2.6	Assembly of PV VLPs in yeast cells	129
4.2.7	TEM imaging of purified PV VLPs	133
4.3	Discussion.....	134
Chapter 5	Optimisation of PV VLP purification	136
5.1	Introduction	136
5.2	Purification methods for Yeast cells.....	138
5.2.1	Cell disruptor method.....	138
5.2.2	Bead-beater method	141
5.2.3	Zymolyase and N ₂ cavitation method.....	142
5.3	<i>S. cerevisiae</i> origin PV VLP yield optimization	144
5.3.1	PV3 VLP purification using zymolyase and N ₂ cavitation method.....	144

5.3.2	RAY3A-D-PV3SC8-3C VLP purification using Zymolyase and cell disruptor method	148
5.4	Purification methods for Insect cells	149
5.4.1	Cell disruptor method	149
5.4.2	N ₂ cavitation method	152
5.5	Discussion	154
Chapter 6	The factors of capsid assembly and contribution to VLP antigenicity	158
6.1	Introduction	158
6.1.1	Antipicornavirus compounds and VP1 mutations	159
6.2	Antigenicity of PV VLPs	161
6.2.1	Insect cells origin VLPs	162
6.2.2	<i>S. cerevisiae</i> origin VLPs	163
6.3	VP1 pocket manipulations	164
6.3.1	Expression of VP1 pocket surface mutants	165
6.3.2	Supplementation in insect cells expression system	168
6.4	VLP stabilising mutations for PV1 at VP4 and VP1	172
6.4.1	Modification of the VP4 N-terminus	175
6.4.2	Modification of the VP1 N-terminus	179
6.5	Discussion	186
Chapter 7	General Discussion	190
Chapter 8	References	195

List of Figures

Figure 1.1. History of PV	21
Figure 1.2. PV infection route to result in poliomyelitis.....	23
Figure 1.3. Poliovirus serotype 1 (Mahoney) genome structure and polyprotein cleavages..	25
Figure 1.4. PV replication in a susceptible cell.....	30
Figure 1.5. A schematic representation of the IRES structure used in enteroviruses	32
Figure 1.6. Schematic representation of 40S ribosome recruitment for the initiation of translation.....	33
Figure 1.7. PV RNA synthesis	34
Figure 1.8. Myristate position in the capsid	37
Figure 1.9. PV capsid assembly and sedimentation coefficient on sucrose gradient.....	38
Figure 1.10. Poliovirus capsid protein schematic representation	39
Figure 1.11. The PV capsid features	41
Figure 1.12. Images for VP1 pocket in PV	43
Figure 1.13. Hypothetical mechanism of capsid (protomer) rearrangement during the uncoating process. A protomer is colour coded for each viral protein, VP1 (blue), VP3 (red) and VP2 (yellow).....	53
Figure 1.14. Baculovirus infection cycle in nature	57
Figure 2.1. Schematic representation of the PV transfer vector.....	84
Figure 2.2. Schematic representation of yeast expression vector transformation and its confirmation flow	90
Figure 3.1. Schematic presentation of PV viral proteins expression cassette showing controls for 3C _{EV71}	99
Figure 3.2. BLAST result of 3C _{EV71} and 3C _{PV}	100
Figure 3.3. The expression cassette designs for all three serotypes of PV.	102
Figure 3.4. WB analysis for VP1 presence following a time course (1-4 days) small-scale <i>Sf9</i> cells infection of Bac-PV1-P1-3C	103
Figure 3.5. WB analysis showing PV P1 cleavage into viral proteins using 3C _{EV71} in <i>Sf9</i> , High Five and <i>Tnao38</i> cells.	108

Figure 3.6. WB analysis demonstrating Ab specificity with <i>Sf9</i> and High Five cells infection with Bac-PV1P1, Bac-PV1P1-3C and Bac-GFP (3 d.p.i)	109
Figure 3.7. WB analysis for presence of P1 and VP1 of Bac-PV1P1-3C infected <i>Sf9</i> cells (3 d.p.i) in various Rupintrivir concentration.	111
Figure 3.8. WB analysis using VP1 antibody for sucrose velocity separation (linear 15-45% sucrose gradient) fractions from Bac-PV1P1-3C infected High Five cells culture	112
Figure 3.9. gSTED images for single High Five cells infected with (A) Bac-PV1P1-3C and (B) Bac-PV1P1 which are labelled with the fluorophores	114
Figure 3.10. TEM image of concentrated sucrose gradient fractions (40% sucrose zone from Figure 3.8).....	115
Figure 3.11. Schematic representation for 3CD transfer vector cassettes	116
Figure 3.12. WB analysis by (A) VP1 antibody (MAB8566) and (B) P1 sera (Rabbit sera) for 3 d.p.i. of <i>Sf9</i> cells infected with Bac-PV1P1-3CDWT, Bac-PV1P1-3CD Δ , Bac-PV1P1-3CDWTFS or Bac-PV1P1-3CD Δ FS	118
Figure 4.1. <i>S. cerevisiae</i> expression vector, pKT10 schematic representation produced by DNA dynamo	126
Figure 4.2. Schematic representation of PV1 VLP expression vector (RAY3A-D-PV1-3C) based on pKT10 produced by DNA dynamo.....	128
Figure 4.3. WB analysis by VP0 detection using anti-VP0 rabbit sera following post-alkaline extraction of RAY3A-D-PV1-3C	129
Figure 4.4. WB analysis for presence of VP1 following RAY3A-D-PV1-3C lysis on 15-45 % sucrose gradient using anti-VP1 (MAB8566, Millipore).....	130
Figure 4.5. WB analysis using VP1 antibody (MAB8566, Millipore) following 2 nd 15%-45% sucrose gradient for lysed RAY3A-D-PV1-3C.....	132
Figure 4.6. TEM imaging for negatively stained VLP of RAY3A-D-PV1-3C , 2 nd 15-45% sucrose gradient, fraction 23	133
Figure 5.1. Schematic representation of common yeast cell wall composition and zymolyase function.....	137
Figure 5.2. WB analysis of VP1 by MAB8566, Millipore following RAY3A-D-PV1-3C treatment with cell disruptor and nycodenz step gradient	140

Figure 5.3. TEM image with negative staining of peak fraction of Figure 5.2.....	141
Figure 5.4. TEM image with negatively stained VLP of RAY3A-D-PV1-3C VLP purified with beads-beater and nycodenz gradient.....	142
Figure 5.5. TEM imaging with negative staining of VLPs from RAY3A-D-PV1-3C prepared by zymolyase and N ₂ cavitation method and nycodenz gradient.....	143
Figure 5.6. Confocal microscope (EVOS) image shows RAY3A-D-PV3SC8-3C cells break down by zymolyase and N ₂ cavitation	145
Figure 5.7. WB analysis for detecting VP1 by MAB8566 (Millipore) following RAY3A-D-PV3SC8-3C VLP purification using zymolyase and N ₂ cavitation method and 10-30% Nycodenz step gradient	146
Figure 5.8. TEM imaging of the 3 interfaces which is seen on Figure 5.7.....	147
Figure 5.9. TEM image with negative staining of RAY3A-D-PV3SC8-3C VLPs after zymolyase and cell disruptor purification and 10-30 % Nycodenz step gradient	149
Figure 5.10. WB analysis for VP1 detection using MAB8566 (Millipore) for Bac-PV1P1-3C VLP following purification with cell disruptor and 15-45 % sucrose gradient.....	151
Figure 5.11. TEM image with negative staining of VLPs in peak fractions (fraction 7 and 8) and bottom fraction (fraction 12) from Figure 5.10	152
Figure 5.12. WB analysis detecting VP1 by MAB8566 for Bac-PV1P1-3C VLP following N ₂ cavitation and 10-30 % Nycodenz gradient. 3 d.p.i. of Bac-PV1P1-3C infected High Five cells were prepared for analysis.....	153
Figure 5.13. TEM image with negative staining for VLPs from Figure 5.12 concentrated fraction 9 at 20-30 % nycodenz interface.....	154
Figure 6.1. Chemical structures of antipicornavirus compounds.....	160
Figure 6.2. Antigenicity ELISA analysis for IPV (PV standard) and Insect cell origin PV VLP detected by N/H specific antibodies at NIBSC	162
Figure 6.3. Antigenicity ELISA analysis to determine the status of RAY3A-D-PV1-3C origin VLPs purified using various purification methods at Reading	164
Figure 6.4. WB analysis for Bac-PV1P1-3C with hydrophobic pocket mutations for capsid stability improvement	167

Figure 6.5. WB analysis using anti-VP1 antibody (MAB8566, Millipore) for Bac-PV1P1-3C mutants at M132, H207, F237 and their combinations (codon optimised) for 3 d.p.i of <i>Sf9</i> cells with Bac-PV1P1-3C mutants prepared in a 6 well dish.	168
Figure 6.6. The analysis of GPV13 effect on VP1 reactivity level in <i>Sf9</i> cells infection by Bac-PV1P1-3C, Bac-Y159W and Bac-Y205W	169
Figure 6.7. WB analysis with anti-VP1 antibody (MAB8566, Millipore) for High Five cells infection by Bac-PV1P1-3C with Pleconaril followed by non-ionic detergent lysis and 10-30 % nycodenz gradient.....	170
Figure 6.8. N/H ELISA analysis for 10-30 % nycodenz gradient peak fraction (Figure 6.7) for Mahoney wt VLPs from High Five cells infection by Bac-PV1P1-3C purified with Pleconaril at Reading.....	171
Figure 6.9. N/H ELISA for VLPs conformation from RAY3A-D-PV3SC8-3C +/- Pleconaril at Reading.....	172
Figure 6.10. PV Mahoney SC6b VLP TEM image by negative staining (A) and N/H ELISA result (B).....	174
Figure 6.11. Schematic representation of VP4 N-terminus mutant sequences exchanged with N-terminus of HIV matrix protein, p17	175
Figure 6.12. WB analysis using anti-VP1 antibody (MAB8566, Millipore) for small scale 3 d.p.i. of Bac-PV1P1-3C (shown as Mah wt), Bac-PV1SC6bP1-3C (Mah SC6b), Bac-PV1SC6bP1Ex10, Ex15 and Ex20	177
Figure 6.13. WB analysis with anti-VP1 antibody (MAB8566, Millipore) for 3 d.p.i. of Bac-PV1SC6bP1Ex10 for <i>Tnao38</i> cells following NP40 lysis, 30 % sucrose cushion and 15-45 % sucrose gradient	178
Figure 6.14. TEM image for negatively stained of VLPs of Mahoney SC6b Ex10 from Figure 6.13 concentrated fraction 7 (3 d.p.i. of Bac-PV1SC6bP1Ex10 for <i>Tnao38</i> cells)	179
Figure 6.15. Schematic representation for N-terminus VP1 mutations designed to contain GS linkers consisting of GGGGSGGGGS in 4 or 5 amino acid shifted positions.	180
Figure 6.16. WB analysis by anti-VP1 antibody (MAB8566, Millipore) for small scale 3 d.p.i. of Bac-PV1SC6bP1VP1_1, VP1_2, VP1_3 and Bac-PV1SC6bP1Ex10 for <i>Tnao38</i> cells	182

Figure 6.17. WB analysis using anti-VP1 antibody (MAB8566, Millipore) for 15-45 % sucrose gradient fractions of 3 d.p.i. of *Tnao38* cells Bac-PV1SC6bP1VP1_2183

Figure 6.18. TEM image for negative staining of VLPs of Mahoney SC6b VP1_2 from concentrated fraction 8 indicated in Figure 6.17 (Bac-PV1SC6bP1VP1_2 infection of 100 mL *Tnao38* cells)..... 184

Figure 6.19. N/H ELISA analysis for concentrated peak fractions from 15-45 % sucrose gradient for PV Mahoney SC6b Ex10 (fraction 7) as seen under TEM in Figure 6.14 and VP1_2 (fraction 8) of Figure 6.18 at Reading.....185

List of Tables

Table 1.1. List of mutants for thermostable Saukett SC8 (Fox <i>et al.</i> , 2017) and Mahoney SC6b (Fox <i>et al.</i> unpublished data).....	51
Table 2.1. List of materials with the manufacturer.....	68
Table 2.2. List of equipment and manufacturer.....	70
Table 2.3. List of expression vectors.....	71
Table 2.4. List of recombinant baculovirus strains.....	73
Table 2.5. List of recombinant yeasts.....	75
Table 2.6. List of Cell lines.....	76
Table 2.7. List of antibodies.....	77
Table 2.8. List of buffers, solutions and media.....	78
Table 2.9. List of commercial Kits.....	82
Table 2.10. Combination of primary and secondary antibodies for a particular detection in WB analysis.....	94
Table 5.1. Summary of cell lysis and purification method used in chapter 5.....	157
Table 6.1. List of VP1 residues facing to the VP1 pocket. Substituting amino acids are indicated in blue. The amino acid structures of leucine and Tryptophan are shown below.....	161

List of Abbreviations

AcMNPV	<i>Autographa californica</i> multi-nuclear polyhedrosis virus
ADH1	alcoholic dehydrogenase I
ARS	autonomous replication sequence
BmNPV	<i>Bombyx mori</i> nuclear polyhedrosis virus
BV	budded virus
CAV	cardiovirus A
CD	cell disruptor
CD155	cluster of differentiation 155
CNS	central nerve system
CPE	cytopathic effect
cre	cis-acting replication element
cVDPV	circulating vaccine-derived poliovirus
d.p.i.	day(s) post infection
D ₂ O	deuterium oxide
DNA	Deoxyribonucleic acid
<i>E. coli</i>	<i>Escherichia coli</i>
eIFs	eukaryotic initiation factors
EPI	Expanded Programme on Immunisation
EV71	Enterovirus 71
FMDV	Foot-and-Mouth-Disease virus
<i>GAP or GAPDH</i>	glyceraldehyde-3-phosphate dehydrogenase
GPEI	Global Polio Eradication Initiative
gSTED	Gated-Stimulated Emission Depletion
h.p.i.	hours post infection
HAV	Hepatitis A virus
HBV	Hepatitis B virus

HIV	Human Immunodeficiency Virus
HPV	Human Papilloma virus
HRP	Horseradish peroxidase
HRV	Human Rhinovirus
Ig	immunoglobulin
IgA	immunoglobulin A
INF α/β	interferon- α/β
IPV	inactivated vaccine
IRES	internal ribosome entry site
ISGs	IFN-stimulated genes
mAb	monoclonal antibody
MOI	multiplicity of infection
mRNA	messenger RNA
MW	molecular weight
NIBSC	National Institute for Biological Standards and Control
NMT	N-myristoyl transferase
NPVs	nuclearpolyhedrosis viruses
NTP	nucleoside triphosphate
NTR	non-translated region
OPV	oral polio vaccine
ORF	open reading frame
OV	occluded virus
<i>P. pastoris</i>	<i>Pichia pastoris</i>
P1,2 and 3	polyprotein1,2 and 3
PCR	polymerase chain reaction
Polio	poliomyelitis
PV	Poliovirus
RdRp	RNA-dependent RNA polymerase
RF	replicative form

RI	replicative intermediate
RNA	ribonucleic acid
<i>S. cerevisiae</i>	<i>Saccharomyces cerevisiae</i>
SDS-PAGE	Sodium dodecyl sulphate polyacrylamide gel electrophoresis
<i>Sf</i>	<i>Spodoptera frugiperda</i>
<i>T. ni</i>	<i>Trichoplusia ni</i>
TEM	Transition Electron Microscopy
TLR9	Toll-like receptor 9
VAPP	Vaccine-associated paralytic polio
VLP	Virus-Like-Particle
VP	viral protein
VPg	viral genome-linked protein
WB	Western blot
WHO	world health organisation
WT	wildtype

Chapter 1 Introduction

1.1 Overview

Polio is the medical term used to describe the consequences of poliovirus (PV) replication in the nervous system, which leads to paralysis. PV is a positive sense single-stranded RNA virus of the *Picornaviridae* family. The majority of PV cases historically were reported among children, leaving them with permanent damage in the lower extremities or death in the worst case. The first outbreaks were reported in the early 19th century in the EU and the United States. The number of paralytic cases increased and peaked at 21,000 cases in the United State in 1952. After the introduction of the polio vaccines; inactivated polio vaccine (IPV) and attenuated oral polio vaccine (OPV), the number of poliomyelitis decreased rapidly and the last incident of poliomyelitis caused by wild type PV in the United States was recorded in 1979. After a decade, WHO proposed a global eradication campaign for PV using OPV because of its efficiency, ease of administration and low cost. Since the launch of project, the number of poliomyelitis cases globally has declined by over 99% but approximately 1000 cases of poliomyelitis have been reported annually since 2000, mostly associated with zones of conflict, which questions the feasibility of eradication. While the number of wild type PV derived poliomyelitis cases has declined however, OPV virus derived poliomyelitis cases, also known as Vaccine-associated paralytic polio (VAPP) have become more prominent as a percentage of the overall cases. The vaccine strain of OPV has shown genomic instability and may evolve into VAPP in some instances. The use of OPV necessarily maintains virus in the environment with the potential to result in future outbreaks if herd immunity drops following the cessation of routine vaccination. In contrast to OPV, IPV does not evolve to a revertant form. However, the cost of production and the necessity of wild type virus culture in high security facilities, which could result in an accidental or intentional release, means this method of production is not feasible for a polio free world. As a result of such considerations, new approaches to PV vaccine development are required. One such approach is the development of PV empty capsid production using recombinant expression systems. These systems allow the production of assembled immunogenic viral capsids, virus-like-particles (VLP) without being infectious. In this project I

will investigate empty PV capsid production in selected foreign expression systems and address possible improvements in capsid stability that could benefit immunogenicity and contribute to the likely take up of this candidate vaccine.

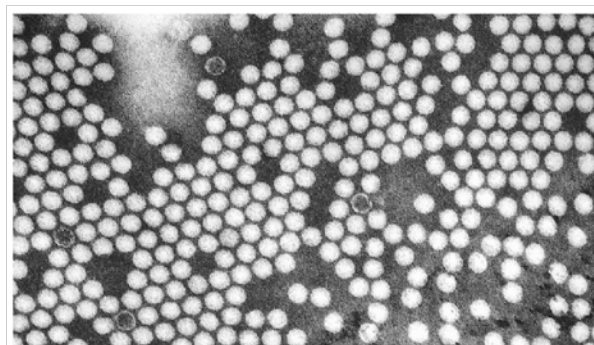
1.2 Poliovirus

The existence of poliomyelitis was recorded on Egyptian hieroglyphic stele (Figure 1.1A) which date from 1580-1350 BC depicting a young man, a supposed king, with a typical leg characteristic of PV paralysis (Galassi *et al.*, 2017). Similarly, mummified bodies with foot deformation typical of weakened limbs date back to a similar age. These historical records indicate that PV has been a health threat to mankind for a long period and that the outcome of infection, paralysis, has not changed. PV infection is normally asymptomatic or only associated with very slight morbidity but depending on the site of virus replication the same infection can give rise to life changing disease.

PV and other members of the *Picornaviridae* family consist of a single stranded RNA genome of positive polarity within a non-enveloped particle (for a review see Tuthill *et al.* (2010)). However, HAV has shown an exception with transient envelope formation on newly released viruses (Feng *et al.*, 2013). Although picornavirus genomes vary in size they are typically between 7-9 kb and the genome structure is universally shared. The genomes encode a single open reading frame (ORF) with non-translated regions (NTRs or untranslated regions/UTRs) that flank the ORF. The ORF is translated into a single large polyprotein and is then matured into individual functional proteins by the action of a virus-encoded proteases reviewed in Racaniello (2013). The picornavirus genome is packed into an icosahedral capsid with a typical size of 30nm diameter and a typical PV electronmicrogram is shown in Figure 1.1B. Sixty copies of each viral protein 1 to 4 (VP1 to VP4), arranged as a single unit, the protomer, are arranged in an icosahedral lattice. VP1 to VP3 form the mature capsid exterior while the mature capsid interior is faced by VP4 (Hogle *et al.*, 1985). PV is one of the most studied picornavirus, in fact one of the most studied animal viruses, as a result of the drive to develop poliovirus vaccines in the 1950s which enabled efficient poliovirus culture and subsequent molecular biological characterisation. Hence poliovirus is often used as a model picornavirus.



(A)



(B)

Figure 1.1. History of PV

(A) Egyptian stele showing a king with deformed limb (GPEI, 2016) (B) Electronmicrogram of PV. The virus particle is positively stained while a few negatively stained empty capsids are visible (CDC, 2017).

1.2.1 History

PV was first recorded as a causative agent of poliomyelitis in 1908 by Landsteiner and Popper (1908). The authors demonstrated the transmission of the disease and its pathology by the injection of a bacteria-free central nerve system (CNS) homogenate from a child showing acute infection into the peritoneum of a rhesus monkey. Studies of the molecular biology and biochemistry of PV progressed with the increase in the paralytic cases in 1950s and a notable milestone for PV research was the propagation of PV *in vitro* with the concomitant ability to study its replication in human cells (Enders *et al.*, 1949). Large-scale virus growth and purification led to PV becoming a model virus in the field of virology with a number of major 'first' studies associated with it. For example, the first animal infectious DNA clone was produced from poliovirus RNA (Racaniello & Baltimore, 1981) and the lack of a 5' cap structure in its messenger RNA (mRNA) was first found in poliovirus (Hewlett *et al.*, 1976; Nomoto *et al.*, 1977a). Amongst these studies, the high-resolution three dimensional structure of PV (Hogle *et al.*, 1985) and the proteolytic processing of the precursor protein into the mature viral proteins (Summers & Maizel, 1968) are highly relevant to this dissertation.

1.2.2 Disease

Most PV infection remains unapparent and asymptomatic. The transmission of PV is via the faecal-oral route. The virus is shed in the faeces of infected individuals, which is then ingested from contaminated water or foodstuffs. The initial replication of PV takes place in the pharynx and/or gastrointestinal tract (Bodian & Horstmann, 1965; Sabin, 1956). After local viral replication, the virus enters into blood stream via the cervical and mesenteric lymph nodes causing primary viraemia (Bodian, 1955; Ren & Racaniello, 1992; Wenner & Kamitsuka, 1957). At this stage of infection, PV may cause abortive poliomyelitis (4-8% of total PV infection), a minor mild illness including fever and gastrointestinal symptoms. The incubation period is about 1-3 days, however the illness may take up to 5 days to be apparent. Less frequently, aseptic meningitis has been reported. This is a non-paralytic, typical viral meningitis with fever and headache and does not involve the CNS parenchyma. The symptoms may last a few days to 2 weeks (Pallansch *et al.*, 2013). In 1 in 200 (0.5%) of infection, secondary viraemia occurs and leads to a paralytic disease, poliomyelitis by affecting motor neurons. The incubation period is about 4-10 days, which is followed by 2-5 days of headache. Then the onset of paralysis becomes apparent. The early symptoms indicative of poliomyelitis are sensory complaints and shooting or aching pain in muscles, which signals virus growth in the tissue (McKinney *et al.*, 1987; Pallansch *et al.*, 2013). Depending on the site of paralysis, the outcome of the symptom is different. When paralysis takes place as a result of virus replication in the spinal cord, it is called spinal polio. The paralysis severity differs from mild weakness to the total loss of use of all four limbs and trunk. In 10-15% of poliomyelitis cases examined the virus is found in the brainstem, bulbar polio. In bulbar polio, the cranial nerves or medullary centres which control the respiratory and vasomotor systems are destroyed by virus replication. Cranial nerves IX and X are most affected. This damage causes pharyngeal and laryngeal muscle paralysis, which makes swallowing and talking difficult. Weakness of the face and tongue muscles is also caused by cranial nerve damage (cranial nerve VII for face and cranial nerve XII for tongue). More seriously, PV replication may affect the brainstem reticular formation which is involved in the control of the respiratory system. The autonomic nerve system damage may result in irregular sweating, urination, defecation and blood pressure (Pallansch *et al.*, 2013). Invasion of the central nervous system by poliovirus is an accidental diversion as there

is no benefit to the virus in replicating in nervous tissue. The survival of the virus depends on viral transmission which in turn requires efficient replication in host gut and shedding in the faeces. The neurological infection ends up as a dead-end for the virus as it offers no release portal to other hosts for a review see Blondel *et al.* (2005). Figure 1.2 summaries the route of PV infection to reach the CNS.

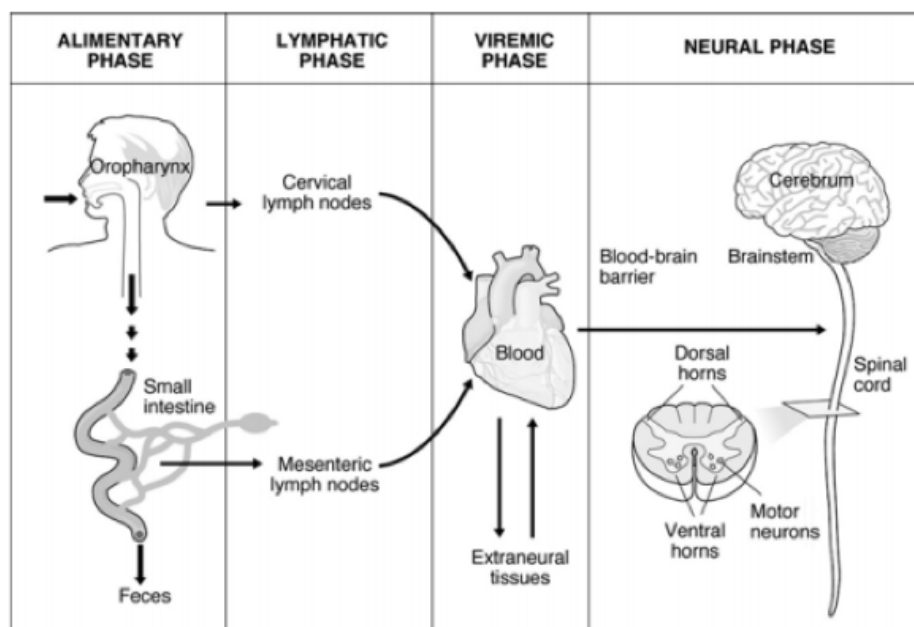


Figure 1.2. PV infection route to result in poliomyelitis.

Primary PV replicates in the oropharynx and/or alimentary mucosal surface. If PV enters the blood stream via the lymph nodes, primary viraemia may take place. PV travels to the organs and tissues by the blood stream. If PV enters the central nerve system via the blood-brain barrier, secondary viraemia may cause poliomyelitis by replication in and destruction of motor neurons. Depending on the PV affected area in the CNS, the symptoms vary. The figure is from a review by Blondel *et al.* (2005).

1.2.3 Taxonomy

The picornaviruses are classified as viruses of the *Picornaviridae* family, a name which comes from pico (meaning small) – RNA virus. There are many members and they can be pathogens of bacteria, animals and plants (Wagner *et al.*, 2008). Within the family, 80 species are classed into 35 genera. Well-known and significant pathogens are PV, enterovirus 71/EV71 (genus *Enterovirus*), hepatitis A virus/HAV (*Hepatovirus*), human rhinovirus/HRV (*Enterovirus*) and foot-and-mouth-disease virus/FMDV (*Aphthovirus*) (Zell *et al.*, 2017) The genus *Aphthovirus* consists of 4 species including foot-and-mouth disease virus (FMDV) and the target host is cloven-footed animals which are infected by FMDV primarily via the upper respiratory tract.

FMDV infects over 70 species of mammals and there are 7 identified serotypes, each of which are consist of numerous subtypes. The genus *Enterovirus* consists of 15 species; Rhinoviruses (RA-C) and 4 human enteroviruses (EV-A to D) and 8 animal enteroviruses (EV-E to –L) (Zell *et al.*, 2017). Within the species, PV and human enteroviruses belong to group EV-C.

The replication of these viruses takes place in the alimentary tract and the virus survives low pH, enabling re-infection via ingestion as reviewed in Blondel *et al.* (2005). PV has three serotypes; type 1, type 2 and type 3 (Bodian *et al.*, 1949). Originally they were classified according to their ability to produce immunity after the initial paralytic infection (Bodian, 1949) which was shown by virus neutralisation assay (Bodian, 1951). Complete genome sequencing revealed that serotype differences are largely characterised by N-terminal amino acid sequences in the capsid proteins, which are normally buried in the capsid. However, these sites are displayed while the capsid conformation undergoes RNA release. Viral infectivity is neutralised if antibodies bind the sequences that are necessary for receptor engagement and virus entry into the cell via the poliovirus receptor which has been mapped as CD155, a cell surface protein involved in epithelial cell junctions with a wide distribution including on intestinal and nervous cells (for review see Racaniello (2013)). The reference virulent strains which are used for IPV productions are Mahoney (type 1), MEF-1 (type 2) and Saukett (type 3) (Plotkin *et al.*, 1999). OPV strains are produced from the attenuated Sabin strains type 1 (LS-c, 2ab), type 2 (P712, Ch, 2ab) and type 3 (Leon 12ab).

1.2.4 Genome

The PV genome consists of 7441 nucleotides and includes 3 distinctive picornavirus regions; the 5' UTR which is covalently bound to a viral genome-linked protein, VPg, a single ORF which is later translated into a single polyprotein and the 3' UTR (Dorschhasler *et al.*, 1975; Kitamura *et al.*, 1981; Spector & Baltimore.D, 1974). Figure 1.3 illustrates the PV genomic structure and its polyprotein cleavages into individual mature proteins (De Jesus, 2007).

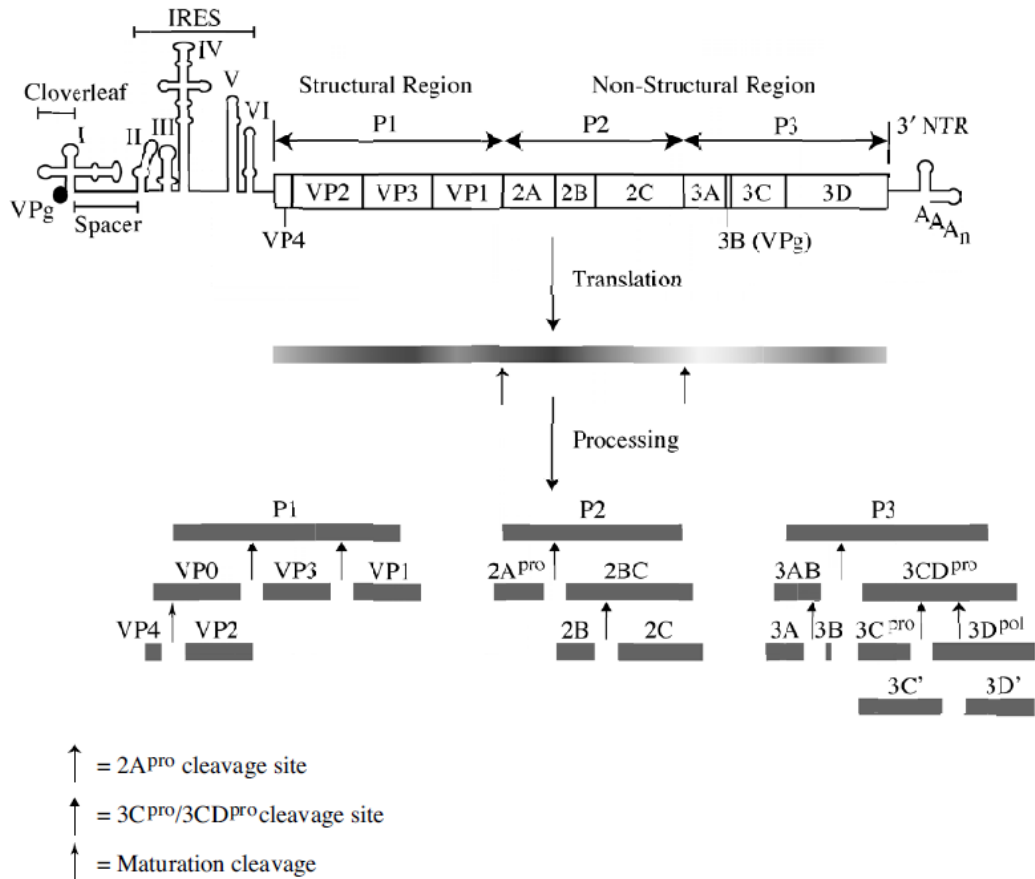


Figure 1.3. Poliovirus serotype 1 (Mahoney) genome structure and polyprotein cleavages.

The 5' non-translated region of the genome contains 6 independent RNA secondary structures which form two functional domains; the clover leaf and the internal ribosome entry site (IRES). VPg binds to the 5' end of the NTR covalently. The 3' NTR consists of 2 structures and a ~60 nucleotide poly(A) tail. The open reading frame (ORF) is cleaved into structural protein, polyprotein 1 (P1) and non-structural proteins (P2 and P3) by virus encoded proteinases. The co-translationally encoded proteases, 2A^{pro} and 3C^{pro}/3CD^{pro} process the polyproteins into mature viral proteins. The figure is from the review by De Jesus (2007).

5' UTR

This region of the PV genome is extensively studied for its usually long sequence. It has been revealed that it contains unique features for RNA replication and translation. The poliovirus 5' UTR consists of 6 domains of RNA secondary structure which play roles in RNA translation and synthesis. The 742 nucleotide long RNA sequence and structure are highly conserved among the serotypes (Skinner *et al.*, 1989; Toyoda *et al.*, 1984). A cloverleaf structure is one of the 5' UTR functioning feature and is formed by the first 88nt of the RNA and facilitates positive-stranded RNA synthesis (Andino *et al.*, 1990). It also functions as a regulator of viral translation by masking the initiation codon from the host cell ribosomes that are seeking the

AUG (Kozak, 1989). The 5' UTR is also the site for an internal ribosome entry site (IRES). The IRES associates with virus modified host cell ribosomes to initiate polyprotein translation. Instead of binding to the canonical 7-methyl guanosine cap structure and then scanning for the kozak sequence, the host ribosome binds to 100 to 150nt upstream of the AUG codon (a *cis*-acting element) and then scans for the AUG codon to initiate translation (Kuge *et al.*, 1989; Pelletier & Sonenberg, 1988). This feature is a major difference between cellular mRNA and PV RNA translation which allows the virus to use host-cell shutoff to minimise cellular translation and favour that of the virus. The spacer regions between the cloverleaf structure and IRES (89-123nt) and from the IRES 3' end to AUG codon (640-742nt) were found to be functional elements as the former region was shown to be involved in RNA replication (Toyoda *et al.*, 2007) while RNA translation is partially regulated by the latter (Arita *et al.*, 2004). The virus RNA cannot be capped as in place of the cap structure of host cell mRNA, the virus has the VPg protein which is a 22 amino acid long virus-encoded protein that covalently binds to the 5' UTR and functions as a primer in RNA synthesis (Lee *et al.*, 1977; Wimmer, 1982).

3' UTR

The 3'UTR is 65nt long and it is highly conserved in polioviruses as well as enteroviruses (Toyoda *et al.*, 1984). Its RNA secondary structure is characterised by the presence of pseudoknot structures which are required for negative-stranded RNA to be synthesised for virus replication (Jacobson *et al.*, 1993). The RNA is terminated by a poly(A) tail which is included in the genome rather than post-translationally added as seen in cellular mRNA poly(A) tail (Wagner *et al.*, 2008).

ORF

This largest part of the genome is later translated into a single polypeptide, the polyprotein, a 250 kDa polyprotein sub-divided into polyprotein1 (P1), P2 and P3 (Figure 1.3) and whose mechanism of translation is described in section 1.3.2.

P1 is translated to the viral structural proteins while P2 and P3 are cleaved to form the viral RNA replication and accessory proteins. The encoded proteases, 2A^{pro} and 3C/3CD^{pro} co-translationally cleave the polyprotein into the final individual functional proteins (Pallansch *et al.*, 1984). 2A protease cleaves the polyprotein at a tyrosine-glycine dipeptide at the junction of P1 and P2 to release the 97 kDa P1 structural precursor protein (Toyoda *et al.*, 1986). This

initial proteolytic processing takes place as self-cleavage and is pre-required for P1 cleavage (Nicklin *et al.*, 1987). P1 is subsequently cleaved into the viral capsid proteins (VP) 0, VP3 and VP1 by the 3C/3CD protease (Hanecak *et al.*, 1982; Ypmawong *et al.*, 1988a). VP0 cleaves further into VP4 and VP2 in a viral protease independent event which occurs when the viral structural protein matures to the procapsid and incorporates RNA (Harber *et al.*, 1991).

P2 and P3 are processed into the stable viral proteins; 2A^{pro}, 2B, 2BC, 2C, 3A, 3AB, 3B (VPg), 3C/3CD^{pro} and 3D^{pol}. These proteolytic cleavages are facilitated by 3C^{pro}/3CD^{pro} catalysis at glutamine-glycine dipeptides (Hanecak *et al.*, 1982). The intermediate proteins, 2BC, 3CD and 3AB have been reported to function in different ways from the final proteins. While 2A protein is essential for proteolytic processing of the polyprotein it is also required for RNA replication as negative strand synthesis during RNA replication was found to be stimulated by the presence of 2A in a cell-free replication system. Although the exact mechanism of 2A involvement in RNA synthesis is not known, it is speculated that 2A may influence cellular protein function during negative strand RNA synthesis (Jurgens *et al.*, 2006). 2A also recognises a tyrosine-glycine cleavage site within the 3D sequence which produces 3C' and 3D' although these are not essential for PV proliferation (Lee & Wimmer, 1988). The other function of 2A is in shut-off of host cell mRNA translation (Hambidge & Sarnow, 1992). The small, hydrophobic, membrane-associated protein, 2B is also required for viral replication as a mutation in 2B led to a defect in PV RNA synthesis (Johnson & Sarnow, 1991). The hydrophobic region of 2B is essential for function and association with membranes where it oligomerises to create a channel, which may result in mature virus release (Agirre *et al.*, 2002). Highly conserved 2C protein consists of membrane-, RNA- and NTP- binding regions (Rodríguez & Carrasco, 1995; Rodríguez & Carrasco, 1993; van Kuppeveld *et al.*, 1997a; van Kuppeveld *et al.*, 1997b) and its amino acid sequence is highly homologous with RNA helicases which are found in most positive stranded RNA viruses. PV 2C unwinds the intermediate double stranded RNA synthesised during RNA replication and guanidine hydrochloride (GuHCl) resistance mutations have been mapped to 2C (Pincus *et al.*, 1986) consistent with the fact that GuHCl inhibits negative strand synthesis and NTPase activity (Pfister & Wimmer, 1999). 2C synthesis disturbs the cellular Golgi apparatus and ER structures to form vesicular structures similar to those produced during RNA synthesis (Aldabe &

Carrasco, 1995; Cho *et al.*, 1994). 2BC is the precursor protein of 2B and 2C and some remains uncleaved during the infection cycle. It seems to have a role in that membrane association for virus release is more efficient with 2BC than with 2B only (Aldabe *et al.*, 1996). 3AB is a precursor for 3A and 3B (Viral Protein genome-linked/VPg) proteins (Semler *et al.*, 1982) and cleaved by 3CD^{pro} to release VPg and 3A (Lama *et al.*, 1994). VPg is crucial in viral replication as it acts as the protein primer for viral RNA synthesis. VPg and 3D^{pol} function is mentioned in section 1.3.3. 3CD is a multi-functional precursor protein which cleaves to give the PV protease, 3C^{pro} and the RNA-dependent RNA polymerase, 3D^{pol}. In spite of the presence of 3D, 3CD functions as only a protease. It cleaves P1 into the structural proteins VP0, VP1 and VP3 and the non-structural proteins, 3AB, 3CD, 3C^{pro} and 3D^{pol} are also cleaved by 3C or 3CD (Harris *et al.*, 1992). 3CD also plays an important role in viral RNA replication, as it facilitates the recruitment of uridynylated VPg and 3D^{pol} (Paul *et al.*, 1998). The cleavage of structural proteins from P1 by 3C/3CD^{pro} is highly relevant to this project as the protease choice for recombinant expression systems is one of the key parameters for efficient synthesis and details of this will be discussed further in chapter 3.

Lulla *et al.* (2019) reported a newly identified protein expressed from an upstream ORF (UP) in echovirus 7 and PV1. UP knockout viruses were attenuated indicating the association with late stage infection in which membrane bound UP facilitates virus release. The findings enabled an understanding of how UP promotes virus growth in the gut and the site of initial contact with susceptible hosts. The study may challenge the single-polypeptide genome strategy for picornaviruses.

1.3 Replication cycle

PV replicates efficiently in the host cell cytoplasm where, as any virus, it takes over cellular function in favour of virus replication. In brief, PV infection initiates with cell attachment via the CD155 receptor (De Sena & Mandel, 1977; Fenwick & Cooper, 1962; Tsang *et al.*, 2001). After capsid uncoating and RNA entry into the cell, VPg is removed from the RNA (Ambros & Baltimore, 1980) and this molecule acts as the viral mRNA used for RNA translation and replication in the host cell cytoplasm. Host cell ribosomes translate the ORF to produce a single

polyprotein which is cleaved into capsid proteins (P1) and non-capsid proteins (P2 and P3) by virus coded protease, 2A^{pro} (Kräusslich *et al.*, 1988; Lawson & Semler, 1990; Pallansch *et al.*, 1984). Structural proteins, VP0, VP1 and VP3 are cleaved from P1 and self-assemble into the capsid (Holland & Kiehn, 1968; Jacobson & Baltimore, 1968a). Non-capsid proteins are required for RNA genome replication in membrane vesicles. VPg accumulates in the membrane structures and acts as primer for negative strand production which is then used as template for more positive strand RNA synthesis (Barton & Flanagan, 1997). Once a copy of the newly synthesised RNA genome is enclosed in the capsid (Nomoto *et al.*, 1977b; Novak & Kirkegaard, 1991), maturation takes place wherein VP0 cleavage into VP4 and VP2 takes place (Harber *et al.*, 1991). Upon cell lysis, PV particles are released to infect new cells for further replication. Distinct steps in the cycle are shown in Figure 1.4.

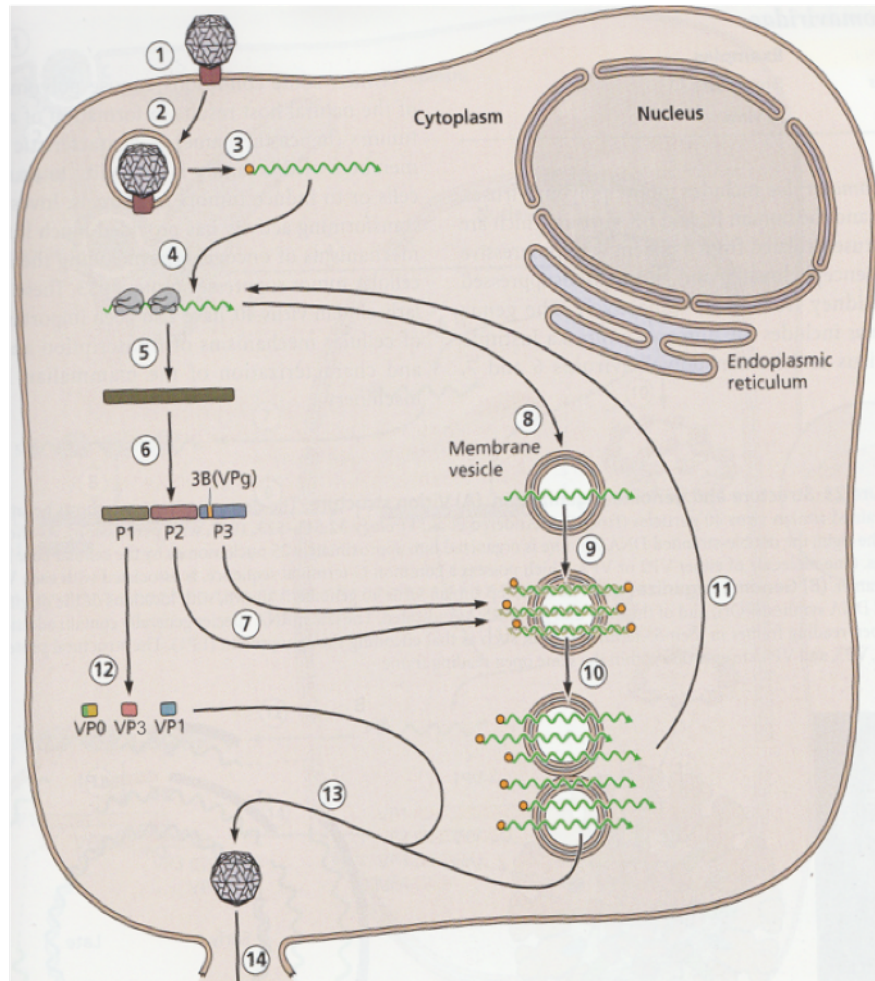


Figure 1.4. PV replication in a susceptible cell.

Each step of replication is illustrated and numbered from virus attachment to exit of the cell. 1) PV particle attachment to CD155 2) Internalisation of CD155-PV complex 3) PV RNA release after capsid uncoating 4) RNA translation by VPg removed viral mRNA by host cell ribosomes to produce 5) Polyprotein 6) Proteolytic processing of polyprotein into capsid protein (P1) and non-capsid proteins (P2 and P3) 7) P2 and P3 derived proteins are used for RNA replication 8) VPg free RNA is recruited for membrane vesicle 9) Double stranded RNA production 10) Production of more positive strand RNA 11) Nascent RNA can be used for further RNA translation after VPg removal 12) P1 cleavage into structural viral proteins (VP0, VP3 and VP1) 13) Encapsidation of RNA genome 14) VP0 cleavage into VP4 and VP2 by capsid maturation, progeny PV virus exit after cell lysis (Flint *et al.*, 2015a).

1.3.1 Poliovirus attachment and entry

The PV infection establishes when the PV particle interacts with the surface poliovirus receptor, PVR, aka cluster of differentiation 155 (CD155) of the host cell. CD155 is a glycoprotein which belongs to the immunoglobulin (Ig) superfamily (Mendelsohn *et al.*, 1989) and consists of extracellular Ig-like domains (D1 to D3), a transmembrane domain and a cytoplasmic tail. D1 interacts with PV particles (Koike *et al.*, 1991; Selinka *et al.*, 1991) and at

physiological temperature, the PV particle undergoes a conformational change; 160S particle to 135S particle (De Sena & Mandel, 1977; Fenwick & Cooper, 1962; Tsang *et al.*, 2001) in which the particle becomes expanded by 4% in size and opens holes at the 2-fold and quasi 3-fold axes. At the same time, the N terminus of VP1 and myristoylated VP4 are externalised (Chow *et al.*, 1987; Curry *et al.*, 1996; De Sena & Mandel, 1977; Fenwick & Cooper, 1962; Fricks & Hogle, 1990). These bind to the host cell surface membrane resulting in pore channel formation (Danthi *et al.*, 2003; Fricks & Hogle, 1990 ; Tosteson *et al.*, 2004; Tuthill *et al.*, 2006). At the same time, the expanded particle is internalised into an endosome form of virus (Brandenburg *et al.*, 2007) where viral RNA genome transport from the viral capsid to the host cell cytoplasm is suspected to occur directly through the channel (Butan *et al.*, 2014).

CD155 is one determinant for PV permissiveness and in the human, CD155 is expressed in a wide range of cells including the usual sites for PV replication (Mendelsohn *et al.*, 1989). Transgenic mice engineered to express Hu CD155 are used as an infection model to test anti-viral responses, e.g. the interferon- α/β (INF α/β) response. When Hu CD155⁺ transgenic mice lacking the INF α/β receptor were injected with PV, replication was seen not only in the CNS but also in liver, spleen and pancreas whereas in Hu CD155⁺ transgenic mice, PV replicated only in the CNS. The expression of IFN-stimulated genes (ISGs) in extraneural tissues was significantly enhanced in CD155⁺ transgenic mice but remained moderate in brain and spinal cord. These findings suggest that an active IFN response is a factor protecting extraneural tissues from PV infection, which agrees well with poliomyelitis prevalence as only 1% of total PV infection results in CNS invasion. Evidently, most cases of PV infection must be limited by the INF α/β response in non-neural tissue (Ida-Hosonuma *et al.*, 2005).

CD155 specific binding by PV is part of the virus host range as although PV infects mainly humans it can also infect Old World primates (Hsiung *et al.*, 1964) where CD155 homologs/orthologs are found. However, efficient PV infection is not established in these animals. In most mammals the amino acid sequence of the D1 domain at is not compatible with PV binding preventing attachment to most mammalian CD155s (Ida-Hosonuma *et al.*, 2003).

1.3.2 Viral RNA translation

Once the viral RNA genome is released into the cytoplasm, host cell enzymes remove the 5' linked VPg (Ambros & Baltimore, 1980) to allow RNA translation resulting in the primary 250kDa polyprotein cleaved mature proteins (Harris *et al.*, 1992; Kitamura *et al.*, 1981; Kräusslich *et al.*, 1988; Lawson & Semler, 1990; Pallansch *et al.*, 1984; Parsley *et al.*, 1999). Translation is initiated by ribosome attachment to the internal ribosome entry site (IRES) (Nicholson *et al.*, 1991; Pelletier & Sonenberg, 1988) rather than ribosomal scanning for an AUG codon for mRNA translation (Kozak, 1989). All picornaviruses utilise an IRES for the initiation of translation (Macejak & Sarnow, 1991) with the enteroviruses using a Type I IRES structure (Figure 1.5). The RNA secondary structure of the IRES allows 40S ribosome subunit recruitment and subsequent translation from the AUG codon, although the optimal sequence of (ACCAUGG) is required for optimal 40S scanning to initiate the polyprotein translation (Kozak, 1986).

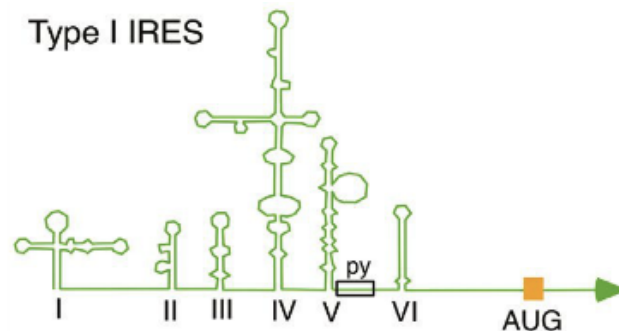


Figure 1.5. A schematic representation of the IRES structure used in enteroviruses

The nucleotide sequences share little conservation, but the secondary structures are important in the recruitment of the ribosome. Once the 40S ribosome subunit is recruited, scanning for the initiation codon occurs and then viral genome translation. The figure is from the review by Racaniello (2013)

In PV infected cells, host cellular mRNA translation is diverted to viral RNA translation. In eukaryotic mRNA translation, translation begins with recruitment of the 40S ribosome subunit and eukaryotic initiation factors (eIFs). In cellular mRNA eIF4E associates with the 5' mRNA cap structure and directs the 40S ribosome subunit onto the mRNA. This is followed by complex formation with eIF4G, eIF3, eIF4A and eIF4E and scanning in the 5' to 3' direction to reach a correct initiation codon. Once the 40S ribosome subunit locates the AUG codon, the 60S ribosome counterpart joins to form an 80S ribosome to commence translation (Hershey & Marrick, 2000; Kozak, 1989). This mechanism is hijacked in favour of the virus for its genome translation in virus susceptible cells as the IRES recruits the host ribosome to translate the viral genome without the requirement for a cap structure at the 5' end, that is, cap-independent translation. In fact PV 2A^{pro} cleaves eIF4G (Hambidge & Sarnow, 1992) effectively inactivating host mRNA cap dependent translation whereas IRES enabled translation occurs with cleaved eIF4G which still forms a complex with eIF3 and eIF4A. Thus, the cleavage of eIF4G can be defined as a switch from host cell mRNA translation to that of the viral RNA and contributes to the major host cell shutoff shown by most picornaviruses. Figure 1.6 shows the eIFs required for eukaryotic mRNA and viral RNA translation.

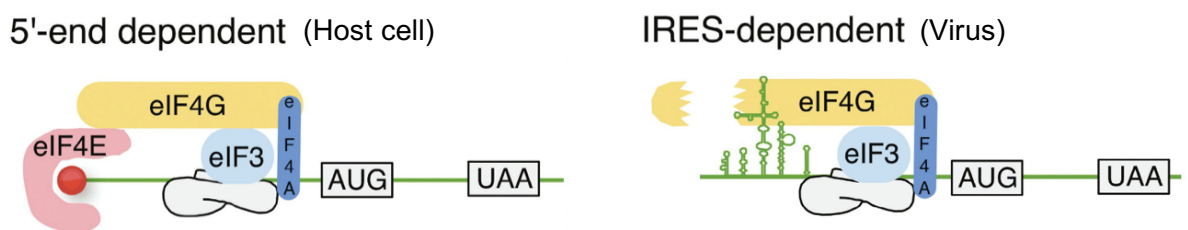


Figure 1.6. Schematic representation of 40S ribosome recruitment for the initiation of translation

(Left) eIF complexes form around mRNA 5'-cap for recruitment of the 40S ribosomal subunit in eukaryotic mRNA translation. (Right) IRES led 40S ribosomal subunit recruitment still occurs with cleaved eIF4G and the rest of eIFs. PV 2A^{pro} cleaves eIF4G leading to a switch in host cell mRNA translation to the viral RNA. The diagrams were adapted from a review by Racaniello (2013).

1.3.3 RNA synthesis

The picornavirus genome is amplified up to 50,000 copies per cell during RNA synthesis which takes place on host cell intracellular membranes termed double-membrane vesicles (Beske *et al.*, 2007; Egger *et al.*, 2000; Schlegel *et al.*, 1996). During RNA synthesis, 3 types of RNA are present in the infected cell. These are positive sense single stranded RNA, replicative intermediate (RI) and replicative form (RF). The most abundant of these are positive sense single stranded RNA. Figure 1.7 illustrates PV RNA synthesis. The incoming genome serves as the initial template for the synthesis of complementary negative strands leading to a full-length duplex RNA called the RF. From this intermediate, several positive strands of RNA are synthesised either to be translated into more viral proteins or used as template to synthesise further negative strand RNA or packaged into virions to be released from the cell (Barton & Flanagan, 1997). Negative strands exist solely as duplex RNA in infected cells (Bienz *et al.*, 1992).

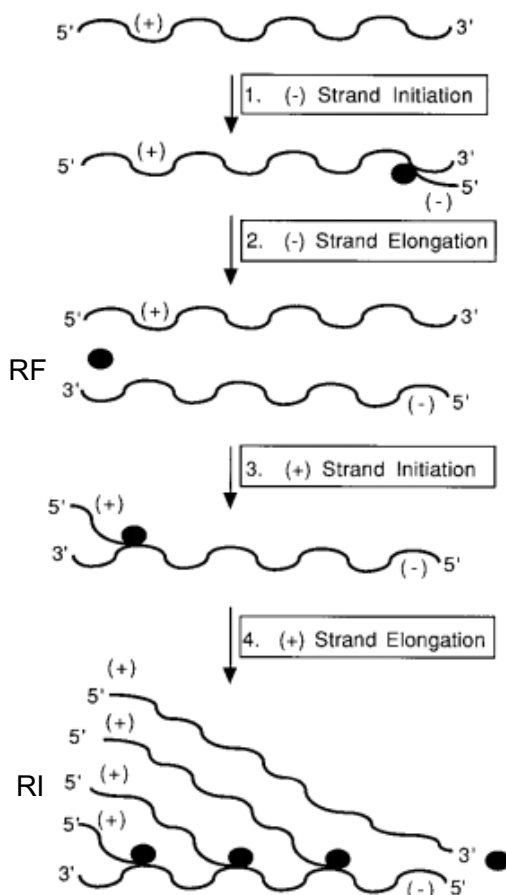


Figure 1.7. PV RNA synthesis

Negative strand synthesis initiation using the positive strand as a template. Once full-length negative strand is produced, those two strands form duplex RNA strand (RF). The negative strand serves to produce multiple nascent positive strands. The black circle indicates the RNA-dependent RNA polymerase, 3D^{pol}. This sketch was adapted from Barton and Flanagan (1997).

The enzyme responsible for RNA synthesis is the RNA-dependent RNA polymerase (RdRp), 3D^{pol}. This 63 kDa protein is a cleaved product from 3CD^{pro}, which functions as a protease. The polymerase requires a poly(U) primer to elongate from the 3' end poly(A) template and this is provided by uridylylated VPg (Paul *et al.*, 1998).

1.3.4 Encapsidation of viral RNA

Once sufficient PV capsids are assembled and RNA synthesised, one copy of the newly synthesised positive-stranded RNA is packaged into the capsid for progeny virus release (Nomoto *et al.*, 1977b; Novak & Kirkegaard, 1991). The exact mechanism of viral genome encapsidation is unknown. An early study suggested that VPg acted as a single protein marker which leads the RNA into the viral particle (Nomoto *et al.*, 1977b). However, it is now known that the negative strand is also bound with VPg protein, yet no negative strand RNA exists in progeny viral particles so this mechanism is incorrect. Later study suggested encapsidation is controlled by multiple viral proteins including 2C^{ATPase} and VP3 which lead to RNA incorporation while the viral capsid is assembling. In this model, when 5 protomers form a pentamer, mature VPg linked positive stranded RNA attaches to it and assembly continues into the provirion which contains the RNA in the interior of the capsid (Liu *et al.*, 2010). This is followed by maturation of the provirion into the infectious virion by VP0 cleavage into VP2 and VP4 (Harber *et al.*, 1991). The detail of PV capsid assembly and structure is discussed in section 1.4.

1.3.5 Exit of the viral particles

Once viral particles are assembled and the genome packaged, PV undergoes extracellular release. PV infected cells start to show cytopathic effects such as condensation of chromatin and shrinkage of the entire cells and it is widely accepted that viral particle release is by final lysis of the host cells. Leakage from the lysosome of the host cell has been suggested to induce cell lysis (Guskey *et al.*, 1970). At the same time however, non-lytic release has been observed without cell lysis in cultured cells (Taylor *et al.*, 2009) and PV particles are found in lysed cells as well as in the media surrounding intact infected cells (Lloyd & Bovee, 1993; Pelletier *et al.*, 1998). CPE is rapid and after only 3-4 hours of PV infection host cell internal membranes are rearranged into double-membraned vesicle (Dales *et al.*, 1965). These vesicles share characteristics with cellular autophagosomes which are responsible for the

regulated self-destruction of unnecessary cellular components (Klionsky, 2005; Mizushima *et al.*, 2002). The proteomes of PV-induced vesicles and cellular autophagosomes has shown that the autophagy proteins LC3 and Atg12 are reduced in PV-induced vesicles indicating that PV compromises the cellular autophagy pathway possibly for non-lytic release (Jackson *et al.*, 2005).

1.4 PV capsid

The poliovirus icosahedral capsid is composed of 60 copies each of 4 viral capsid proteins, VP1 (~33 kDa), VP2 (~30 kDa), VP3 (~26 kDa) and VP4 (~7.5 kDa). The capsid structure is conserved within all picornaviruses, albeit with slightly different capsid sizes. The capsid serves to protect the RNA genome from the environment and in consequence, requires a rigid structure. However, the structure is also required to be ready to release the RNA once it attaches to the receptor on a permissive cell. Therefore, the capsid is a metastable structure.

1.4.1 Capsid assembly

PV capsid assembly undergoes sequential steps involving intermediates identified by their antigenicity and sedimentation coefficient on sucrose gradients. This is illustrated in Figure 1.9. The process requires considerable specificity and coordination among the viral proteins. The assembly of the PV capsid initiates with the proteolytic processing of P1 and the production of the protomer which sediments at 5S and contains 1 copy of each VP0, VP3 and VP1. The protomer matures into a pentamer consisting of 5 copies each of VP0, VP3 and VP1, sedimenting at 14S (Phillips & Fennell, 1973; Watanabe *et al.*, 1965). Pentamer stabilisation is maintained by protein-protein contacts as well as clustering of the myristate chain present at the N terminus of VP4 at the five-fold axis (Figure 1.8). Myristoylation thus provides a factor of PV capsid stability and assembly (Marc *et al.*, 1990; Moscufo *et al.*, 1991). The gathering of 12 pentamers forms the empty capsid which sediments at 80S (Jacobson & Baltimore, 1968b). This capsid has not yet gained PV RNA but does so when it finally assembles into the 160S mature capsid (Jacobson & Baltimore, 1968a). The interchange among the 14S pentamer, 80S procapsid and 160S mature capsids is dynamic and the precise point at which RNA is incorporated remains unclear. However, cleavage of VP0 into VP4 and VP2 is

speculated to occur concomitant with encapsidation of the viral genome. The mature capsid shows elevated stability compared to the empty capsid suggesting that VP0 cleavage is another part of the requirement to produce a stable particle (Guttman & Baltimore, 1977).

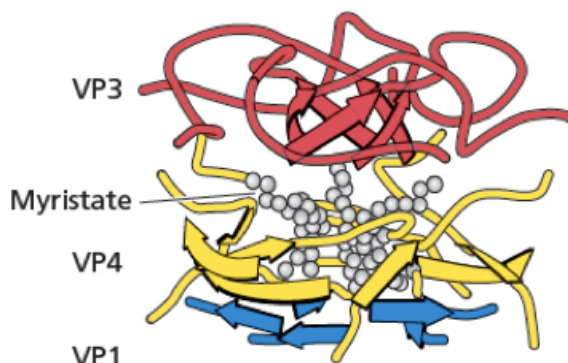


Figure 1.8. Myristate position in the capsid

At the 5 fold axis, five N termini of VP3 assemble into a parallel β sheet structure which interacts with another β sheet structure produced by VP4 and VP1 via the myristate group. Myristoylation is a post-translation addition to VP4. Until proteolytic processing of VP0 into VP4 and VP2 completes, the internal structure is not fully assembled. The figure is from Flint *et al.* (2015b)

1.4.2 Capsid proteins

X-ray crystallography enabled the determination of the PV structure. VP1, VP2 and VP3 were shown to be constructed with a common 'core' architecture consisting of an eight-stranded β -barrel connected by 2 loops and flanked by C- and N- terminal extensions, termed a " β -barrel jelly-roll". Figure 1.10 illustrates the b) VP1, c) VP2 and d) VP3 structures while a) represents the core structure arranged in a wedge-like structure. One wall of the wedge is made of antiparallel β sheets consisting of C, H, E, F β -strands. The other wall and floor is occupied by the other β sheets (B, I, D, G β -strands) which bend at the wall-floor junction. The difference in sequences of the β -strand connecting loops and the N- and C- terminal extensions gives VP1, VP2 and VP3 their conformational distinction. By contrast VP4 has a distinctive structure with its extended conformation resembling the N-termini of VP1 and VP3 (Hogle *et al.*, 1985).

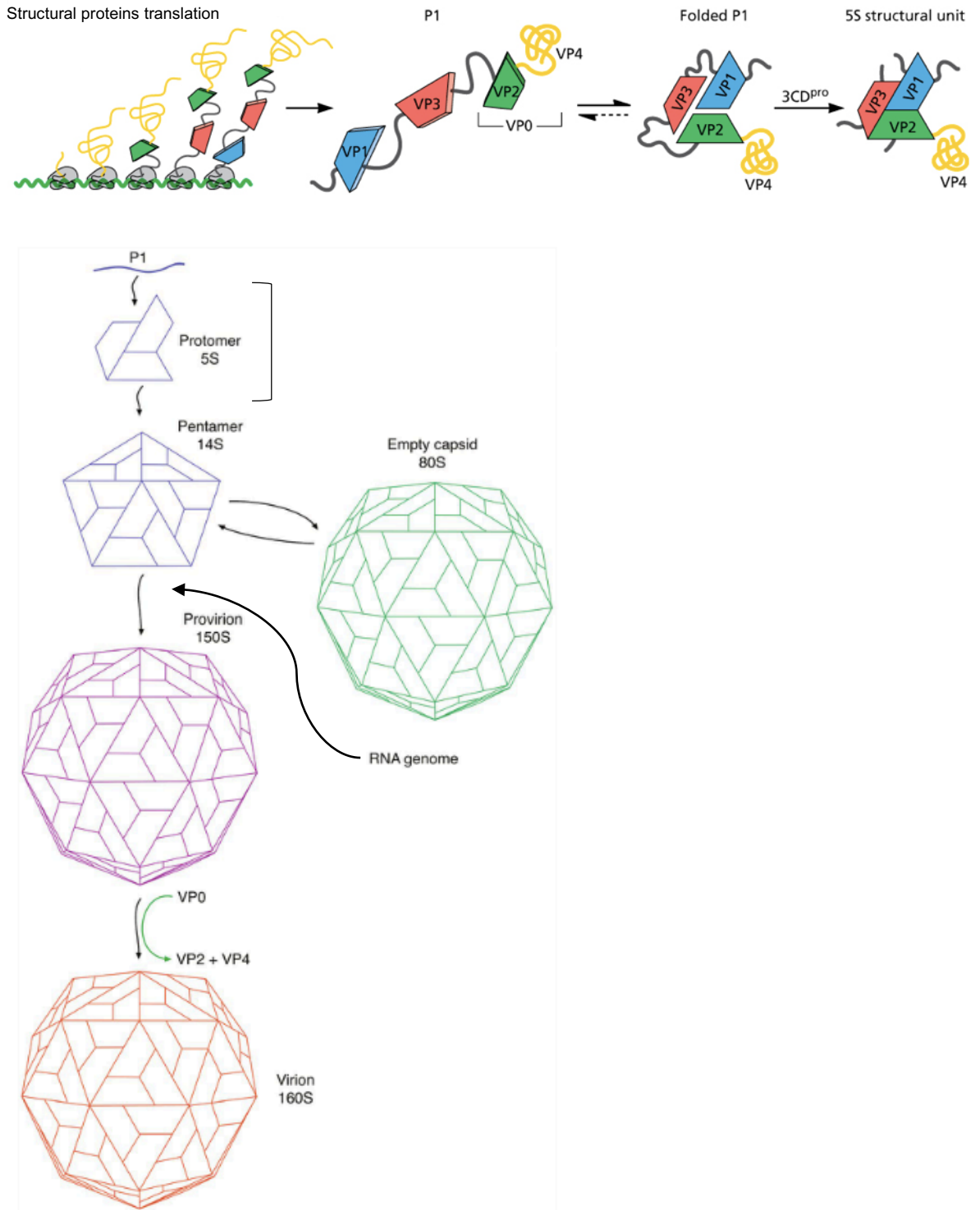


Figure 1.9. PV capsid assembly and sedimentation coefficient on sucrose gradient

The series of 4 images at the top of page illustrates the polyprotein precursor translation by ribosomes through to assembly of 5S protomer consisting of VP1, VP2 and VP0. 5 of protomers self-assemble into pentamers, 14S, and 12 pentamers may form the empty capsid of 80S. Encapsidation of RNA turns the empty capsid into a provirion, 150S and VP0 cleavage into VP4 and VP2 completes the maturation and produces the virion, 160S. The figures are modified from a review by Racaniello (2013).

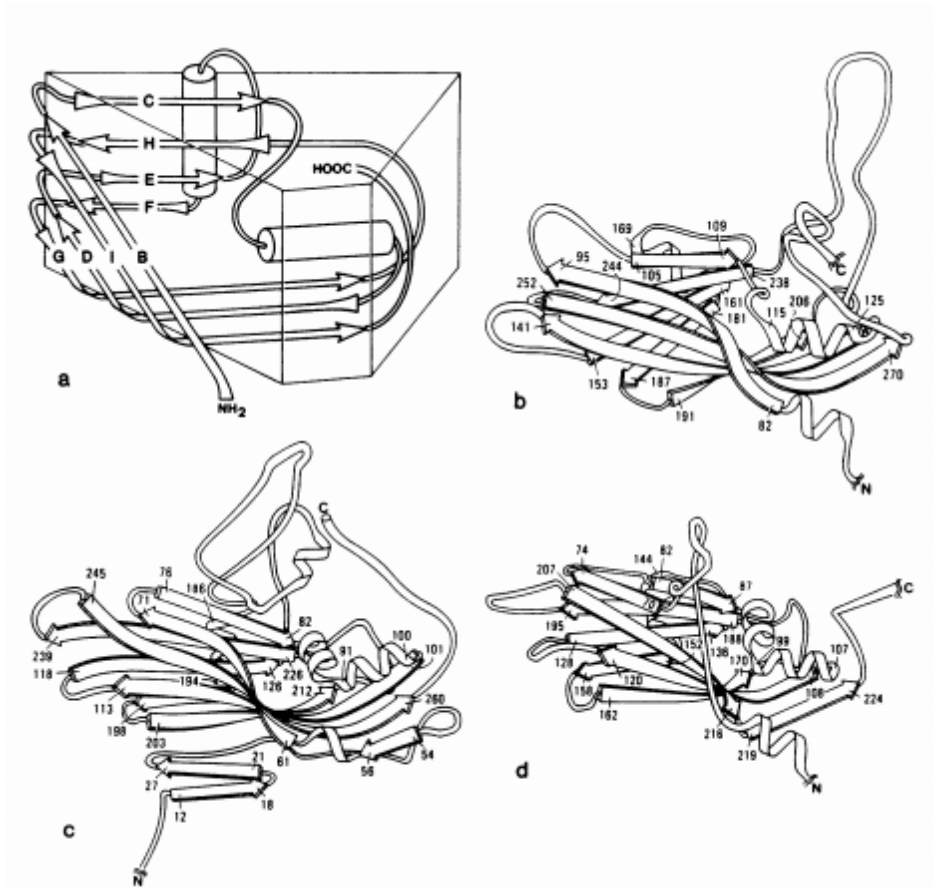


Figure 1.10. Poliovirus capsid protein schematic representation

(a) The 'core' structure of the viral capsid proteins arranged in an eight-stranded wedged-shape antiparallel β barrel. The β strands are given letters B to I (in N to C terminus order). Four (B, I, D and G) strands forms a β -sheet in the front of structure. The back of the structure consists of the C,H,E and F β -sheet. The loops connecting these two sheets are denoted by the strands which is the loop connects (i.e. GH loop). The structurally conserved α -helices are represented by cylinders. (b) VP1, (c) VP2 and (d) VP3 share a 'core' structure with different loop length and C and N termini. The long loop end of the VP1 is arranged into a 5 fold axes. The end of VP2 and the VP3 β -barrel are packed on the 3-fold axes. The figures are from Hogle *et al.* (1985).

1.4.3 External capsid surface

The external surface of the capsid is constructed by a network of VP1, VP2 and VP2 C-termini and loops connecting the β -sheets. These are arranged into surface features which include a star-shaped structure called the "mesa" seen at the 5-fold axes and a 3-bladed "propeller"-shaped structure at the 3-fold axes (Figure 1.11a). The features are isolated by a groove surrounding the mesa and a depression separating the 3-fold axes structures and 2-fold axes (Hogle *et al.*, 1985). A key feature called the "canyon" is formed by the joining of the groove

around the mesa. This is the site for receptor attachment, its recessed nature shielding it from the generation of neutralising antibodies (Belnap *et al.*, 2000; He *et al.*, 2000; Xing *et al.*, 2000). The external surface of the capsid presents the major neutralising antigenic sites. For PV, these sites are located in VP1, VP2 and VP3 regions of the sequence (Minor *et al.*, 1986). As conformational change occurs as the PV capsid undergoes particle attachment to the receptor, those sites are exposed and neutralising antibody can bind them.

1.4.4 Internal capsid surface

The internal surface of the capsid is decorated with the N-terminal extensions of VP2, VP3 and VP1 and with VP4. Protein-protein interactions function to stabilise the capsid (Figure 1.11b) and include a plug for a channel consisting of 5 copies of VP3, found on the inner side of the 5-fold axes. The plug is formed by 5 copies of the intertwisted N-termini of VP3, called a twisted parallel β -tube. The structure is surrounded by 5 copies of a 3-stranded β sheet formed by the myristoylated VP4 N-termini and residues from the VP1 N-terminus (Figure 1.11c). The structure stabilises the structure as it is maturing from protomer to pentamer (Hogle *et al.*, 1985). The other internal shell feature is a 7-stranded β -sheet formed by a 2-stranded β hairpin from the N-terminus of VP2 sandwiched by a 4-stranded CHEF sheet (C, H, E and F β -sheet as seen in Figure 1.10) of VP3 and a peptide from the N-terminus of VP1, both of which are from the neighbouring pentamer. The structure cements neighbouring pentamers together to achieve stabilisation of the overall PV icosahedral structure (Figure 1.11d) (Filman *et al.*, 1989).

The interior of the capsid is partially filled with a 1500 nucleotide long RNA which may also contribute to capsid stability. CAV20 and PV chimeric virus particle showed an interaction among 2C and VP3 (Liu *et al.*, 2010) and VP1 (Wang *et al.*, 2012a) suggesting a contribution to capsid assembly and encapsidation of newly synthesised RNA.

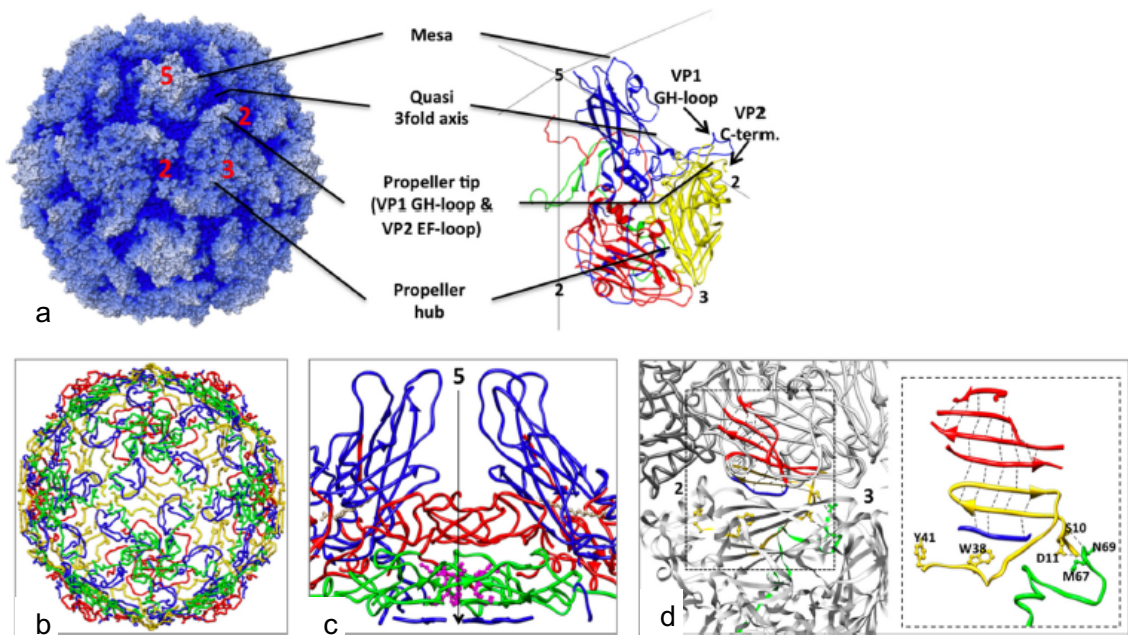


Figure 1.11. The PV capsid features

(a) The radical-depth cued model of poliovirus capsid (Right). The numbers indicate the locations of the icosahedral axes. The ribbon presentation shows a protomer (Left). The viral capsid proteins are colour coded; blue for VP1, yellow for VP2, red for VP3 and green for VP4. (b) The inner shell network of poliovirus depicted by VP4 and N-termini of VP1, VP2 and VP3 (c) The 'plug' structure at the 5-fold axes is formed by the N-terminal peptides of VP3, VP4 and VP1 (d) The sandwich structure consist of 2 neighbouring pentamers. The upper 4 strands from the CHEF sheet of VP3 sits on the neighbouring α -hairpin of VP2. The VP1 strand sits in the bottom of the complex. Modified from Levy *et al.* (2010).

1.4.5 VP1 hydrophobic pocket

Many picornavirus capsids have a hydrophobic space in the core of VP1, beneath the canyon as indicated in Figure 1.12A, the cleft revealed by atomic structures where the receptor, CD155 in the case of poliovirus, binds. This space is termed the hydrophobic pocket and there are a total of 60 pockets as indicated in yellow in Figure 1.12B in an assembled picornavirus capsid, corresponding to the number of VP1 proteins. In the available atomic structures for most enteroviruses these pockets are found to contain lipids derived from the host cell called 'pocket factors' (Filman *et al.*, 1989). The pocket factor is not a unique molecule as analysis of bovine enterovirus virions has shown mixed types of lipids, although palmitic acid and myristic acid represent the majority (Smyth *et al.*, 2003). In poliovirus type 1 and type 3, the pocket is filled with sphingosine. Those fatty acids being determined from the electron density features of the

crystallographic study (Filman *et al.*, 1989). During receptor binding in the canyon, a depression of the canyon floor results in deformation of the VP1 pocket and ejection of the pocket factor. In consequence, the capsid conformation changes and uncoating occurs, leading ultimately to the release of the RNA genome into a new cell. However, this conformational change is prevented when hydrophobic antiviral drugs such as WIN compounds, shown in Figure 1.12C and discussed in detail in 1.6.1, are present in the pocket as they are designed to bind tightly, lock the cavity and counteract canyon depression which then prevents virus entry by inhibiting the capsid conformation changes that occur after receptor binding (Grant *et al.*, 1994; Muckelbauer *et al.*, 1995; Rossmann, 1994; Smith *et al.*, 1986). This is the functional basis of their antiviral activity. When a pocket factor is dislodged, capsid destabilisation leads to the externalisation of the N termini of VP4 and VP1. These orchestrate genome release across the 2-fold axis and into the host cell most likely via a pore formed from VP4 (Tuthill *et al.*, 2006). Thus, in viral capsid uncoating, the pocket factor plays a role as a picornavirus infection initiation switch (Plevka *et al.*, 2013) and it follows that this switch might be fixed in an off conformation, pocket locked, by manipulating the VP1 cavity and so act to control virion thermal stability (Filman *et al.*, 1989; Macadam *et al.*, 1989).

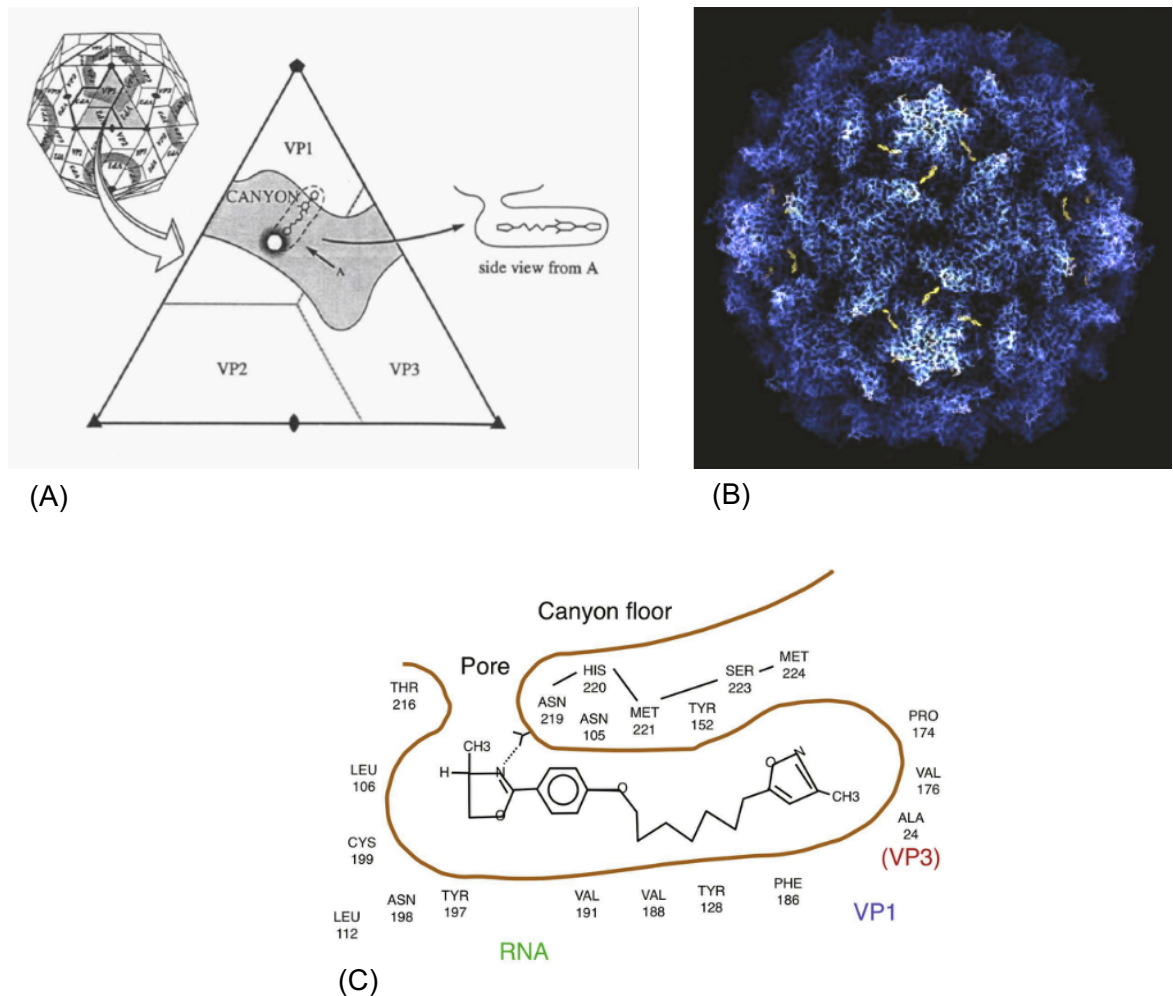


Figure 1.12. Images for VP1 pocket in PV

(A) A sketch of the picornavirus icosahedral capsid with canyon at the 5-fold axes. The hydrophobic pocket location in the canyon is illustrated, as is a cross section of the hydrophobic pocket with WIN compound (Oliveira *et al.*, 1993). (B) A radial depth-cued representation of poliovirus with a pocket binding WIN compound (R78206) indicated in yellow. The imaging method demonstrates dimensional depth by colouring the atoms closer to the core of PV particle with a deeper blue colour. White/pale blue colour indicates that the atoms are projecting away from the capsid. (C) A cross section of a pocket with pocket compound (WIN52084) bound. The original lipid in the pocket was replaced by this compound which inhibits infectivity. The image shows residues facing into the pocket. Although mostly from VP1, one residue of VP3 also contributes to the structure. The images B and C were from the review by Racaniello (2013).

1.5 PV infection control

PV infection was rare until the 20th century. At that time PV was in general circulation and infants encountered it within 6-12 month of age when they were still under maternal antibody protection. This resulted in mild infections and PV immunity development. Following the industrial revolution, urbanisation progressed in the cities and public sanitation was greatly

improved. This delayed the first PV contact with infants. These unprotected infants then became susceptible to PV infection (Nathanson & Kew, 2010) and the increase in PV naïve infants led to poliomyelitis epidemics (Centers for Disease Control and Prevention, 2012). The growing number of poliomyelitis cases led the development of PV vaccines which are currently still used world-wide. The early success of those vaccines led to the WHO campaign for WT PV eradication and while that has been very effective, vaccine revertant poliomyelitis has become prominent as the total number of cases dropped. In the case of a wholly PV naïve population, an endemic outbreak would be predicted and because of this possibility, an infection management plan is necessary for the post-eradication future even though WT PV eradication has not been achieved yet for all serotypes.

1.5.1 Current vaccines

Jonas Salk produced inactivated PV vaccine (IPV) and its introduction achieved a reduction in paralytic poliomyelitis cases from 13.9 cases in 100,000 in 1954 to 0.5 cases in 100,000 in 1961 (Centers for Disease Control and Prevention, 2012). Virulent WT PV, inactivated by formalin, is administered by intramuscular injection (Salk, 1960). In 1961, live attenuated oral PV vaccine (OPV) was proven to be effective by Albert Sabin and the current OPV is named Sabin after the inventor. Monovalent OPVs were licensed prior to trivalent OPV which was licensed in 1963. Since then, OPV has replaced IPV because of the ease of administration (the droplet alone or on a sugar cube), the induction of mucosal immunity and the public health benefit of some live vaccine virus spreading from immunised to non-immunised individuals (Sabin, 1985). Sufficient OPV replication in the alimentary tract imitates natural PV infection which elicits neutralising antibodies, serum antibodies and secretory immunoglobulin A (IgA), resulting in the induction of local intestinal mucosal immunity and terminating PV shedding in healthy individuals (Ghendon & Robertson, 1994; Hird & Grassly, 2012; Ogra *et al.*, 1968; Valtanen *et al.*, 2000). The spread of the attenuated virus among close contacts of the vaccinated individuals resulted in prevention of WT PV transmission which normally takes a faecal-oral route of infection (Nomoto & Arita, 2002). These benefits of OPV were considered to be sufficient advantage to tolerate a low level of vaccine-associated paralytic poliomyelitis (VAPP) which is caused by a low level of reversion of the vaccine virus at the peak of the epidemic. VAPP cases occur at 1 every 2 to 3 million doses of OPV. However, from 1980 to

1999, this revertant infection became responsible for 95% of the paralytic poliomyelitis cases in the United States as wild-type circulating PV infection declined. Further studies showed recombination between PV serotypes (Romanova *et al.*, 1980; Tolskaya *et al.*, 1983) and 3 Sabin vaccine strains in vaccine recipients (Cammack *et al.*, 1988; Cherkasova *et al.*, 2005). These data confirmed the evolution of OPV into circulating vaccine-derived poliovirus (cVDPV) and after the last case of WT PV poliomyelitis in the United States in the 1970s, VAPP could no longer be overlooked, regardless of the low number of cases it produced. Soon after, an 'enhanced-potency' IPV was shown to be effective to induce comparable immunity to OPV and the occurrence of VAPP and the availability of the new IPV influenced the OPV administration policy in the United States and led to the exclusive use of the improved IPV immunisation from 2000. The switch from OPV and IPV has also been seen in most western countries (Centers for Disease Control and Prevention, 2012). Although improved IPV appears to be a superior vaccine to OPV, IPV has to be noted for differences from OPV; the cost is relatively high when compared to OPV and there is a requirement for healthcare professional training for intramuscular injection (Ehrenfeld *et al.*, 2009). In addition, levels of protective immunity are remarkably distinctive. In contrast to OPV intestinal mucosal immunity, IPV induces only serum antibodies rather than secretory IgA (Ogra *et al.*, 1968) which translates to only limited resistance to PV infection in the intestine (Henry *et al.*, 1966). In addition, as IPV is effective only for IPV-vaccinated individuals, the community herd immunity required to be maintained to achieve prevention of PV transmission via the faecal-oral route is lost (Nomoto & Arita, 2002). In 2015, WT type 2 PV eradication was announced and trivalent OPV was switched to divalent OPV by the removal of type 2 OPV. The type 2 OPV component has been estimated to be responsible for up to 38% of VAPP so the use of type 1 and type 3 divalent OPV is not only part of the trajectory for OPV withdraw but should also lead to a cessation of VAPP caused by type 2 OPV (The Global Polio Eradication Initiative, 2015).

1.5.2 PV eradication and its difficulties

The effective administration of OPV led to the end of WT PV transmission in 1979 in the United States. The global eradication of smallpox accelerated the idea of the global eradication of a major human disease and in 1988 the World Health Organisation (WHO) announced the Global Polio Eradication Initiative (GPEI) aiming at global WT PV eradication by 2000. It is

proposed that breaking WT PV transmission will be necessary to achieve this goal. In the United States, in 1960s, national immunisation days were launched to immunise children under 5 with OPV whether or not they had been previously immunised. This strategy was successful and eliminated PV from susceptible populations and reduced WT PV circulation and the same strategy was applied to the global eradication project. OPV was chosen as the means of vaccination because of its immune response and the ease of administration. A great reduction in poliomyelitis cases was seen immediately after the start of project. However, ~1000 cases of WT PV infection per annum in the world were still reported by the time the project limit had reached 2000 (Ehrenfeld *et al.*, 2009). Since then a low number of WT PV derived cases have been regularly reported meaning that the disease is still not eradicated (i.e. less than 100 cases since 2015) (WHO, 2017). If WT PV eradication is successful, complete poliomyelitis eradication will be the ultimate goal and in order to achieve it, a number of factors must be considered that prevent eradication. There have been outbreaks of paralytic poliomyelitis associated with VDPV in Haiti and the Dominican Republic and the responsible virus was found to be a recombinant between type 1 OPV and an unidentified enterovirus. This outbreak indicated that VDPV had the ability to transmit (Kew *et al.*, 2002). Another outbreak in northern Nigeria in 2006 was caused by a revertant of type 2 OPV. In the area concerned, there was a year without PV immunisation which increased the population of PV naïve individuals. The reintroduction of immunisation then caused a rapid spread of the vaccine virus which allowed it to evolve to be a pathogenic VDPV (Adu *et al.*, 2007; CDC, 2007). Thus, when herd immunity declines, there is a tendency of the vaccine virus to evolve towards VDPV which suggests that vaccination has to be continued at a high level for some years after eradication. In addition, there is a chronic environmental source of VDPV. Individuals, normally with B cell deficiency, can be chronically infected with the vaccine virus resulting in constant shedding of progeny VDPV years after OPV immunisation. The virus evolves by acquiring mutations to be a more virulent VDPV within the host (Blomqvist *et al.*, 2004; Shulman *et al.*, 2006) and demonstrates that the use of OPV cannot ever achieve the ultimate goal of poliomyelitis eradication. Inadequate immunisation coverage is another factor delaying the eradication. Most areas which remain endemic are regions of military conflict where health workers cannot easily reach the target population. Alternatively, they are regions with political or cultural disbelief in vaccine

safety or general resistance against large health campaigns. These obstacles demonstrate the limitations to the poliomyelitis eradication campaign and question the current strategy by WHO to cease OPV vaccination 3 years after the last case of poliomyelitis. The rationale for this plan is to prevent VAPP and OPV evolution to a more virulent VDPV. However, OPV termination leaves a PV susceptible population (Ehrenfeld *et al.*, 2009) and these findings suggest the necessity to sustainably protect the entire population and, in turn, the need for a new generation of vaccines.

1.5.3 Post-PV eradication world and vaccination

Although OPV has contributed to the eradication of WT PV, OPV vaccine is the source for VAPP cases and circulating VDPV which may result in outbreaks as noted in 1.5.2. After WT PV eradication, the protection benefit of OPV becomes less than the risk of poliomyelitis cases. It is therefore inevitable that OPV is discontinued to achieve the eradication of poliomyelitis (Dowdle *et al.*, 2003). A computer model of PV introduction into a PV naïve population has suggested that a PV outbreak is unavoidable (Thompson *et al.*, 2008). Historically, the population immunity to PV was high due to the circulation of wild strains which enabled children to develop immunity (in the pre-industrialisation era) or via effective vaccination schemes. But the cessation of immunisation in isolated communities followed by outbreaks of usual severity has shown what would happen following PV re-introduction to an immunologically susceptible population, such as after eradication (Adu *et al.*, 2007; CDC, 2007; Ehrenfeld *et al.*, 2009). It is an unfortunate but foreseeable fact too that accidental PV release from research or vaccine production establishments or intentional release of virulent PV as a bioterrorism weapon could have severe consequences in low herd immunity populations (Collett *et al.*, 2008; Nomoto & Arita, 2002).

In order to maintain a polio-free world, the whole population has to be protected continuously and this could be achieved by indefinite PV immunisation with a suitable vaccine that did not suffer from the accepted limitations of IPV and OPV. A number of new PV immunisation strategies have been proposed for a polio-free world including use of the enhanced-potency IPV as in the shift from OPV to IPV in high income countries. However, a world-wide switch to IPV is prevented by difficulties such as the production cost, the administration route and the production size required to meet global demand. In addition, IPV vaccines are formulated using

virulent viruses which poses PV containment and safety issues for the manufacturing facilities (Ehrenfeld *et al.*, 2009). It is debatable whether WT PV could be considered as truly eradicated while a vaccine was produced using WT PV (Chumakov & Ehrenfeld, 2008). Other IPV improvement approaches have been also investigated. IPV production from OPV/Sabin strain is one such approach as this is proposed to be safer as the current OPV vaccine viruses will be used for the inactivation. Another approach has investigated the production of IPV derived from a stable attenuated PV strain but with the virulent IPV reference strain capsid (Ehrenfeld *et al.*, 2009). This new IPV is expected to achieve a lower cost than current IPV, avoid virulent PV release but to have equal or enhanced immunogenicity (Ehrenfeld *et al.*, 2009). As the biosecurity of production is less, the cost should be lowered which could result in being able to supply the vaccine demand for the world. However, as discussed, as it is IPV mucosal immunity will not be induced and the production methods still relate to the earlier debate by Chumakov and Ehrenfeld (2008) on whether PV could be considered as truly eradicated while producing a vaccine using replicating PV. For the post-eradication world, ideally antigens would be produced without any PV live culture and this could be offered by recombinant vaccines technologies which approaches immunogen production from a different angle.

1.6 Thermal stability

Further to current vaccine issues related to VAPP for OPV and IPV inability to induce intestinal mucosal immunity, which does not contribute to the herd immunity, as well as bio security concerns for the production of vaccines involving live PV culture both vaccines exhibit an instability which is one of the worst amongst common childhood vaccines. It is essential for the vaccines to be transported in a temperature controlled environment. However, this cold-chain requirement is not always easy for logistical and economic reasons (Pipkin & Minor, 1998; WHO, 2006).

The PV immunogenicity loss is caused by heating and was originally observed by antigen complement fixation assays (Hummeler & Hamparian, 1958; Mayer *et al.*, 1957) where, on heating, immunogenic antigen is converted to non-immunogenic antigen. Hummeler and Hamparian (1958) called the immunogenic antigen N (Native) antigen and the non-

immunogenic antigen H (Heated). Conversely, Mayer *et al.* (1957) labelled the immunogenic antigen as D and the non-immunogenic antigen C based on their sedimentation position in gradients; fractions from a sucrose gradient were collected from the top of the tube and named A, B and so on. The authors showed that C antigen reacts with acute human sera while convalescent sera reacted with D antigen. In addition, C antigenic particles were found to have lost their RNA when the capsid conformation changed from the D antigenic form (Breindl, 1971).

The addition of compounds isolated as antipicornaviral drugs, such as the oxazolinyloxazoles (the so-called WIN compounds) developed by Sterling-Winthrop Inc, (McSharry *et al.*, 1979) and the pyridazinamines, developed by Janssen (Andries *et al.*, 1992) were shown to maintain capsid conformation and improve stability, preventing capsid denaturation or conformation change on heating.

While the thermostability is an issue for PV vaccines, PV shed from infants who had received OPV indicated that PV could overcome this sensitivity which was later found to be due to an acquired point mutation in the case of PV3 virus (Minor, 2012). Additional mutations were also identified to suppress the temperature sensitivity by culturing Sabin type 3 vaccine at elevated temperature. This method of identifying mutation was then applied to find thermal stabilising mutations for each serotype. PV empty capsids, formed by infection of such viruses in the presence of guanidine chloride showed that improved stability was retained, as was immunogenicity (Fox *et al.*, 2017). With this rationale, current vaccine issues discussed in 1.5 may be resolvable as it is clear that WT empty capsids are unstable and change their conformation to the H form readily (Basavappa *et al.*, 1994). Thermostable mutations in PV1 virus were selected similarly and a number of mutations, located mostly at intersubunit interfaces, were identified and these viruses produced N conformation thermostable empty capsids (Adeyemi *et al.*, 2017) which could be applied for VLP production.

From the mutations identified by the studies of Fox *et al.* (2017) and Adeyemi *et al.* (2017) subunit interfaces seem to contribute to the thermostability of empty capsids. These regions are also closely associated with capsid conformation change during uncoating as shown by resolving 135S (Butan *et al.*, 2014) and 80S (Levy *et al.*, 2010) structures.

In the following chapters, some of the thermostabilising methods such as VP1 pocket manipulation by pocket factor binding or pocket filling mutations, introduction of thermostabilising mutations and the potential contribution of capsid uncoating are investigated to attempt to produce a high level of N conformation VLPs.

1.6.1 Antipicornavirus compounds

Small molecules such as antiviral 'WIN' compounds that inhibit the viral capsid conformational change bind the pocket and regulate viral infection (Rossmann, 1994). When these compounds bind to the PV pocket, the natural pocket factors are replaced and capsid conformational change is limited to a minimum (Smith *et al.*, 1986). The precise effects of the compounds differ in individual viruses. In HRV14, the binding of these compounds induces a capsid conformational change so that the virus particle fails to attach to the receptor (Pevear *et al.*, 1989). In PV, the WIN compounds showed inhibition of capsid uncoating but not the attachment to the host receptor (Rossmann, 1994). The relationship between the residues that line the pocket and the action of pocket factors has been demonstrated by PV mutants which are dependent on the WIN compounds for viral replication. Without the WIN compound these mutants were of the H conformation at 37 °C and missing VP4 (Mosser & Rueckert, 1993) which can now be interpreted as the result of externalisation of VP4 during capsid uncoating and the conformation change from 135S to 80S (Butan *et al.*, 2014). Thus, pocket factors are integral to capsid stability and polioviruses with these compounds are more stable.

1.6.2 Thermostable PV mutants

The successful identification of thermostable mutations in the Sabin type 3 vaccine strain showed VP3 residue 91 changed to phenylalanine from serine (Minor, 2012). The mutation is at the interface of the protomers (Filman *et al.*, 1989) explaining how it contributes to the temperature sensitivity of virus growth and capsid assembly (Macadam *et al.*, 1991).

Similar mutations could improve empty PV capsids, enabling robust production in foreign expression systems. For thermostable Saukett empty capsids, mutations identified in Sabin type 3 were introduced into strains Leon and Saukett resulting in 8 amino acid changes from IPV Saukett which is now called Saukett SC8 (Fox *et al.*, 2017). When this sequence was used for plant expression studies, one of the candidate foreign expression platforms used for VLP

assembly, both wt Saukett and Saukett SC8 VLPs were purified and visualised under TEM but those of Saukett SC8 were better formed. Antigenicity analysis showed that the SC8 VLPs had an N conformation and its ability to produce protective immunity was confirmed by transgenic mice immunisation and challenge with Saukett virus (Marsian *et al.*, 2017). The study indicated that a combination of thermostability engineering and foreign expression could produce PV VLP that were a potential candidate vaccine.

Mahoney thermostabilising mutations were also identified by Fox *et al.* (2017) and Mahoney SC6b (Fox *et al.* unpublished data) was found to be most thermostable mutant to produce empty capsid rather than Mahoney SC7 described in Fox *et al.* (2017). Table 1.1 shows the list of mutations introduced in the thermostable mutants. The study was running concurrently to our project as a part of consortium. Therefore, thermostable mutants became available in the middle of project and were adopted at that time, as noted in the following chapters.

Table 1.1. List of mutants for thermostable Saukett SC8 (Fox *et al.*, 2017) and Mahoney SC6b (Fox *et al.* unpublished data)

Saukett SC8	Mahoney SC6b
T4067A	R4018G
L2018I	T2025A
L2215M	D2057E
D2241E	L3119M
H3019Y	Q3178L
L3085F	H1248P
T1105M	
F1132L	

1.6.3 Capsid stabilising region

Studies of 135S (Butan *et al.*, 2014) and 80S (Levy *et al.*, 2010) suggested a capsid uncoating mechanism which involves dynamic change in the structure. Figure 1.13 shows the suggested conformation change on one protomer. When the mature PV capsid is altered to the 135S capsid, the N-terminus of VP1 associates with a hole at the 2-fold axis produced by capsid

rearrangement and a further change produces another bigger hole at the quasi-3-fold axis. The N-terminus moves to the bigger hole, promoted by capsid change and later it is externalised to bind to the tip of VP2 propeller, a feature on the capsid surface which occurs at the junction of two protomers. VP4 is also involved in the uncoating reaction by translocating from the inner surface of the capsid, where it may help mature virion stability (Hogle *et al.*, 1985), to the outer surface. The N-terminus of VP4 is known to be myristoylated which is believed to be essential for protomer association and pentamer formation (Ansardi *et al.*, 1992). The formation of an EV71 80S-like VLP without VP4 and its potency as a vaccine (Wang *et al.*, 2018) has since cast doubt of the contribution of VP4 to VLP assembly, it may simply be needed for entry.

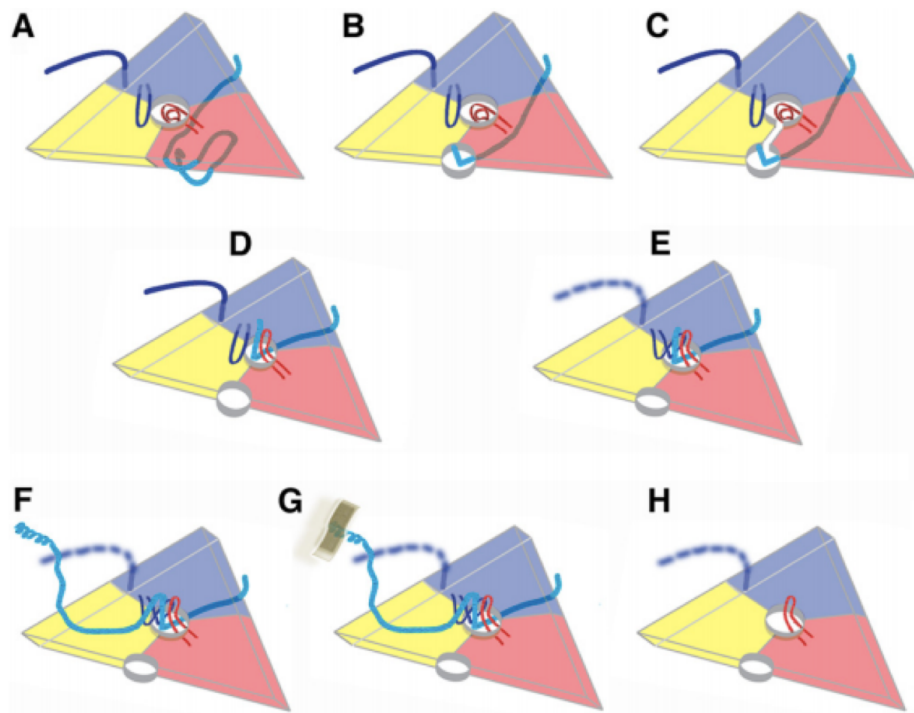


Figure 1.13. Hypothetical mechanism of capsid (protomer) rearrangement during the uncoating process. A protomer is colour coded for each viral protein, VP1 (blue), VP3 (red) and VP2 (yellow).

(A) 160S mature capsid before the uncoating. The rigid structure is provided by the C terminus and GH loop of VP1 (Navy line) binding in the VP2 propeller structure proximity. The quasi-3-fold hole is filled with coiled VP3 GH loop (red line). N terminus of VP1 (light blue line) stays beneath the inner capsid across VP1 to VP3. (B) The expanded virion during breathing of PV capsid. The N terminus of VP1 is externalised through a newly formed 2-fold hole. (C) VP1 extension moves to quasi-3-fold hole from the 2-fold hole. (D) GH loop of VP3 changes to form hairpin structure which results in opening of the quasi-3-fold hole and prepares the binding site for the externalised VP1 to bind. At this point, VP4 is already lost while RNA is still present in the capsid. (E) The C terminus and GH loop of VP1 (Navy) become disordered. (F) The N terminus of VP1 extends from the tip of the VP2 propeller structure. (G) The extended N terminus of VP1 reaches to the host membrane, the beginning of a virus-host connection. (H) After complete or partial loss of RNA, 135S turns into an 80S expanded empty capsid with the quasi-3-hole and 2-fold hole. The N terminus of VP1 returns to the inside of the capsid (Garriga *et al.*, 2012; Lin *et al.*, 2011; Wang *et al.*, 2012b). The C terminus and GH loop of VP1 remain disordered for PV. The figure is from Butan *et al.* (2014).

1.7 Recombinant VLP vaccines

Recombinant vaccines are a type of vaccine produced by combining recombinant DNA technology with foreign gene expression systems. The target viral gene is transferred into non-pathogenic viruses, bacteria, yeasts, insect cells, plant cells or mammalian cells to express the immunogenic protein(s) as reviewed in Flint *et al.* (2015c). Recombinant virus-like-particle (VLP) vaccines are one of the recombinant vaccine production approaches as the capsid

proteins of non-enveloped and some enveloped viruses assemble to a capsid structure on their own as long as they are producing in sufficient quantity. The assembled capsid structure is identical or near identical to native virus particles so conformational epitopes are maintained to induce neutralising antibodies and a protective immune response. The obvious difference in viral particles and VLPs is the content of the capsids. VLPs contain no viral genetic material so are non-infectious, and do not need inactivation (Chackerian, 2007). This is another advantage of VLPs because chemical inactivation can contribute to conformational epitope change and if this occurs vaccine efficiency is lowered. VLP vaccines for the human market are already in use for hepatitis B virus (HBV) and human papilloma virus (HPV). The HBV vaccine prevents HBV chronic infection which can otherwise lead to liver cirrhosis and hepatocellular carcinoma. The vaccine consists of the HBV surface antigen which self-assemble into a VLP like structure. The licensed vaccine expression is done in yeast cells. HPV vaccines consist of VLPs made using sequences of strains 6, 11, 16 and 18 which are the main strains causing cervical cancer in women. The major capsid protein, L1 of HPV is known to assemble on its own to form VLPs even though the natural capsid also contains a small amount of a second protein, VP2. The current licenced HPV vaccines contain VLPs produced either in yeast cells or in insect cells for a review see Mohsen *et al.* (2017).

VLP vaccine development for picornaviruses has been demonstrated for EV71 in foreign expression systems such as the baculovirus expression system (Chung *et al.*, 2006) and yeast, *Saccharomyces cerevisiae* (Li *et al.*, 2013). As EV71 and PV both belong to the enteroviruses, the technologies developed for EV71 should be transferable to PV. Indeed, PV VLP production has been attempted previously in various expression systems. Immunogenic PV empty capsids were produced by recombinant baculovirus expression following the insertion of the complete ORF and poly(A) tail sequence into the baculovirus genome (Urakawa *et al.*, 1989) although yields were very low. Later, Jore *et al.* (1994) showed PV empty capsid production in *S. cerevisiae* although these capsids were not immunogenic unless a pocket binding compound was added, in which case the immunogenicity was altered to a form that induced neutralising antibodies (Rombaut & Jore, 1997). Despite these successes, the production of PV VLP vaccines has not progressed. Possibly the baculovirus production method could have been seen as over labour-intensive at the time of the study and for PV empty capsid production

in *S. cerevisiae*, the pleconaril requirement may have been seen as a prohibitive increase in cost. With the current requirement for new PV vaccines for use after eradication, PV VLP vaccines need to be revisited, a member of the project consortium associated with the work described here produced good levels of immunogenic empty PV capsid from plants (Marsian *et al.*, 2017) using the thermostable mutants described by Fox *et al.* (2017). Recently, thermostable immunogenic PV VLPs were also produced using baculovirus expression systems (Xu *et al.*, 2019). With the excellent track records of both baculovirus and yeast expression system for current marketed VLP vaccines, those expression systems required re-investigation as methods to produce immunogenic PV empty capsids.

1.8 Baculovirus expression system

Expression systems are regarded as recombinant protein production platforms which offers high-level expression especially for complex and biologically active proteins (Stern & Wiley, 1992). The successful production of commercialised vaccines for HBV and HPV in such systems demonstrates their potential in commercial manufacturing. Baculoviruses are lethal pathogens for lepidopteran, dipteran and hymenopteran larvae. Baculoviruses are ingested daily but as they do not replicate in vertebrates they are not considered a risk (Heimpel *et al.*, 1973). Normally baculovirus expression work is carried out in biosafety level 1 containment laboratories and the safety required is minimal (O'Reilly *et al.*, 1992). The term 'baculo' refers to the rod-shape capsids which are 40-50nm in diameter and 200-400nm in length. The genomes are double-stranded, circular and covalently closed molecules of ~80-200kb (Burgess, 1977). The extendable capsid is capable of accommodating large DNA inserts which is a useful character for the recombinant protein expression platform (Fraser, 1986). Several well-characterised insect cell lines are widely available for laboratory use. *Spodoptera frugiperda* (Sf9 and Sf21) cells originating from the fall armyworm are the most widely used (Vaughn *et al.*, 1977) but *Trichoplusia ni* (*T. ni*, commercially known as High Five™) (Granados *et al.*, 1994; Wickham & Nemerow, 1993) and *Tnao38* cells (Hashimoto *et al.*, 2010) from the cabbage looper are alternate expression hosts. All insect cell lines grow well in suspension culture at 27°C and this can be beneficial for the expression of temperature sensitive functional

proteins which cannot tolerate 37°C (Reynisdóttir *et al.*, 1990). The expression system was first described for the production of human IFN- β in insect cells using a recombinant baculovirus in which the highly active polyhedrin promoter was used for the expression of the foreign gene (Smith *et al.*, 1983). Later, another late baculovirus promoter, for the p10 gene, was found to be equally powerful and both these promoters have been used for numerous recombinant protein expression examples. Expression in insect cells exhibits most of the post-translational modification characteristics of other eukaryotic cells, such as mammalian cells and this may influence the functional activity and immunogenicity of some expressed proteins (Luckow & Summers, 1988; O'Reilly *et al.*, 1992).

1.8.1 Baculovirus

Two baculoviruses are commonly used for the foreign gene expression; *Autographa californica* multi-nuclear polyhedrosis virus (AcMNPV) and *Bombyx mori* nuclear polyhedrosis virus (BmNPV). Both genomes are ~130kb and are found complexed with the nucleoprotein as a nucleocapsid. Two forms of virus exist in infected cells, budded viruses which are enveloped with a loose membrane studded with surface projections, *aka* peplomers, on one apex and occluded virus, which lack the surface structures and is found in crystalline arrays in the nucleus of infected cells. In nucleopolyhedrosis viruses (NPVs) such as AcMNPV, the polyhedral occlusion bodies are known as polyhedra and contain multiply embedded nucleocapsids (Van der Beek *et al.*, 1980). The virus budded from the plasma membrane, budded virus (BV), is responsible for cell to cell spread within the infected insect while the occlusion derived virus (ODV) is responsible for transmission between hosts, the occlusion structure providing protection from desiccation and UV damage (O'Reilly *et al.*, 1992). The peplomers which is a key difference in the BV and ODV forms of virus is the presence of the viral-encoded glycoprotein, gp64 which is only found in BV. Gp64 functions for cell entry via adsorptive endocytosis followed by membrane fusion (Volkman & Goldsmith, 1983). Natural infection in the wild is via the ODV form which is ingested by browsing larvae. When it reaches the midgut, the crystalline polyhedrin matrix is solubilised by the alkaline environment and the embedded virions are released to enter midgut cells. The BV form of virus produced is released into the larvae's open circulatory system which allows the BV to spread throughout the body and the larvae becomes a sac filled with baculovirus virions. Eventually it ruptures to release

ODV and start the cycle in a new host. Figure 1.14 shows the baculovirus replication cycle in nature from ingestion of occlusion body, through virus replication in the midgut producing 2 forms of viruses to release from the host cell to a new host.

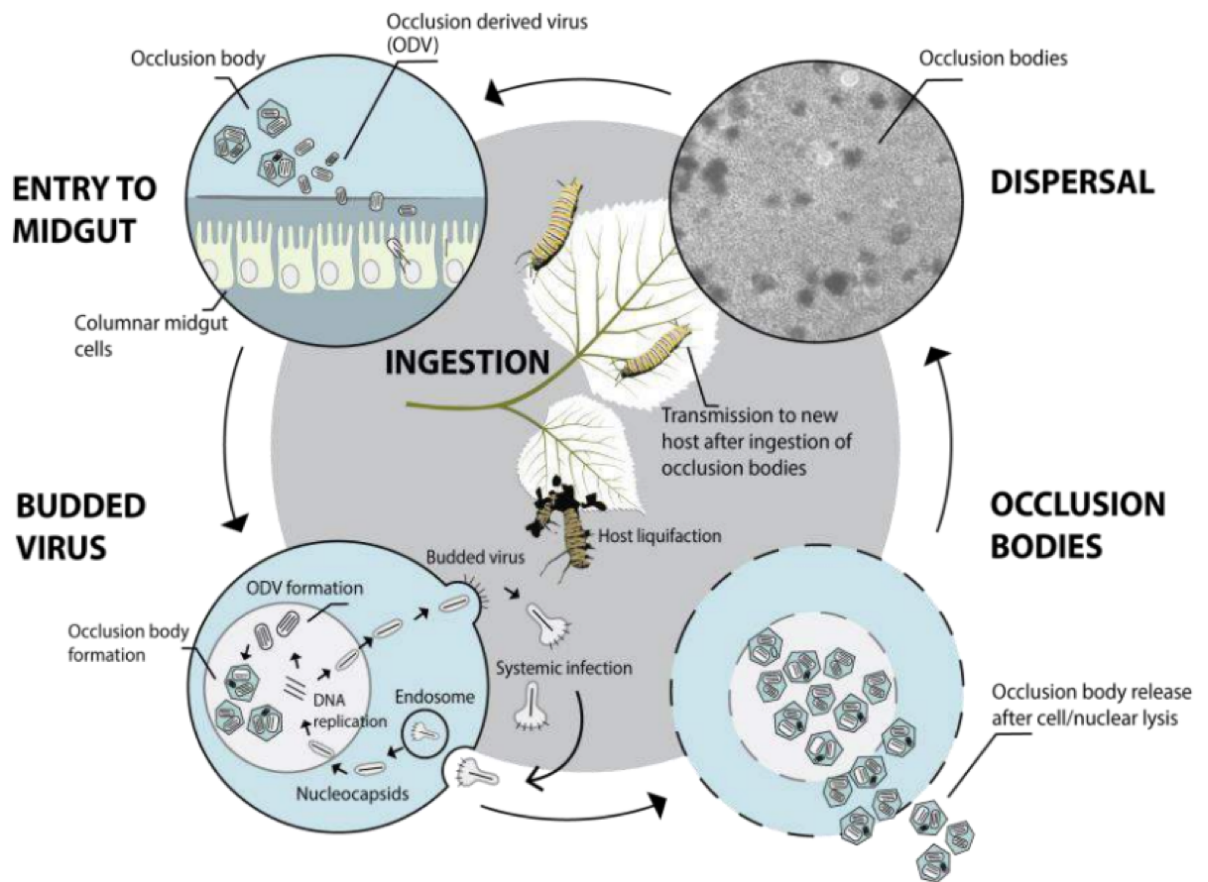


Figure 1.14. Baculovirus infection cycle in nature

Baculovirus occlusion body enters a susceptible larva by ingestion. Alkalinity in gut disturbs the occlusion body and releases occlusion derived virus, a form of baculovirus and initiates virus replicates in the midgut. DNA replication takes place in host cell nucleus and is packed into budded virus (BV), the other form of baculovirus for internal infection. Meanwhile, occlusion derived virus is packed into occlusion body which is packed with polyhedrin. Eventually the host cell dies and releases the new occlusion bodies into the environment and the cycle restarts. The figure is from OET (2019)

In insect cell culture, baculovirus replication undergoes 3 phases: early, late and very late. In cell culture entry by adsorptive endocytosis releases the nucleocapsid which travels from the cytoplasm to the nucleus where early transcription begins (Chisholm & Henner, 1988). Within 6 hours post infection (h pi), the virus enters viral DNA replication, the host cell loses its chromatin structure and is enlarged. Early proteins from the early viral promoters, expressed

by the host RNA polymerase on nuclear entry, establish the conditions for DNA replication to begin (Charlton & Volkman, 1991).

In the late phase, the viral DNA replicates, late proteins are expressed and BVs are assembled. This period lasts from 6h to 24 h pi and BV production is logarithmic at 12-20 h pi but declines thereafter (Knudson & Harrap, 1976; Lee & Miller, 1979). During this period, nucleocapsids assembled in the nucleus travel to the plasma membrane where they incorporate gp64 during the budding process. An important point to note is that an entire replication cycle can be completed without the requirement of the ODV phase, a fundamental property of the recombinant baculovirus system.

In the very late phase, occlusion-specific protein expression and morphogenesis take place and by the end of this phase, the infected cell nucleus is filled with occlusion bodies. In cell culture conditions cell lysis begins around 60 h pi and protein synthesis has effectively ceased by 72 h pi as it enters cell death or lysis. The very late phase lasts ~two days and is characterised by the synthesis of polyhedrin and p10 both of which are produced from specific very late promoters. As ODV forms of virus are not required for the tissue culture replication, these very late genes can be deleted, or replaced with genes of interest. The resulting recombinant virus is still able to establish a productive cycle in culture but now expresses the target gene product during the very late phase of expression. The use of very late promoters and the lack of the ODV form of virus are therefore key features of the recombinant baculovirus expression system.

1.8.2 Baculovirus expression vector

Although Smith *et al.* (1983) showed the high-level expression of a foreign gene product by replacing the *polh* gene in the baculovirus genome the system did not spread widely as it was not as a convenient platform as bacterial or yeast expression systems. An early difficulty was the low rate of recombinant baculovirus production which was in the order of 0.1-1% of the progeny virus. At this time, distinguishing the recombinant virus from wild type virus was based on loss of the ODV phenotype as observed by light microscopy and many rounds of plaque assay were required to isolate a pure recombinant virus. Later this was vastly simplified by the use of linearised baculovirus DNA in place of the circular form during transfection. A unique restriction site was inserted in the *polh* locus (Kitts *et al.*, 1990). Linear DNA is not infectious

unless rescued to the circular form by recombination with the transfer vector and with this implementation the rate of recombinant baculovirus formation rose to ~30%. Further modifications included the deletion of *orf1629* which is an essential gene adjacent to the *polh* locus. As before correction of this deletion was achieved by recombination with the transfer vector, which restored infectivity at the same time as incorporating the gene of interest giving up to 97-98% recombinant formation (Kitts & Possee, 1993). In parallel, a method was developed which used the baculovirus genome cloning into a bacterial artificial chromosome (bac) in *Escherichia coli* (*E. coli*). A transfer vector is still use but site specific transposition is used to incorporate the gene of interest into the bac in *E. coli* (Luckow *et al.*, 1993). This technology, commercialised as the Bac-to-Bac system is widely used as the transposition event is done entirely using plate genetics with appropriate antibiotic selection. While the various technical improvements increased the yield of recombinant baculovirus a background of wild type virus was still encountered, requiring a plaque assay to prevent outgrowth of the wild type virus during recombinant amplification (van Oers *et al.*, 2015). A later improvement combined the bacmid and linearisation approaches by mutating ORF 1629 by gene knockout so that even circular DNA was non-infectious until recombined. This modification achieved 100% recombinant baculovirus production (Zhao *et al.*, 2003). A similar strategy was applied for a commercially available bacmid DNA, *flashBAC*[™] by Oxford Expression Technologies (King *et al.*, 2007) and is the method used in the work described here. In addition, *flashBAC*[™] DNA is deleted for two non-essential gene encoding a cathepsin like protease and a chitinase which are normally used for cell lysis but have been shown to lessen overall recombinant protein yields (Hitchman *et al.*, 2011; Lu *et al.*, 2002; Possee *et al.*, 1999; Thomas *et al.*, 1998).

1.8.3 Transfection

The delivery of both *flashBAC* GOLD DNA and the purified transfer vector are achieved by liposome based transfection. Positively charged liposomes and negatively charged DNA bind each other to form a complex that enters cells (Felgner *et al.*, 1994). Once the DNA is internalised a proportion undergoes recombination in the nucleus restoring the circular baculovirus genome and allowing early gene expression to occur. A full replication cycle ensues resulting in the harvest of a recombinant virus which expresses the recombinant gene in the very late phase of the cycle.

1.8.4 Post-translational modification

One of the advantageous characteristics of the baculovirus expression system is the typically eukaryotic post-translational modifications, which include phosphorylation, glycosylation, acylation, disulphide bond formation and proteolytic processing (Miller, 1988). In the case of PV expression, the N terminus of VP4 is modified by N-myristoylation by N-myristoyl transferase (NMT) which does not occur in bacteria but has been reported as essential to assembly (Ansardi *et al.*, 1992). However, NMT functions in insect cells so VP4 is myristoylated as required for VLP assembly. To this extent post-translational modification is essential for the assembly of authentic empty capsids to elicit an effective immune response as a VLP vaccine.

Protein folding

VLPs consist of multiple proteins that require correct folding of each protein for assembly to occur (Liu *et al.*, 2013). The insect cell cytoplasm is equipped with chaperons and foldases such as Hsp70 to fold and assemble polypeptides without forming aggregates (Ailor & Betenbaugh, 1999; Sokolenko *et al.*, 2012). The efficiency of foreign protein folding in insect cells compared to mammalian cells is not fully known and may differ for different proteins depending on their complexity.

Glycosylation

The one post translational modification that does differ between insect and mammalian cell is glycosylation (Chen *et al.*, 2010). The baculovirus expression system produces glycoproteins and is widely used for this purpose for recombinant proteins as efficiency can exceed the production possible in mammalian cells. However, while glycosylation starts similarly for both insect and mammalian cells, the subsequent processing in insect cells is much more limited. Insect cells cannot produce complex mammalian style N-glycans, instead producing high mannose glycans unless used with engineered insect cell lines aimed at mimicking mammalian processing (Altmann *et al.*, 1999; Jarvis, 2003). In the case of PV VLPs however glycosylation differences should not be a concern as none of the capsid proteins are glycosylated.

1.8.5 Purification of VLPs

For pharmaceutical and scientific use, baculovirus-insect cell origin proteins are required to be free from baculovirus particles due to their adjuvant activity as agonists of Toll-like receptor 9 (TLR9) (Abe *et al.*, 2005). If it is not removed physically or biochemically, the immunogenic

response to the VLP may be jeopardised or there may be an unacceptable inflammatory reaction at the site of immunisation (Vicente *et al.*, 2011). When synthesised recombinant proteins and baculovirus particles have similar properties, the separation process may be complicated and this is the case for the purification of VLPs. Traditional velocity or density gradient ultracentrifugation is capable of separating VLPs from baculovirus particles or nucleocapsids but it is labour intensive, time consuming and scale limiting and its productivity for the final product is questionable as it still contains impurities (Huhti *et al.*, 2010; Liu *et al.*, 2013). As a result simpler stepwise operations were also widely used, for example, low speed centrifugation, precipitation and ultrafiltration or diafiltration have been employed (Maranga *et al.*, 2002). Chromatography may be also added after filtration or precipitation, with size exclusion chromatography acting to polish the final product after filtration (Peixoto *et al.*, 2007). For example, norovirus VLPs were purified by polyethylene glycol precipitation followed by anion exchange chromatography (Koho *et al.*, 2012; Lin *et al.*, 2015). Although chemical inactivation of baculovirus infectivity is possible, for example by formaldehyde, VLP antigenicity may be affected by the treatment (Liu *et al.*, 2013; Vicente *et al.*, 2011). A novel development, rather than relying on biophysical and biochemical methods, has been the introduction of an engineered baculovirus to ease the purification. Deletion of the *vp80* gene in baculovirus genome produces recombinant baculovirus which cannot form either BVs or ODVs, without affecting the level of foreign gene expression (Marek *et al.*, 2011). The recombinant is grown in a helper cell line which provides this function *in trans* but non helper cells are used for the protein expression phase. This application simplifies the purification method particularly for secreted proteins which are harvested from the supernatant of infected cells, which would include VLPs produced in insect cells (Lin *et al.*, 2015) although this particular method has not been reported for the production of VLPs.

1.8.6 Baculovirus expression system application for this project

The expression system was used throughout this project as the default eukaryotic platform for PV gene expression with 1) high yield and 2) post-translational modification. These two characteristics suit an examination of the system for PV VLP based vaccine production. VLP conformation is critical to obtain an immunogenicity that is as good as or better than OPV or IPV. The high expression rate is driven by the strong very late baculovirus promoters which

has the potential to make baculovirus-insect cells derived VLPs a cost effective product. Nevertheless, another expression system was tested as part of this project.

1.9 Yeast expression system

The yeast system similarly offers the higher eukaryotic cell characteristics but combines this with the advantages of mass microbial cultivation. Although prokaryotic expression systems such as *E. coli* have been successful for many simple products, recombinant protein localisation in inclusion bodies is a frequently encountered problem and for complicated proteins such as VLPs bacteria have proved problematic (Porro *et al.*, 2005; Sorensen, 2010). Where it has been investigated, picornavirus assembly to the fully assembled capsid has failed (Goodwin *et al.*, 2009) although recently the apparent assembly of FMDV in *E. coli* was reported (Puckette *et al.*, 2017). Yeast cells however, retain the simplicity of bacterial culture: high growth rate and low cost while offering eukaryotic post-translational modification (Porro *et al.*, 2011). The availability of yeast molecular and genetic resources is another advantage that can be applied for a VLP vaccine production platform (Goffeau *et al.*, 1996). Using these benefits, vaccines for HBV and HPV have been approved for human use (Bill, 2015) and by their adoption, yeast cell expressed products have shown their safety and immunogenicity. Currently, baker's yeast, *Saccharomyces cerevisiae* (*S. cerevisiae*) is the most commonly used strain for expression systems and is used in the production of licensed vaccines. Other yeasts such as *Pichia pastoris* (*P. pastoris*) are also used widely in research laboratories. Their potential cannot be neglected as they offer different expression rates and expression conditions and may contribute to solving some expression difficulties such as hyperglycosylation and protein retention in the periplasm which results in partially degraded proteins along with proper conformational proteins (Romanos *et al.*, 1992). The variety of host cell characteristics is one of the reasons to choose yeast as an expression system and yeast host cell choice is still increasing for specific expression requirements of individual recombinant proteins.

For recombinant protein production, the desired heterologous gene is transformed into the yeast cells where it may integrate into the yeast genome or exist as a freely replicating episome.

In order to obtain a high yield of the heterologous protein, a highly transcribed promoter is essential and the choice of promoter may require the use of a specific host cell, as is the case for expressing using the methanol inducible promoter AOX in *P. pastoris* (Macauley-Patrick *et al.*, 2005). After the recombinant protein is produced, the purification method will differ depending on protein location and will need to be determined for each heterologous protein, as it is for any other expression system.

1.9.1 Transformation of heterologous genes

Following cloning a heterologous gene sequence into a yeast expression plasmid (see below) the gene is introduced into yeast by transformation in one in main 3 methods, spheroplast preparation, lithium acetate (LiAc) method or electroporation (Porro *et al.*, 2005). Spheroplast preparation is achieved by disturbing the yeast cell wall using 2-mecaptoethanol and delivering the heterologous gene containing plasmid DNA with carrier DNA. The LiAc method is similar to spheroplasts preparation but includes 5 elements: LiAc, polyethylene glycol (PEG), heat shock at 42°C, single-stranded carrier DNA, and use of intact mid-log phase cells, all of which contribute to a higher transformation efficiency. Electroporation has also been investigated for yeast cell transformation and its initial low transformation rate was improved by supporting the electrically compromised cell in a buffer with 1M sorbitol (Kawai *et al.*, 2010). The improvements in each transformation method have resulted in all being used with some preferred for individual host cells or the size of transforming material e.g. yeast artificial chromosomes. However, for simplicity and easy preparation the LiAc method is an obvious choice for yeast cell transformation and was the method used here.

1.9.2 Yeast cell selection markers

To select transformed yeast cells auxotrophic markers are commonly used although later vectors make use of novel antibiotic selection, e.g. zeocin. As a result of the large repertoire of yeast mutants engineered yeast cells with critical enzyme deficiencies can survive by taking up a heterologous vector carrying a compensatory gene along with the desired heterologous DNA sequence. In theory, only the successful transformant survives in selective media which is lacking the specific biosynthesis product. For example, *URA3* gene which encodes orotidine-5'-phosphate decarboxylase is involved in pyrimidine biosynthesis while *HIS3* (L-histidine

synthesis), *LEU2* (L-leucine), *TRP1* (L-tryptophan) and *MET15* (L-methionine) are all employed as auxotrophic markers (Pronk, 2002). To overcome the cross-feeding possible when plating high density culture, engineered cells may include other auxotrophic markers to ensure a clean selection (Porro *et al.*, 2005). For example, for the *URA3* marker gene the essential biosynthetic intermediate uridine 5'-monophosphate of *S. cerevisiae* can be produced by 2 pathways, via the *URA3* gene product or by pyrimidine conversion to uracil by uracil phosphoribosyl-transferase (*FUR1*). Yeast cells with both mutations (Δ *URA3* and Δ *FUR1*) enable a plasmid-origin *URA3* gene as a selection marker even in uracil-containing culture as the double mutants are lethal (Pronk, 2002).

1.9.3 Transformation vectors for yeast cells

Cloning of the desired DNA is normally carried out in *E. coli* using a shuttle plasmid capable of replication in both yeast and bacteria for ease of gene manipulation. Transformation vectors are available as integrative vectors and extrachromosomal vectors based on autonomous plasmids and episomal plasmids (Singh & Heinemann, 1997). The integrative plasmids rely on recombination into the yeast chromosomal DNA for foreign gene expression and to enable this the plasmid has to contain DNA homologous to a specific yeast locus, although random recombination may also occur (Porro *et al.*, 2005). The method is known for low foreign gene transfer frequency but, if the correct integration takes place it is very stable when cultured in selective medium. Extrachromosomal vectors replicate in yeast cells as they contain a yeast origin of replication, an autonomous replication sequence (ARS) such as the naturally occurring 2 μ circle. This facilitates high heterologous gene carriage but with lower stability although this is improved by introduction of centromeric sequence at the expense of a lower copy number. Episomal plasmids offers the most suitable characteristics overall for yeast expression vectors but are not available for all possible host yeasts. At present, there is no universal transformation vector which offers stability of foreign gene and high copy number limiting to some degree the host cells that are chosen.

1.9.4 Promoters

Transcription efficiency for any heterologous gene relies on the promoter in use and a wide variety of promoters are available, including homologous or heterologous, inducible or

constitutive (Porro *et al.*, 2005). Yeast promoters typically consist of 3 domains, an upstream activation sequence, TATA elements and initiator elements and are often over 500bp in length. Glycolytic enzyme promoters including alcoholic dehydrogenase I (*ADH1*), phosphoglycerate kinase and glyceraldehyde-3-phosphate dehydrogenase (*GAP* or *GAPDH*) are powerful promoters that are widely used. Highly inducible promoters such as *GAL1* are also used with addition of galactose for induction and glucose for suppression. Inorganic phosphates, temperature and metal ions have also been used for inducing promoters (Berlec & Strukelj, 2013). Inducibility is useful when a foreign protein is toxic but for higher expression efficiency, constitutive promoters are preferred and the *GAP* promoter is used in the work described here (Porro *et al.*, 2005).

1.9.5 Heterologous protein purification

The location of any recombinant protein in yeast cells alters the downstream process of extraction; cytoplasmic proteins offer very high expression level but difficult extraction whereas secreted proteins are much easier to purify. As yeast cell walls are robust structure, high pressure homogenization is necessary to access the cytosolic contents and during this process, some loss of the expressed protein is inevitable. In the case of VLPs the lysis procedure also has to be compatible with maintenance of the capsid structure. It is notable that for the HBV vaccine the surface antigen is extracted from yeast cells in a denaturing protocol and renatured post-purification (Yamazaki, 1988). Such a strategy would not be compliant with a multi-protein VLP such as a picornavirus capsid. Although secretion would be useful there are few universal rules for secretion from yeast make this currently unworkable for capsids expression.

The encouraging data on the use of yeast as an expression host for PV VLPs is the previous experience with PV in *S. cerevisiae*, albeit at low levels (Jore *et al.*, 1994; Rombaut & Jore, 1997) and the more recent data on the production of enterovirus 71 VLPs in both *S. cerevisiae* and *P. pastoris* (Li *et al.*, 2013; Zhang *et al.*, 2015). In these reports, P1 and its protease 3CD were employed to produce the individual viral proteins VP1, VP3 and VP0. While co-transformation of P1 and 3CD plasmids produced VLPs (Zhao *et al.*, 2013) the yield was low when compared to P1 and 3CD combined on a single expression plasmid (Zhang *et al.*, 2015; Zhou *et al.*, 2016). It is clear that the expression strategy made a difference in VLP yield and

these findings, control over the balance of viral proteins expressed, suggest that a similar strategy for PV could be beneficial (Kim & Kim, 2017).

1.10 Aims of the project

The aims of this project are to investigate the assembly, characterisation and development of recombinant PV capsids using the baculovirus and yeast expression systems. While PV is a candidate for the third virus ever to be eradicated from the world, the feasibility of achieving this remains in debate. There are two types of vaccine currently available; OPV and IPV. OPV, whilst proving the greatest immune response, could give rise to revertants that could serve as a source of the wild virus in the population even after incidents of disease have ended. IPV does not generate revertants but large scale growth of the live virus under level 3 containment is required. Therefore, new concepts for PV vaccines are required for the post-polio world. The project will use technology developed at the University of Reading to assemble empty picornavirus capsids in insect cells and to apply this also to yeast. Such capsids trigger an immune response without being infectious and represent a novel candidate polio vaccine. Further engineering, which would not be feasible with infectious virus, such as improved stability, is also possible.

The project will utilise the following approaches for assembly, characterisation and development of recombinant PV capsids:

1) PV VLP production in baculovirus and yeast expression systems

Picornavirus 3C^{pro} cytopathic effects, which jeopardises natural host cell function, have suggested the need for an adjustment in 3C activity to serve as an appropriate P1-2A processing protease in the baculovirus expression system. Dual control of 3C^{pro} resulted in FMDV VLP expression in which suitable P1-2A and 3C^{pro} molar ratios were met by the inclusion of a human immunodeficiency virus (HIV) frameshift and mutating 3C^{pro} itself (Porta *et al.*, 2013). Similarly, for the successful expression of EV71 VLPs the EV71 3C^{pro} included a mutation at the conserved residue involved in substrate recognition, S128A, which lowered the enzymatic activity significantly (Cui *et al.*, 2011). As a result, in this work a genetic construct

optimised for FMDV expression was adapted for PV VLP production by replacing the P1 region with PV P1 and the 3C^{pro} region with EV71 3C^{pro} containing the S128A mutation. The use of the EV71 3C^{pro} for processing PV structural proteins has not been previously reported. Improvements in VLP purification methods will be also discussed as part of the optimisation of production.

2) Improvement of PV capsid stability

IPV has shown instability at elevated temperatures and in some chemical conditions (Plotkin, 1991; 1997). The poliovirus uncoating mechanism was visualised to show externalisation of the N termini of VP1 and VP4 (Bostina *et al.*, 2011; Butan *et al.*, 2014; Lin *et al.*, 2011). This finding indicates that molecular engineering at these sites could be used to prevent premature opening and achieve a more stable capsid. Such mutations may be lethal for the virus as it would be unable to uncoat but this is not applicable when empty capsids are used.

3) Capsid conformation status alteration

PV VLPs originating from *S. cerevisiae* are found not to be conformation inducing protective immunity (H-form). Addition of VP1 pocket binding drug in the culture and purification procedure changed the VLPs into immunogenic conformation (N-form) (Rombaut & Jore, 1997). To follow this up the same P1-3C^{pro} cassettes developed for insect cell expression will be assessed for yeast PV VLP expression. Alteration of the conformational status will be attempted with the addition of pleconaril and another capsid binding drug, GPV13 (De Colibus *et al.*, 2014) and an assessment of the H/N-form of VLPs made.

Chapter 2 Materials and General Methods

In this section, routinely used general methods for this project are explained. When stated commercially available kits were used following the manufacturers' protocols.

2.1 Materials

2.1.1 Chemical reagents, enzymes and columns

Chemical reagents, enzymes and columns used in this project is listed in the table below

Table 2.1. List of materials with the manufacturer

Manufacturers/distributers	Chemicals
ThermoFisher scientific, US	Ethanol, Methanol, glucose, sucrose, sodium chloride (NaCl), sodium acetate, Ethylenediaminetetraacetic acid (EDTA), Tris, Tween™ 20, bacteriological agar, potassium chloride (KCl), sodium phosphate dibasic (Na ₂ HPO ₄), potassium phosphate monobasic (KH ₂ PO ₄), 5M hydrochloric acid (HCl), 10 M sodium hydroxide (NaOH), FastDigest restriction enzymes, T4 DNA ligase, Zeba 7K MWCO spin column, Immobilon-P transfer membrane, protein-free T20 (TBS) blocking buffer (Thermo Scientific), clear flat-bottom nonsterile 96-well plate, Bolt™ 4-12 % Bia-Tris Plus gels, Novex™ sharp pre-stained protein standard and TMB Stable
Invitrogen, US (through ThermoFisher scientific, US)	Lipofectin Transfection Reagent, Bolt™ Bis-Tris Plus Gels, 10-well, Bolt™ LDS sample buffer, SilverQuest™ Silver staining kit
Merck Millipore, US (through ThermoFisher scientific, US)	Amicon Ultra 100K MWCO 0.5, 4 and 15 mL

Sigma-Aldrich, US (Merck Millipore, US)	Lithium acetate, salmon sperm DNA, polyethylene glycol, Nonidet™ P-40, Benzonase®, cOComplete ULTRA EDTA-free tablets, DL-Dithiothreitol (DTT), D-sorbitol, HEPES sodium salt, glycerol, bromophenol blue, 2-Mercaptoethanol, guanidine chloride, bovine serum albumin (BSA), sulfuric acid (H ₂ SO ₄), yeast nitrogen base without amino acid, yeast synthetic drop-out medium supplement without uracil, ampicillin sodium salt, pleconaril, PEG-8000 (P2139), Rupintrivir, poliomyelitis vaccine (inactivated) BRP, lithium acetate (LiAc), Salmon sperm DNA, Polyethylene glycol, bovine serum albumin (BSA), Nycodenz, Phenylmethylsulfonyl fluoride (PMSF), Coomassie Brilliant Blue R250, sodium carbonate (Na ₂ CO ₃), sodium bicarbonate (NaHCO ₃), dimethyl sulfoxide (DMSO), foetal calf serum (FCS)
New England Biolabs, US	Phusion® High-Fidelity PCR Master Mix with HF Buffer
Local supermarket	Dried milk
BD bioscience, US	Fixation/Permeabilization solution kit
Geneflow, UK	ChemiFast Western blot detection agent
National Diagnostic, US (through Geneflow, UK)	20 % sodium dodecyl sulphate solution (SDS), 50X Tris-acetate-EDTA (TAE), 10X Tris-Glycine SDS PAGE buffer, Tris-buffered saline buffer (TBS) and 10X Tris-glycine Electroblothing buffer
AGCT, UK (through Geneflow, UK)	Agarose
AMS Biotechnology, UK	Zymolyase 100T
GE Healthcare Life science, US	Whatman™ 3MM Chromatography Paper
MP Biomedicals, US	Lysing matrix C tube

Oxford Technologies, UK	Expression	<i>flashBAC</i> GOLD
Beckman Coulter, US		Ultra-Clear Thinwall tube for SW40 (13.2ml) and Ultra-Clear Thinwall tube for SW32 Ti (38.5ml)
MatTek, US		poly-D-lysine glass-bottom 35 mm sterile dish
Agar scientific, UK		Uranyl acetate, Formvar/Carbon 300 Mesh Copper grid
Bio-Rad Laboratories, US		Mini-PROTEAN® TGX™ Gel, 10 well, 30 µl
National institute for biological standards and control (NIBSC)		PV standard for IPV

2.1.2 Specialised equipment

Table 2.2. List of equipment and manufacturer

Manufacturers/distributors	Equipment
Lifetechnologies, US	Countess® Automated Cell Counter
Bio-Rad laboratories, US	BioLogic LP
Stanstead Fluid Power Ltd, UK	Lab Homogenizer Cell Disruptor
MP Biomedicals, US	FastPrep®-24 Classic Instrument
Parr Instrument Company, US	N ₂ cavitation vessel (40 ml capacity)
ThermoFisher Scientific, US	EVOS FL Cell Imaging System
Eppendorf, Germany	Bench top centrifuge (5418)
Bechman coulter, US	Optima™ L-90K Ultracentrifuge
Eppendorf, Germany	Biophotometer
BioComp Instruments	Gradient Master Base Unit
ATTO, Japan	HorizBLOT
Syngene, UK	G: Box imager
Tecan, Switzerland	Infinite 200 Microplate Fluorescence Reader
Leica, Germany	gSTED microscope
Joel, Japan	2100Plus TEM

2.1.3 Vectors

In this project, a cassette system was used for expression in insect and yeast cells. The cassette consists of P1, the first 10 amino acids of PV 2A, a HIV-1 frameshift sequence and an EV71 origin 3C protease sequence which carries a S128A mutation (3C_{EV71}). The vector is based on pOPINE (Berrow *et al.*, 2007), itself a modification of pTriEx1.1 (EMD Chemicals Inc, 2011).

Table 2.3. List of expression vectors

Vector	Description	Source
pOPINE EV71 P1-2A_FS_3C _{EV71}	pOPINE vector contains EV71 cassette	Cone (2015)
pOPINE Mahoney P1_2A_FS_3C _{EV71}	pOPINE vector contains PV Mahoney cassette	This work
pOPINE MEF-1 P1_2A_FS_3C _{EV71}	pOPINE vector contains PV MEF-1 cassette	This work
pOPINE Saukett SC8 P1_2A_FS_3C _{EV71}	pOPINE vector contains PV Saukett with SC8 mutation cassette	This work
pTriEx1.1 Mahoney P1	pTriEx1.1 vector contains PV Mahoney P1 sequence	This work
pTriEx1.1 GFP	pTriEx1.1 vector contains GFP sequence	Host lab
pET15b-3CD μ 10	3CD Δ sequence source. Serine insertion at the junction of PV wild type 3C and 3D prevents 3CD cleavage	NIBSC
pOPINE Mahoney P1_2A_3CDWT	pOPINE vector contains Mahoney P1, first 10 aa of 2A and PV wild type 3CD sequence	This work

pOPINE Mahoney P1_2A_3CDΔ	pOPINE vector contains Mahoney P1, first 10 aa of 2A and 3CD with S insertion at 3C/3D	This work
pOPINE Mahoney P1_2A_FS_3CDWTFS	pOPINE Mahoney P1_2A_3CDWT with FS sequence between 2A and 3CD	This work
pOPINE Mahoney P1_2A_FS_3CDΔFS	pOPINE Mahoney P1_2A_3CDΔ with FS sequence between 2A and 3CD	This work
pKT10	pKT10, a yeast 2μ expression vector which uses uracil as the nutritional marker	Dr Yuko Morikawa, Japan
pKT10 Mahoney P1_2A_FS_3C _{EV71}	pKT10 inserted with PV Mahoney cassette	This work
pKT10 Saukett SC8 P1_2A_FS_3C _{EV71}	pKT10 inserted with PV Saukett SC8 cassette	This work
pOPINE Mahoney P1_2A_FS_3C _{EV71} - M132L, M132W, M132W-H207W, M132W-F237W, H207W-F237W, M132W-H207W-F237W (Triple), Y159W, Y159W-Y205W, Y205W, H207W, F237W	pOPINE vector contains PV Mahoney cassette with VP1 mutation at the specific locations	This work
pKT10 Mahoney P1_2A_FS_3C _{EV71} - M132L, M132W, Y159W, Y205W and M132W-Y207W-F237W (Triple)	pKT10 vector contains PV Mahoney cassette with VP1 mutation at the specific locations	This work
pOPINE Mahoney SC6b P1_2A_FS_3C _{EV71}	pOPINE vector contains PV Mahoney with SC6b mutation cassette	This work

pOPINE Mahoney SC6b P1 Ex10, Ex15 and Ex20, _2A_FS_3C _{EV71}	pOPINE vector contains PV Mahoney SC6b mutation cassette with various degree of HIV matrix protein p17 inserted at VP4 N-terminus	This work
pOPINE Mahoney SC6b P1 VP1_1, VP1_2 and VP1_3, _2A_FS_3C _{EV71}	pOPINE vector contains PV Mahoney SC6b mutation cassette with GS linker inserted at VP1 N-terminus	This work

2.1.4 Recombinant baculovirus strains

Table 2.4. List of recombinant baculovirus strains

Virus	Vector used	Description
Bac-PV1P1-3C	pOPINE Mahoney P1_2A_FS_3C _{EV71}	Recombinant baculovirus produced to express PV Mahoney (PV1) viral proteins
Bac-PV2P1-3C	pOPINE MEF-1 P1_2A_FS_3C _{EV71}	Recombinant baculovirus produced to express PV MEF-1 (PV2) viral proteins
Bac-PV3P1-3C	pOPINE Saukett SC8 P1_2A_FS_3C _{EV71}	Recombinant baculovirus produced to express thermostable PV Saukett (PV3) SC8 viral proteins
Bac-PV1P1	pTriEx1.1 Mahoney P1	Recombinant baculovirus produced to express PV Mahoney (PV1) P1
Bac-GFP	pTriEx1.1 GFP	Recombinant baculovirus produced to express GFP

Bac-PV1P1-3CDWT	pOPINE Mahoney P1_2A_3CDWT	Recombinant baculovirus produced to express Mahoney VPs by PV wild type 3CD cleavage
Bac-PV1P1-3CD Δ	pOPINE Mahoney P1_2A_3CD Δ	Recombinant baculovirus produced to express Mahoney VPs by PV mutated 3CD cleavage
Bac-PV1P1-3CDWTFS	pOPINE Mahoney P1_2A_FS_3CDWTFS	Recombinant baculovirus produced to express Mahoney VPs by FS down regulated PV wild type 3CD
Bac-PV1P1-3CD Δ FS	pOPINE Mahoney P1_2A_FS_3CD Δ FS	Recombinant baculovirus produce to express Mahoney VPs by FS down regulated PV mutated 3CD
Bac- M132L, M132W, M132W-H207W, M132W-F237W, H207W-F237W, M132W-H207W-F237W (Triple), Y159W, Y159W-Y205W, Y205W, H207W, F237W	pOPINE Mahoney P1_2A_FS_3C _{EV71}	Recombinant baculovirus produced to express PV Mahoney (PV1) viral proteins with the VP1 mutations shown
Bac-PV1SC6bP1-3C	pOPINE Mahoney SC6b P1_2A_FS_3C _{EV71}	Recombinant baculovirus produced to express thermostable PV Mahoney (PV1) SC6b viral proteins

Bac-PV1SC6bP1Ex10, Ex15 and Ex20	pOPINE Mahoney SC6b P1 Ex10, Ex15 and Ex20, _2A_FS_3C _{EV71}	Recombinant baculovirus produced to express PV Mahoney (PV1) SC6b viral proteins with VP4 N-terminus mutants
Bac-PV1SC6bP1VP1_1, VP1_2 and VP1_3	pOPINE Mahoney SC6b P1 VP1_1, VP1_2 and VP1_3, _2A_FS_3C _{EV71}	Recombinant baculovirus produced to express PV Mahoney (PV1) SC6b viral proteins with VP1 N-terminus mutants

2.1.5 Recombinant yeasts

Table 2.5. List of recombinant yeasts

Yeast	Vector used	Description
RAY3A-D-PV1-3C	pKT10 Mahoney P1_2A_FS_3C _{EV71}	Recombinant RAY3A-D engineered to express PV Mahoney (PV1) viral proteins
RAY3A-D-PV3SC8-3C	pKT10 Saukett SC8 P1_2A_FS_3C _{EV71}	Recombinant RAY3A-D engineered to express PV Saukette SC8 (PV3) viral proteins
RAY3A-D-PV1-3C - M132L, M132W, Y159W, Y205W and M132W-Y207W-F237W (Triple)	pKT10 Mahoney P1_2A_FS_3C _{EV71} - M132L, M132W, Y159W, Y205W and M132W-Y207W-F237W (Triple)	Recombinant RAY3A-D engineered to express PV Mahoney (PV1) viral proteins with desired VP1 mutations

2.1.6 Cell lines

Table 2.6. List of Cell lines

Cell line	Description	Source
Sf9	A clonal derivative of Sf21 (IPLB-SF21-AE) cell line derived from pupal ovarian tissues of the fall armyworm, <i>Spodoptera frugiperda</i> . They are susceptible to baculovirus infection. Sf9 cells are more uniform in sizes than Sf21 cells which helps the identification of plaques. Doubling time: 24 hours	ThermoFisher, US
High Five™	BTI-Tn-5B1-4 cell line originated from the ovarian cells of cabbage looper, <i>Trichoplusia ni</i> . The recombinant protein yield is higher than Sf9 cells. The cell line contains TNCLV, an alphanodavirus. Doubling time: 18 hours	ThermoFisher, US
Tnao38	BTI-Tnao38 cell line originated from a clonal isolate of the High Five™ (BTI-Tn-5B1-4) cell line. The recombinant protein yield is at the same level as High Five™ cells. TNCLV is absent. Doubling time: 20 hours (Hashimoto <i>et al.</i> , 2012)	Blissard lab, US
Stellar cells	Chemically competent <i>E. coli</i> HST08 strain for high efficiency transformation	Clontech, US
RAY3A-D	<i>S. cerevisiae</i> laboratory adapted auxotrophic mutant strain (<i>MATa/α ura3/ura3 his3/his3 leu2/leu2 trp1/trp1</i>) (Ruggieri <i>et al.</i> , 1989)	Dr Yuko Morikawa, Japan

2.1.7 Antibodies

Table 2.7. List of antibodies

Antibody	Use	Manufacturer
Anti-poliovirus Blend Ab, MAB8566	Detection of PV VP1 for all serotypes	Millipore, Germany
Rabbit anti-VP0 sera, Day 39	Detection of PV VP2 for all serotypes	Reading
Rabbit anti-VP3 sera	Detection of PV VP1 for all serotypes	Host lab collaborator
Rabbit anti-PVP1 sera	Detection of PV P1 for all serotypes	Host lab collaborator
Mouse anti-baculovirus p39 sera	Detection of baculovirus major baculovirus structural protein	Host lab collaborator
Polyclonal Goat Anti-mouse Immunoglobulins/HRP, P0447	Anti-mouse antibody conjugated with HRP	Dako, Denmark
Polyclonal Goat Anti-rabbit Immunoglobulins/HRP, P0448	Anti-rabbit antibody conjugated with HRP	Dako, Denmark
Oregon green 488	Fluorophore conjugated anti-mouse Ab	ThermoFisher Scientific, US
STAR440SXP	Fluorophore conjugated anti-rabbit Ab	Abberior GmbH, Germany
SH16 for PV1	PV1 capture Ab for N/H ELISA	NIBSC, UK
R Skt live	PV3 capture Ab for N/H ELISA	NIBSC, UK

234	PV1 N specific Ab for N/H ELISA	NIBSC, UK
520	PV3 N specific Ab for N/H ELISA	NIBSC, UK
1588	PV1 H specific Ab for N/H ELISA	NIBSC, UK
517.3	PV3 H specific Ab for N/H ELISA	NIBSC, UK

2.1.8 Buffers, solutions and media

Table 2.8. List of buffers, solutions and media

Buffer / solution	Description	Manufacturer
PBS	137 mM NaCl 2.7 mM KCl 10 mM Na_2HPO_4 1.8 mM KH_2PO_4	Central school service (CSS) in the University
TBS	50 mM Tris base 150 mM NaCl adjust to pH 7.5 with HCl	CSS or purchased from National Diagnostics
Lonza InsectXPRESS with L-Glutamine	Commercial media supports the growth of insect cell lines such as <i>Sf9</i>	Lonza, Switzerland
Softening medium	100 mM HEPES-KOH, pH9.4 10 mM dithiothreitol (DTT) 25 mM EDTA	Host lab modifying from Odorizzi (2003)
Spheroplasting medium	2 % glucose 50 mM HEPES-KOH, pH 7.2 1 M Sorbitol 1 mM EDTA	Host lab, modifying from Odorizzi (2003)

Break buffer	PBS pH 7.2 1 % NP40 1.7 mM EDTA cComplete ULTRA EDTA-free tablet	Host lab, based on Kim <i>et al.</i> (2010)
Homogenization buffer	250 mM sucrose 10 mM Hepes pH7.2 1 mM EDTA 1 mM DTT cComplete ULTRA EDTA-free tablet	Host lab, modifying from Wang <i>et al.</i> (2014)
YPD media	20 g Bacto peptone 10 g Yeast extract in diH ₂ O to 950 mL for autoclave 20 % sterile glucose was added to be 2 % final concentration after autoclave	CSS
YPD media agar	YPD media High grade agar	CSS
TE buffer	10 mM Tris base 1 mM EDTA adjusted to pH 8.0 with HCl	Reading
LiAc mix	100 mM LiAc in TE buffer	Host lab referred from Herskowitz (2012)
PEG mix	40 % PEG in 100 mM LiAc mix	Host lab referred from Herskowitz (2012)
Synthetic dropout (SD) media for pKT10	Yeast nitrogen base without amino acids Yeast synthetic dropout medium supplement	CSS

	50 % sterile glucose	
SD media agar for pKT10	Yeast nitrogen base without amino acids Yeast synthetic dropout medium supplement High grade agar (without uracil) 50 % sterile glucose	CSS
Buffer 1	1X PBS 1 mM CaCl ₂ 0.5 mM MgCl ₂	Host lab
Blocking/wash buffer for gSTED sample preparation	1X PBS 2 % BSA	Host lab
2XSDS loading buffer	125 mM Tris-HCl pH 6.8 25 mM EDTA 4 % SDS 20 % Glycerol 0.4 % Bromophenol Blue 286 mM 2-Mercaptoethanol	Host lab
10X Tris-Glycine SDS PAGE Buffer	0.25 M Tris base 1.92 M Glycine 1 % (w/v) SDS	National Diagnostics, US
20X Bolt™ MES SDS running buffer	Exact content is not known. Expected to contain; MES, 2-(N-morpholino)ethanesulfonic acid) Tris base SDS	Invitrogen, US

Coomassie stain	250 mg Coomassie Brilliant Blue R250 10 % Glacial acetic acid 10 % Methanol 80 % diH ₂ O	Host lab
10X Tris-Glycine Electroblotting Buffer	0.25 M Tris base 1.92 M Glycine pH 8.4	National Diagnostics, US
TBST	1X TBS 0.2 % (v/v) Tween™ 20	Host lab
WB blocking buffer	5 % (w/v) dried skimmed milk TBST	Host lab
Renaturing buffer	20 mM Tris-HCl 1 mM EDTA 0.5 mol/L NaCl 0.05 % Tween™ 20 1 M Guanidine hydrochloride 5 % dried skimmed milk	Host lab referred from Jia <i>et al.</i> (2013)
Carbonate coating buffer	15 mM sodium carbonate 35 mM sodium bicarbonate	Host lab
PBST	1X PBS 0.1 % Tween™ 20	Host lab
blocking solution for western blot	PBST 1 % BSA	Host lab
assay diluent	1X PBS 1 % BSA	Host lab

2.1.9 Commercial Kits

Table 2.9. List of commercial Kits

Kit	Manufacturer
Gel extraction and MinElute kits	QIAGEN, Germany
In-Fusion cloning kit	Clontech, US
QIAprep Spin Miniprep kit	QIAGEN, Germany
QIAquick PCR Purification kit	QIAGEN, Germany
Yeast Plasmid Isolation kit	Clontech, US
GeneJET Gel Extraction and DNA Cleanup Micro Kit	ThermoFisher Scientific, US
GeneJET Plasmid Miniprep Kit	ThermoFisher Scientific, US
SilverQuest™ Silver staining kit	Invitrogen, US

2.2 Cloning

2.2.1 Construction of expression vector for insect cell expression system

This section explains the construction of the PV1 (Mahoney) expression vector for insect cell.

All subsequent studies are based on this expression vector.

Insect cell transfer vectors

The PV1 expression vector (pOPINE Mahoney P1_2A_FS_3C_{EV71}) was constructed based on the existing EV71 expression vector which had already shown expression of EV71 capsid proteins that assembled into empty capsids (Cone, 2015). The EV71 expression vector was produced by inserting the capsid polyprotein (P1) sequence, first 10 amino acid sequence derived from 2A, HIV frameshift sequence and 3C protease with the S128A mutation into the base pOPINE expression vector. These 4 features (P1-2A-FS-3C) in the expression cassette, were introduced downstream of the p10 promoter by In-Fusion cloning (Clontech, US) (Berrow *et al.*, 2007). In-Fusion cloning is a method that allows the introduction of DNA fragments into any vector following unique primer design. The 5' end of the primer contains 15 nucleotides which are homologous to the linearised vector. The 3' end also requires an analogous homologous sequence in the insert. The total length of sequence added is around 40

nucleotides. Linearised vector and PCR product are recognised by In-Fusion Cloning enzyme and the activity fuses the homologous sites to produce a new transfer vector. During this process unique restriction sites were added to the cassette system; a *Bst*EII site at position 0 of the P1 sequence and a *Not*I site at the junction between 2A and the FS. A *Bsu*36I site was placed at the end of 3C sequence. Figure 2.1 illustrates the transfer vector and its details. These sites allow the swapping of a P1-2A sequence for the resident EV71 sequence. A PV P1-2A synthetic gene with unique *Bst*EII and *Not*I sites was produced by Lifetechnologies (US). Both EV71 expression vector and the synthetic vector were digested with *Bst*EII and *Not*I, and then isolated by gel extraction (MinElute Gel Extraction kit and QIAquick Gel Extraction Kit, QIAGEN, Germany). The linearised EV71 transfer vector and PV P1-2A fragment were ligated by T4 DNA ligase (Thermo scientific, US) and then transformed into Stellar *E. coli* chemically competent cells. After antibiotic selection, plasmid DNA was prepared using plasmid preparation kits (QIAprep Spin Miniprep Kit or EndoFree Plasmid Maxi Kit, QIAGEN, Germany) and screened with *Scal* digest, a marker for the PV sequence. Positives were verified by DNA sequencing (Source BioScience, UK). For expression of MEF-1, Saukette SC8 and Mahoney SC6b the sequences were gifted by Andrew Macadam, NIBSC and synthetic DNA for P1 region of all clones were synthesised as GeneArt Strings (ThermoFisher, US) which contained *Bst*EII site at 5' and *Not*I at the 3' end. Those P1 regions replaced the resident PV1 region at the restriction sites in the backbone vector. Following ligation, transformation and DNA sequencing, pOPINE MEF-1 P1_2A_FS_3C_{EV71}, pOPINE Saukett SC8 P1_2A_FS_3C_{EV71} and pOPINE Mahoney SC6b P1_2A_FS_3C_{EV71} were produced.

pTriEx1.1 Mahoney P1

pTriEx1.1 Mahoney P1 was produced by ligation cloning. pTriEx was digested with either *XhoI* and *NcoI* to linearise. The linearised vector was cleaned by GeneJET Gel Extraction and DNA Cleanup Micro Kit (ThermoFisher Scientific, US). Mahoney P1 region including flanking restriction sites, *XhoI* and *NcoI* were amplified by PCR using Phusion® High-Fidelity DNA polymerase master mix (NEB, US) which is described below. The transformation, plasmid preparation and sequencing of newly produced plasmid were performed as explained above.

pOPINE Mahoney 3CD

pOPINE Mahoney P1_2A_FS_3C_{EV71} was modified to accommodate the 3CD sequences. 3CDWT and 3CDWTFS were cloned from the authentic virus sequence, a gift from Toby Tuthill. pET15b-3CD_μ10 expression plasmid contains an extra serine at the 3C-3D junction to prevent auto-cleaving (Parsley *et al.*, 1999) and was used as the source of the 3CD sequence for 3CD Δ and 3CD Δ FS. The 3CD fragment was amplified following the same method as section 2.2.2 using primers which contain the cassette system unique restriction sites, *NotI* and *Bsu36I* to replace the resident 3C. Two types of forward primers were designed, 3CDF and 3CDFSF. 3CDF was designed for constructs that do not contain the frameshift sequence, which are 3CDWT and 3CD Δ . 3CDFSF was used to introduce the HIV frameshift sequence into both 3CDWTFS and 3CD Δ FS. The PCR product and the PV1 parental vectors were digested with *NotI* and *Bsu36I*. Following the ligation of 3CD fragment with the backbone vector and transfection into *E. coli* competent cells, newly constructed plasmids were purified and sequenced as explained above.

Yeast cell expression vector

The cassette consists of the P1-2A-FS-3C_{EV71} from the insect cell expression vector was amplified by PCR as per 2.2.2. Restriction site substitutions were included in the priming oligonucleotides (*BstEII* to *EcoRI* and *Bsu36I* to *StuI*) to facilitate cloning into the yeast vector pKT10. The PCR product was cleaned with GeneJET Gel extraction and DNA Cleanup Micro Kit (ThermoFisher, US). pKT10 was digested by *EcoRI* which was followed by the reaction cleanup using the same GeneJET kit. The purified PCR product was inserted into the linearised pKT10 by In-Fusion cloning (Clontech, Japan). The newly formed vector was transformed into

E. coli competent cells. The plasmid was purified using GeneJET Plasmid Miniprep Kit and verified by DNA sequencing (Source Bioscience, UK) prior to transformation of yeast.

VP1 mutant expression vectors

The mutations were inserted by overlap site-directed mutagenesis (Ho *et al.*, 1989) in the baculovirus expression vector (pOPINE Mahoney P1_2A_FS_3C_{EV71}) followed by re-cloning via the restriction digest and ligation method. By site-directed mutagenesis, primers carrying the desired mutation were used for PCR to introduce the mutation in the product and re-amplify the full-length product. Following the procedure, *AgeI* and *NotI* double digest was carried out for both PCR product and the parental vector. The ligation with PCR product with newly introduced mutation and the double-digested pOPINE Mahoney P1_2A_FS_3C_{EV71} produced the baculovirus vector with the desired mutation. For the yeast expression vector, the *AgeI* and *NotI* fragment which ultimately contained the mutation, were cloned into the exact restriction sites of pKT10 Mahoney P1_2A_FS_3C_{EV71}.

2.2.2 Polymerase chain reaction (PCR)

Phusion® High-Fidelity DNA polymerase master mix (NEB, US) was chosen for all amplifications for its low error rate in DNA amplification.

The PCR is performed following the manufacturer's protocol. The reaction mixture is prepared to contain 0.5 µM forward and reverse primers, template DNA (5ng), 1X Phusion® High-Fidelity PCR Master Mix with HF Buffer (NEB, US) and Nuclease-free water to make up to the final volume. After the reaction mixture is placed in a thermocycler and the following condition is applied; initial denaturation at 98 °C for 30 seconds and then 30-35 cycles of 98 °C for 10 seconds (denaturation), 45-72 °C for 30 seconds (annealing) and 72 °C extension, whose time was adjusted according to the product size, and 1 cycle of final extension at 72 °C for 10 minutes. The PCR product was visualised by agarose gel electrophoresis to ensure the purity. The PCR product of correct size was purified using QIAquick PCR Purification Kit (QIAGEN, Germany).

2.3 Insect cell culture

Sf9 cells, High Five cells and *Tnao38* cells are insect origin cells. They were used in routine virus passage and/or expression. In order to minimise the contamination to these cells, they were handled under sterile condition in a laminar flow hood. Insect cells were grown in Insect-XPRESS™ Media (Lonza, Switzerland). The suspension cultures were placed in a 28 °C shaking incubator and sub-cultured every 3-4 days. On 3rd or 4th day of passage, a cell count was obtained using a Countess® Automated Cell Counter (Lifetechnologies, US) to decide the cell dilution for next passage. *Sf9* cells and T.ni cells were adapted to grow in serum free insect media. *Tnao38* cell was culture in insect media with 2% FCS.

2.3.1 Transfection and recombinant baculovirus production

Sf9 cell were transfected with *flashBAC* GOLD (Oxford Expression Technologies, UK), using lipofectin (Invitrogen, US), the transfer vector and nuclease free water. Each well of 6 well dish was seeded with 1×10^6 *Sf9* cells (50 % confluence). The transfection mixture was incubated for 15 minutes at room temperature and transferred into the well with 1ml of serum free insect media. The 6 well dish was incubated in a 28 °C incubator and the following day, the media was changed to 2 ml of media containing 2 % FCS. On 7th day from transfection, the recombinant virus was harvested by centrifugation at 13000 rpm for 3 minutes. The supernatant, which contains recombinant virus, was passaged to fresh cells settled in 6 well dishes. Subsequent passages were followed every 4 or 5 days until virus titre was so high that CPE become visible under a microscope.

2.3.2 Recombinant protein expression

Small-scale infection

Once a recombinant virus was produced, a small size infection using a 6 well dish was set up to assess the recombinant protein expression. Each well was seeded with the cell type of choice (for the first test, normally the *Sf9* cells) at 50 % confluence (1×10^6). 200 µL of the virus stock (10 % of total infection size) was added and the infection progress was monitored under an inverted microscope. At 3 days post infection the infected cells were harvested by gentle pipetting and centrifuged at 13000 rpm for 3 minutes to separate cell pellet and supernatant.

The pellet was re-suspended with PBS at 1/20 volume of the original infection volume (i.e. 2 ml infection = 100 μ L).

Rupintrivir 3C protease inhibition

Six well dish small-scale infections using the PV1 recombinant baculovirus were set up. At 3 hours p.i., 10-fold serial dilutions of Rupintrivir in insect cell media starting at 330 nm to 0.33 nm were added to the individual wells. Two days later, the infected cells were harvested and the cell pellet was re-suspended in the same manner as described above.

2.3.3 Protein expression scale up

A large volume of recombinant virus is required to scale up the protein expression to obtain purified VLP. Monolayer cultures were used for amplification of the virus stock. Cell culture flasks were seeded with a suitable number of Sf9 cells to achieve 50% confluence. Once recombinant virus was added, the flask was incubated in 28°C incubator. On the 7th day, CPE was easily observed. The cells were lifted by gentle tapping and collected and then centrifuged at 4500 rpm, 20 minutes at 4 °C. The supernatant containing recombinant baculovirus was pooled and stored at 4 °C. When a sufficient amount of recombinant virus is obtained, a suspension culture was prepared to be 1x10⁶ cells/ml to commence the infection. 10 % of total infection volume of virus stock representing an MOI of ~3 was added to the cell culture and placed in the incubator for 3 or 4 days until its viability reached 30-40%. The infected cells were harvested by centrifugation at 4500 rpm, 20 minutes at 4°C. The pellet was stored at -80°C.

2.4 Yeast cell culture

RAY3A-D (*MATa/a ura3/ura3 his3/his3 leu2/leu2 trp1/trp1*), a strain of *Saccharomyces cerevisiae* was used for PV VLP production. The strain was kindly gifted by Dr Yuko Morikawa, Kitasato University, Tokyo, Japan. For RAY3A-D and recombinant yeast expression culture, YPD media was used. During the transformation, synthetic dropout (SD) media was utilised. The expression vector has a uracil marker. Therefore, SD media lacking uracil was used. For parental yeast growth, culture was prepared at 250 rpm shaking at 30 °C overnight. For the expression, the temperature was lowered to 20 °C for slower yeast growth.

2.4.1 Yeast cell transformation and its confirmation

pKT10 with the PV cassette expression vectors were transformed into *S. cerevisiae* using the lithium acetate (LiAc) protocol described by Herskowitz (2012). RAY3A-D was grown in YPD media over night to reach saturation. The following day, the saturated cells were diluted in the fresh 100 ml media at an OD₆₀₀ reading of 0.2 and grown to reach OD₆₀₀ 0.5-0.7 at 30°C, 250 rpm. The cultures were harvested at 3000 rpm for 5 minutes. The cell pellet was washed in 5 ml LiAc mix (100 mM LiAc in TE buffer) and recovered by centrifugation. 1 ml of LiAc mix was added to the pellet and 100 µL aliquots were taken per transformation. 1 µg pKT10 expression vector with the PV cassette, 50 µg salmon sperm DNA as a carrier and 0.7 ml PEG mix (40 % PEG in LiAc mix) were added and vortexed. The cells were incubated at 30 °C for 30 minutes and then heat-shocked at 42 °C for 20 minutes. The cells were then centrifuged at 3000 rpm for 30 seconds. The pellet was dispersed in 200 µL sterile diH₂O and plated out onto SD media agar. For RAY3A-D transformed cells, uracil lacking media was utilised. The plate was incubated at 30 °C for 3-4 days. Once the colonies were observed on the plate, a glycerol stock for the transformed yeast cells were prepared. The colonies were resuspended in 0.5 ml of the synthetic dropout media, sterile glycerol to 25 % was added and was kept in a -80 °C freezer for the future use. At the same time, the transformed plasmid was re-isolated to confirm successful transformation using a yeast plasmid isolation kit (Clontech, US). The purified plasmid was transformed back into Steller *E. coli* cells (Clontech, US). pKT10 plasmid has the bacterial origin of replication and an antibiotic resistant marker therefore it can be recovered into *E. coli* cells. After growing the inoculation overnight, the plasmid was purified from the *E.coli* cells and DNA sequencing verified the transformation as described in section 2.2.1. The steps from the transformation to the confirmation of the presence of the expression vector are summarised in Figure 2.2.

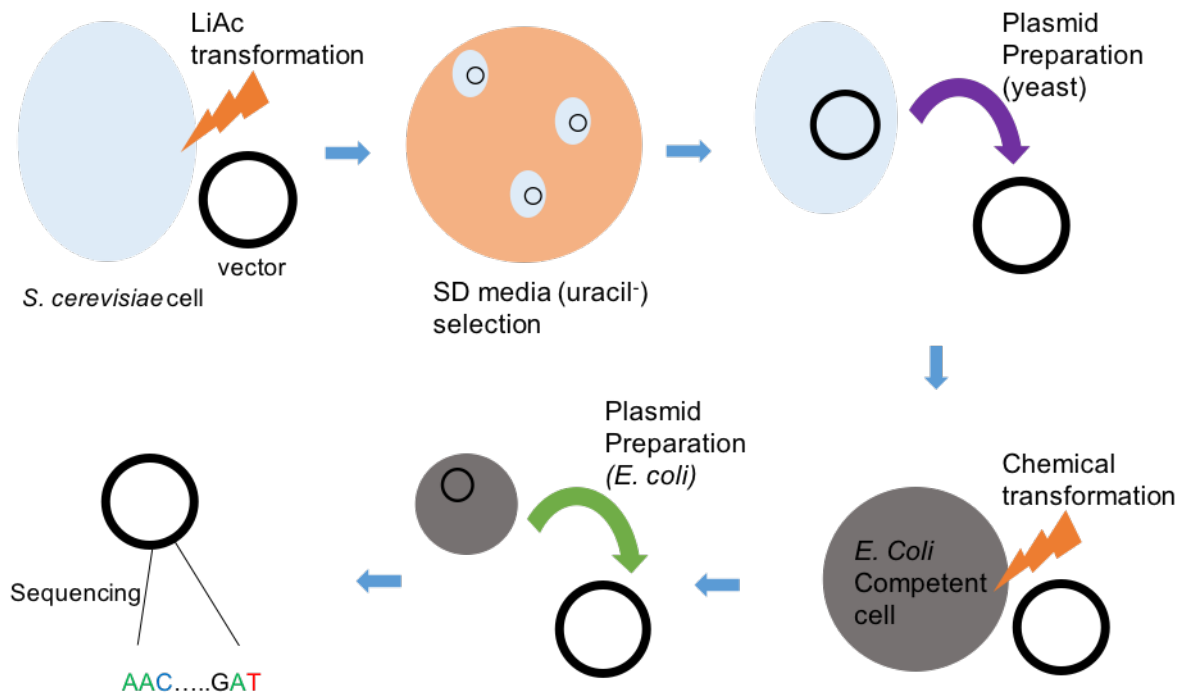


Figure 2.2. Schematic representation of yeast expression vector transformation and its confirmation flow

Once the expression vector is constructed, it was transformed into *S. cerevisiae* cells by LiAc transformation method. Then the selection of the cells combined with the expression vector carrying *URA3* gene was carried out on the SD media lacking uracil. For the confirmation of positive transformation, the expression vector was purified from the yeast cells and transformed back into competent *E. coli* cells to purify the plasmid. The vector was prepared from the *E. coli* cells and then sequenced to confirm its identity.

2.4.2 PV VLP expression by *S. cerevisiae*

For each culture preparation, transformed yeast cell glycerol stocks were streaked on SD media agar for the start culture. The culture was prepared by incubating scraped yeast cells from the plate at 30 °C overnight at 250 rpm. The following day, the saturated media were transferred to seed YPD medium for the expression phase. The expression medium at starting OD₆₀₀ of 0.2 was incubated at 20 °C overnight at 250 rpm and left to grow to the desired density. The culture was harvested by centrifugation at 5000 rpm for 20 minutes at 4°C. If it was not required immediately, the pellet was stored at -80°C.

2.5 Purification of recombinant PV empty capsid

The method described in this chapter especially for yeast cell derived VLPs was later improved. The changes will be described in chapter 5.

2.5.1 Cell lysis

Insect cell

For VLP purification from the insect cells, the pellet was re-suspended with 10X volume of PBS for the pellet weight. Afterwards, a total concentration of 1 % Nonidet® P40 (Fluka, US) in PBS and 20 units/ml Benzonase® nuclease (Sigma-Aldrich, US) and 1 cComplete™ ULTRA protease inhibitor tablet (Roche, Switzerland) were added and incubated in ice for 60 minutes. Clarifying by centrifugation removed unbroken cells and nuclei leaving the supernatant which contained the PV VLP.

Yeast cell lysis by cell disruptor

The harvested PV VLP yeast cells were resuspended in ice cold buffer 1 supplemented with 1 tablet of cComplete™ ULTRA protease inhibitor (Roche, Switzerland). First, the cell disruptor cooling system equipped with glycerol was switched on 30 minutes prior to the operation. The system was purged with ice cold diH₂O and then ice-cold buffer 1 (without protease inhibitor). The pressure was set to 2.5 bar (280 MPa). The sample was loaded onto the system. The sample consistency was checked to be free from clumps or high viscosity and 10 ml sample volumes were pressurised in one press. The sample temperature was monitored for PV VLP stability.

2.5.2 Ultracentrifugation

The ultracentrifugation condition, including medium, centrifuge speed, time, and gradient was changed through the project to improve the yield. Here, the basic procedure is described. The condition for each ultracentrifugation will be noted later where appropriate.

Two types of ultracentrifugation; velocity centrifugation and isopycnic centrifugation have been used. The first type separates the particles into distinct zones on the basis of the size and shape (which contribute to the sedimentation rate). Normally sucrose is chosen to form a gradient. In the second type, the particles undergo separation by differences in their buoyant

density. Once the centrifugation starts, the particles migrate to the equilibrium point where the particle's buoyant density and the gradient density are the same. At this point, the isodensity level, the sample does not migrate any further (Mazzone, 1998). A sucrose cushion is a simple form of pre-gradient (Dijkstra & Jager, 1998). In our project, 30 % sucrose was used because assembled capsids can migrate through this sucrose layer to reach the bottom of the centrifuge tube. Any other smaller substances cannot enter the layer, hence, they are separated. This process is used as a first selection step before the final gradient step.

After the cell lysis or supernatant concentration, debris was removed by clarification centrifugation at 15,000 rpm, 30 minutes at 4°C. The clarified supernatant was loaded onto the 30% sucrose layer and centrifuged at 30,000 rpm for 16 hours at 4 °C. Depending on the supernatant size, it was loaded into Thinwall Ultra-Clear tubes for either the SW32 Ti rotor (38.5ml capacity) or SW40 rotor (13.2 ml). The formed pellet at the bottom of tube was resuspended in a small volume (~800 µL) of appropriate buffer. The resuspension was centrifuged at 15,000 rpm, 30 minutes at 4 °C in a refrigerated bench top centrifuge to remove insoluble aggregates and the supernatant was removed from the tube and stored on ice. The newly formed pellet was resuspended in a small volume of buffer and centrifuged again. The combined supernatant was then loaded onto the sucrose gradient consisting of a 20-60 % discontinuous sucrose gradient with 5 % increments or a linear 15-45 % sucrose gradient produced by a gradient master base unit (BioComp Instrument, Canada). The gradient maker prepares a linear gradient of the media automatically by mixing the most and least concentrated media at a specific angle, with a specific rotation and length of time. Ultracentrifugation at 30,000 rpm or 21,000 rpm at 4 °C for 16 hours separated the VLPs into different zones and the sample was fractionated from the top of the gradient.

Occasionally, a 2nd ultracentrifugation was done to improve the VLP purity. Following the analysis of 1st gradient, the chosen fractions were pooled and diluted to remove the sucrose or passed through a Zeba 7K MWCO desalting spin column. Once the removal of sucrose was completed, the eluate was concentrated using an Amicon Ultra 4 ml or 15 ml cassette to lay a small volume on top of the 2nd sucrose gradient and ultracentrifuged as described above.

2.6 SDS-PAGE and Western blot assay

Samples for western blot were prepared by adding 2X SDS loading buffer (2.1.8) or 4X Bolt™ LDS sample buffer (Invitrogen, US) containing 2-mercaptoethanol. For insect cells from a small-scale infection, 5×10^4 cells were loaded per well. In order to denature the sample completely, they were vortexed for 30 seconds, centrifuged briefly at maximum speed and boiled for 10 minutes at 100 °C. The samples were then blended for 30 seconds to reduce viscosity with a vortex and centrifuged again for 5 minutes at 13000 rpm. Sodium dodecyl sulphate gel electrophoresis (SDS-PAGE) was run to separate the denatured protein samples using a Mini-PROTEAN® TGX™ Gel, 10 well, 30µl (Bio-Rad Laboratories, US) with 1X Tris-Glycine SDS PAGE buffer (National Diagnostics, US) or Bolt™ Bis-Tris Plus Gels, 10-well (Invitrogen, US) with 1x Bolt™ MES SDS running buffer (Invitrogen, US). Once the gels finished running, they were either stained for visualisation by coomassie staining (2.1.8) or silver stained by the SilverQuest™ Silver staining kit (Invitrogen, US) or transferred for western blot. For western blot, the gel was then transferred onto an Immobilon-P transfer membrane (Merck Millipore, US) by semi-dry transfer. The transfer membrane and Whatman™ 3MM Chromatography Paper (GE healthcare, US) were soaked in 1X Tris-glycine electroblotting buffer (National Diagnostics, US) supplemented with methanol. The transfer sandwich (3 layers of chromatography paper, membrane layer and another 3 layers of chromatography paper) was prepared on a HorizBLOT (Atto, Japan). After the transfer, the membrane was incubated in either Western blot (WB) blocking buffer, Protein-free T20 (TBS) blocking buffer (Thermo Scientific Pierce, US) or at 4 °C or renaturing buffer at RT overnight. The membrane was incubated with TBST (2.1.8) 3 times (5 minutes each) to wash off any excess carry over from the previous step. The membrane was then incubated with primary antibody for 1hour together with the same buffer used in the blocking step except in the cases of renaturing buffer. For membrane blocked with renaturing buffer, Protein-free T20 (TBS) blocking buffer was used for antibody incubation. On completion, membranes were washed 3X 5 minutes in TBST. When the primary antibody is not conjugated with horseradish peroxidase (HRP), a secondary antibody conjugated with HRP was incubated to probe for the primary antibody. Typical Ab combinations for a particular antigen detection are listed in Table 2.10.

ChemiFast (Syngene, UK) was used as a chemiluminescent detection agent to react with HRP.

The antigen was detected by G:Box imager (Syngene, UK) to produce a digital image.

Table 2.10. Combination of primary and secondary antibodies for a particular detection in WB analysis.

The detail of the antibodies are listed on Table 2.7

Detection	Primary Ab	HRP conjugated secondary Ab
VP1 detection	Anti-poliovirus Blend Ab (MAB8566, Millipore at 1:5000)	Polyclonal Goat Anti-mouse Immunoglobulins/HRP (P0447, Dako at 1:2000)
VP0 detection	Rabbit anti-VP0 sera (Day 39, Host lab at 1:2000)	Polyclonal Goat Anti-rabbit Immunoglobulins/HRP (P0448, Dako at 1:2000)
VP3 detection	Rabbit anti-VP3 sera (Collaborator at 1:2000)	Polyclonal Goat Anti-rabbit Immunoglobulins/HRP (P0448, Dako at 1:2000)
P1 detection	Rabbit anti-PVP1 sera (Collaborator at 1:2000)	Polyclonal Goat Anti-rabbit Immunoglobulins/HRP (P0448, Dako at 1:2000)
p39 detection	Mouse anti-baculovirus p39 sera (Collaborator at 1:2000)	Polyclonal Goat Anti-mouse Immunoglobulins/HRP (P0447, Dako at 1:2000)

2.6.1 Rapid analysis of VP expression in Yeast

This procedure enabled rapid analysis for the recombinant protein extraction from *S. cerevisiae* (Kushnirov, 2000). For the expression analysis of PV VPs, colonies grown on YPD agar were scraped off and resuspended in 100µL distilled water. Alternately, a fraction of liquid culture (2.5 OD₆₀₀U/ml) which provided roughly 2.3 mg of yeast pellet in wet weight, was resuspended in distilled water. Then, 100 µL of 0.2 M NaOH was added and incubated for 5 minutes at room temperature. After pelleting in the bench top centrifuge at 14000 rpm for 5 minutes, the sample was resuspended in 50 µL 1X SDS loading buffer, boiled for 3 minutes, then pelleted. The

prepared samples were analysed by WB following the SDS-PAGE and semi-dry transfer as described in section 2.6.

2.7 Microscopy

Two types of imaging were utilised for this project to visualise PV VLP. Gated-Stimulated Emission Depletion (gSTED) microscopy situated at the Research Complex at Harwell. Dr Christopher Tynan helped to operate the microscope. Transmission Electron Microscopy, Joel TEM available at The University of Reading. Dr Peter Harris and Miss Amanpreet Kaur gave technical training.

2.7.1 Gated-Stimulated Emission Depletion (gSTED) microscopy

gSTED microscopy produces high resolution images utilising improved fluorescence confocal imaging and is especially user friendly for live cell imaging. STED microscopy generates the images by using two different beams, excitation laser beam and STED beam. The excitation beam strikes the sample conjugated with fluorophore whereupon the fluorophore emits Stoke's shifted emission photon. It scans the fluorophore in a section of interest pixel by pixel. The STED beam defines the excitation strike spot by surrounding it. With two beams, the central area of STED beam fluorescence detection is enhanced to produce the final image (Vega, 2014).

Small scale infection with recombinant baculovirus was carried out in poly-D-lysine coated glass-bottom 35 mm sterile dishes (MatTek, US) following section 2.3.2. After 2 days infection, the virus and media was discarded from the dish. Infected cells were fixed and permeabilized using a Fixation/Permeabilization kit (BD Bioscience, US). The solution was washed off with blocking/wash buffer, PBS with 2 % BSA. Then the specimen was blocked in blocking/wash buffer for 1h. After aspirating the buffer, the primary antibody against the target protein was diluted in the same buffer and incubated for 1h. The fixed sample was washed with the blocking/wash buffer 3 times, 5 minutes incubation each. Fluorophore conjugated secondary antibody was diluted in the same buffer and used to incubated the specimen in the dark for 1h. After a 2nd wash, the sample was sealed with parafilm and kept in dark until the specimen observation. The standard operation manual was followed for imaging. The choice of imaging

wavelength according to the fluorophore is important for high resolution image. For Oregon green 488, manufacturer recommends to detect the wavelength around 514 nm. At the same time, STED beam intensity was adjusted to improve the resolution.

2.7.2 Transmission Electron Microscopy

Once samples were adjusted for correct concentration in a buffer for TEM imaging, a couple of microliter was laid on a piece of parafilm. Two droplets of diH₂O were placed next to the sample. These are flowed by two droplets of 0.45 µm filtered 2 % uranyl acetate. Once all the solutions were prepared on the parafilm, formvar/carbon 300 mesh copper grid was floated on with shiny side facing the sample. After 5 minutes incubation, any excess sample on the grid was removed by filter paper. The grid was transferred onto the first diH₂O and moved to second. The excess solution was blotted with the filter paper. Then the grid was placed on the uranyl acetate for 5 minutes. Then moved to second droplet and the excess was removed by filter paper. After preparing the grid, it was stored in a grid box. The TEM was operated following a standard protocol. For PV VLP visualisation, high tension was set for 200 kV. Typically, PV VLP images were obtained around X27,500 magnification. Higher magnification is desired for PV VLP particle size.

2.8 N/H ELISA

This ELISA protocol was modified from the original protocol offered by the National Institute for Biological Standards and Control (NIBSC).

A clear flat-bottom immune nonsterile 96-well plate (Thermofisher, US) was coated with poliovirus capture antibody (SH16 for PV1 at 1:500 and R Skt live for PV3 at 1:2000) diluted in carbonate coating buffer (2.1.8) for at least 16 hours prior to the assay. Once the plate is coated, the plate was sealed and placed in a lunch box with a humidified atmosphere. The box was stored in 4 °C. The following day, the plate was washed with PBST (2.1.8) 3 times. Then the plate was incubated in blocking solution (2.1.8) for 30 minutes at room temperature.

In the meantime, sample dilutions were prepared. The European PV standard was diluted in assay diluent to 1:20 for the start dilution (2.1.8). The dilutions of the purified samples from the expression systems varied on each occasion. Duplicate of samples were prepared for N and

H specific antigen analysis. Columns 1 to 5 was used for N specific ELISA and columns 7 to 11 for H specific ELISA. The samples were added in column 1 and 7. From the columns, 5 series of 1:2 dilutions were made. One row was added with assay diluent to serve as a blank. The plate was sealed and placed in the humidified atmosphere lunch box. It was incubated at room temperature for 2h.

After the incubation, the plate was washed with PBST 3 times. Then diluted monoclonal antibodies for N and H were then added to the wells. N specific antibodies (234 for PV1 and 520 for PV3) were diluted in 1:200 in assay diluent. The same dilutions were used for H specific antibodies (1588 for PV1 and 517.3 for PV3). The plate was placed in the same box and incubated at room temperature for 1h.

After the plate was washed 3 times with PBST, goat anti-mouse HRP conjugated antibody (2.1.7) at 1:1000 in assay diluent was added to the wells. The plate was incubated in the same manner as above, which was followed by a 3 plate washes with PBST.

For detection, TMB Stable (Thermofisher, US) was added to the well and incubated up to 30 minutes at room temperature. In order to stop the TMB stable reaction with HRP, 0.25 M H_2SO_4 was added. The optical density at 420 nm was read by a Tecan plate reader, with Magellan 6 software. The result was exported from the programme to an excel sheet and OD vs serial dilution graphs were plotted.

Chapter 3 Capsid protein expression and assembly in insect cells

3.1 Introduction

3.1.1 VLP production in insect cells

Previous studies on the expression of FMDV empty capsids in insect cells defined the minimal proteins required; the structural polyprotein (P1), the self-cleaving 2A peptide and the 3C protease (Lewis *et al.*, 1991; Roosien *et al.*, 1990). Using these components, a P1-2A construct synthesised the FMDV structural polyprotein but a P1-2A-3C cassette failed in the expression of significant amounts of the individual structural proteins. The study suggested that the 3C protease activity led to 3C cleavage of host cell proteins as well as P1 precursor cleavage (Porta *et al.*, 2013). To overcome this, it was suggested that 3C protease activity down regulation would be required for the efficient synthesis of the mature viral structural proteins and this was achieved by the addition of two 3C regulators. The first regulation was done by the introduction of a mutation in the 3C enzyme shown to reduce activity *in vitro* (Sweeney *et al.*, 2007). The second level of regulation was the addition of a HIV-1 ribosomal frameshift signal between P1-2A and 3C. The signal consists of two distinctive structural features. A hexameric 'slippery site' consisting of 6T nucleotides followed downstream by a stem-loop, an RNA secondary structure thought to cause ribosomal pausing (Dinman *et al.*, 2002). These two elements are linked by a spacer sequence (2A first 10 amino acids) and together they facilitate ribosome slip back by one base in the 5' direction, and then start a new reading frame from the -1 frame codon. The level of slippage of the HIV frameshift is reported to be about 1 in 20 translation events (Wilson *et al.*, 1988). A schematic representation of the HIV-1 frameshift is shown in Figure 3.1. The use of this signal acts to translate P1-2A as the majority product and P1-2A-FS-3C as the minority product, effectively reducing the level of 3C compared to the level of P1. The combined use of these regulators effectively reduces 3C toxicity and allows the build-up of sufficient cleaved mature picornavirus capsid proteins for empty capsid assembly to occur (Porta *et al.*, 2013).

An analogous mutation affecting 3C activity, serine 128 to alanine, has been shown for EV71, another member of the *Picornavirus* family (Cui *et al.*, 2011) suggesting a similar strategy could work for empty capsid production for enterovirus members. Indeed, previous work in the host laboratory showed that EV71 capsids could be assembled in insect cells using the same cassette design as that described for FMDV (Cone, 2015). As the sequences of the EV71 3C and that of poliovirus 3C are very similar as shown in Figure 3.3, the modified EV71 3C sequence was used for the construction of equivalent cassettes for the expression of PV empty capsids. For the structural P1 region, IPV virulent reference strain sequences of the three PVs, Mahoney/PV1, MEF-1/PV2 and Saukett/PV3 were chosen for the initial production of PV VLP. However, during the course of the work, viruses with improved stability were described (Fox *et al.*, 2017) and VLPs made in plants using a the same, improved, sequence from PV3 Saukett were shown to be more stable than the WT sequences (Marsian *et al.*, 2017). Therefore, in later experiments a sequence variant, Saukett SC8, was used for insect cell expression rather than the wild type sequence.

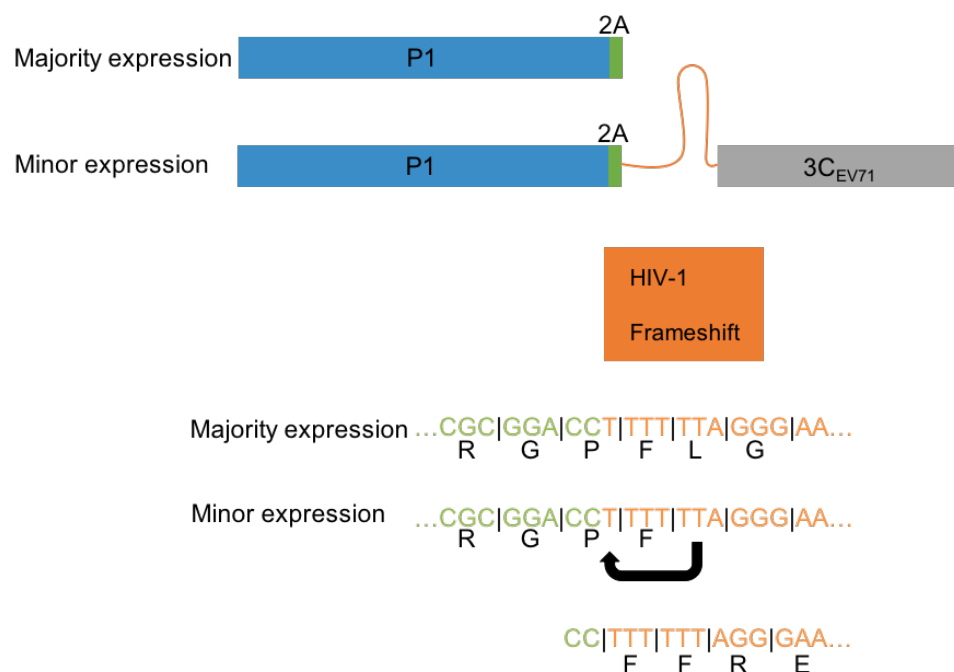


Figure 3.1. Schematic presentation of PV viral proteins expression cassette showing controls for 3C_{EV71}

P1 region is coloured in blue and is followed by the first 10 amino acids of 2A in green. The HIV-1 frameshift is shown in orange connected to the 3C grey region. The orange area focuses on the nucleotide sequence at the frameshift slipping site. The majority of expression terminates after the host cell ribosome drops off from ORF1 but a minority of the ribosomes continue translating in the -1 frame after the frameshift sequence (Wilson *et al.*, 1988).

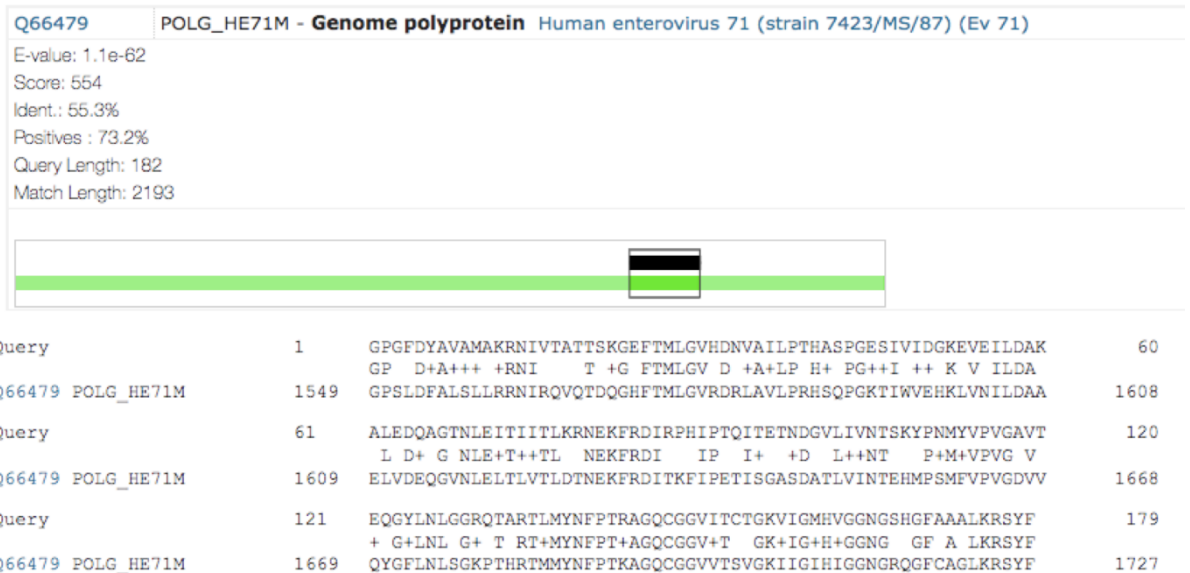


Figure 3.2. BLAST result of 3C_{EV71} and 3C_{PV}

The result aligned 3C_{PV} and 3C_{EV71} to find the amino acid sequence homology. The result was produced by UniProt.

3.1.2 Protease for P1 processing

The difference in the roles of 3C and 3CD^{pol} in the proteolytic processing of P1 has been previously investigated. In the picornaviral replication cycle, 3C is one of the proteases which is responsible for cleavage of the polyprotein at a Gln-Gly junction into functional mature protein products (Kuo *et al.*, 2008), including temporary intermediate products (Lawson & Semler, 1990). These intermediate products have functions which are different from the final cleaved products. One of such products is the viral polyprotein 3CD as discussed in 1.2.4. Comparative studies using poliovirus 3C and 3CD protease showed that 3CD protease cleaves more efficiently than 3C, although 3C contains the enzymatic active site (Andino *et al.*, 1993; Harris *et al.*, 1994; Jore *et al.*, 1988; Mosimann *et al.*, 1997; Ypmawong *et al.*, 1988a; Ypmawong *et al.*, 1988b). These data suggested that certain 3D regions act as a 3C activity enhancer. While the mechanistic details are poorly understood, the necessity for 3D in P1 cleavage was shown in several studies (Jore *et al.*, 1988; Parsley *et al.*, 1999; Ypmawong *et al.*, 1988b). A 3CD construct which contains a serine insertion at the junction between 3C and 3D to eliminate the auto-cleavage of 3C and 3D showed enhanced cleavage of PV viral proteins produced by bacterial expression (Parsley *et al.*, 1999). These historical findings led to the use of 3CD in recombinant expression systems to produce empty PV capsids using P1 and 3C/3CD. Ansardi *et al.* (1991) showed co-infection of one recombinant vaccinia virus expressing P1 and the other 3CD resulted in PV viral proteins expression in HeLa cells. The

sucrose gradient fractionation pattern was found to be consistent with sedimentation of PV empty capsids and electron microscopy showed empty capsids with a capsid centre penetrated by stain and of suitable size and shape. Similarly PV VLP production in *Saccharomyces cerevisiae* used P1 and 3CD expression vectors (Rombaut & Jore, 1997). However, the host laboratory has shown that FMDV and EV71 VLPs are produced in insect cell expression system using a single transfer vector with a regulated 3C rather than co-expression of P1 and 3CD. These findings suggest that there is a need to study the preferred protease in the insect cell system for the expression of PV empty capsids via a single expression cassette.

In this chapter, the synthesis of PV viral proteins by the recombinant baculovirus expression system and their assembly to PV VLPs is investigated. Optimisation experiments include an investigation of PV VLP production by the preferred protease, 3C or 3CD.

3.2 The expression of viral proteins for PV1, PV2 and PV3

3.2.1 Construction of insect cell expression vector

The expression vector construction was carried out as per 2.2.1. Figure 3.3 summarised the cassette system used for all the PV serotypes. Using existing expression vectors that had previously shown EV71 VLPs assembly in insect cells (Cone, 2015) the sequence of P1_{EV71} and first 10 amino acids of 2A was removed from the vector pOPINE EV71 P1_2A_FS_3C and replaced by PV P1 (Mahoney/PV1, MEF-1/PV2 and Saukett/PV3) and the first 10 amino acids of 2A to construct equivalent insect cell expression vectors with the potential to assemble PV VLPs following baculovirus expression. The vectors produced were pOPINE Mahoney P1_2A_FS_3C_{EV71}, pOPINE MEF-1 P1_2A_FS_3C_{EV71}, and pOPINE Saukett SC8 P1_2A_FS_3C_{EV71}. In addition, to provide a suitable control for the non-cleaved polyprotein, pTriEx1.1 Mahoney P1 was also produced for the expression of PV P1 only. The method is detailed in 2.2.1.

3.2.2 Synthesis of VP0, VP3 and VP1 by 3C_{EV71}

Expression vector transfection and recombinant baculovirus production, followed by small-scale infections and WB to examine protein expression and cleavage were carried out as

described in 2.3.1, 2.3.2 and 2.6. Recombinant baculoviruses, Bac-PV1P1-3C, Bac-PV2P1-3C, Bac-PV3P1-3C, Bac-PV1P1 and Bac-GFP (expression control) were produced following the transfection of the relevant expression vectors and virus passage to generate high titre stock.

EV71 cassette



PV cassette



Figure 3.3. The expression cassette designs for all three serotypes of PV.

The colour scheme was maintained the same as Figure 3.1.

To assess the genetic cassette design for the expression of PV proteins, a time-course of infection was carried out using Bac-PV1P1-3C infection of *Sf9* cells. A six well dish was seeded with $\sim 10^6$ *Sf9* cells per well and infected with 0.1 mLs of the PV1 recombinant baculovirus stock for 1 hr at room temperature. The inoculum was then removed and replaced with 2 mLs of culture medium. A single well of the infection was harvested each day. The baculovirus inoculum had a titre of $\sim 5 \times 10^7$ pfu/ml giving an MOI of ~ 5 for this and subsequent experiments. Approximately $1/20^{\text{th}}$ of the harvested well, that is $\sim 5 \times 10^4$ insect cells were analysed per well of a precast Bolt™ Bis-Tris Plus 4-12% gels (Invitrogen, US). VP1 detection was carried out by WB using a mixture of monoclonal antibodies, MAB8566, to all 3 PV serotypes (Millipore) (Figure 3.4). A ~ 32 kDa band, which was identical to the calculated VP1 MW, was visible in the infected insect cells from day 1 to day 4 with the intensity peaking at day 3. A minor intermediate band was visible at ~ 57 kDa, possibly representing VP3-VP1, and a high MW band, possibly an aggregate of protein and DNA, was also present near the slot. No discreet

band of P1 was apparent suggesting complete polyprotein processing. Some non-specific binding of the anti-VP1 Ab was seen to non-infected *Sf9* cells but the band intensities were very low and the cross reaction did not obscure the VP1 band present in the test lanes. This result confirmed that the expression vector functioned as designed and that VP1 is produced by P1 proteolytic processing. It also showed that a 3 days infection was optimum for the detection of PV viral proteins, a time course typical of baculovirus expression driven by very late promoters (O'Reilly *et al.*, 1992).

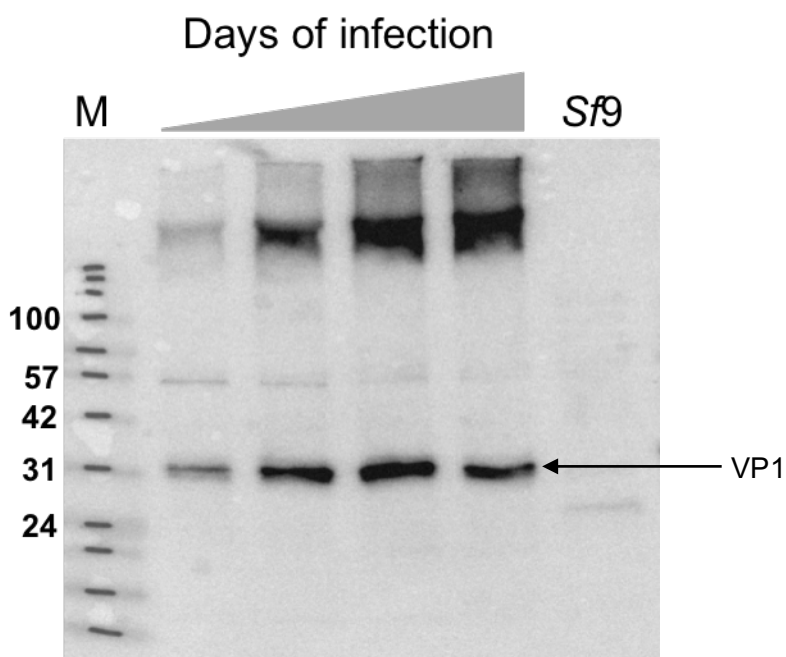


Figure 3.4. WB analysis for VP1 presence following a time course (1-4 days) small-scale *Sf9* cells infection of Bac-PV1-P1-3C

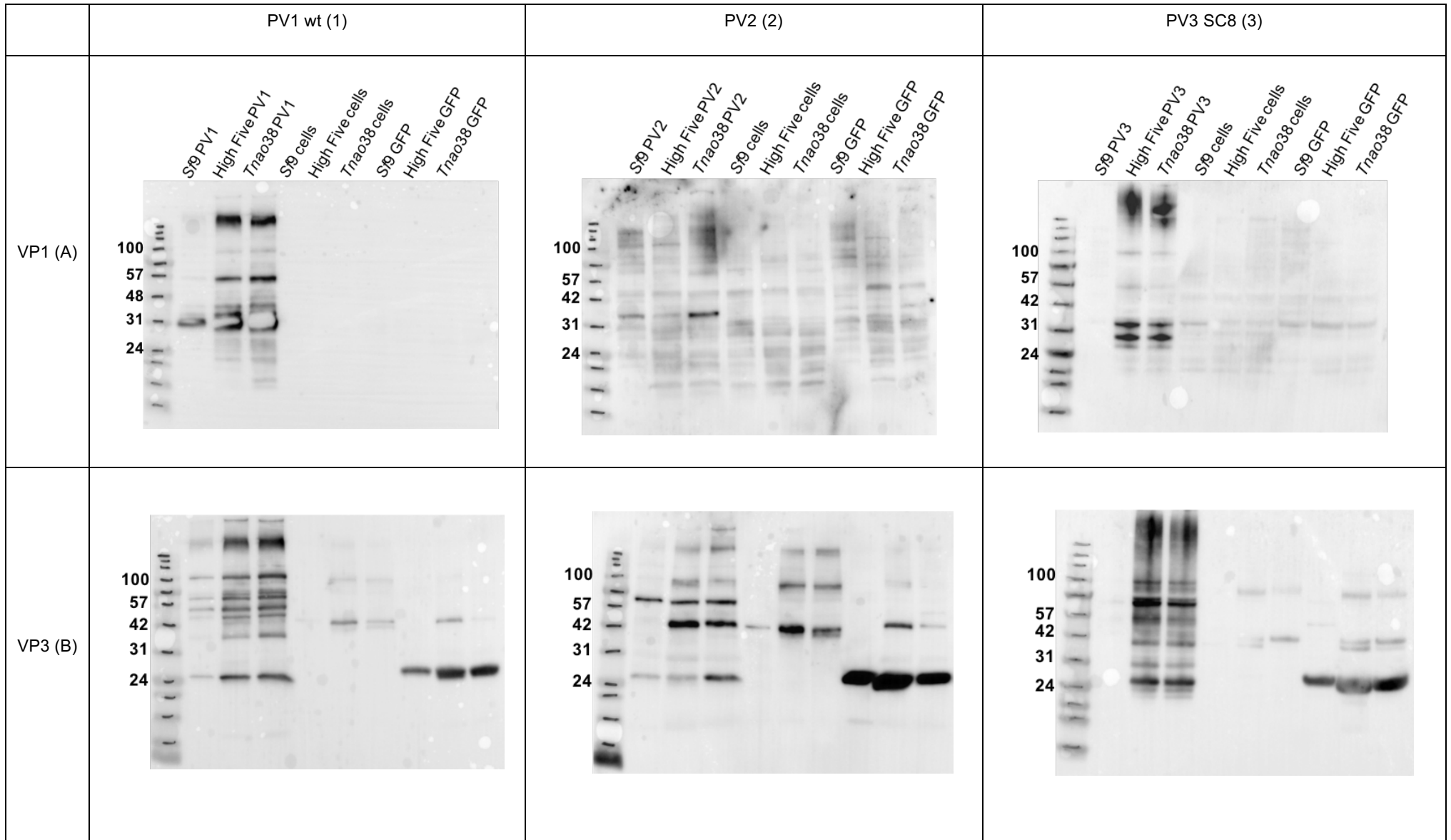
The reactivity at 32kDa band increased to 3rd d.p.i. and slightly declined on 4th d.p.i. *Sf9* cells were included as a negative control (far right). Protein molecular markers are shown to the left of the gel (M) and are in kilodaltons. Mini-PROTEAN TGX Any kD gel (BIO-RAD) and BLUeye Pre-Stained Protein Ladder (Geneflow) were used.

To confirm that the expression of PV1 VP1 was typical of all the serotypes constructed, small-scale 3 day infections by Bac-PV1P1-3C, Bac-PV2P1-3C and Bac-PV3P1-3C were also prepared in *Sf9* cells. In addition, to assess the role of the host cell line on expressed protein yield, High Five cells and *Tnao38* cells both originally from *T.ni* were also infected in an identical format. Infection by the Bac-GFP recombinant and insect cells only acted as infection and mock controls. At 3 day p.i. the cells were harvested and processed for WB as before. In these assays, in addition to the use of a VP1 specific antibody, polyvalent sera specific for VP0

and VP3 (gifted by Dr Jane Cardoso, Universiti Sains Malaysia) were also used as primary antibodies. The WB analysis showed efficient PV1 P1 cleavage into VP1 (Figure 3.5A1) as before but also the presence of VP3 (Figure 3.5B1) and VP0 (Figure 3.5C1) as expected of authentic 3C mediated maturation of PV1 (Figure 3.5 left panels, column 1). In addition, the equivalent constructs for PV2 (Figure 3.5 middle panels, column 2) and PV3 (Figure 3.5 right panels, column 3) showed that these serotypes too are expressed and cleaved into their requisite mature viral proteins. When the signal intensity of the test tracks (lanes 2-4) was compared it was found that the yields of PV proteins were in the order *Tnao38* ≥ *High Five* >> *Sf9*, irrespective of the serotype used. When the different serotypes were compared it was evident that PV2 expression (middle panels) was lower than either PV1 or PV3.

In the case of PV2 expression of VP1 (Figure 3.5A2) it was possible that the lower intensity is in part due to the MAB8566 mixture (anti-VP1 Ab) as the MEF-1 VP1 sequence at residue 295 is different from the Sabin type 2 sequence which was used for production of the mAb (Gary *et al.*, 1997). However a lower yield from PV2 was also apparent on the blots probed by VP3 (B) or VP0 (C) blots, the latter being barely detectable, suggesting that the PV2 sequence is generally more poorly expressed. The reasons for this are unclear. The patterns of antigen expression revealed by the blots were generally similar although in the case of VP1 detection for PV3 (Figure 3.5A3) a slightly smaller band was detected in addition to the VP1 band. This might suggest some altered processing in different cell lines but could also reflect the affinity of the antibodies in the polyclonal sera for certain breakdown products. As the sera have not been formally epitope mapped this cannot be confirmed by inspection of the epitope sequences. The Anti-VP3 sera bound a major band at molecular weight 27 kDa for PV1, PV2 and PV3 consistent with predicted MW of VP3. (Figure 3.5B1-3). The VP3 antiserum also showed a high background binding to GFP in the expression control lanes. In contrast the VP0 serum had a low background and bound specifically to a 40kDa band as predicted for the MW of the VP0 product (Figure 3.5C1 and C3). A range of background bands were present on the blots but their origin is not known. Figure 3.5D showed that the baculovirus capsid protein p39 was detected at similar rates in all infections suggesting equivalent rates of infection thus supporting the conclusions concerning different levels of PV antigen expression based on

serotype and cell line. Higher molecular weight bands in PV lanes, which are visible in (A), (B) and (C) may represent unprocessed or partially processed P1.



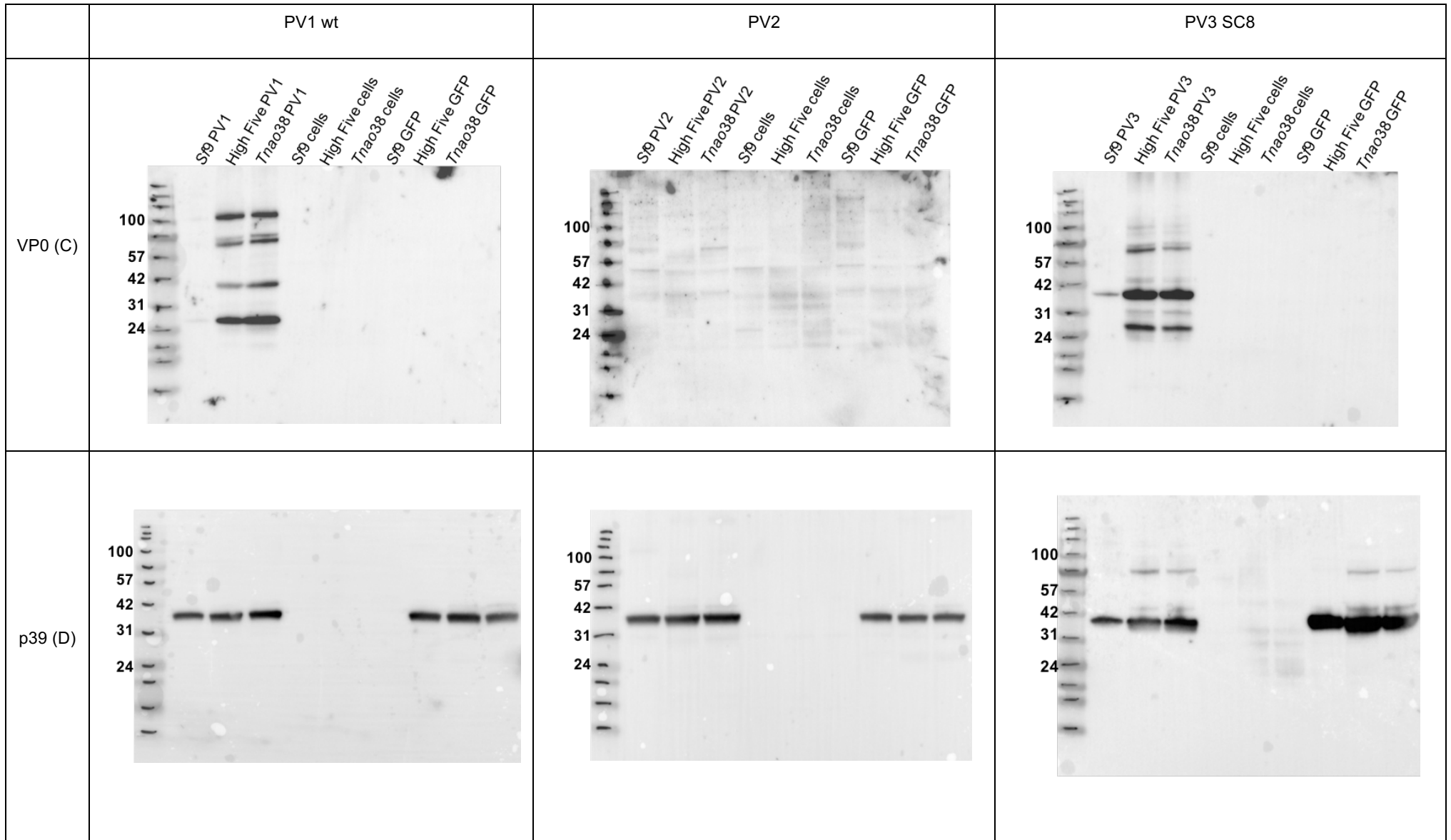


Figure 3.5. WB analysis showing PV P1 cleavage into viral proteins using 3C_{EV71} in *Sf9*, High Five and *Tnao38* cells.

3 d.p.i. of Bac-PV1P1-3C, Bac-PV2P1-3C and Bac-PV3P1-3C (Skt SC8) infected cells were analysed for proteolytic processing. The WB for PV1 (A-D1), PV2 (A-D2) and PV3 (A-D3) contain identical samples and were probed using different primary antibodies; MAB 8566 for VP1 detection (A), anti-VP3 for VP3 detection (B), anti-VP0 detection (C) anti-p39 for p39 detection (D). Primary antibodies were detected with horseradish peroxidase-conjugated secondary antibodies (Polyclonal Goat Anti-mouse Immunoglobulins/HRP, P0447 for A and D and Polyclonal Goat Anti-rabbit Immunoglobulins/HRP, P0448 for B and C) and detected by chemiluminescence, ChemiFast. The white area apparent in the 32kDa band in blot (A) indicates the antigen detection is over the exposure limit. Protein molecular makers are shown to the left of the gel (M) and are in kilodaltons. Bolt™4-12% Bis-Tris Plus Gels (ThermoFisher) and BLUeye Pre-Stained Protein Ladder (GeneFlow) were used.

3.2.3 Confirmation of P1 cleavage by the 3C_{EV71} protease

The data in Figure 3.5 indicated that the P1 precursor of all PV serotypes can be processed by the 3C_{EV71} protease. To confirm that this specificity was the result of 3C protease activity alone, the processing in insect cell was assessed following infection by Bac-PV1P1 (without 3C_{EV71}), which expresses unprocessed P1 and Bac-PV1P1-3C (with 3C_{EV71}), which produced cleaved viral proteins. The expressed PV proteins were detected by WB as before. Both High Five and *Sf9* cells infections were analysed, along with insect cells only as mock infection and infection by Bac-GFP as infection control. Cells were harvested and processed at 3 days p.i. WB analysis presented in Figure 3.6 shows that the anti-VP1 mAb detected P1 in both *Sf9* and High Five lanes at the predicted molecular weight of 100kDa (lanes at left of gel). When the 3C_{EV71} protease is present however, P1 is cleaved into VP1 (Figure 3.6A lanes at right of gel). The p39 image (Figure 3.6B) indicates that baculovirus infection was somewhat less for the 3C expressing viruses although this does not detract from the conclusion that PV P1 processing is the result of co-expression with P1 of the EV71 3C protease.

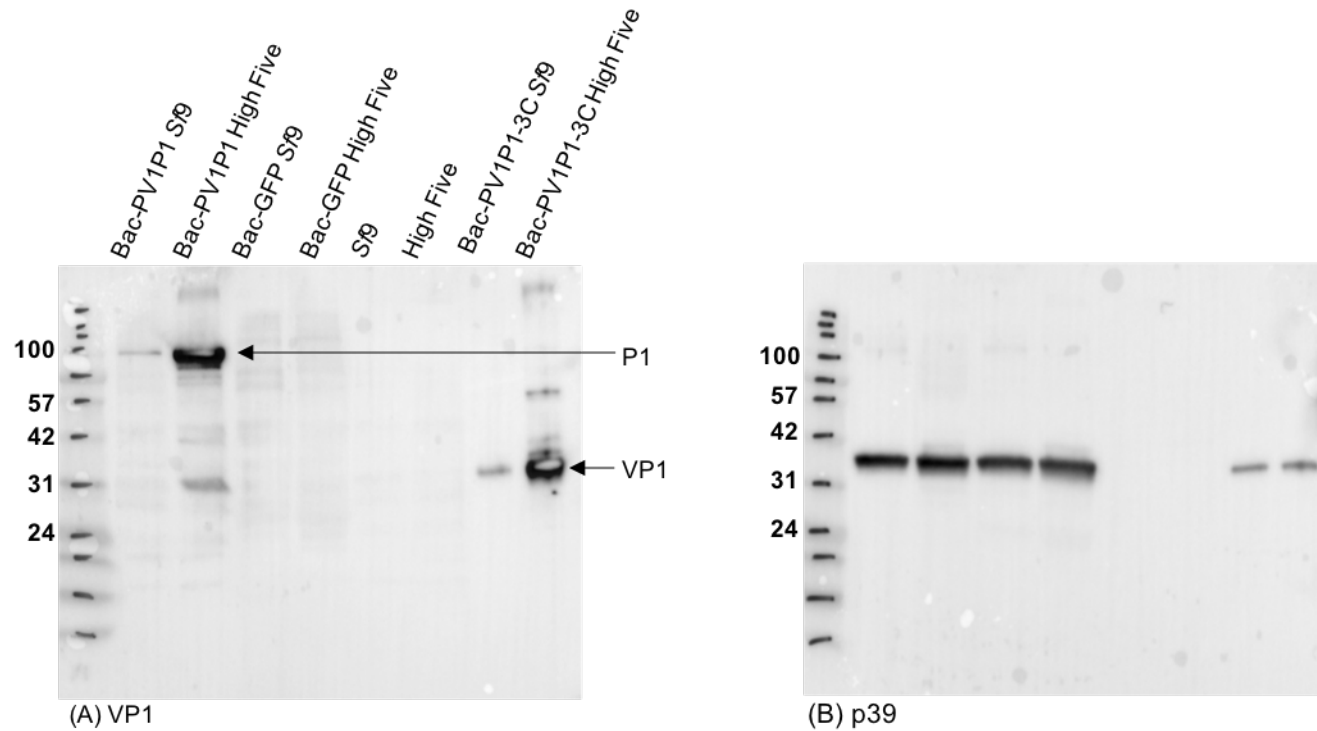


Figure 3.6. WB analysis demonstrating Ab specificity with *Sf9* and High Five cells infection with Bac-PV1P1, Bac-PV1P1-3C and Bac-GFP (3 d.p.i)

(A) VP1 detection. Bac-PV1P1-3C lane, MAB8566 showed a faint 100 kDa band which corresponds to the expected size of P1. In Bac_PV1P1 High Five lane, a higher intensity 100 kDa band was observed as well as a faint ~32 kDa band which is consistent with the theoretical VP1 size. Bac-PV1P1-3C High Five lane showed a high intensity ~32 kDa band. Bac-PV1P1-3C also indicated antigen detection at ~32 kDa at lesser intensity than one in High Five cells. Bac-GFP *Sf9*, Bac-GFP High Five, *Sf9* and High Five lanes showed minimum non-specific binding. (B) p39 detection indicating the baculovirus infection level. Protein molecular makers are shown to the left of the gel (M) and are in kilodaltons. Bolt™4-12% Bis-Tris Plus Gels (ThermoFisher) and BLUeye Pre-Stained Protein Ladder (Geneflow) were used.

To confirm further the role of EV71 3C protease in PV P1 cleavage, WB antigen detection was used to assess expression of P1 and P1 + EV71 3C protease in the presence of the inhibitor Rupintrivir (formally AG7088). This compound binds irreversibly to the cysteine in the 3C active site. Rupintrivir is effective for all HRV strains (Binford *et al.*, 2007; Dragovich *et al.*, 1998) and for is also effective for EV71 due to 3C sequence homology with rhinovirus 3C (Binford *et al.*, 2005). *In vitro* study with mammalian cell expression has shown that the 3C inhibition occurs without cytotoxicity (Lee *et al.*, 2008) suggesting that similar concentrations of drug can be used to investigate the 3C_{EV71} activity inhibition by Rupintrivir during PV P1 proteolytic cleavage in insect cells. Accordingly, small-scale infection using Bac-PV1P1-3C in the presence of various concentrations of Rupintrivir were prepared and the infected Sf9 cells were analysed by VP1 and P1 detection on WB at 3 days post infection as described in 2.3.2.

WB of the samples showed the highest reactivity to unprocessed P1 at 330nM Rupintrivir, decreasing to no detectable P1 at 0nM of drug. A 75kDa band may indicate partial P1 cleavage by a cellular protease at all Rupintrivir concentrations (Figure 3.7A). In contrast, the anti-VP1 image (Figure 3.7B) showed no VP1 detection in the 330nM and 33nM Rupintrivir lanes. As Figure 3.6 showed the anti-VP1 mAb binding ability to P1, 33nM Rupintrivir or higher may be cytotoxic for insect cells unlike in mammalian cells. VP1 was present at Rupintrivir concentrations lower than 3.3nM. These data confirm that PV P1 proteolytic processing into mature viral proteins is 3C_{EV71} dependent in insect cells.

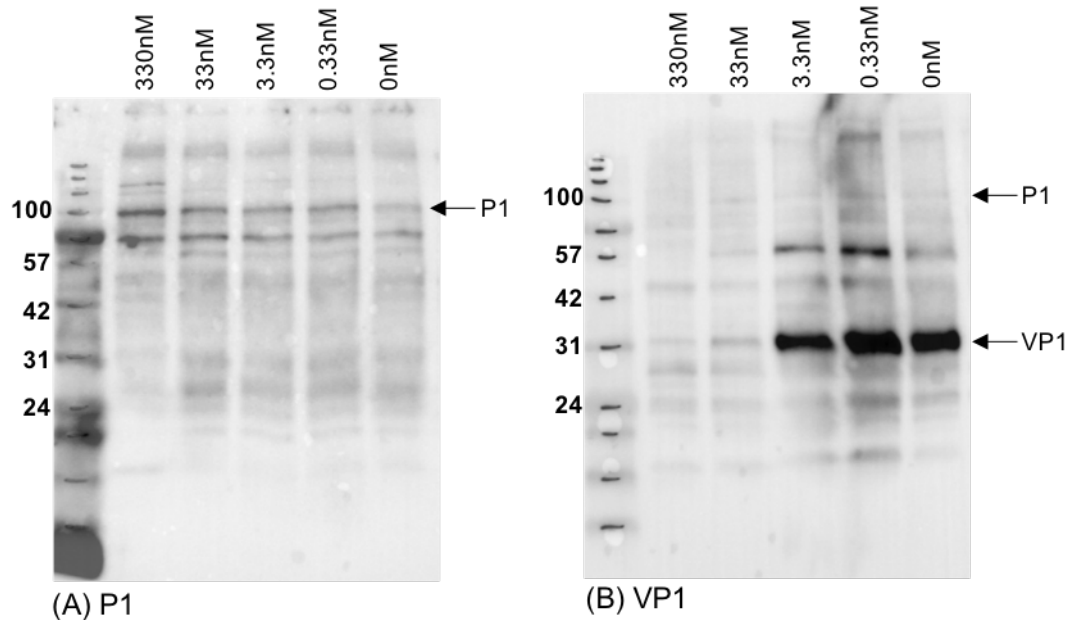


Figure 3.7. WB analysis for presence of P1 and VP1 of Bac-PV1P1-3C infected *Sf9* cells (3 d.p.i) in various Rupintrivir concentration.

(A) Rabbit anti-PVP1 sera detected P1. The reactivity was highest at 330nM Rupintrivir and lowest at no Rupintrivir present. Reactivity at ~75kDa was seen though the serial dilution. (B) MAB8566 mAb detection of VP1 was poor at the concentration of 330nM and 33nM Rupintrivir. At the concentration of 3.3nM and lower, VP1 was detected. Markers to the left (M) of the gels are in kilodaltons. Bolt™4-12% Bis-Tris Plus Gels (ThermoFisher) and BLUeye Pre-Stained Protein Ladder (Geneflow) were used.

3.3 PV VLP assembly

Following PV viral protein expression in all insect cell types, the self-assembly of those viral proteins was analysed using well-characterised methods in order to identify assembled virus-like particles. In this project, ultracentrifugation, imaging by super resolution confocal microscopy, gSTED, and transmission electron microscope (TEM) were employed.

3.3.1 Ultracentrifugation

In order to investigate PV VLP assembly in the insect cells, velocity ultra-centrifugation in which sucrose is used as a medium was used to identify the assembled, 80S-like empty PV capsid, if present. The insect cell culture size was scaled-up to 1L and infection done with the Bac-PV1P1-3C as per 2.3.3. It was followed by non-ionic detergent based cell lysis and a 2 step ultracentrifugation process; a 30% sucrose cushion to remove impurities which are smaller than the PV VLPs, and 15%-45% sucrose gradient to band VLPs at the expected sucrose

concentration away from other molecules (section 2.5). After 16h centrifugation, 1ml fractions from the top of the gradient were taken and 30 μ L of each fraction was mixed with SDS loading buffer for SDS-PAGE, followed by transfer to the PVDF membrane and analysis by VP1 detecting WB (section 2.6). The aggregate found at the bottom of the tube was resuspended in a volume of PBS equal to the lysate load.

Figure 3.8 shows that a VP1 band was present in lanes from the 30%-35% sucrose concentration which is the characteristic of naturally occurring PV empty capsid migration following sucrose velocity separation. A faint VP1 band was observed in the 20% and 25% sucrose fractions which could represent non-fully assembled VLPs i.e. PV protomers or pentamers. The faint VP1 band in the 40% zone may be the result of aggregation at the bottom of the tube which was visible in lane P. Together the data in Figure 3.8 suggested the assembly of the PV VLP in insect cells using baculovirus expression system.

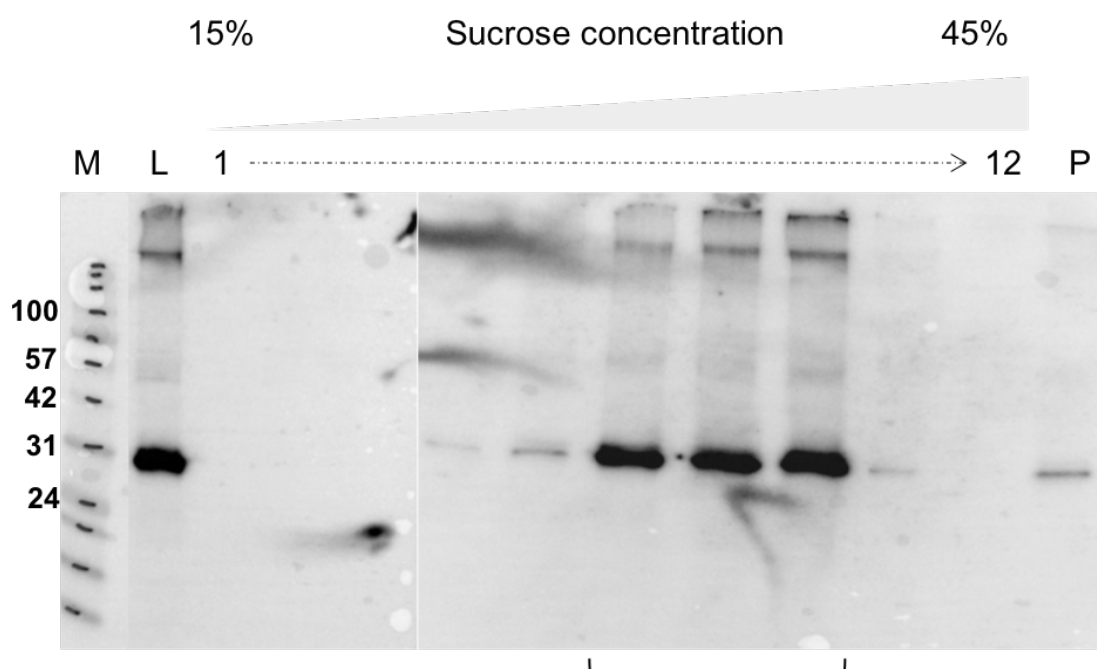


Figure 3.8. WB analysis using VP1 antibody for sucrose velocity separation (linear 15-45% sucrose gradient) fractions from Bac-PV1P1-3C infected High Five cells culture

Fractions containing top of gradient (15% sucrose) to the bottom of gradient (45% sucrose) were run across 2 gels. The result image is composite of the gels. VP1 band (~32 kDa) appeared from 30% sucrose to 35% (indicated) sucrose concentration. Faint VP1 bands occur in the 20%, 25%, 40% sucrose and lane P (pellet resuspension) lane were visible. Lane L is for insect cell lysate load for this ultracentrifugation. Protein molecular markers (lane M) are shown to the left of the gel and are in kilodaltons. Mini-PROTEAN TGX Any kD gel (BIO-RAD) and BLUEeye Pre-Stained Protein Ladder (Geneflow) were used.

3.3.2 gSTED imaging of VLPs and P1 in insect cells

Following the WB gradient result suggesting PV VLP assembly (Figure 3.8), visual confirmation of the assembled VLPs was desirable. Super resolution gSTED microscopy achieves a magnification and resolution suited for imaging particles within a single insect cell. For the imaging, High Five cell infections with Bac-PV1P1-3C and Bac-PV1P1 were prepared in glass-bottomed 35mm sterile dishes as before. The sample preparation is detailed in 2.7.1. At 2 days post infection the Bac-PV1P1-3C and Bac-PV1P1 infected cells were fixed and processed for immunolabelling with anti-VP1 antibody and anti-P1 serum respectively. Primary antibody binding was detected by fluorophore conjugated secondary antibodies. Anti-mouse Oregon green 488 antibody was used for anti-VP1 antibody and anti-rabbit antibody, STAR440SXP for anti-P1 sera.

Figure 3.9 revealed an enlarged nucleus in the centre of the insect cells which is a typical cytopathic effect among baculovirus infected cells and abundant globular particles scattered in the cytosol for Figure 3.9A and linear filamentous or aggregated signal for Figure 3.9B. Judging from the distinctive imaging patterns, the globular 488 fluorescence is likely to represent PV VLPs and the filamentous aggregate unassembled P1 PV polyproteins. The substantial change in image based on the presence or absence of the 3C protease in the expressing construct suggested that the gSTED images also support the self-assembly of the viral proteins into the VLPs within expressing insect cells.

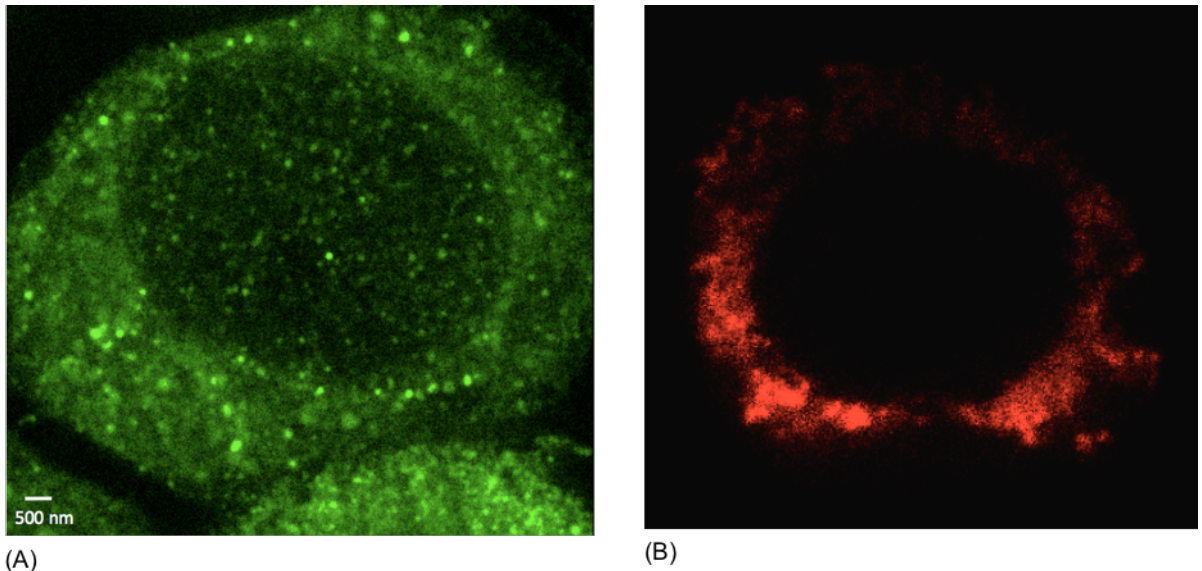


Figure 3.9. gSTED images for single High Five cells infected with (A) Bac-PV1P1-3C and (B) Bac-PV1P1 which are labelled with the fluorophores

(A) The cell was immunolabelled with MAB8566 and then Oregon Green 488. In the cytosol, numerous fluorophore labelled globular structures were found. (B) anti-P1 rabbit sera and STAR440SXP was used for P1 imaging. Filamentous or aggregated structures were immunolabelled. Both cells showed enlarged nuclei as a result of the baculovirus infection.

3.3.3 TEM imaging

TEM imaging is traditionally used for virus visualisation as images can show the size and state of particles, for example if they are regular assemblies. Empty capsids and virus particles have a distinguishing appearance which again supports the fact of capsid assembly in this study. Direct imaging of the peak fractions from the gradient (Figure 3.8) would confirm the presence of empty PV capsid. The pooled peak fractions were concentrated for EM grid preparation as described in 2.7.2. Figure 3.10 showed one PV empty particle and unknown structures smaller than the particle, possibly polymerised actin. The particle size of ~36nm is somewhat large for PV VLPs (expected size 30nm) but the particle could be “expanded” and the stain penetration gives the characteristic appearance of a PV empty capsid suggesting VLP production. In chapter 5, improved PV VLPs purification methods are discussed which reduce background and boost yields to visualise more PV VLPs.

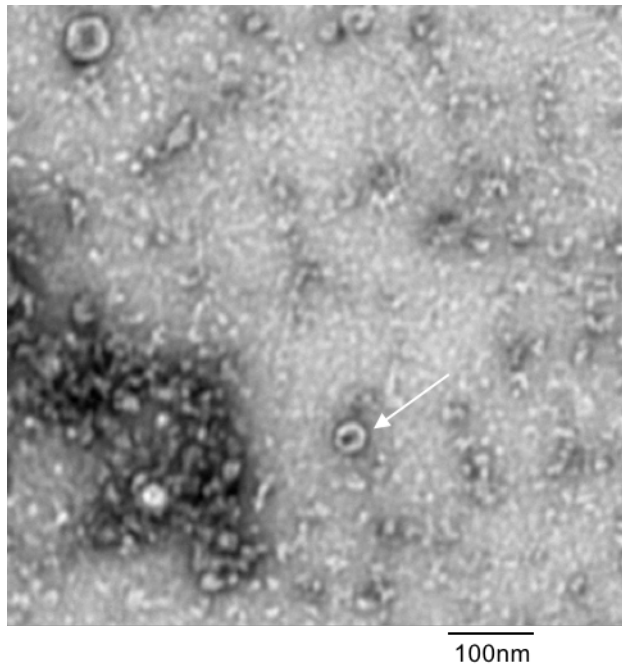


Figure 3.10. TEM image of concentrated sucrose gradient fractions (40% sucrose zone from Figure 3.8)

White arrow indicates the VLP sized 36nm with negative staining. Fragmented structures which are smaller than the VLP as also present. 2 % uranyl acetate was used as stain on a carbon coated formvar copper grid (Agar scientific).

3.4 VLP yield optimisation

3.4.1 Cleavage efficiency enhancement in transfer vector

Figure 3.10 indicated the presence of the PV VLP, however the yield was low. In order to increase the VLP production, the optimum protease choice for the transfer vector was investigated. As the protease used for P1 proteolytic processing has been largely 3CD historically, the function in the host lab setup (baculovirus expression system with single transfer vector to express P1 and its protease which is 3C_{EV71} rather 3C_{PV}) was tested. Four different expression vectors pOPINE Mahoney P1_2A_3CDWT, pOPINE Mahoney P1_2A_3CDΔ, pOPINE Mahoney P1_2A_FS_3CDWTFS and pOPINE Mahoney P1_2A_FS_3CDΔFS were constructed following the method described in 2.2.1. These constructs append the PV 3CD protease to the P1 polyprotein either as the WT or non-processed forms and with or without an intervening frameshift sequence. Figure 3.11 shows cartoons of the cassettes used in the expression vectors. After their transfection and production of recombinant baculovirus as described, small scale infection using Sf9 cells were carried out (2.3.2) and the expression products at 2 days post infection analysed by WB for VP1 and P1 as before and as described in 2.6.



Figure 3.11. Schematic representation for 3CD transfer vector cassettes

The serine insertion for at 3C-3D junction is denoted with Δ . The colour scheme was maintained the same as for Figure 3.1 and Figure 3.3.

WB analysis of the *Sf9* cells infected with Bac-PV1-3CDWT, Bac-PV1-3CD Δ , Bac-PV1P1-3CDWTFS, Bac-PV1P1-3CD Δ FS and Bac-PV1P1-3C (positive control) were carried out along with *Sf9* cells (negative control) using VP1 antibody (Figure 3.12A) and P1 sera (Figure 3.12B). Figure 3.12A showed a ~32kDa band which is likely to be VP1 visible for Bac-PV1-3CDWT and Bac-PV1-3CD Δ . The intensity is much lower than VP1 reactivity in infections by the previously described Bac-PV1P1-3C. The lanes also showed reactivity at 100kDa band which is possibly P1, ~42 kDa, ~50kDa and ~26kDa. The latter 3 reactivities do not fit to the size of 3CD partially processed P1 and are possibly cellular protease degradation products. The reactivity at both P1 and VP1 indicated that 3CD is acting as a protease capable of processing P1 to some degree but the efficiency is much lower than that observed with the modified $3C_{EV71}$. There was no obvious reactivity for Bac-PV1P1-3CDWTFS or Bac-PV1P1-3CD Δ FS. WB analysis for P1 (Figure 3.12B) showed a similar detection pattern although reactivity for processed VP1 was lower than with use of the VP1 serum in Figure 3.12A. The distinctive difference was reactivity at ~155kDa which fits with the predicted P1+3CD size for Bac-PV1-3CDWT, Bac-PV1-3CD Δ , Bac-PV1P1-3CDWTFS and Bac-PV1P1-3CD Δ FS. The results suggested that use of the PV 3CD protease or its non-cleaved variant with this

particular configuration of P1 and protease did not improve the level of VP1 synthesis and in turn would not increase the PV VLP yield although it should be noted that none of samples were purified and visualised. The choice of the protease for further chapters therefore remains 3C_{EV71} with a down regulation mutation S128A preceded by the HIV-1 frameshift.

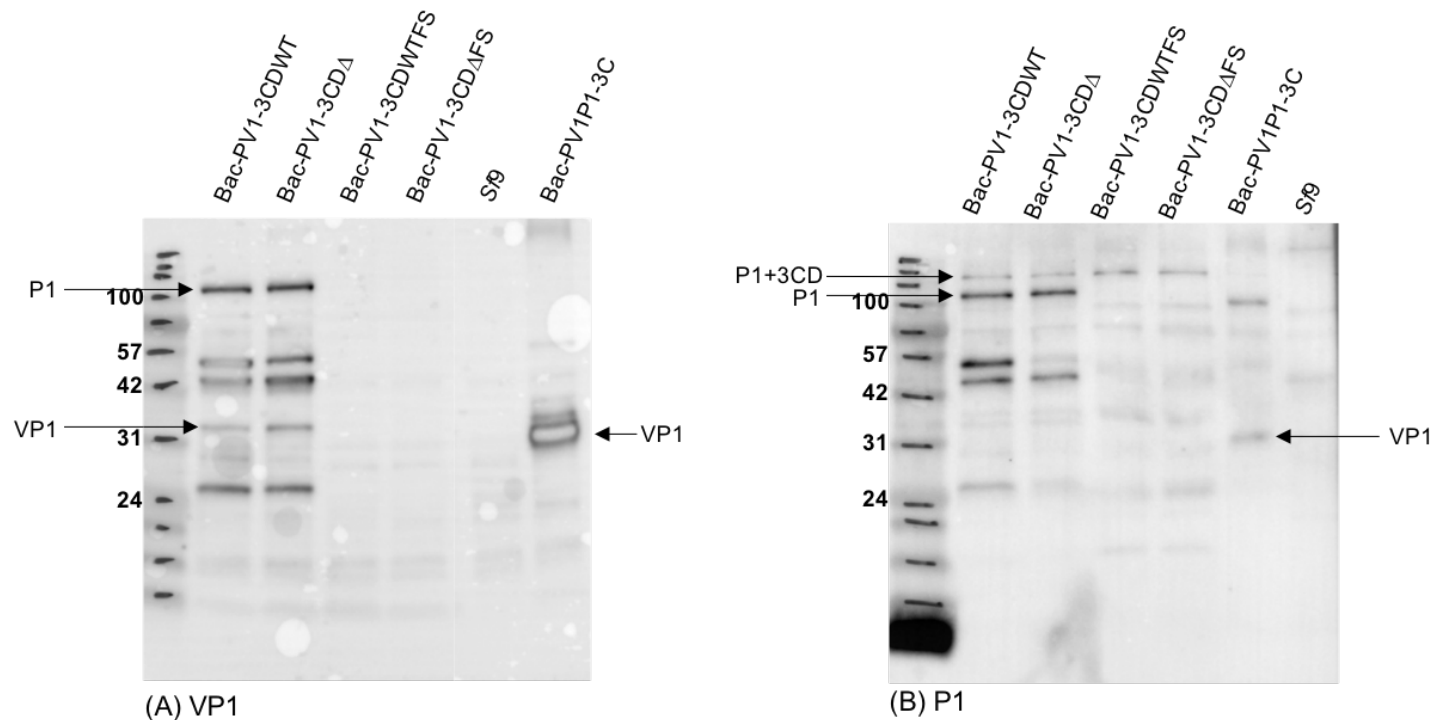


Figure 3.12. WB analysis by (A) VP1 antibody (MAB8566) and (B) P1 sera (Rabbit sera) for 3 d.p.i. of *Sf9* cells infected with Bac-PV1P1-3CDWT, Bac-PV1P1-3CD Δ , Bac-PV1P1-3CDWTFS or Bac-PV1P1-3CD Δ FS

(A) Bac-PV1P1-3CDWT and Bac-PV1P1-3CD Δ showed a similar pattern and level of expression. Bands corresponding to the expected size of uncleaved P1 (~100kDa) and its processed products, VP1 (~32kDa) were visible as well as ~55 kDa, ~50kDa and ~26kDa reactivity. The VP1 band intensity in Bac-PV1P1-3CDWT and Bac-PV1P1-3CD Δ was much lower than Bac-PV1P1-3C indicating lower protease activity. There was no evident band for Bac-PV1P1-3CDWTFS, Bac-PV1P1-3CD Δ FS and *Sf9*. (B) Reactivities at ~42 kDa, ~50 kDa and ~100 kDa (P1) occur in Bac-PV1P1-3CDWT and Bac-PV1P1-3CD Δ at similar intensity as (A). A band at ~26kDa appears on the lanes, but the intensity is lower. In addition, there was reactivity at ~150 kDa (P1+3CD) in the lanes. The reactivity also occurred in Bac-PV1P1-3CDWTFS and Bac-PV1P1-3CD Δ FS lanes indicating inefficient protease cleavage. Protein molecular markers are shown to the left of the gel (M) and are in kilodaltons. Bolt™4-12% Bis-Tris Plus Gels (ThermoFisher) and BLUeye Pre-Stained Protein Ladder (Geneflow) were used.

3.5 Discussion

The minimal picornavirus components necessary for capsid assembly, as described by others, were used here in a single transfer vector consisting of P1, 2A and modified 3C, designed to provide equimolar expression of each mature viral protein and lead to the self-assembly of the VLPs in insect cells. The balanced expression of PV P1 and a functional protease, EV71 3C, ensured the equimolar expression of mature viral proteins and is achieved by the presence of the HIV-1 frameshift signal and a mutation in 3C (S128A). The HIV-1 frameshift controls ribosome translation efficiency and while most of the translation products terminate after P1-2A translation, 5% of ribosomes are able to translate the full of P1-2A-FS-3C sequence resulting in protease production. The introduced mutation at S128A for 3C_{EV71} was shown previously to lower toxicity without compromising the P1 processing function (Figure 3.1). The homology between 3C_{EV71} and 3C_{PV} as shown in Figure 3.2 also supports its use to cleave mature PV viral proteins from the P1 precursor. Three reference strains (but a thermostable mutant for PV3 Skt SC8 as described in chapter 1) of PV P1 were introduced into the existing EV71 expression cassette (Figure 3.3) and all shown to cleave P1 into VP0, VP3 and VP1 (Figure 3.4 and Figure 3.5) although there were differences in the expression levels observed. 3C_{EV71} processing was investigated by comparing P1 expression alone with that of P1-3C and Figure 3.6 showed that, without the protease, P1 remained as an unprocessed protein. Further, the addition of Rupintrivir, a broad picornavirus 3C inhibitor, inhibited P1 cleavage (Figure 3.7). These data confirmed the ability of 3C_{EV71} to process PV P1 in the insect cell expression system. The self-assembly of cleaved viral proteins into PV empty capsids was also investigated. WB analysis of fractionated lysates obtained following ultracentrifugation showed VP1 reactivity in the 30-40% sucrose part of the gradient (Figure 3.8). As naturally occurring empty PV particles sediment in similar sucrose concentrations, these were likely to be self-assembled into empty PV capsids, and this was supported further by gSTED imaging of single insect cells infected with Bac-PV1P1-3C which showed distinctive punctate loci in the cytosol (Figure 3.9). Cells infected with Bac-PV1P1 showed only diffuse staining consistent with unprocessed antigen. Figure 3.9 indicates that the viral proteins self-assembled to the VLPs with the distinctive images. Figure 3.10 showed only one particle with the typical stain penetration appearance and a

measured diameter of 36nm, somewhat large for a PV VLP. However, picornavirus particles can undergo expansion in the procapsid (Cifuentes *et al.*, 2013) or post receptor binding state (Belnap *et al.*, 2000) leading to the conclusion that this could be a single example of *bona fide* PV VLP. Clearly further preparations with better yield will be needed to improve this. As part of such improvements, VLP yield improvement through the use of an alternate protease, the PV 3CD protease, was investigated. PV 3CD^{prol} has been widely used for recombinant PV empty capsid expression, although not in the context of the cassette system used here. Wild type PV protease 3CD (3CDWT) and a mutated 3CD^{pro}, which prevents 3C-3D autocleavage (3CD Δ), were tested. In addition, to mimic the cassette in use, the HIV frameshift sequence was added to both proteases (3CDWTFS and 3CD Δ FS). Although the expression study analysis by WB using the antibody against VP1 showed some P1 cleavage into VP1 (32kDa) in Bac-PV1P1-3CDWT and Bac-PV1P1-3CD Δ infected cells, reactivity was much less than the Bac-PV1P1-3C (the EV71 3C carrying S128A) expressed VP1. For Bac-PV1P1-3CDWTFS and Bac-PV1P1-3CD Δ FS, there was no visible reactivity (Figure 3.12A). This result suggested that 3CDWT or 3CD Δ were not as efficient as proteases as the regulated 3C_{EV71} in the insect cell expression, at least not in the genetic configuration used here. When WB was done with a rabbit serum detecting P1 a band consistent with the expected molecular weight of P1+3CD was present in Bac-PV1P1-3CDWT and Bac-PV1P1-3CD Δ infection in addition to the bands detected by the VP1 serum. However, in Bac-PV1P1-3CDWTFS and Bac-PV1P1-3CD Δ FS infected cells only P1+3CD was detected (Figure 3.12B). The results may suggest that 3CD levels were too low in this case to ensure further processing despite the equivalent cassette allowing efficient protease processing in the case of P1 and 3C_{EV71}. The protease origin, EV71 vs PV, could have a role in this difference or perhaps the large 3CD enzyme needs to be made at a higher level to be active. In a particular timeframe, less 3CD protease is available for P1 proteolytic processing compared to 3C_{EV71}, simply as translation takes longer. Whatever the reason, these results indicate that the regulated 3C_{EV71} was the most suitable protease for future infection experiments.

In conclusion, novel constructs were designed for PV VLP production in the insect cell expression system. The chapter demonstrated the synthesis of viral proteins and their self-

assembly into PV VLPs. Although gSTED imaging indicated abundant PV VLP production, further improvement in the purification protocols are needed to obtain higher PV VLPs yields.

Chapter 4 Poliovirus capsid protein expression and assembly in *Saccharomyces cerevisiae*

4.1 Introduction

Mature PV viral protein (VP0, VP1 and VP3) synthesis and their self-assembly into VLPs in insect cells was shown in chapter 3. The expression was achieved by the single baculovirus expression vector which harbours the structural polyprotein, P1, a linker sequence derived from 2A, a unique HIV-1 frameshift sequence and a modified protease, 3C_{EV71}. The production of EV71 VLP (Cone, 2015) and PV VLP in insect cells demonstrated that P1-2A-FS-3C_{EV71} cassette system did not show cellular toxicity as it was seen in FMDV VLP production without 3C down regulation and brought about equimolar amounts of each viral protein by equivalent cleavage at each mature protein junction, resulting in PV VLP assembly. However, even though a variety of purification methods were attempted there was some difficulty to repeatedly purify VLPs and often no or low numbers of particles were visible under TEM. The presence of baculovirus nucleocapsids was also a confounding factor. As a result, it was of interest to search for other expression platforms for VLP production, particularly those that did not depend on the use of a virus vector. Yeast cell expression systems offer the combined benefits of eukaryotic and prokaryotic expression system. This system still has the simplicity of bacterial culture preparation and low cost but does not have the disadvantages of eukaryotic cell culture: inconvenience, low yield and high maintenance. In addition, expression in yeast cells is able to produce recombinant proteins with post-translational modifications which may be essential to produce functional proteins. For example, the binding of eukaryotic chaperones such as HSP90 and GSH has been suggested to be important for some picornavirus assembly (Jiang *et al.*, 2014). The benefits of yeast cell expression for vaccine production has been demonstrated by the success of products for HBV and HPV, both of which have been approved for human use (Bill, 2015). Accordingly, *Saccharomyces cerevisiae* is an attractive expression system for VLP products.

The concept of empty PV capsids as a vaccine drew researchers' attention in the early 1990s when PV VLPs were produced in mammalian cells (Ansardi *et al.*, 1991), insect cells (Urakawa *et al.*, 1989) but also yeast cells (Jore *et al.*, 1994). Jore *et al.* (1994) demonstrated the assembly of PV VLPs in *S. cerevisiae* by co-expression of a P1 vector and a 3CD vector, both cloned into yeast replicating vectors, also known as autonomously replicating sequence (ARS) vectors. The vector contained the inducible *GAL* promoter and following induction, VP0, VP1 and VP3 were shown to be produced and self-assemble into empty particles. However, when competition immunoprecipitation assay was done, it showed that the produced VLPs were of the H (Heated) conformation of capsid which is unsuitable for vaccine use. It is important to note that the sequences used for all expression studies at that time were wild type. There was no data on the selection of more stable variants or the use of structure based mutants that might alter conformation. In a subsequent study, Rombaut and Jore (1997) succeeded to produce the N (Native) conformation of empty capsid by supplementation with the antiviral compound, Pirodavir, to the yeast culture and throughout the purification steps, allowed the conversion of the H antigenic VLPs to N antigenic VLPs, with the level of conversion related to the level of drug added. Immunisation of mice demonstrated that yeast origin VLPs purified in the presence of Pirodavir elicited anti-N antibodies in neutralisation assays.

In this chapter, the yeast expression experiment was revisited using the same expression cassette that produced VLPs in insect cells (chapter 3). Following an investigation of PV VLP synthesis in yeast cells, a number of lysis and purification techniques were assessed; including a cell disruptor and sucrose gradient banding. Any VLP present were assessed by antigen distribution on sucrose gradients by WB and by visualisation under TEM.

4.2 Yeast expression system

For this study, Dr Yuko Morikawa, Kitasato University, Japan gifted a strain of *S. cerevisiae*, RAY3A-D (*MATa/α ura3/ura3 his3/his3 leu2/leu2 trp1/trp1*) and a yeast expression vector pKT10 as this combination of vector and host had proved successful for the expression of HIV VLPs (Sakuragi *et al.*, 2002).

4.2.1 RAY3A-D

S. cerevisiae RAY3A-D (*MATa/α ura3/ura3 his3/his3 leu2/leu2 trp1/trp1*) was first used by Ruggieri *et al.* (1989) and has since been used as the host strain for recombinant protein expression. The genotype indicates the dominant (upper case) and recessive (lower case) genes in the yeast strain (Tropp, 2012). For instance, RAY3A-D has *MATa/α* gene, however it lacks *URA3*, *HIS3*, *Leu2* and *TRP1* genes. *MATa/α* is the mating type of the yeast cells. The propagation of *S. cerevisiae* has two modes; vegetative budding and mating. The former mode is used by haploid cells containing either *MATa* or *MATα*. The mating types are controlled by 2 different alleles of mating type (*MAT*) locus. *MATa* and *MATα* fuse together to produce *MATa/α* diploid cells when mating. *S. cerevisiae* is normally found as stable diploid cells. In nature, the diploid cells are produced in response to the low nutrition environment when cells carrying opposite mating type aggregate and stick together. Haploid budding is arrested and finger-like tips are extended from the opposite mating type cell to fuse (Landry *et al.*, 2006; Tropp, 2012).

The rest of the genotype indicates the common genes used for selection. Yeast expression in *S. cerevisiae* has historically used auxotrophic selection rather than the antibiotic selection used in bacteria because of a high frequency of antibiotic resistant mutations and low antibiotic efficacy in some strains of yeast. 'Auxotrophy' is defined as the incapability of an organism to produce an essential component of their nutrient requirement (Patrick, 2014). This deficiency in the synthesis is due to the lack of the genes which encode the necessary enzymes. Typical genes used for selection in *S. cerevisiae* are *URA3*, *HIS3*, *Leu2* and *TRP1*. The designation and numbers indicate the particular genetic locus (Tropp, 2012). The *URA3* gene encodes orotidine-5-phosphate decarboxylase, an enzyme which contributes to pyrimidine ribonucleotide synthesis (*Saccharomyces* Genome Database, 2016; Umezu *et al.*, 1971). The other genes similarly encode for the enzymes involved in the synthesis of amino acids; *HIS3* (L-histidine), *Leu2* (L-leucine) and *TRP1* (L-methionine) (Pronk, 2002). With the lack of those genes, the auxotrophic strains of yeast fail to grow in simple media unless a copy of a functional gene is added to restore the ability to encode the biosynthetic enzyme. If the host cell acquires an expression vector with a relevant gene, the recombinant yeast cell is now able to synthesise the nutrient and can survive in a medium lacking that particular nutrient. Host cells without the

relevant gene cannot grow (Patrick, 2014). For RAY3A-D, the genotype indicates that it lacks 4 genes, therefore it grows only when the media is supplemented with uracil, histidine, leucine and methionine or in rich media, such as YPD.

4.2.2 pKT10

pKT10 has a *URA3* gene as a selective marker, the 2 μ plasmid for replication and a constitutive promoter and terminator derived from the glyceraldehyde-3-phosphate dehydrogenase (GAPDH) gene (Morikawa *et al.*, 2007; Tanaka *et al.*, 1990) as shown in Figure 4.1. pKT10 is classified as a YE_p (yeast episomal plasmid) vector and also contains bacterial plasmid DNA for DNA manipulation and plasmid purification in *E. coli* (Curran & Bugeja, 2000). The *URA3* gene acts as the auxotrophic marker and restores ODCase activity to synthesise uracil. Transformed yeast are selected in media without uracil allowing positive selection against yeast cells which have not gained the expression vector (Jones, 1992; *Saccharomyces* Genome Database, 2016). Due to its 2 μ backbone, pKT10 is maintained at 50 to 100 copies per haploid genome in yeast cells (Berlec & Strukelj, 2013; Maloy, 2004) providing some gene dosage effect. The GAPDH gene promoter is chosen for pKT10 because of its high level of constitutive activity, a factor in vector efficiency (Curran & Bugeja, 2000). Heterologous termination sequences are often not recognised by *S. cerevisiae* resulting in unstable extremely long mRNAs and to avoid this issue a yeast terminator, the termination sequence of GAPDH, is present at the 3' end of the inserted gene as is usual for YE_p vectors (Curran & Bugeja, 2000).

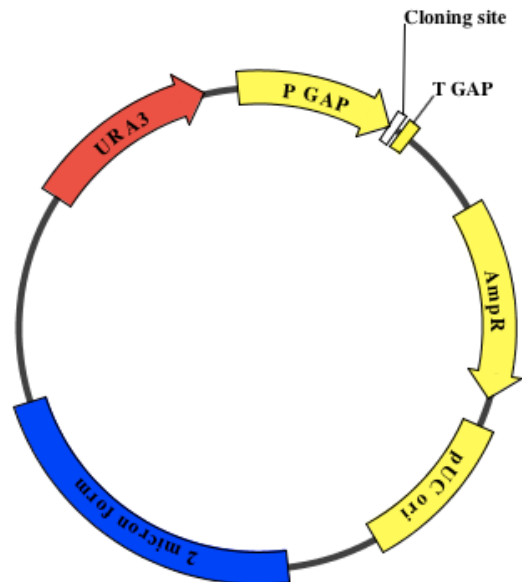


Figure 4.1. *S. cerevisiae* expression vector, pKT10 schematic representation produced by DNA dynamo

The vector consists of URA3, 2 μ form, pUC ori, ampicillin resistance, and GAPDH promoter and terminator. URA3 and 2 μ maintain the recombinant plasmid in yeast to express foreign protein using GAPDH promoter and terminator. pUC origin and ampicillin resistance genes are essential for simplified DNA cloning in *E. coli*. The vector was gifted by Dr Yuko Morikawa

4.2.3 Yeast cell wall disruption

For the recovery of recombinant protein expressed in yeast cells, it is essential to disrupt yeast cells efficiently. The yeast cell wall is known for its robust structure. The cell wall mainly consists of mannoprotein and fibrous β 1, 3 glucan, with a minor portion including β 1,6 glucan and chitin which also contribute to its structure. The β 1,3 glucan and chitin complex form the yeast inner cell wall, the glycosylated mannoproteins the outer cell wall and the β 1,6 glucan holds the inner and outer cell walls together. This three layered structure gives a packed structure and limits cell permeability (Lipke & Ovalle, 1998) but is a challenge for subsequent purification. Accordingly, a cell disruptor was assessed for cell lysis in which 10 ml of compacted yeast cells was pressurised within 5 seconds, a mechanical force that ruptures the cells. The advantage of the cell disruptor was the wide choice of the pressure; 10 MPa to 410 MPa and once a suitable pressure was found, the result should be repeatable. One consideration for this lysis method was that the sample temperature should not rise due to pressurising. As the PV VLPs are not thermostable, this method could be challenging and any assembled VLP conformation could be altered or disassembled by the process. The sample

temperature was therefore constantly monitored during the lysis and processing. Synthesis of viral proteins and their assembly into VLPs

4.2.4 Expression vector cloning

To examine the possibility of PV VLP assembly in yeast, a suitable yeast expression vector was constructed. The cassette, consisting of a contiguous sequence encoding P1 (PV1 Mahoney) and 3C, with various control elements, was explanted from the insect cell expression vector described in chapter 3 and cloned into the pKT10 yeast cell expression vector to produce RAY3A-D-PV1-3C. The cloning procedure is detailed in section 2.2.1. In brief, the expression cassette (P1-2A-FS-3C_{EV71}) was amplified by PCR with a forward and reverse primer which each introduced unique restriction sites (*EcoRI* and *StuI*) found in the MCS of pKT10. The PCR product was digested with the requisite enzymes and inserted into pKT10 using the same restriction sites. The schematic representation of expression vector is shown in Figure 4.2. The final plasmid was sequenced to confirm the desired construction. The vector was then transformed into the RAY3A-D strain of *S. cerevisiae* using the LiAc method (Herskowitz, 2012). The transformed cells were selected on synthetic defined (SD) media agar lacking uracil. After several days of incubation at 30 °C, colonies were visible whereas the plating of non-transformed cells gave no colonies. To confirm the transformants, colonies were grown in small scale (10mls) and any episome present extracted using a yeast plasmid extraction kit. Extracted vector was then transformed back into competent *E. coli* cells and those transformants again grown for plasmid isolation. The recovered vector was assessed by restriction digest and selected samples were sent for DNA sequencing. All transformants had *bona fide* yeast PV vectors as initially designed. The complete process is summarised in Figure 2.2 in section 2.4.1.

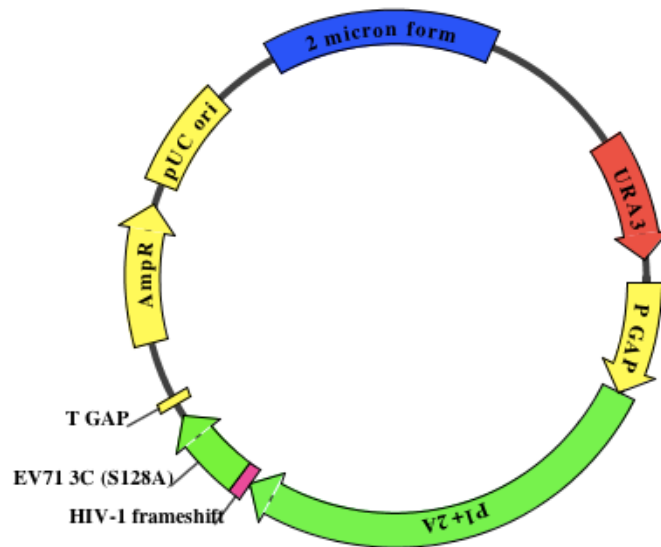


Figure 4.2. Schematic representation of PV1 VLP expression vector (RAY3A-D-PV1-3C) based on pKT10 produced by DNA dynamo

PV VLP cassette consisting of P1-2A-HIV-1 frameshift-modified 3C_{EV71} was inserted into pKT10 cloning site which was shown in Figure 4.1.

4.2.5 Viral protein expression

Once transformation into RAY3A-D was confirmed, an expression analysis for the presence of PV antigen was carried out. Following overnight growth in YPD media recombinant yeast cells were disrupted by alkaline extraction (Kushnirov, 2000) which denatures the entire cell and its contents as described in section 2.6.1. The alkaline extract was analysed by SDS-PAGE and the separated proteins processed for western blot. PV1 VLP expressing insect cells were included as a control. Figure 4.3 shows PV antigen detection by anti-VP0 rabbit sera by WB. The image showed a sharp band at ~40kDa in PV1 yeast lanes which co-migrated with a band present in the insect cell origin PV1 VLPs. No band at ~100kDa was observed, suggesting the efficient proteolysis of P1 and background reaction was generally low. This result suggested that PV antigen expression and its cleavage by 3C was occurring in yeast cells.

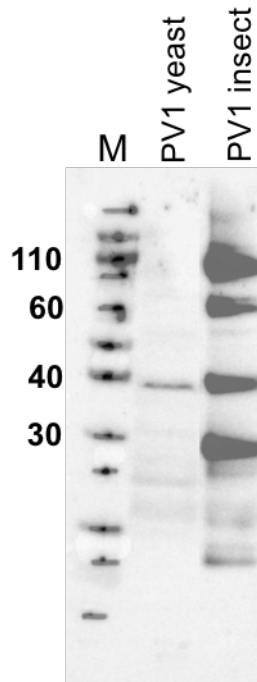


Figure 4.3. WB analysis by VP0 detection using anti-VP0 rabbit sera following post-alkaline extraction of RAY3A-D-PV1-3C

A sharp band at ~40 kDa corresponding the species corresponding VP0 molecular weight was seen in the PV1 yeast lane. PV1 insect lane showed reactivity at various sizes. ~100kDa band may indicate P1 partial proteolytic processing. Protein molecular markers are show to the left of the gel (M) and are in kilodaltons. Bolt™4-12% Bis-Tris Plus Gel (ThermoFisher) and Novex™ sharp pre-stained protein standard (ThermoFisher) were used.

4.2.6 Assembly of PV VLPs in yeast cells

As processed antigen was present in the selected transformants, one isolate was grown at larger scale for the assessment of PV antigen size in solution. To do this 100ml of culture was grown to 1.04 OD₆₀₀U/ml and prepared as described in 2.4.2. The harvested cell pellet was lysed by cell disruptor (2.5.1) with the temperature monitored throughout the process. Once lysis was complete, unbroken cells and large debris was removed by centrifugation (15000rpm for 30 minutes at 4°C) and the clarified sample was purified further by ultracentrifuge, first by sedimentation through a 30% sucrose cushion and then by sedimentation of the resuspended pellet on a 15%-45% linear sucrose gradient, carried out at 21000rpm, 4°C for 16h using a SW40 rotor. Details of the procedure are as described in 2.5.2. The gradient was fractionated manually from the top by taking 1ml samples from the meniscus and 30µL of every 1ml fraction were analysed on WB as before using an antibody to VP1.

Figure 4.4 shows the distribution of VP1 throughout the 15%-45% linear sucrose gradient. No western blot signal was present at the top or bottom of the gradient in keeping with the pre-banding cushion step which selects for high MW antigen. While some non-specific bands were detected throughout the gradient the most prominent feature is a ~30kDa band in fraction 5 and in fractions 7-9. The peak intensity found in fraction 7-9 corresponds to a sucrose concentration of around 35% while the more minor peak in fraction 5 corresponds to ~25% sucrose. Clearly, VP1 as a soluble monomer or assembled into a VP1-VP0-VP3 (MW ~100 kDa) protomer would be insufficiently large to enter the gradient so this banding pattern suggests that VP1 antigen expressed in yeast cells following cleavage of the P1 precursor is assembled into larger molecular weight complexes. These large MW complexes could include pentamers (MW ~500kDa) in fraction 5 and fully assembled VLPs (MW ~6000kDa) in fractions 7-9.

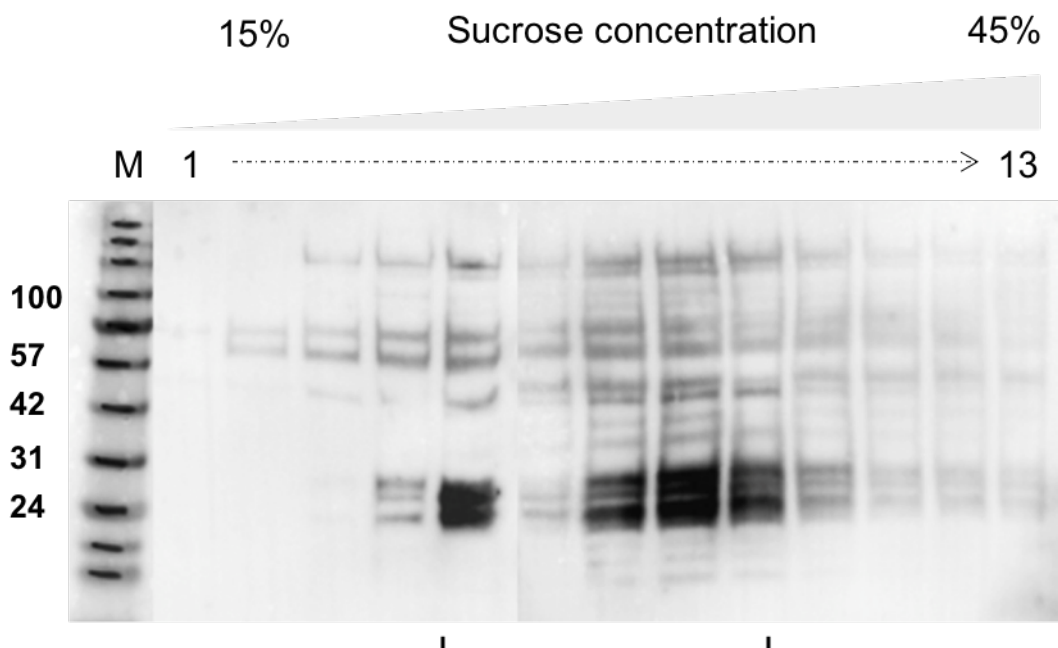


Figure 4.4. WB analysis for presence of VP1 following RAY3A-D-PV1-3C lysis on 15-45 % sucrose gradient using anti-VP1 (MAB8566, Millipore)

A total of 13 fractions were analysed on 2 gels which have been merged here. The prominent reactivity is at ~30kDa in fractions from the middle of the gradient (indicated) corresponding to a sucrose concentration of ~35% consistent with empty PV capsids. VP1 reactivity in fraction 5 may represent banding of protomer or pentamer subunits. Higher MW bands at ~ 60kDa could be VP3-VP1 intermediates. Protein molecular markers are shown to the left of the gel (M) and are in kilodaltons. Bolt™4-12% Bis-Tris Plus Gels (ThermoFisher) and BLUeye Pre-Stained Protein Ladder (Geneflow) were used.

However, as Figure 4.4 also showed various bands detected by the anti-VP1 Ab, consistent with some degradation of VP1, a further round of purification was completed. To do this, the peak fractions, 7-9, were pooled together and the concentration of sucrose reduced by a three-fold dilution with PBS. The sample was then loaded onto a second sucrose gradient, again developed by centrifugation at 21000rpm, 4°C for 16h using the SW32 rotor. The procedure is detailed in 2.5.2. The gradient was fractionated from the top of the tube as before, producing 40 fractions, and alternate fractions were analysed by SDS-PAGE and western blot as before. The WB analysis for VP1 detection is presented in Figure 4.5. The WB images showed a similar detection pattern by the anti-VP1 Ab to the fractions from the first gradient with VP1 detection in fraction 12 to fraction 30. Some VP1 was seen in fraction 40, possibly due to aggregation as this was the fraction containing the pellet formed at the bottom of the tube. The pattern of VP1 detection reflected that in the first gradient; a minor peak in fraction 15 and a more major spread peak in fraction 22 to 24. As before the 2nd peak was around 35% consistent with a high molecular weight assembly containing VP1, plausibly VLPs.

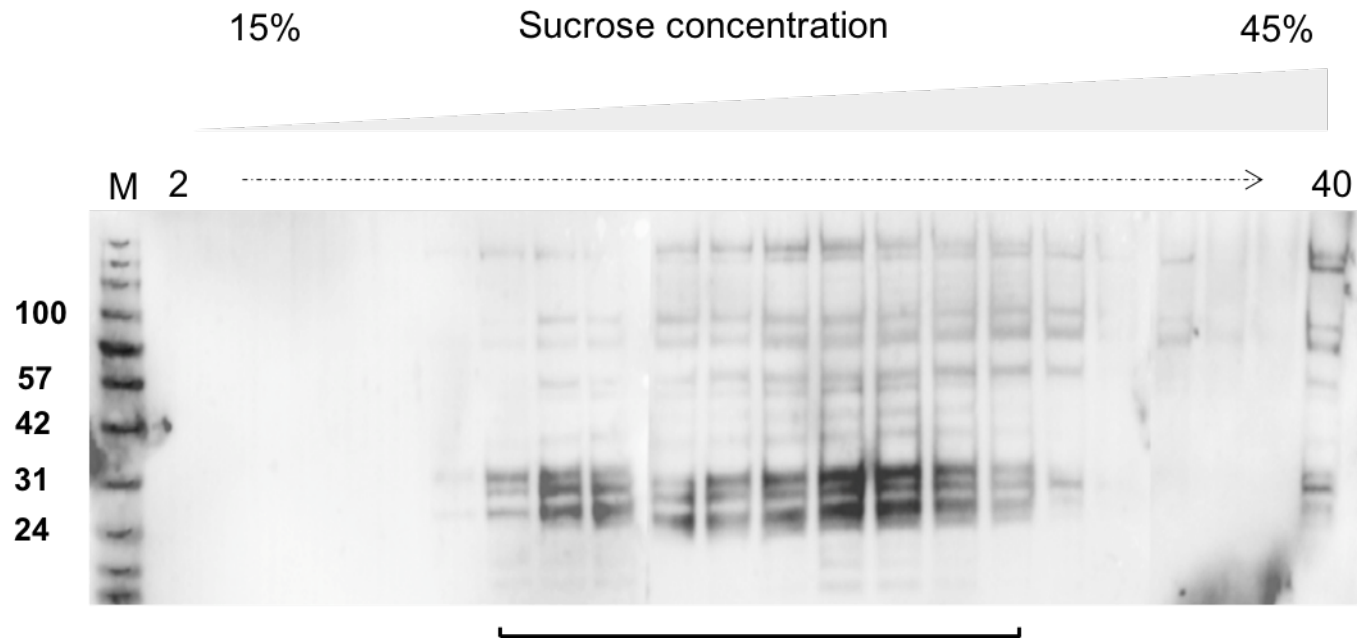


Figure 4.5. WB analysis using VP1 antibody (MAB8566, Millipore) following 2nd 15%-45% sucrose gradient for lysed RAY3A-D-PV1-3C

Fractions 7-9 of Figure 4.4 were pooled and applied as the sample. 1ml fractions were taken from the top of the tube after the ultracentrifugation. Alternate fractions except fraction 14-18 (every fractions) were run on 3 gels. The resultant blot image is a composite of these. Reactivity at ~30 kDa occurs in fractions 14 to 30 (indicated). Reactivity in fraction 40, the bottom of the gradient including the pellet, may indicate aggregation. Protein molecular markers are shown to the left of the gel and are in kilodaltons. Bolt™4-12% Bis-Tris Plus Gels (ThermoFisher) and BLUeye Pre-Stained Protein Ladder (Geneflow) were used.

4.2.7 TEM imaging of purified PV VLPs

Ultracentrifugation suggested the assembly of PV VP1 antigen into a species corresponding to molecular weight broadly in the same range as that shown for 80S PV VLPs in the sucrose gradient (Jiang *et al.*, 2014). As a result, the most obvious technique to confirm the presence of VLPs would be direct visualisation. Accordingly, the peak fraction (fraction 23 from the second gradient) was prepared following the method described in section 2.7.2.

Figure 4.6 shows TEM images for fraction 23 which contained particles with the dimensions expected of poliovirus empty capsids with average size of 46.7nm. The background image also displayed globular forms, possibly assembly intermediates or particles that had broken as a result of the TEM preparation methods as well as some large cells debris. From this image, VLP seem to be present although the TEM was indistinct and the level of intactness uncertain. This was encouraging but indicated the need for improvement in the culture condition, the lysis and the purification method if VLPs for PV assembled in yeast were to be confirmed.

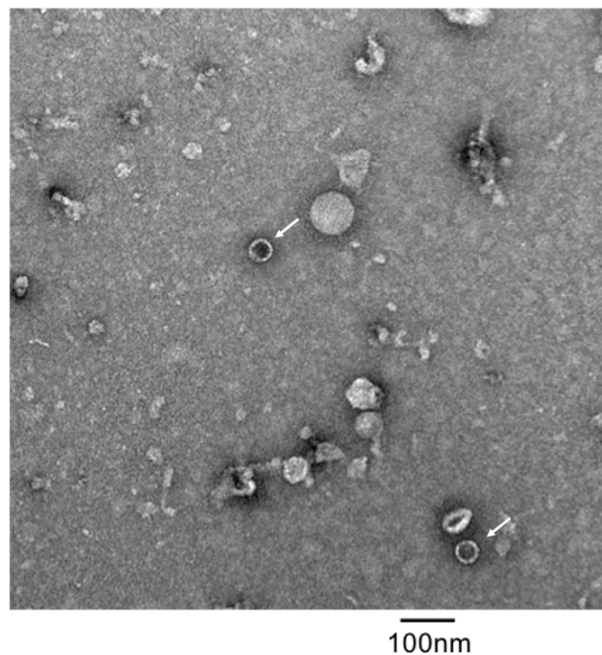


Figure 4.6. TEM imaging for negatively stained VLP of RAY3A-D-PV1-3C , 2nd 15-45% sucrose gradient, fraction 23

Fraction 23, a peak fraction from Figure 4.5 showed two VLPs which is indicated with arrows. Globular forms which are at lower half image and debris are also present in the fraction. The average VLP size was 46.7 nm. 2 % uranyl acetate was used as stain on a carbon coated formvar copper grid (Agar scientific).

4.3 Discussion

Following difficulty in the separation of VLPs from baculovirus capsids following expression in insect cells, a yeast expression system for the production of PV VLPs was explored. PV VLP synthesis in *S. cerevisiae* was first shown by Jore *et al.* (1994) but the VLPs produced were of the H conformation, which does not induce protective immunity in mice. Subsequently, the same authors produced VLPs of the N conformation following expression in *S. cerevisiae* by the addition of a "pocket" binding drug which was discussed in chapter 1 (Rombaut & Jore, 1997). These publications demonstrated that the yeast cytoplasm was a suitable environment for the assembly of VLP but, surprisingly, no follow-up study has been done on PV VLP production in *S. cerevisiae*. With improvements in biotechnology, this platform for PV VLPs production should be investigated further. For our in-house expression system in *S. cerevisiae*, the cassette system used for insect cell expression was introduced in the expression vector, pKT10. Following its transformation into a laboratory strain of *S. cerevisiae*, RAY3A-D to produce RAY3A-D-PV1-3C, the synthesis of viral proteins from P1 by 3C protease was analysed. PV related proteins appeared to be synthesised as both WB analysis with anti-VP0 sera indicated antigen of the expected molecular weight (Figure 4.3). Analysis for the self-assembly of PV VLPs was carried out by sucrose gradient after cell lysis was carried out by the cell disruptor. The antigen detection pattern for the sucrose gradient fractions (Figure 4.4 and Figure 4.5) peaked in the mid fractions of the gradient, although evidence of considerable degradation was present with bands detected at 35kDa – 30kDa, and this pattern matched the distribution of naturally occurring 80S empty PV VLPs in sucrose gradients suggesting self-assembly into VLPs. Concentrated peak fractions from the sucrose gradient under TEM confirmed the presence of capsid like structures (Figure 4.6) although the size is larger than the expected corresponding size of 30nm. These two findings indicated the assembly of the VLPs although the number of VLPs found by TEM imaging was low, possibly associated with either transient heating during lysis or the degradation of the VP1 signal seen on western blot. Nevertheless, VLP production in yeast strain RAY3A-D using the cassette system previously constructed for baculovirus expression but moved into yeast expression vector pKT10 has

repeated the work published by Jore *et al.* (1994) although improvements in the purification method will be needed to enhance VLP yield.

Chapter 5 Optimisation of PV VLP purification

5.1 Introduction

In chapter 4, PV1 wildtype Mahoney VLP purification from yeast cells was carried out using a cell disruptor which revealed some broken PV VLP with a homogenous background that, consistent with the numbers and sizes, were suspected to be protomers and pentamers (the initial and intermediate assembly units of picornavirus capsids). While yeast expression may be useful therefore, the implication that PV VLP were disassembling during the purification method suggested this might not be the most suitable extraction procedure for PV VLPs. Hence, an improvement in the yeast cell lysis method was required. For yeast cell preparation, numerous methods have been published. Amongst these are methods in which the cells are homogenized by high pressure, by glass bead vortexing or by enzymatic lysis. In order to find the most suitable method for yeast cell lysis to obtain good quality PV VLP several of these purification methods were assessed. Both cell disruptors and bead-beaters utilise mechanical forces to physically break the cells. Lyu *et al.* (2015) showed the production of antigenic EV71 and EV71/CAV chimeric VLPs from *S. cerevisiae* using high pressure homogeniser. Rombaut and Jore (1997) succeeded to produce PV VLPs from *S. cerevisiae* using bead-beating although sample vortexing was also supplemented with detergent. For the experiments described here, the lysis method described by Kim *et al.* (2010) was adapted for PV VLPs using a bead-beater, the FastPrep-24™ with Lysing Matrix C (the type of bead used). When mechanical force is used to lyse a sample heat is produced as a by-product and as PV VLPs have thermostability issues (the N and H antigenic forms), the heat generated during lysis has to be monitored to minimise the possibility of VLP damage. For this, the cell disruptor was equipped with a cooling system as described by Lyu *et al.* (2015). Samples were pre-chilled in ice and also periodically during processing. Sample temperature was closely monitored during the process to prevent PV VLP disassembly. In addition to cell disruption by physical means a non-physical lysis approach was also assessed for PV VLP purification. A yeast cell wall lyticase, zymolyase, enabled the removal of the yeast cell wall to leave only the yeast plasma membrane. Zymolyase is derived from *Arthrobacter luteus* and hydrolyses the β -1,3 glucan

layer of the yeast cell wall to disturb its structure (Kitamura & Yamamoto, 1972). Figure 5.1 summarises the yeast cell wall structure and indicates the function of zymolyase. After the removal of the yeast cell wall, spheroplasts, which consist of membrane bound yeast cells in an isotonic solution, are produced. At this stage, membrane dissolution can be accomplished by gentle non-thermal cell disruption using N₂ decompression. Wang *et al.* (2014) reported a *S. cerevisiae* subcellular fraction which maintained its functional integrity using zymolyase and N₂ cavitation. The benefit of N₂ cavitation is that its operation temperature and gentle processing preserve sample function. In the process, N₂ gas is forced into solution inside cells in a pressurised chamber. When the pressure is suddenly released, the dissolved nitrogen comes out of solution as bubbles which expand the membrane and cell which eventually bursts (Parr Instrument Company, 2015).

In addition to the method of yeast cell lysis, improvements in PV VLP separation were also tested by switching to Nycodenz as the ultracentrifuge medium for isopycnic centrifugation rather than velocity gradients. In this method, particles undergo separation by differences in their buoyant density and particles migrate to the equilibrium point where their buoyant density and the gradient matrix density are equal. At this point, the isodensity level, the sample does not migrate any further (Mazzone, 1998).

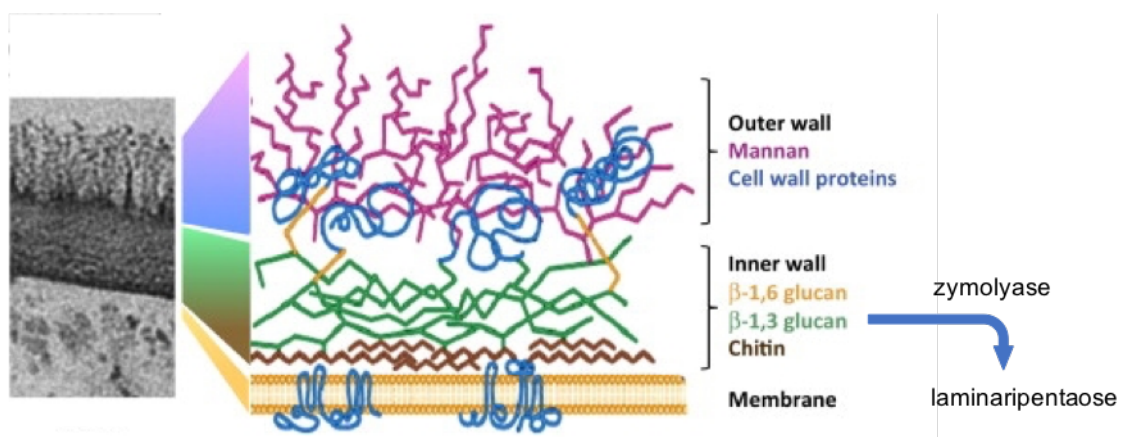


Figure 5.1. Schematic representation of common yeast cell wall composition and zymolyase function

Once yeast outer wall is weakened, zymolyase hydrolyses β-1,3-glucan and releases laminaripentaose. The Figure was modified from Brown *et al.* (2014).

In order to maximise the yield of stable PV VLPs by these various methods, a further change, the use of PV3 Skt SC8 as the P1 open reading frame in the expression vector, was also made during these experiments. PV3 Skt SC8 was already reported to produce more stable VLPs based on experiments making small amounts of empty VLPs in mammalian cells (Fox *et al.*, 2017) and larger quantities in plants (Marsian *et al.*, 2017). Their expression here was done as described for PV1 in chapter 4, essentially a change of the P1 region in the resident vector to produce *S. cerevisiae* producing PV3 Skt SC8 VLP, RAY3A-D-PV3SC8-3C. Finally, the yeast cell culture size was also increased to obtain higher amounts of PV VLPs. Yeast cell cultures were grown for 2 days as described in Lyu *et al.* (2015).

In all a total of 3 purification methods are assessed to decide the optimal method for PV VLP purification from yeast cells and the optimized methods used with PV3 Skt SC8 to obtain thermostable PV VLPs in higher amount. As an aside the purification method was also used for purification of VLPs from insect cells to discern if the VLP yields were improved.

5.2 Purification methods for Yeast cells

5.2.1 Cell disruptor method

Yeast cell expression cultures were prepared as described in 2.4.2. 2 L of RAY3A-D-PV1-3C liquid culture was grown overnight to ~2.0 ODU/ml as described in Lyu *et al.* (2015). The yeast cell pellet was resuspended in PBS pH 7.2, 1 mM PMSF, 1 mM β -mercaptoethanol and applied to the cell disruptor. The cells were pressurised to 1800 bar twice and the temperature of the sample exiting the cell disruptor was recorded. Then, NP40 was added to be final concentration of 1 % and incubated in ice for 1h after which the cells were centrifuged at 10000 rpm, 4 °C for 30 minutes to obtain the supernatant. PEG8000 to a final concentration of 8 % (w/v) and NaCl (to be 0.2 M) were added to the supernatant for PEG precipitation. The mixture was gently stirred at 4 °C overnight. The following day, it was centrifuged at 10,000 xg, 4 °C for 1 hour and the pellet was resuspended in PBS, pH 7.2. Following clarification, the supernatant was loaded onto a 30 % sucrose cushion and centrifugation carried out at 21,000 rpm, 4 °C for 16 hours. The pellet was resuspended as described in 2.5.2. After a clarifying spin, it was loaded onto a 10-30 % Nycodenz step gradient of 10 % increments, each layer 2.5

ml. The layered tube was centrifuged at 28,000 rpm, 4 °C for 3 hours using SW40 rotor. After the spin, the tube showed 2 visible bands, 1 band at the interface of sample load and the 10 % Nycodenz layer and 1 band between the 20 % and 30 % layers. 1 ml fractions were collected from the top except for the visible bands which was collected separately. These fractions were analysed by WB for PV VP1 detection. Figure 5.2 shows very faint VP1 detection in the PV standard lane at 35 kDa but neither of the bands at 75 kDa and 30 kDa visible on fraction 9-12 of the gradient blot image matched the VP1 band size indicated by PV standard. However the reactivity at Nycodenz concentration of 20-30 % is consistent with PV empty capsids. In general, PV empty capsids are obtained around the concentration of 25 % for Nycodenz rather 35 % for sucrose. Despite this size abnormality the peak fraction was observed under TEM following the method described in section 2.7.2. Figure 5.3 shows a very low level of VLPs found by TEM with typical VLP characteristics. Thus, despite an uncertain western blot assembled PV VLPs were found in the expected fractions by direct EM observation. However, yields were very low and it was concluded that physical disruption was unlikely to be a method of choice for VLP release without considerable further optimization.

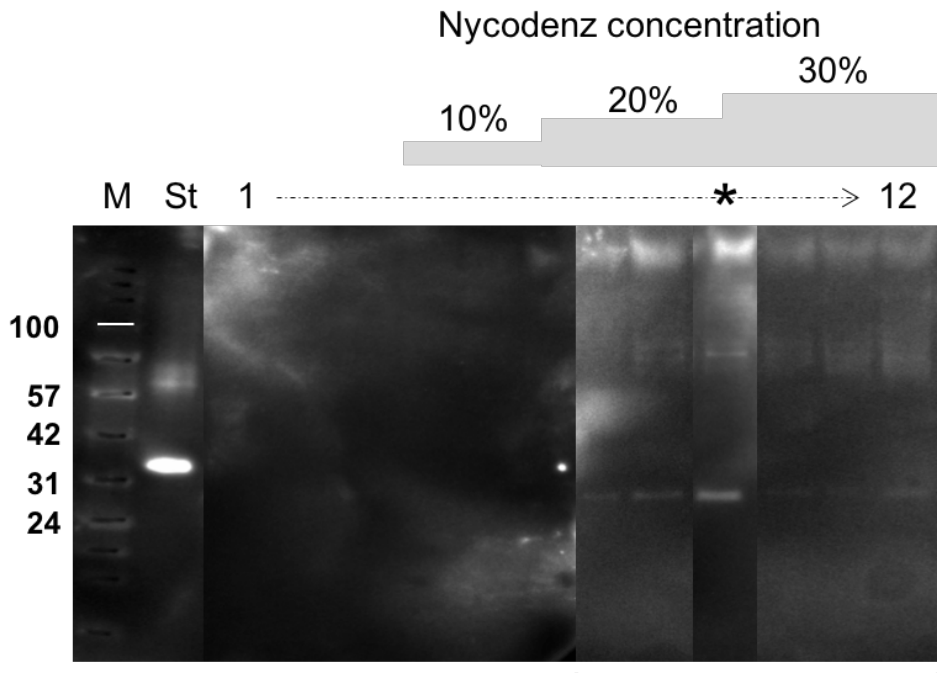


Figure 5.2. WB analysis of VP1 by MAB8566, Millipore following RAY3A-D-PV1-3C treatment with cell disruptor and nycodenz step gradient

A total of 12 fractions were analysed across 2 gels which are merged in this figure. Reactivity at ~30 kDa and ~75 kDa is visible at fractions 7 to 12 (indicated), peaking in fraction 9 which corresponds to a visible band layer at the 20%/30% interface. Protein molecular markers (M lane) are shown to the left of the gel and are in kilodaltons. St lane contains PV standard (European PV standard) which acts as a control for VP1 detection. Bolt™4-12% Bis-Tris Plus Gels (ThermoFisher) and BLUeye Pre-Stained Protein Ladder (Geneflow) were used.

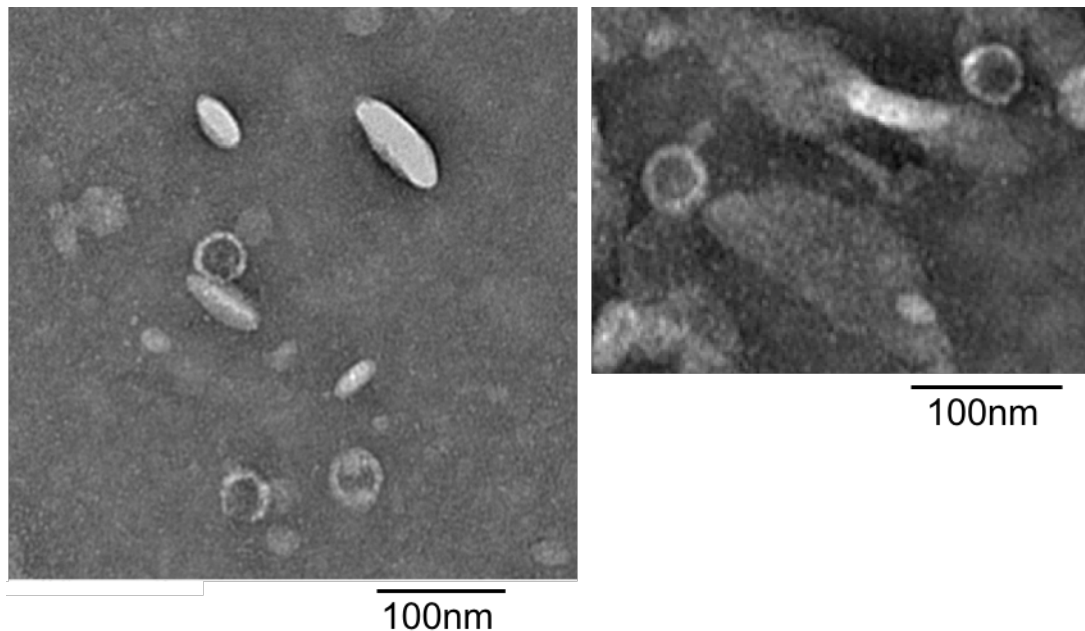


Figure 5.3. TEM image with negative staining of peak fraction of Figure 5.2.

The concentrated 20 % and 30 % nycodenz interface fraction which is indicated with * on Figure 5.2 was stained with 2% uranyl acetate prior to micrograph. (Left) One complete shape VLP which indicated by the penetration of stain and the morphology was seen in the centre with two more below, possibly damaged. (Right) Two further VLPs with some impurities. The average VLP size on the images is 37nm. 2 % uranyl acetate was used as stain on a copper grid with carbon coated formvar film (Agar scientific).

5.2.2 Bead-beater method

A 2L yeast cell culture was grown to 1.5 ODU/ml following the culture preparation explained in 2.4.2 and the method used was modified from the yeast cells lysis method of Kim *et al.* (2010). The cells (wet weight 8.6 g) were resuspended in ice-cold breaking buffer (section 2.1.8) at 1:1 ratio with the cell pellet wet weight. The resuspension was then transferred to MP bio Lysing Matrix C tubes and homogenization carried out for 8 times at 6.0 M/S for 30 seconds. The cells were rested for 5 minutes on ice between beat cycles to prevent a temperature rise. The pooled homogenate was centrifuged at 15000 rpm, 4 °C for 30 minutes and the supernatant applied to a 30 % sucrose cushion as before. The pelleted sample was dissolved in PBS pH 7.2 and the clarified sample was ultracentrifuged in 10-30 % Nycodenz gradients as described. The interface layers between the sample load and the 10 % layer as well as between the 20 % and 30 were collected and analysed as above.

TEM imaging was obtained from the 20-30 % interface (Figure 5.4). Only one VLP like particle was observed (Figure 5.4, left and right in different magnifications) and generally speaking,

both images have a white background which might suggest the grid was covered with an unknown material which obscured clear imaging. As the background was too high to determine true VLP assembly and there was uncertainty about the degree of temperature rise during the homogenization bead beating was abandoned as a likely final extraction procedure, at least for this scale of culture.

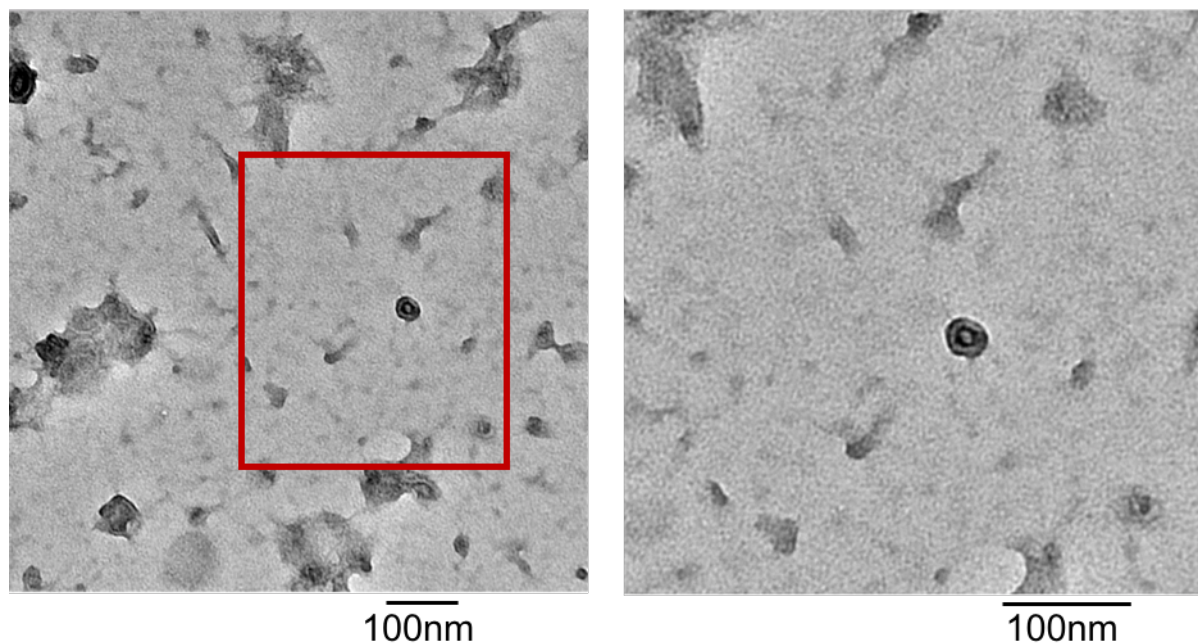


Figure 5.4. TEM image with negatively stained VLP of RAY3A-D-PV1-3C VLP purified with beads-beater and nycodenz gradient.

Figure 5.4 was prepared from 20 % and 30 % nycodenz interface. (Left) A particle holds VLP morphology and stain penetration was seen but it appears slightly compressed compared to VLP from Figure 5.3. (Right) The identical field image to the left at higher magnification. There is unknown material all over the grid. The size of this particular VLP is 30.4 nm. 2 % uranyl acetate was used as stain on a copper grid with carbon coated formvar film (Agar scientific).

5.2.3 Zymolyase and N₂ cavitation method

A 300 ml yeast cell culture was prepared as before to 1.5 ODU/ml. The procedure followed was based on Wang *et al.* (2014) with some modifications. The cell pellet (0.9 g wet weight) was washed in 10 ml PBS pH 7.2, 10mM DTT and finally taken up in 10 ml 1.2 M sorbitol and centrifuged again. The pellet was resuspended in 6 ml 1 M sorbitol, 1 mM EDTA, 10 mM sodium citrate and zymolyase 100T was added to the mixture at 5 µg/ml and then incubated at room temperature with rotation at 250 rpm for 1.5 hours. The sample was then centrifuged

and resuspended in 30 ml homogenization buffer (HM / section 2.1.8) and this process repeated once more. The resuspension was loaded into the N₂ cavitation vessel and incubated with nitrogen gas at 500 psi for 10 minutes and then at 350 psi for 10 minutes. After that the treated sample was clarified at 15,000 rpm, 4 °C for 20 minutes and the supernatant applied to a 30 % sucrose cushion and centrifuged at 28,000 rpm, 4 °C for 3 hours. The collected pellet was allowed to re-suspend overnight in PBS pH 7.2 and then clarified before being loaded onto a 10-30 % Nycodenz gradient and ultracentrifuged at 27,000 rpm, 4 °C for 3 hours. The resultant tube showed a 20-30 % interface band only. 1ml fractionation was done from the top of the tube and the interface band was concentrated (as per section 2.7.2) and visualized under TEM.

Figure 5.5 shows assembled VLP present in this fraction with a typical empty capsid staining pattern in each case, and a diameter of typically ~35 nm, broadly as expected for PV VLPs. Debris is also present but the background obtained from these images was much lower than that seen in Figure 5.4. At this point, this method seemed to be the most efficient purification method and could be applied to much larger culture volumes.

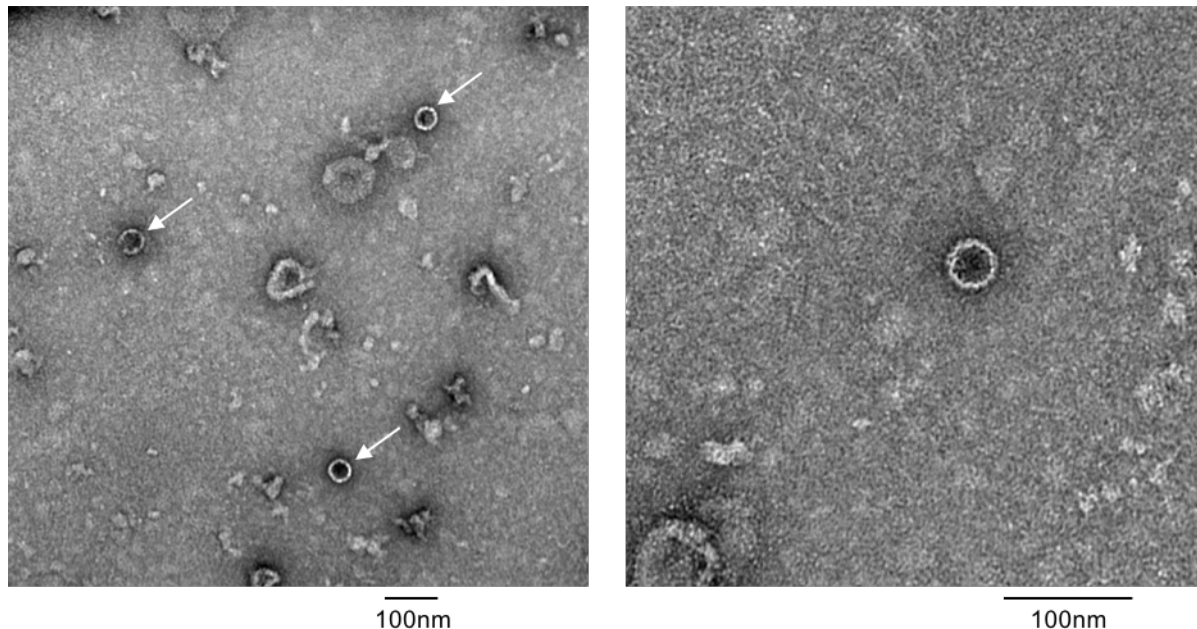


Figure 5.5. TEM imaging with negative staining of VLPs from RAY3A-D-PV1-3C prepared by zymolyase and N₂ cavitation method and nycodenz gradient.

Concentrated 20–30% nycodenz interface fraction was stained with 2% uranyl acetate for the microgram. (Left) PV VLP showing the negative staining of empty capsid. Three particles were imaged in total although one (on the left) appeared incomplete. (Right) TEM image at higher magnification. The capsid diameter is ~ 35nm. 2 % uranyl acetate was used as stain for copper grid with formvar carbon film (Agar scientific)

5.3 *S. cerevisiae* origin PV VLP yield optimization

In this section, PV VLPs prepared using the PV3 Skt SC8 sequence were extracted with zymolyase and N₂ cavitation or cell disruptor methods as described. To do this the plasmid pKT10 Saukett SC8 P1_2A_FS_3C_{EV71} was constructed by replacing the resident PV1 Mahoney sequence with that of Skt SC8 flanked with *EcoRI* and *StuI* (cloning explained in section 2.2.1). Once the plasmid was confirmed by sequence analysis, the PV3 expression vector was transformed into *S. cerevisiae* RAY3A-D and successful transformants re-extracted, transformed back into competent *E. coli* cells and plasmid preparation again done to confirm the transformation by DNA sequencing as described in 2.4.1.

5.3.1 PV3 VLP purification using zymolyase and N₂ cavitation method

A 2L liquid culture of PV3 Skt SC8 expressing *S. cerevisiae* was prepared to 2.3 ODU/ml which gave a 13.5 g wet weight pellet and processed as before - the procedural details are described in 2.4.2. The cell pellet obtained was processed using zymolyase and N₂ cavitation method as described but with small modifications to adapt the method to the culture size, that is larger volumes of buffer and the addition of a cComplete ULTRA EDTA-free protease inhibitor tablet prior to the loading of the sample into the N₂ cavitation vessel. Small fractions of cells were taken out before and after N₂ cavitation and examined by EVOS confocal microscopy to confirm cell lysis. The confocal microscopy image shows the typical yeast cell lysis using this method (Figure 5.6). The clarified lysis supernatant was ultracentrifuged as described earlier. The resultant centrifuge tube gave 3 distinct bands; a 1st interface between sample load and 10 % Nycodenz layer, a 2nd interface between the 10 % and 20 % layers and a 3rd interface between the 20 % and 30 % layers. 1 ml fractions were collected from the top of the tube except for the visible bands, which were taken separately. A pellet at the bottom of the gradient was also resuspended in PBS and stored.

The fractions from the Nycodenz gradient were analysed by VP1 WB (Figure 5.7). The image indicated detection of a high intensity band around 30 kDa in the middle of Nycodenz gradient as had been observed for Figure 5.2, although now more intense. In order to confirm the presence of PV VLP, TEM imaging for all 3 interfaces were carried out following the method described in section 2.7.2 (Figure 5.8). At each interface, lower magnification image is shown

on the left to illustrate the wider field to provide VLP number as well as purity. Whereas a higher magnification image (right) gives more accurate VLP size estimation. Grids of the 1st interface sample showed material of a size smaller than typical PV VLPs with few regular features while grids of the 2nd interface showed some PV VLPs present in a high background similar to Figure 5.4 with average size of 46.9 nm (+/- SEM = 4.01, n=10). The 3rd interface layer contained VLPs which have average VLP size of 32.5 nm (+/- SEM = 1.98, n = 6) and typical characteristics but also contained other debris. These images confirm the purification of PV3 Skt SC8 VLPs from yeast using a combination of enzymatic removal of the cell wall and gentle pressure induced lysis.

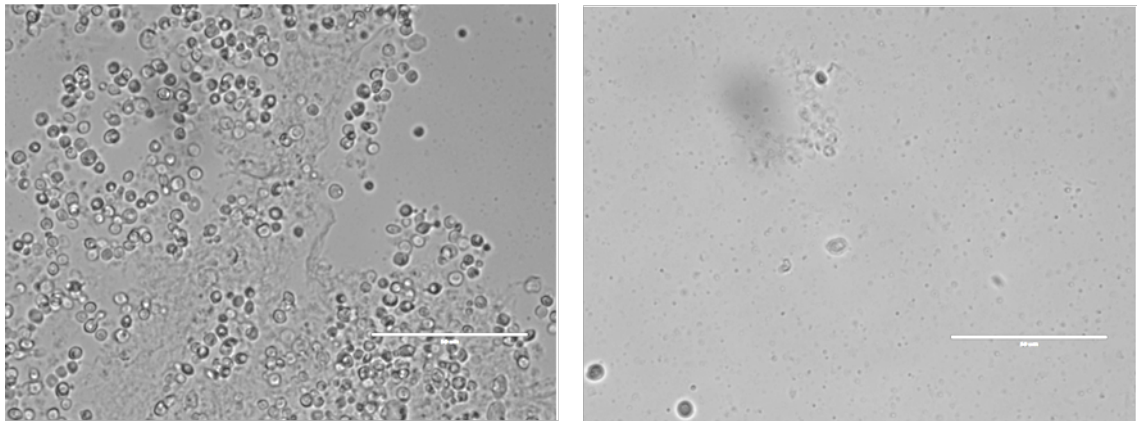


Figure 5.6. Confocal microscope (EVOS) image shows RAY3A-D-PV3SC8-3C cells break down by zymolyase and N₂ cavitation

(left) *S. cerevisiae* cells are still intact before N₂ cavitation. There were almost no RAY3A-D-PV3SC8-3C cells left post N₂ cavitation (right).

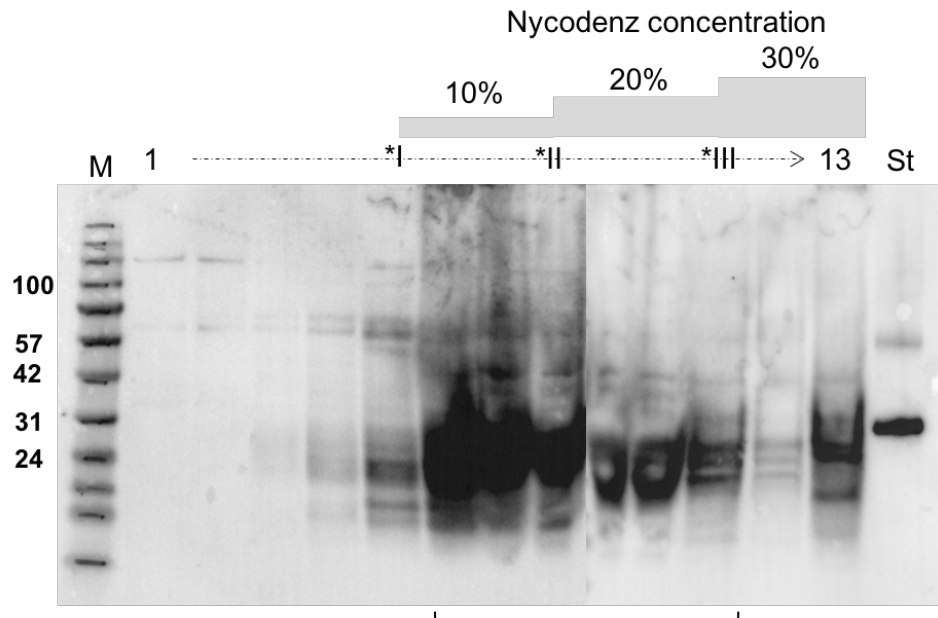
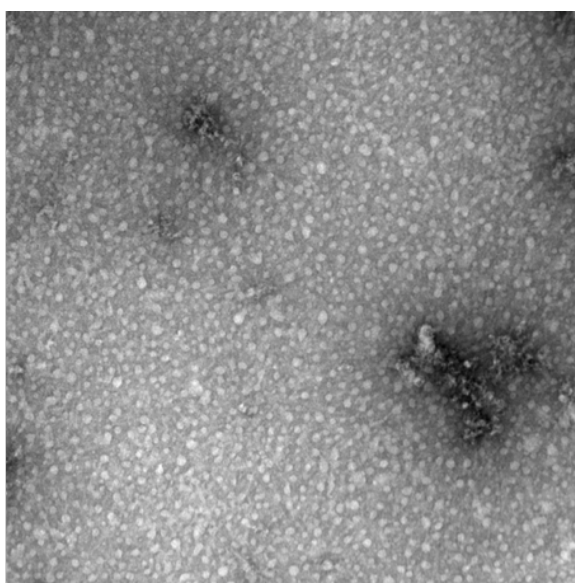
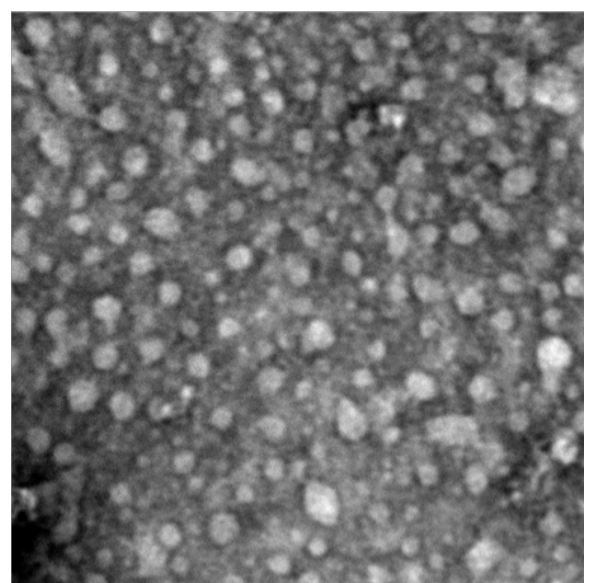


Figure 5.7. WB analysis for detecting VP1 by MAB8566 (Millipore) following RAY3A-D-PV3SC8-3C VLP purification using zymolyase and N₂ cavitation method and 10-30% Nycodenz step gradient

The fractions from the gradient and PV standard were run on 2 gels which are merged for this presentation. Visible interface layers were fractionated separately and denoted *I - *III. 30 kDa bands were detected in fractions 6-11 as indicated. The intensity peaked in fractions 9 and 10 (20% Nycodenz concentration) while reactivity in the 10% fractions was also strong. Fraction 13 reactivity may indicate aggregation as the pellet was collected with the last fraction. Protein molecular markers are shown to the left of the gel (M) and are in kilodaltons. PV standard, far right lane (St) is for a PV1 reactivity control. Bolt™4-12% Bis-Tris Plus Gels (ThermoFisher) and BLUeye Pre-Stained Protein Ladder (Geneflow) were used.



1st Interface



100nm

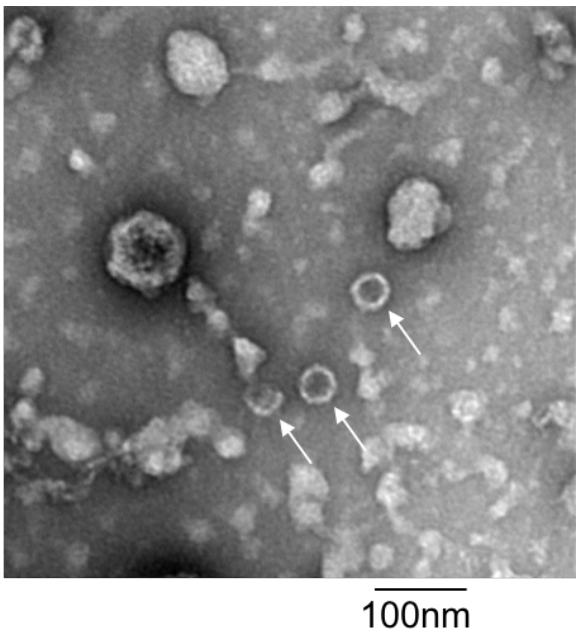
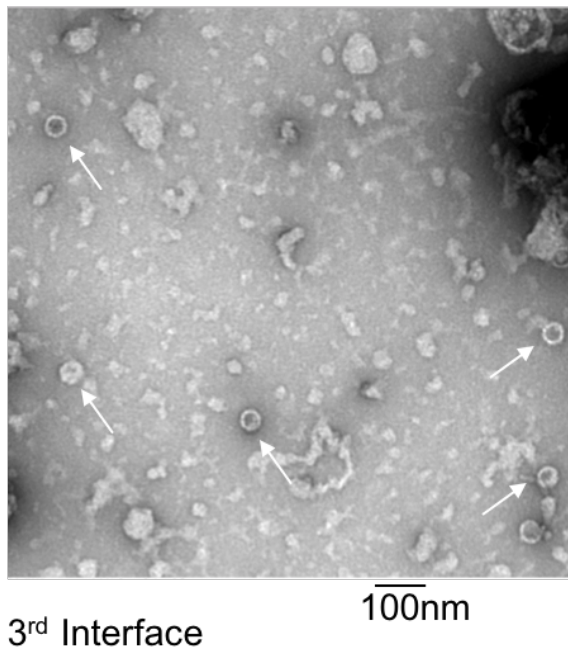
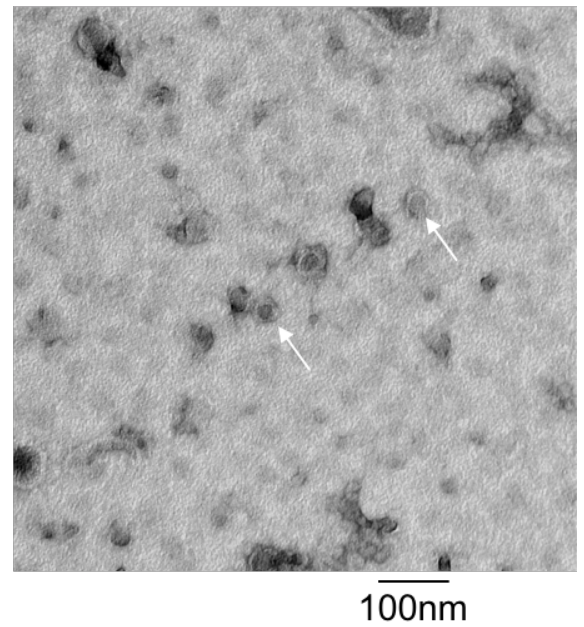
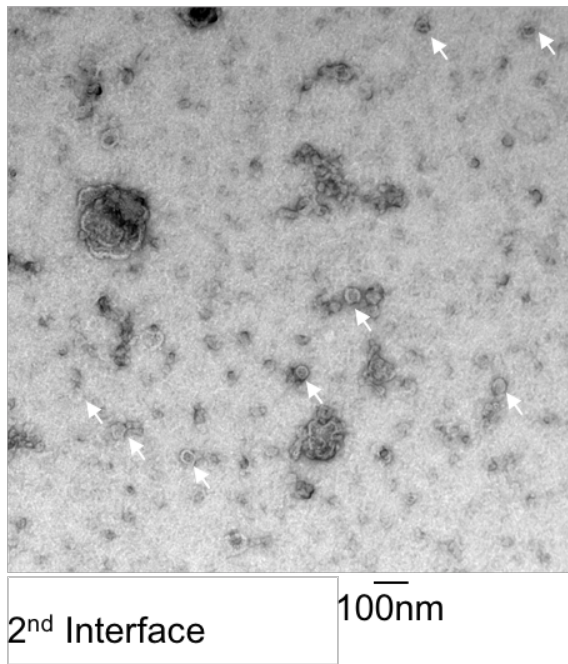


Figure 5.8. TEM imaging of the 3 interfaces which is seen on Figure 5.7.

White arrows in the images indicate VLPs, characterised by stain penetration and the morphology. The 1st interface showed numerous stained structure sizes from 10 nm to 26 nm with irregular shapes. The 2nd interface images appeared as a white background image, similar to Figure 5.4. There were some VLPs characterised by the stain penetration with distorted shapes. Average VLP size is 42.9 nm (+/- SEM = 4.01, n=10). The 3rd interface fraction contained VLPs which are more uniformly shaped, although some seem broken. Average VLP size was 32.5 nm (+/- SEM = 1.98, n = 6). A background was present in this fraction but it was lower than that in the 2nd interface fraction. 2 % uranyl acetate was used as stain on a copper grid with carbon coated formvar film (Agar scientific).

5.3.2 RAY3A-D-PV3SC8-3C VLP purification using Zymolyase and cell disruptor method

A yeast cell culture was grown for 2 days to reach 17.7 ODU/ml, 21.0 g wet weight per litre of culture. The cells were treated as the same way as in section 5.3.1. However, the buffer volume was adjusted to compensate for the bigger cell pellet. Zymolyase processing was done in 120 ml buffer and lysis performed by cell disruptor, 9 strokes of 250 MPa were required for complete destruction as shown by light microscopy. The sample temperature was maintained < 20°C throughout. Clarification, sucrose cushion and then 10-30% Nycodenz gradient were done as before (section 5.3.1). The gradient showed 2 visible bands at the 10-20 % and 20-30 % interface as well as a pellet at the bottom of the tube. 1 ml fractions were taken from the top and the fractions containing visible bands were concentrated for TEM imaging. One fraction below the 20-30 % interface fraction was also concentrated for TEM (section 2.7.2).

TEM images revealed PV VLPs in the 20-30 % interface sample with average size of 43.8 nm (+/- SEM of 1.78, n = 7), as expected from the other optimisation experiments described. A fraction below the interface also contained PV VLPs (Figure 5.9) with average size of 42.0 nm (+/- SEM of 2.70, n = 17). Previously, experiments appeared to suggest that zymolyase and N₂ cavitation was not efficient when the yeast culture was left to grow beyond mid-log phase as the cell wall becomes very thick and the physical disruption required to break it is too harsh for the PV1 VLPs used for initial experiments. Here however, using PV3 VLPs the physical disruption appeared compatible with VLP isolation although it should be noted that no measurement of H/N antigenic form was done for these samples, nor were any structures obtained to substantiate the VLP structure. Nevertheless, yeast expression is clearly a viable option for PV VLP production and suitable methods can be found to extract VLP intact from large scale cultures.

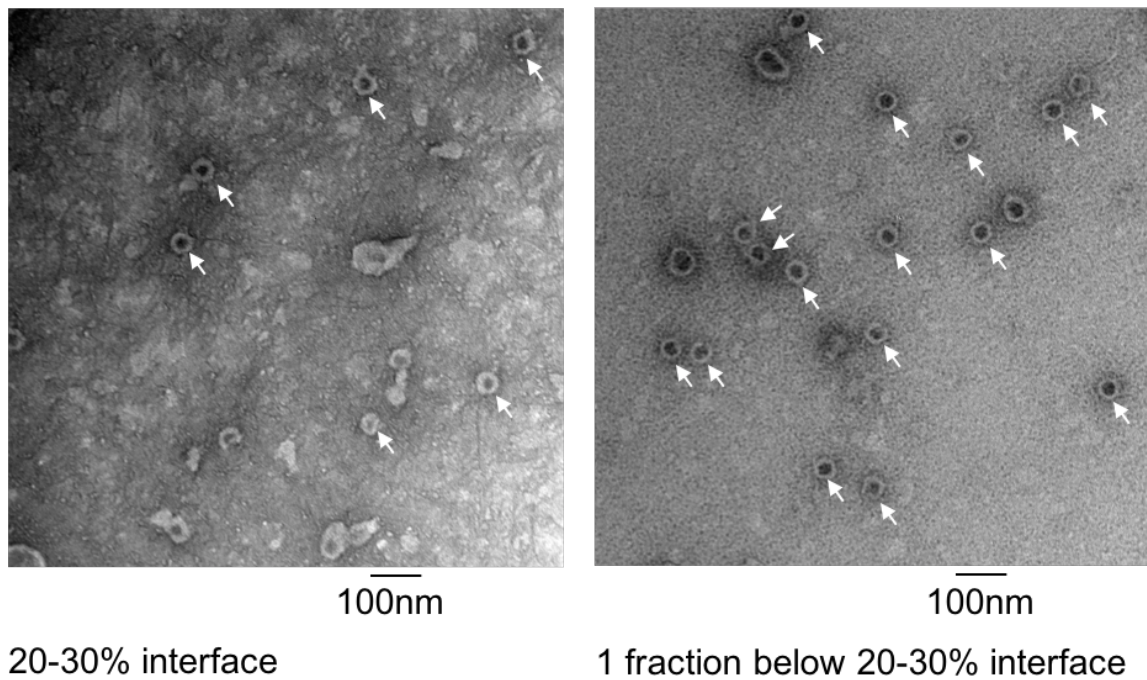


Figure 5.9. TEM image with negative staining of RAY3A-D-PV3SC8-3C VLPs after zymolyase and cell disruptor purification and 10-30 % Nycodenz step gradient

(Left) Concentrated 20-30 % interface was observed. There were some VLPs as well as some background structures. The average size of VLPs is 43.8 nm (+/- SEM of 1.78, n = 7). (Right) A fraction below the 20-30 % interface (concentrated) showed VLPs with average size of 42.0 nm (+/- SEM of 2.70, n = 17). Some structures with stain penetration which sizes up to 75 nm were also visualised. 2 % uranyl acetate was used as stain on a copper grid with carbon coated formvar film (Agar scientific).

5.4 Purification methods for Insect cells

The lysis methods described in this chapter were designed for the processing of yeast cultures but having shown some improvement over the period of testing, it was interesting to ask if the same methods would allow purification of PV VLPs from insect cells. Thus, the cell disruptor and N₂ cavitation methods were assessed as methods to lyse insect cells expressing PV1 VLPs as described in chapter 3.

5.4.1 Cell disruptor method

Suspension cultures of High Five cells, following infection with Bac-PV1P1-3C, were prepared as per 2.3.3. The cells were resuspended in 25 ml PBS pH 6.8, 1 mM CaCl₂, 0.5 mM MgCl₂ supplemented with cOmplete ULTRA EDTA-free protease inhibitor tablet. The resuspension was pressurised to 70 MPa and only one stroke was required for insect cells disruption as

judged by light microscopy. The sample temperature was maintained at $< 20^{\circ}\text{C}$ throughout. Thereafter NP40 was added to be 1 % (v/v) and incubated in ice for 1 hour. The supernatant obtained after 15000 rpm, 4°C for 30 minutes centrifugation was processed as before and loaded onto a 15-45 % linear sucrose gradient and ultracentrifuged at 21,000 rpm, 4°C for 16 hours. It was fractionated from the top of the tube and each fraction was analysed by WB for the presence of VP1 (Figure 5.10). The procedures are detailed in section 2.5 and 2.6. VP1 appeared from fraction 2 to fraction 13 and also in the resuspended pellet fraction. Among the fractions, the VP1 band intensity fluctuated with a peak in fraction 7 and 8 which then declined. VP1 intensity increased again in fraction 12. Assembled PV VLP were expected in the middle of the gradient and TEM visualisation of fraction 7, 8 and 12 was carried out after concentration by spin-filter as per section 2.7.2. The images are shown in Figure 5.11. The concentrated sample for fraction 7 and 8 showed VLP particles of average size of 38.6 nm with \pm SEM of 2.56, $n = 7$ with a high background of smaller material. Fraction 12 also revealed particles around VLP size but many were distorted or broken. Fragmented baculovirus particles were also present in the debris. This fraction is likely to be aggregated material which has trapped some PV VLPs and the level of VLP here might be lessened by improved extraction so that the pellet fraction is reduced. Nevertheless, the lysis of High Five cells using a cell disruptor allowed the observation of PV VLP under TEM and indicates another possible method purification.

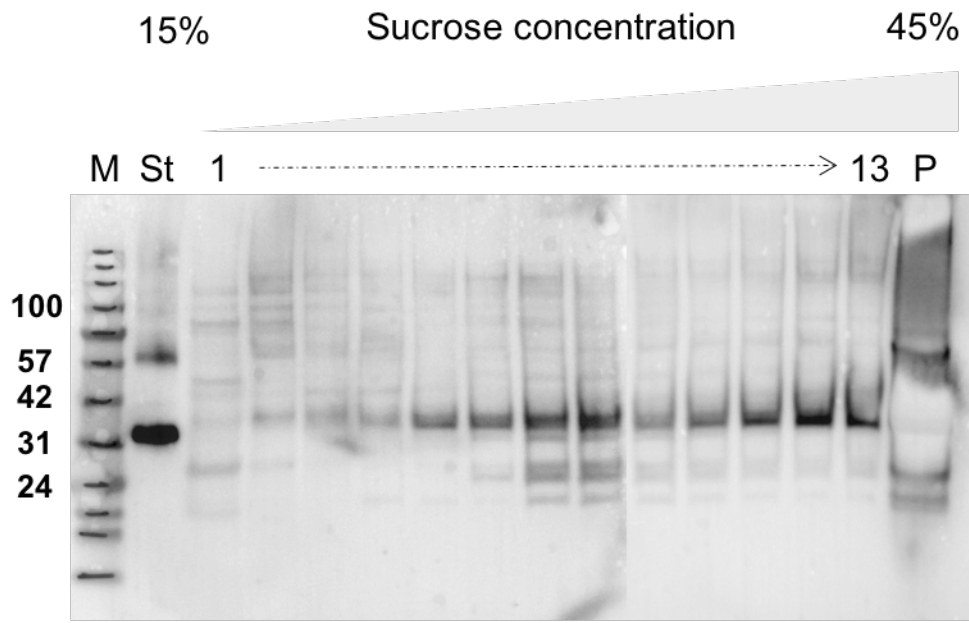


Figure 5.10. WB analysis for VP1 detection using MAB8566 (Millipore) for Bac-PV1P1-3C VLP following purification with cell disruptor and 15-45 % sucrose gradient

35 kDa bands were detected throughout the gradient. However the intensity reached peak at fraction 7 and 8 as indicated then again at fraction 11 to 13. The St lane is the PV standard included as VP1 detection control. The P lane in right hand side WB is loaded with pellet resuspension. Protein molecular markers are shown to the left of the gel (M) and in kilodaltons. Bolt™4-12% Bis-Tris Plus Gels (ThermoFisher) and BLUeye Pre-Stained Protein Ladder (Geneflow) were used.

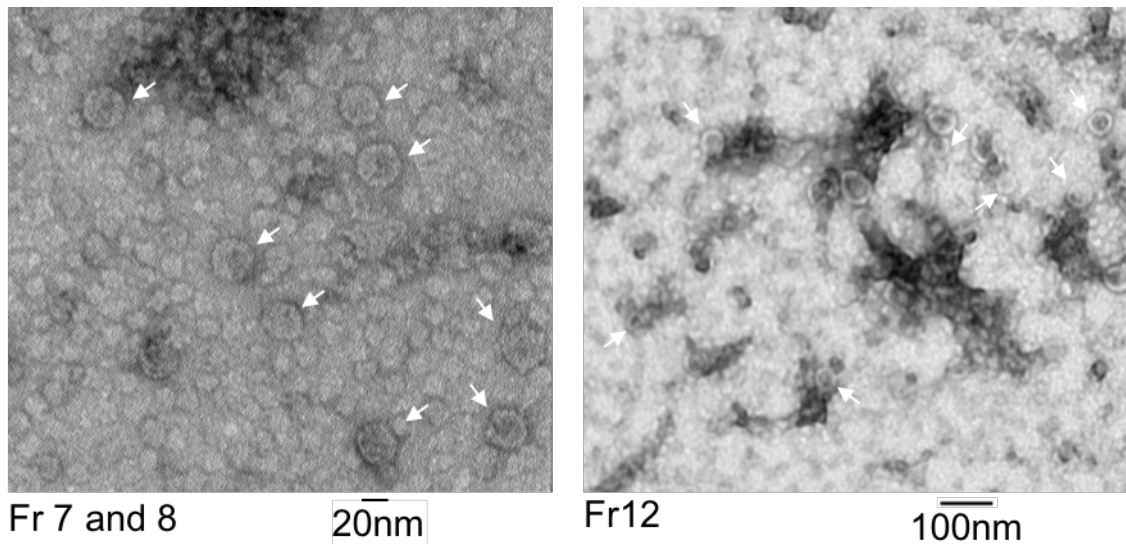


Figure 5.11. TEM image with negative staining of VLPs in peak fractions (fraction 7 and 8) and bottom fraction (fraction 12) from Figure 5.10

White arrows in the images indicate possible VLPs. (Left) Peak fractions showed some VLPs with various forms. However the stain penetration typical to VLP is not seen. The average size of VLP is 38.6 nm with +/- SEM of 2.56, n = 7. (Right) Smaller positive stained structures similar to Figure 5.8 1st interface was seen in the field. Fraction 12 showed some probable VLPs as well as background material. 2 % uranyl acetate was used as stain on a copper grid with carbon coated formvar film (Agar scientific).

5.4.2 N₂ cavitation method

As the N₂ cavitation is a gentle non-thermal method for lysis of cells, the insect cells were also lysed using this method for purification of Bac-PV1P1-3C VLPs. The procedure developed for yeast cells was used with a slight change in nitrogen gas incubation pressure and duration. High Five cells in 200 mL suspension culture infected with Bac-PV1P1-3C as before were resuspended in ice-cold 25 ml homogenization buffer (2.1.8). The cells were pressurised at 500 psi for 30 minutes in N₂ cavitation vessel. Thereafter, the sample was incubated with NP40, clarified and used as the load to a 30 % sucrose cushion followed by a 10-30 % Nycodenz gradient. After the ultracentrifugation (section 2.5.2) there was no visible clear band but the 30 % layer appeared hazy. At the bottom of the tube, a pellet was formed. 1 ml fractionation from the top of tube was carried out as before.

The fractions were analysed with WB for the presence of VP1. The blot images are shown in Figure 5.12. VP1 detection fluctuated and peaked at fraction 9 and declined until the aggregate at the bottom of tube, as before. Fraction 9, i.e. the interface fraction between 20 % and 30 % Nycodenz, was concentrated and observed under TEM as per section 2.7.2. Figure 5.13 reveals the presence of PV VLP (average size of 41.8 nm with +/- SEM of 2.85, n = 28) and

other vesicle like structures of with various sizes. The lower magnification image (left) showed both PV VLP and baculoviruses, characterised by the long rod shape. Those images suggested that N₂ cavitation is efficient for PV VLP purification. However, this method requires further optimisation due to baculovirus content and VLP size variety.

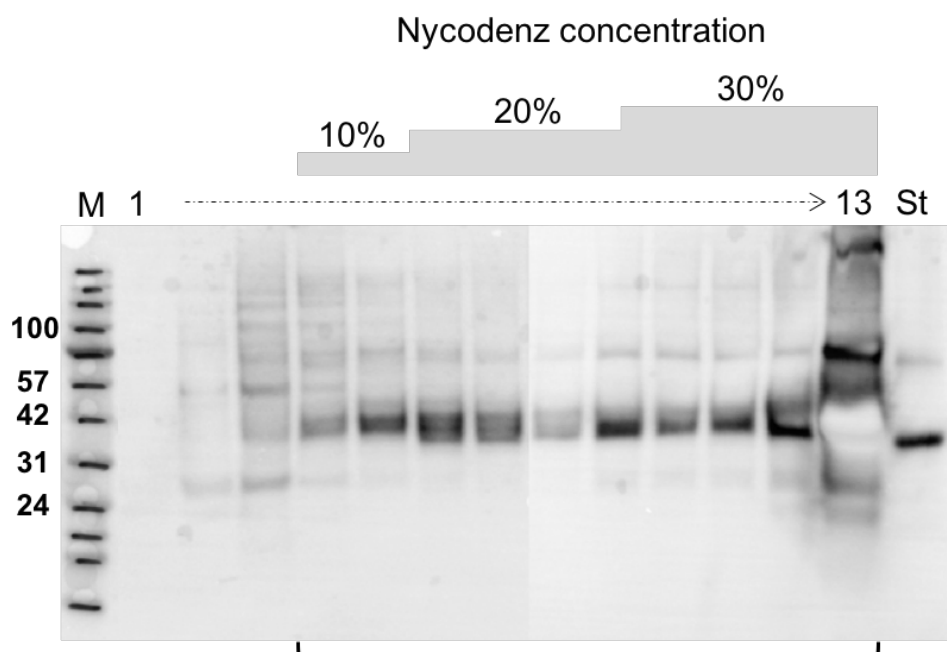


Figure 5.12. WB analysis detecting VP1 by MAB8566 for Bac-PV1P1-3C VLP following N₂ cavitation and 10-30 % Nycodenz gradient. 3 d.p.i. of Bac-PV1P1-3C infected High Five cells were prepared for analysis.

Total of 13 fractions were run on 2 gels. The image above is composite. ~37 kDa reactivity occurs across Nycodenz layers (fraction 4 to 13 as indicated). Fraction 9 at 20-30 % nycodenz interface showed increased reactivity. The reactivity decreased for fr10 and started to increase again from fraction 11 and reached the highest at 13. Far right lane (St) contains PV standard as VP1 reactivity control. Protein molecular markers are show to the left of the gel (M) and are in kilodaltons. Bolt™4-12% Bis-Tris Plus Gels (ThermoFisher) and BLUeye Pre-Stained Protein Ladder (Geneflow) were used

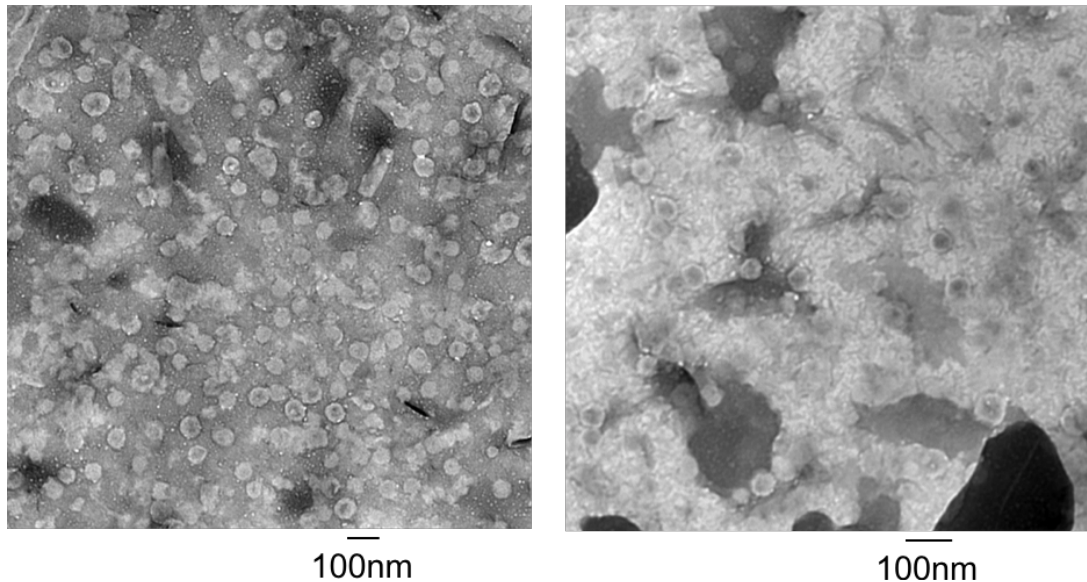


Figure 5.13. TEM image with negative staining for VLPs from Figure 5.12 concentrated fraction 9 at 20-30 % nycodenz interface

(Left) There are numerous PV VLPs which is characterised with stain penetration and average size of 41.8 nm with \pm SEM of 2.85, $n = 28$ and rod shaped baculoviruses. (Right) A field from the same grid indicated some background material as seen in Figure 5.11 fraction 12. 2 % uranyl acetate was used as stain on a copper grid with carbon coated formvar film (Agar scientific).

5.5 Discussion

In this chapter, cell lysis and different separation techniques were assessed for the successful release of intact VLPs, primarily from yeast. Table 5.1 summarises the purification methods used and the result obtained. The best findings were also transferred to PV1 wildtype VLP isolation from insect cells. Three different methods were studied to improve the purification for PV1 Mahoney wildtype VLP originated from *S. cerevisiae* as preliminary data shown in chapter 4 had indicated that yeast cell lysis that maintained VLP conformation was difficult. Thus, cell homogenization by pressure, bead-beating and enzymatic lysis with membrane disruption by N_2 cavitation were used for yeast cell lysis. The cell disruptor method showed low VP1 detection on the WB (Figure 5.2) and a low level of VLP under TEM (Figure 5.3). On the grids, other material was also observed on the grids. Although the yield and purity was not optimal, the method purified PV VLPs to some degree and was relatively easy to perform. It was noted that temperature control was an important consideration for this method. The bead-beater method also led to the visualisation of some empty VLPs but the background was high preventing confirmation of VLP dimensions and structure (Figure 5.4). Both of the methods that used mechanical force showed a temperature rise during the procedure, a key concern

for the thermostability of PV VLPs. The zymolyase and N₂ cavitation method also showed the presence of PV VLP (Figure 5.5) and had the advantage of low operational temperature, useful for PV VLP purification. With these benefits, zymolyase with N₂ cavitation was considered to be the most suitable method for PV1 VLP purification from yeast cells. A consistent observation when western blotting was done for the detection of mature VP1 from yeast expression cultures was the presence of a 30 kDa band, rather than the anticipated 35 kDa. On a western blot all proteins are denatured prior to electrophoresis and a VP1 subunit nicked by proteolysis would be detected by blot even if the folded VP1 protein remained intact in solution, as in a VLP. It has been shown that trypsin digest of PV substantially reduces its ability bind to cell surfaces (Piirainen *et al.*, 1996) and that in the context of VLPs, the N terminus of VP1 can be exposed, depending on buffer conditions (Basavappa *et al.*, 1998). Moreover the antibody used to detect VP1 is known to bind to the C-terminus of the protein (Gary *et al.*, 1997) so cleavage to the 30 kDa form must occur N terminal to the bound epitope. Together it is reasonable to suppose that, in the yeast background, or during sample processing the N terminus of VP1 may become exposed to protease and subject to nicking or degradation. Evidently however VLPs remain intact although their conformation and the effect of such cleavage on yield was not assessed.

As these studies were ongoing a variant form of PV3, the PV3 Skt SC8 mutant, was shown to have increased thermostability (Fox *et al.*, 2017; Marsian *et al.*, 2017) and a new construct using this sequence was adopted for expression and production. As PV1 VLP yield had improved by the use of the zymolyase and N₂ cavitation method, this method was also applied to the new Skt SC8 strain. The zymolyase and N₂ cavitation method successfully processed the cells from a 2 L culture (Figure 5.6) providing a distribution pattern of VP1 reactivity on WB (Figure 5.7) which suggested a higher yield of VLPs. The improved PV3 Skt SC8 thermostability and direct observation by TEM (Figure 5.8) confirmed VLP presence. The zymolyase and cell disruptor method produced Figure 5.9 and again indicated an increased number of VLPs and less impurity in the equivalent fractions to the zymolyase and N₂ cavitation method. Although a strict side-by-side comparison was difficult, the increased VLP yield suggested that the use of strains with improvised thermostability contributed to an increase in VLP purity and should be adopted whenever available.

The yeast cell purification trials led to some experimental trial of the same methods for PV VLP isolation from insect cells. The cell disruptor method demonstrated VP1 reactivity in the middle fractions of a 15-45 % sucrose gradient (Figure 5.10), typical of where empty capsids band. The TEM imaging of the peak fraction revealed a high background but abundant VLPs (Figure 5.11). The WB result (Figure 5.13) for the N₂ cavitation method indicated that VP1 peak reactivity at 20-30 % interface layer of Nycodenz gradient, which corresponded to the finding from the yeast cell purification protocol. Again, TEM image (Figure 5.12) confirmed numerous VLPs as well as baculovirus capsids (obviously missing in the Yeast derived images). Thus, these purification trials benefited the VLP extraction from insect cells and the quality of the VLP is obvious, although there is impurity and vector baculoviruses are present.

Overall this chapter has shown an effective method for the purification of PV VLPs from yeast cells using zymolyase and N₂ cavitation. Possibly the cell disruptor method is more efficient for the thermostable VLP purification from yeast cells as the potential for physical disruption of the VLP is less. Both cell disruptor and N₂ cavitation methods improved VLPs yields and these methods could be very beneficially used for insect cells also if baculovirus removal is achieved by some other means.

Table 5.1. Summary of cell lysis and purification method used in chapter 5

	Yeast cells					Insect cells	
PV type	PV1 wildtype			PV3 Skt SC8		PV1 wildtype	
Method	Cell disruptor	Beads- beater	zymolyase + N ₂ cavitation	zymolyase + Cell disruptor	zymolyase + N ₂ cavitation	Cell disruptor	N ₂ cavitation + NP40
Ultracentrifugation	10-30 % Nycodenz	10-30 % Nycodenz	10-30 % Nycodenz	10-30 % Nycodenz	10-30 % Nycodenz	15-45 % Sucrose	10-30% Nycodenz
VP1 detection by WB	30 kDa 75 kDa	X	X	X	30 kDa 60 kDa	35 kDa	35 kDa 60 kDa
TEM	A few VLPs High background	A VLP Highest background	A few VLPs Moderate background	Several VLPs Moderate background	A few VLPs Moderate background	Distorted particles High background	Numerous VLPs Baculovirus co-purified

Chapter 6 The factors of capsid assembly and contribution to VLP antigenicity

6.1 Introduction

Although there are two types of vaccine available for poliovirus, neither are a suitable choice for the post eradication world due to the requirement for live virus culture. At the same time any vaccine replacing the existing OPV and IPV stocks is expected to improve other current limitations, such as the thermostability of the vaccines as discussed in chapter 1.

Since the studies success in VLP production in *S. cerevisiae* (Rombaut *et al.*, 1994) and its conformation change to immunogenic VLP (Rombaut & Jore, 1997) as detailed in chapter 4, no follow-up of this observation has appeared in the literature and investigation of the improved stability of VLPs from *S. cerevisiae*, or any other recombinant system, by the addition of Pirodavir or similar compounds has not been reported.

Other than the VP1 pocket region, the association of protomers to form a pentamer is driven by dynamic capsid change during the assembly process of picornaviruses and detailed PV capsid rearrangement has been studied in 135S (Butan *et al.*, 2014) and 80S particles (Levy *et al.*, 2010). As discussed in chapter 1, dynamic capsid change involves the N-terminus of VP4 and the N-terminus of VP1 and the assumption is that they may make a contribution to capsid assembly and stability. During the course of these investigations, the Mahoney SC6b sequence, a thermostable variant, also became available and was used to produce VLP incorporating those mutations.

This chapter focuses on attempts to improve VLP stabilisation to produce VLPs that are predominantly or wholly in the N conformation. The experiments target the site known to be the binding site for Pirodavir-like antiviral drugs, the hydrophobic pocket in the mature VP1 protein in expectation that they will make a contribution to capsid stability and VP4 and the N-terminus of VP1 which are contributing to pentamer formation.

First, the conformation of VLPs produced in the baculovirus and *S. cerevisiae* expression systems was assessed using ELISA with mAbs specific for the N or H conformational forms.

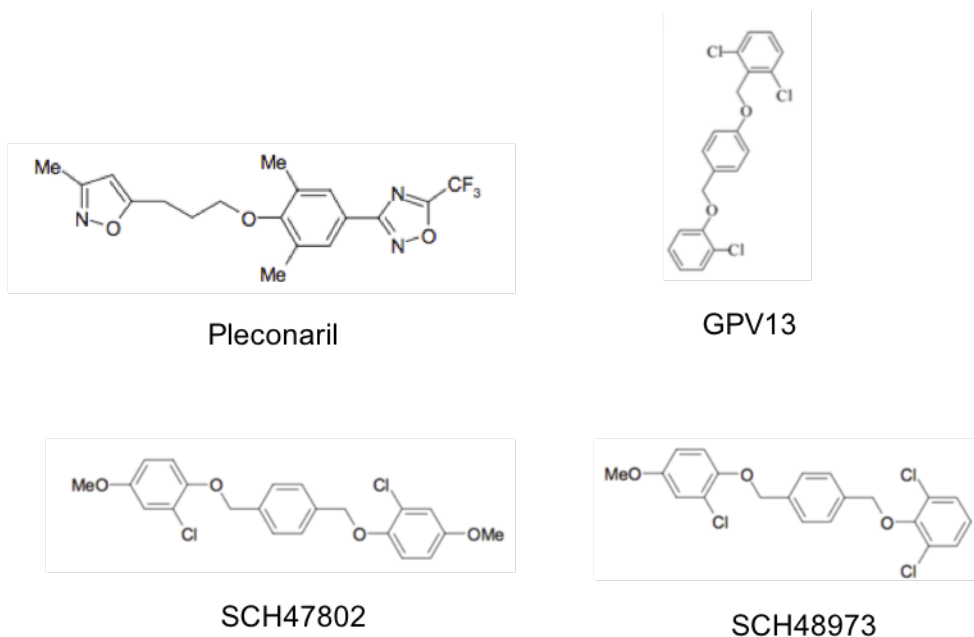
Next, manipulation of the occupancy of the VP1 pocket is investigated by introducing amino acid mutations that alter the side chains that protrude into the hydrophobic space. Then an attempt was made to supplement cultures and purification steps with antiviral compounds such as Pleconaril and GPV13 (De Palma *et al.*, 2008b) to address whether conformational change can be achieved post expression. Finally the contribution of VP4 and the N-terminus of VP1 to VLP assembly are tested individually by exchanging VP4 amino acids with another myristoylated protein and by the addition of short GS linkers to the N-terminus of VP1.

6.1.1 Antipicornavirus compounds and VP1 mutations

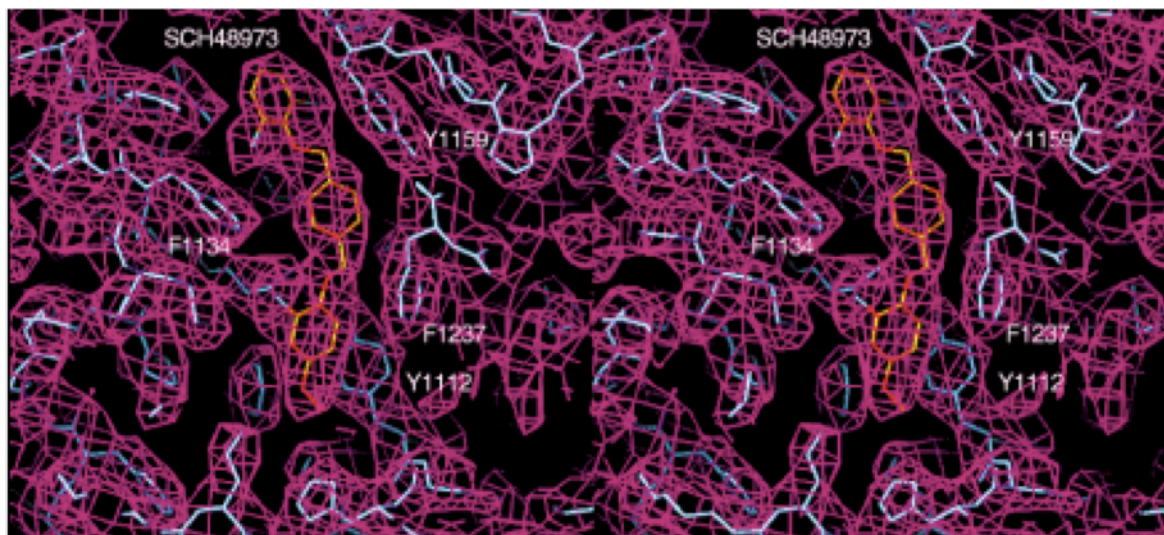
As discussed in chapter 1 and 4, antipicornaviral compounds such as WIN compounds were originally designed to bind VP1 pocket at high affinity to inhibit capsid conformation change and prevent the infection. For PV, the binding mode of those compounds was found to inhibit conformational change but is still able to bind the receptor (Rossmann, 1994). This feature is therefore suited as a strategy for stabilising VLP and indeed, Pirodavir addition improved VLPs produced in *S. cerevisiae* by changing H conformation VLP to N conformation (Rombaut & Jore, 1997).

In this chapter, Pleconaril and GPV13 (Figure 6.1) are used as the pocket binding compounds to prevent N antigen conversion to H antigen. Pleconaril, also known as WIN63843 was produced as part of the WIN compound development and inhibition of viral uncoating was observed widely for enteroviruses (Florea *et al.*, 2003; Pevear *et al.*, 1999). Pleconaril entered clinical trials as a HRV inhibitor for the common cold treatment but its development has since ceased (De Palma *et al.*, 2008b). In PV, De Palma *et al.* (2008a) demonstrated that Pleconaril inhibited Sabin PV2 and PV3 replication although it was less efficient towards Sabin PV1. Very similar activity was obtained for Pirodavir, the capsid binding compound used by (Rombaut & Jore, 1997) for capsid stabilisation of *S. cerevisiae* derived VLPs. This suggests that Pleconaril may be as effective as Pirodavir in maintaining the N conformation of VLPs. GPV13 is similar to a SCH47802 analogue, SCH48973 (Figure 6.1A) produced by Schering-Plough (De Colibus *et al.*, 2014). The antiviral properties of these compounds were observed in PV2 along with several echoviruses and coxsackieviruses (Cox *et al.*, 1996; De Palma *et al.*, 2008b). The crystallographic imaging (Figure 6.1B) showed the binding of SCH48973 to the VP1 pocket and has confirmed that the site of the binding is almost identical to that of the natural pocket

factors (De Palma *et al.*, 2008b; Lentz *et al.*, 1997). The effect of GPV13 on PV VLP is not known. However as binding in the VP1 pocket prevents the conformational change, it is expected to behave as a capsid stabiliser.



(A)



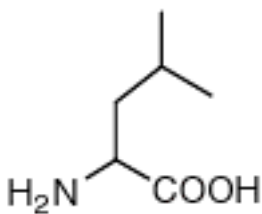
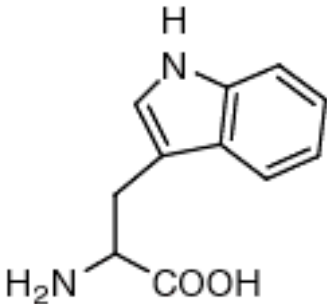
(B)

Figure 6.1. Chemical structures of antipicornavirus compounds

(A) Pleconaril, SCH47802, SCH48973 (De Palma *et al.*, 2008b) and GPV13 (De Colibus *et al.*, 2014). (B) Crystallography of PV2 VP1 filled with SCH48973. The compound is labelled with yellow backbone. Some of residues close to the compound are indicated (De Palma *et al.*, 2008b).

An alternate approach to antipicornaviral compound binding to the VP1 pocket to conserve the capsid N status for PV capsids may be the introduction of hydrophobic side chains via VP1 residues facing into the VP1 pocket. The pocket is then filled permanently as if by a pocket factor or antiviral compound. Suitable residues for change in VP1 were chosen from modelling *in silico* carried out by project collaborators at the University of Oxford and the introduction of leucine (aliphatic amino acid) and tryptophan (aromatic amino acid) in their place was chosen. Tryptophan contains an indole structure made up of a benzene ring which contributes to VP1 pocket filling because of its bulky structure. Leucine was selected as a milder choice than tryptophan as it too contains a hydrophobic side chain but does not have the bulky structure of tryptophan.

Table 6.1. List of VP1 residues facing to the VP1 pocket. Substituting amino acids are indicated in blue. The amino acid structures of leucine and Tryptophan are shown below

	VP1 residue	
Mutation	M132L, M132W, M132W-H207W, M132W-F237W, H207W-F237W, M132W-H207W-F237W (Triple), Y159W, Y159W-Y205W, Y205W, H207W, F237W	
	Leucine (Leu, L) = Aliphatic 	Tryptophan (Trp, W) = Aromatic 

6.2 Antigenicity of PV VLPs

The antigenicity of PV VLPs was analysed by enzyme-linked immunosorbent assay (ELISA) sandwich assay by Sarah Knowlson at NIBSC. The immunosorbent plate wells were coated with a PV particle capture Ab which does not induce conformational change of PV particles and the PV sample applied. The immobilised PV is then probed with conformation specific mAbs (either N or H specific mAb). A conjugated secondary Ab is added to the wells for

enzyme-substrate interaction. The detail of antibodies used and procedures were described in section 2.8. As a positive control for N antigen, IPV reference material available from NIBSC was included in the assay.

6.2.1 Insect cells origin VLPs

Three day infections of 1 L High Five cells with Bac-PV1P1-3C were prepared to obtain the cell pellet as described in 2.3.3. After the VLPs were purified from insect cells by cell lysis followed by 30 % sucrose cushion and 15-45 % linear sucrose gradient (section 2.5), the immunogenic conformation of VLPs was examined by ELISA as described in 2.8. Insect cells expressing poliovirus VLPs showed the H-conformation (Figure 6.2) suggesting an inability to raise neutralising antibodies if used as a vaccine. The IPV control showed its N dominant characteristics validating the assay format.

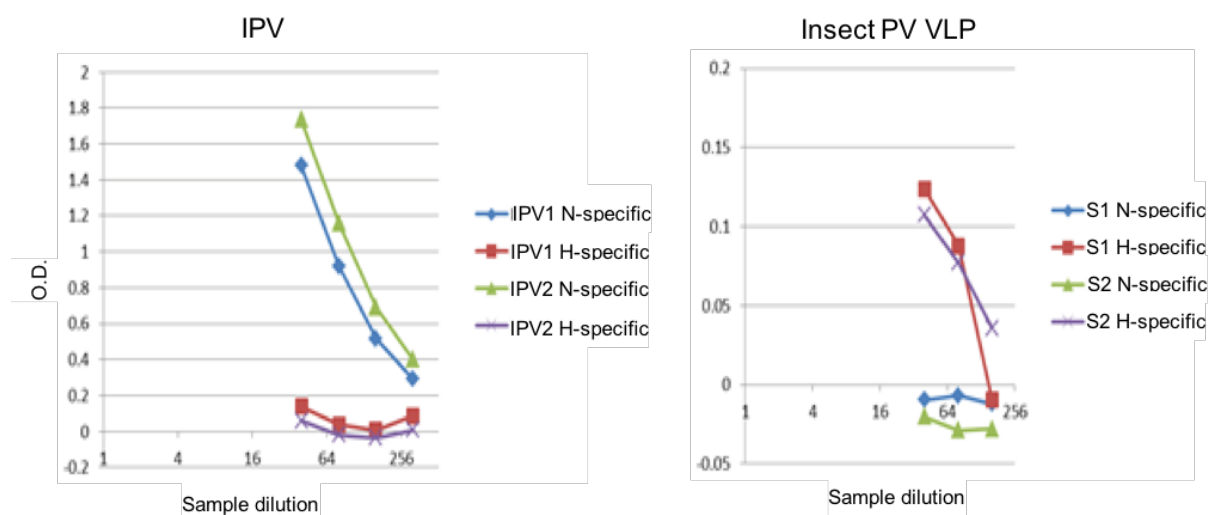


Figure 6.2. Antigenicity ELISA analysis for IPV (PV standard) and Insect cell origin PV VLP detected by N/H specific antibodies at NIBSC

Duplicates of IPV and VLP samples were analysed. (Left) IPV sample are predominantly N specific starting at the 2-fold dilution from 1/40 to 1/320 while H specific remained low readings throughout the dilution. (Right) the same dilution was applied for insect PV VLPs. Insect cell sample O.D. readings were much lower than IPV. N-specific readings were observed at 1/40 and 1/80. At 1/160, N specific readings reached non-significant readings and remained unchanged through the later dilutions.

6.2.2 *S. cerevisiae* origin VLPs

Yeast expressed PV VLPs were also tested for the antigenicity by N/H ELISA at Reading and purified samples from three different purification methods (see chapter 5) were included. The individual culture and purification methods are detailed in section 5.2. Previously, VLPs produced in *S. cerevisiae* were identified as H confirmation (Rombaut & Jore, 1997), so the expectation was for H antigenicity. However, the data in Figure 6.3 indicated that the antigenicity varied according to the purification method used. ELISA for IPV validated the assay for detection of N antigenic particles (Figure 6.3, Left) and VLPs purified by zymolyase and N₂ cavitation (shown as N₂ Bomb on the ELISA result) showed almost equal amounts of N and H specific antigen (Figure 6.3, Centre). The N-specific Ab binding showed a decline according to dilution consistent with the presence of N antigenic VLPs although the readings were generally low when compared to the IPV assay. This method of purification also provided the highest number of VLPs (Figure 6.3, right) and this in part may reflect higher OD reading for both N and H Abs when compared to the other two purification methods. VLPs purified by the cell disruptor (CD) method failed to give significant readings for either N or H- specific Ab although VLPs were confirmed by TEM (Figure 5.3) and should have been captured by the trapping layer. Plausibly, the heat generated by the CD caused changes that prevented binding but further work would be required to prove this. VLPs extracted by the bead-beater showed a constant decline in N-specific Ab binding with dilution but unchanged OD reading for the H-specific Ab. TEM of this sample showed very few visible VLPs, consistent with a poor binding overall. From these data it seems possible that N conformation VLPs could be produced in *S. cerevisiae* at some level but that the preservation of the conformation may depend on treatment. Broadly, the numbers of VLP and level of intactness as demonstrated by TEM were in accord with the ELISA data and it would be useful to re-investigate the steps in each purification method using only N specific mAb reactivity as a relevant readout of VLPs present.

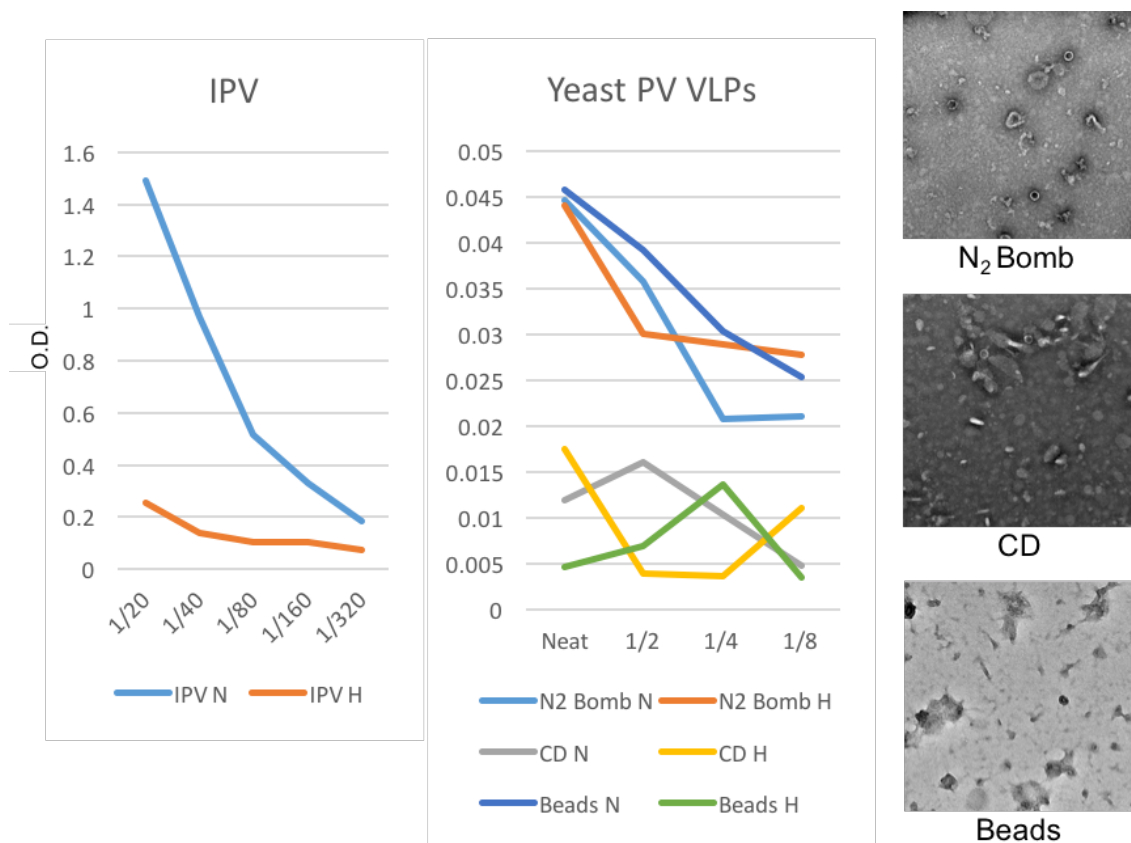


Figure 6.3. Antigenicity ELISA analysis to determine the status of RAY3A-D-PV1-3C origin VLPs purified using various purification methods at Reading

(Left) IPV as the assay control showed mainly N specific particles. 1/20 IPV was used in 2-fold serial dilution up to 1/320. (Centre) VLPs from of RAY3A-D-PV1-3C which are purified by using either N₂ Bomb (N₂ cavitation), CD (cell disruptor) or Beads beater. Undiluted concentrated sample were applied and 2-fold serial dilution to 1/8 were carried out. N₂ Bomb samples showed similar readings for both N and H through the dilutions. The N and H specific readings for VLP prepared by CD remained unchanged, un-correlating with the dilution. VLPs prepared by bead beater showed higher N specific readings and the pattern declined with the dilution while H specific readings were lower and remained significantly unchanged throughout the dilutions. (Right) TEM images of negatively stained VLP samples used for ELISA assay (from chapter 5).

6.3 VP1 pocket manipulations

The results of VLP conformation tests for material from both insect cells and *S. cerevisiae* showed that, even if N-type VLPs were present, they were not the major products. Therefore, attempts at conversion of the H conformation to the N conformation of VLP are required. As discussed, the hydrophobic VP1 pocket plays an important role in the thermostability of PV and occupation of the pocket by the introduction of mutations in residues lining it. Other capsid

stabilisation methods, that is, the addition of pocket binding compounds will be discussed in Section 6.4.

6.3.1 Expression of VP1 pocket surface mutants

Molecular modelling carried out by collaborators at University of Oxford predicted the VP1 residues that line the pocket where side chain changes could act to fill the space are listed in Table 6.1. The mutations were introduced into pOPINE Mahoney P1_2A_FS_3C_{EV71} for the expression in insect cells as described in 2.2 and recombinant baculoviruses listed in 2.1.4 are produced (section 2.3.1). Small scale infections with *Sf9* cells were performed to examine the expression of PV proteins and their cleavage measured by VP1 WB as before. There is a dynamic equilibrium in expressing cells between assembled and disassembled capsids with the latter being prone to degradation, as has been shown to also be the case for other picornaviruses (Katpally & Smith, 2007). In the case of improved stability therefore the level of the VP1 product as seen by the WB band intensity should increase as a result of less capsid degradation.

The WB analysis (Figure 6.4) shows very different levels of VP1 antigen detection associated with each mutation made. Bac-M132L, Bac-Y205W and Bac-H207W showed clear VP1 bands albeit substantially less than the level of VP1 produced by the parental construct Bac-PV1P1-3C. One of the isolates of Bac-Y159W essentially abolished expression. The two isolates of Bac-Y159W arose as, during the course of the work, two forms of the parental PV1 Mahoney sequence were used, the first was cloned from the virus sequence donated by collaborators at NIBSC and was not codon optimised whereas the other was produced using a *Sf9* codon optimised synthetic DNA fragments. This change arose as the cost and availability of the synthetic approach reduced substantially over the course of the project, becoming the default method. A comparison among the non-codon optimised showed Bac-Y159W to be detrimental whereas the codon optimised Bac-Y159W was tolerated. This indicates a role for codon optimised in the expression level seen and leaves the exact effect of Bac-Y159W in question. However Bac-M132L, Bac-Y205W and Bac-H207W reduced expression.

The expression of the remaining VP1 pocket mutants, many multiple, which now used codon optimised sequences throughout, was also analysed by WB VP1 detection (Figure 6.5). The lanes for Bac-F237W, Bac-M132W-F237W, Bac-Triple mutants and Bac-PV1P1-3C showed

VP1 levels similar or equal to the parental construct. However, in the case of Bac-M132W-F237W, Bac-H207W-F237W expression of VP1 was substantially reduced. These results may indicate that only the F237W mutation is able to be tolerated for expression, and therefore the assembly of VLPs. The combination mutants with F237W also showed different VP1 expression levels. Although M132W-F237W and the triple mutations showed expression, H207W-F237W did not. The data in Figure 6.4 and Figure 6.5 indicate that capsid stability is indeed affected greatly by the residues that line the VP1 pocket, validating the approach to improved stability. However, none of the introduced mutations, single or multiple, benefited VP1 levels, all were deleterious to some degree indicating the challenge of predicting the outcome of even minor changes in the structure of a large assembled complex.

To ensure that the data obtained in insect cells was not an artefact of the expression background some of the VP1 pocket lining mutations were introduced also into the *S. cerevisiae* expression system. Based on the data of Figure 6.4 and Figure 6.5, the mutants M132L, M132W, Y159W, Y205W and triple (M132W-Y207W-F237W). pKT10 Mahoney P1_2A_FS_3C_{EV71} - M132L, M132W, Y159W, Y205W and M132W-Y207W-F237W (Triple) were transformed to produce recombinant RAY3A-D with VP1 pocket mutants RAY3A-D-PV1-3C-M132L, M132W, Y159W, Y205W and M132W-Y207W-F237W (Triple) as per section 2.4.1. However they were not codon optimised for *S. cerevisiae* expression as they were to be compared like with like. After the transformation and confirmation of the desired mutations in each case, 3 day old colonies were analysed by WB analysis using anti-VP1 antibody following NaOH disruption as explained in 2.6.1. The result showed no significant VP1 expression (data not shown).

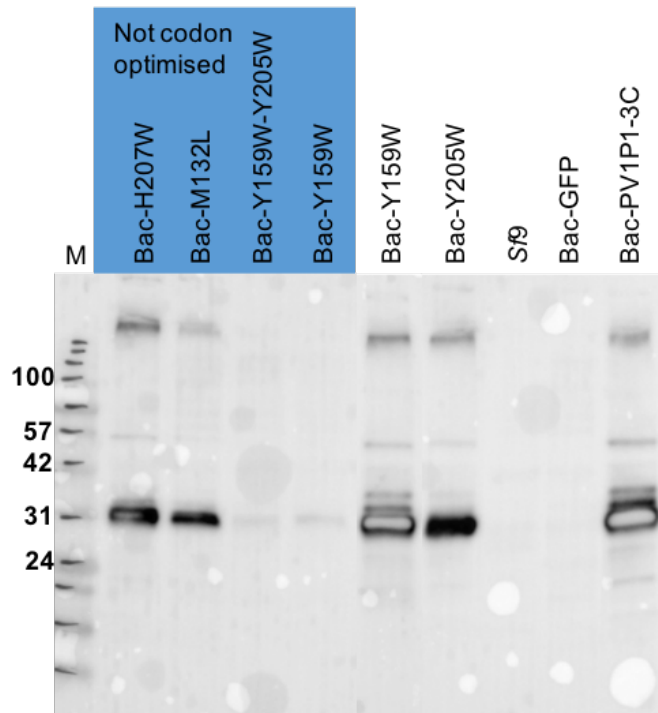


Figure 6.4. WB analysis for Bac-PV1P1-3C with hydrophobic pocket mutations for capsid stability improvement 3 d,p,i of Sf9 cells with corresponding recombinant baculovirus in 6 well dish was loaded on the gel. The image is composite of 2 gels. Samples in blue box indicates non-codon optimised P1 in their transfer vector. The blot showed the different level of antigen detected by VP1 antibody (MAB8566, Millipore). Bac-H207W, M132L, Y205W mutants showed ~35kDa reactivity which is VP1, however the level is not as high as Bac-PV1P1-3C. Y159W variant constructs showed different levels of VP1 reactivity. Non-codon optimised Bac-Y159W showed low antigen level at ~35 kDa. Sf9 cells codon optimised Bac-Y159W showed VP1 reactivity which was slightly lower than Bac-PV1P1-3C. Sf9 lane contains only the cells to act as negative control. Bac-GFP lane was included as mock baculovirus infection. Protein molecular markers are show to the left of the gel (M) and are in kilodaltons. Bolt™4-12% Bis-Tris Plus Gels (ThermoFisher) and BLUEye Pre-Stained Protein Ladder (Geneflow) were used.

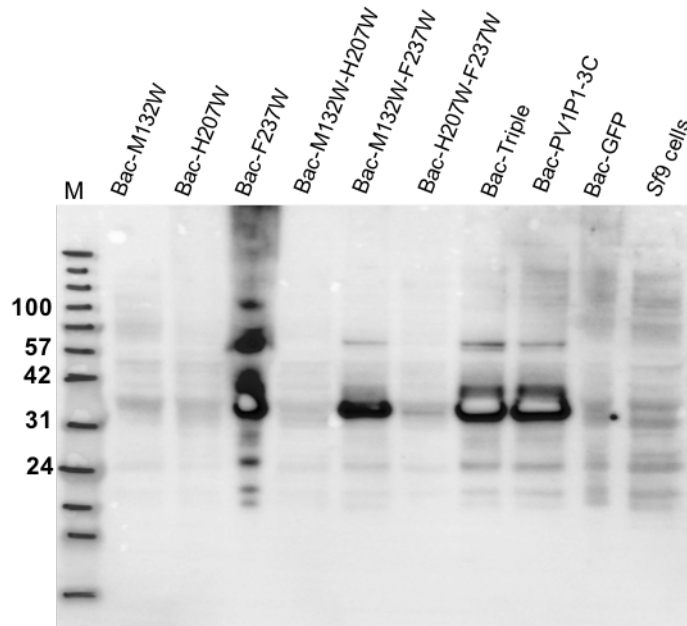


Figure 6.5. WB analysis using anti-VP1 antibody (MAB8566, Millipore) for Bac-PV1P1-3C mutants at M132, H207, F237 and their combinations (codon optimised) for 3 d.p.i of *Sf9* cells with Bac-PV1P1-3C mutants prepared in a 6 well dish.

VP1 reactivity (~37kDa) were seen in lanes for F237W, M132W-F237W, Triple mutants (M132W-H207W-F237W) and Bac-PV1P1-3C at the rate of M132W-F237W<F237W=Bac-Triple=Bac-PV1P1-3C. The other mutants showed rather background reactivity which was seen in *Sf9* cells (negative control) and Bac-GFP (mock baculovirus infection) lanes. Protein molecular markers are show to the left of the gel (M) and are in kilodaltons. Bolt™4-12% Bis-Tris Plus Gels (ThermoFisher) and BLUeye Pre-Stained Protein Ladder (Geneflow) were used.

6.3.2 Supplementation in insect cells expression system

GPV13

After setting up small scale infection as described in 2.3.2, the insect cell media was changed +/- GPV13 at 8 h.p.i. 10 µg/ml GPV13 (the same concentration as Pirodavis used by Rombaut and Jore (1997) and significantly higher concentration than Lentz *et al.* (1997) used for solving the PV2 Lansing structure at 0.4 µg/ml) was added to a 2-day infection of Bac-PV1P1-3C, Bac-Y159W and Bac-Y205W. At the time of the experiment, they were the only *Sf9* codon optimised mutants which had different VP1 expression levels (Figure 6.4). Alongside, the same infections without GPV13 acted as controls. The harvested cells were analysed by WB using anti-VP1 antibody (section 2.6). The result is shown in Figure 6.6, left. The antigen level of WT Bac-PV1P1-3C infection without GPV13 (PV-) serves as control. Bac-PV1P1-3C infection with GPV13 (PV+) showed a higher level of antigen on the WB while for Bac-Y159W infection,

Y159W+ demonstrated a lower level of VP1 reactivity compared to Y159W-. On the other hand, Y205W+ showed an increased VP1 detection compared to Y205W-. The antigen comparison graph (Figure 6.6, right) indicated that WT PV+ VP1 reactivity was stimulated about 1.4 times while Y159- showed about a 20% higher VP1 reactivity than Bac-Y159W+. In contrast, Bac-Y205W+ showed at least a 4 times higher reactivity than Y205W-.

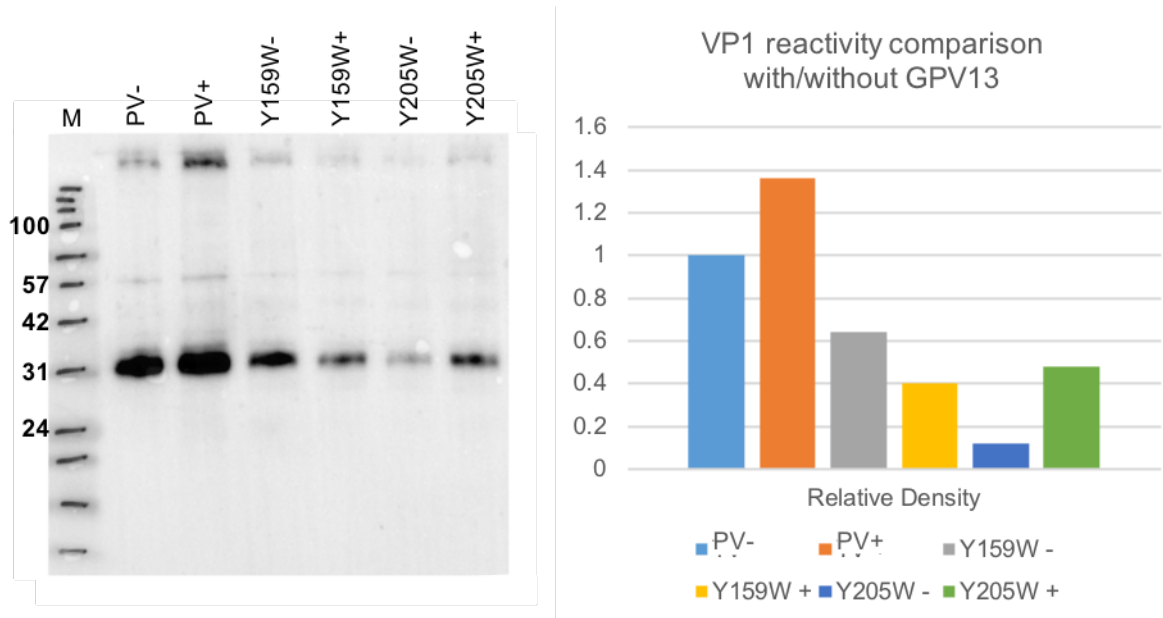


Figure 6.6. The analysis of GPV13 effect on VP1 reactivity level in *S/9* cells infection by Bac-PV1P1-3C, Bac-Y159W and Bac-Y205W

(Left) WB analysis by anti-VP1 antibody (MAB8566, Millipore). GPV13+/- infection was prepared with Bac-PV1P1-3C (PV+/-), Bac-Y159W (Y159W+/-) and Bac-Y205W (Y205+/-). ~35kDa VP1 reactivity was seen in all lanes, but the levels are different. The VP1 reactivity for PV+ and Y205W+ was higher than PV- and Y205W-, however not for Y159. Protein molecular markers are show to the left of the gel (M) and are in kilodaltons. Bolt™4-12% Bis-Tris Plus Gels (ThermoFisher) and BLUeye Pre-Stained Protein Ladder (Geneflow) were used. (Right) VP1 reactivity quantitative comparison. PV+ is calculated to produce 1.4 times more antigen than PV-. Y159W+ displayed roughly 20% lower VP1 reactivity than Y159W-. Y205W+ showed 4 times higher detection than Y205W-.

Pleconaril in insect cells expression system

The other PV pocket binding drug, Pleconaril was also investigated for its effectiveness for increasing VP1 expression, which in turn indicates increased stability. Pleconaril was added to High Five cells infection (250ml) with Bac-PV1P1-3C at the concentration of 10 µg/ml, sufficient for all VLPs produced from *S. cerevisiae* to be in the N-specific conformation (Rombaut & Jore, 1997). The concentration of Pleconaril was maintained during the purification. The insect culture preparation detail is described in 2.3.3. In order to test the VLP

formation, the cell lysis and 10-30 % nycodenz step gradient was carried out (section 2.5). Following the WB analysis to determine the peak fractions from the gradient (section 2.6), the sample was examined by N/H ELISA as detailed in section 2.8. The WB analysis using anti-VP1 antibody (Figure 6.7) showed VP1 reactivity in lanes for fraction 7-13, peaking at fraction 7, 8 and 9. This reactivity at around 20 % nycodenz is equivalent to 35 % in sucrose and suggests the formation of VLPs. The middle fraction, fraction 8 was analysed by N/H ELISA at Reading to assess VLP conformation (Figure 6.8). The result indicated that the VLPs are neither N nor H antigenic form although the assay format was confirmed by the PV standard. The levels of VLP were low as judged by the WB of gradient samples, but it was clear that the addition of Pleconaril did not dramatically convert the H antigenic VLPs to N antigenic VLPs in insect cells.

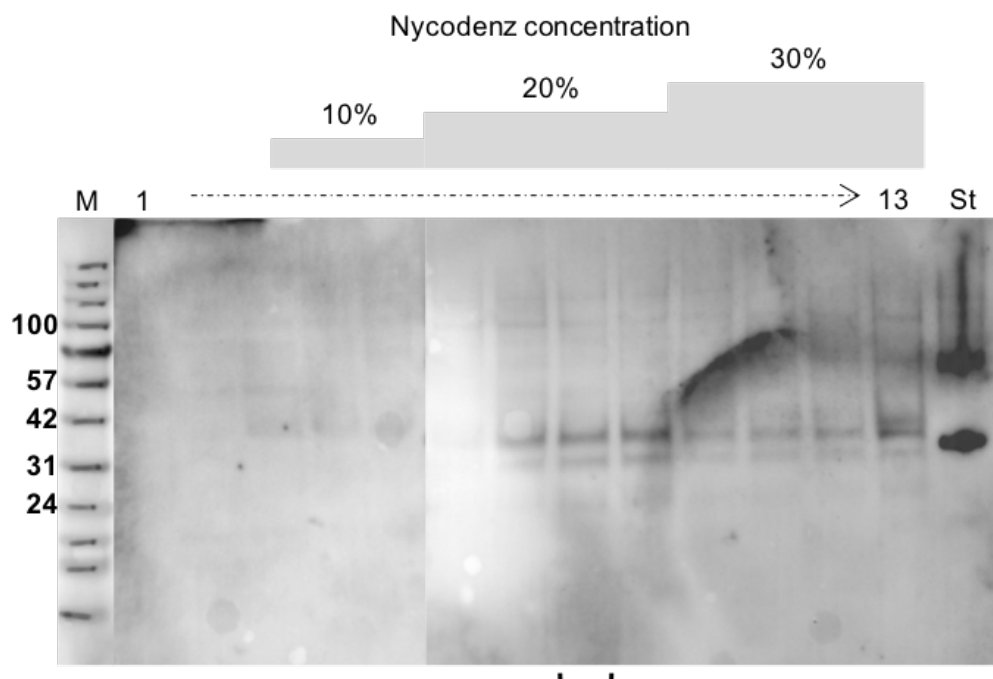


Figure 6.7. WB analysis with anti-VP1 antibody (MAB8566, Millipore) for High Five cells infection by Bac-PV1P1-3C with Pleconaril followed by non-ionic detergent lysis and 10-30 % nycodenz gradient

The figure is composite of 2 gels. VP1 reactivity was shown in fraction 7-13 which peaked at fraction 7-9 and faded towards the bottom of tube except for fraction 13. Fraction 8 (indicated) was used for N/H ELISA analysis. There was no apparent VP1 reactivity from fraction 1 to 6. Far right lane (St) contains PV standard as VP1 reactivity control. Protein molecular markers are show to the left of the gel (M) and are in kilodaltons. Bolt™4-12% Bis-Tris Plus Gels (ThermoFisher) and BLUeye Pre-Stained Protein Ladder (Geneflow) were used.

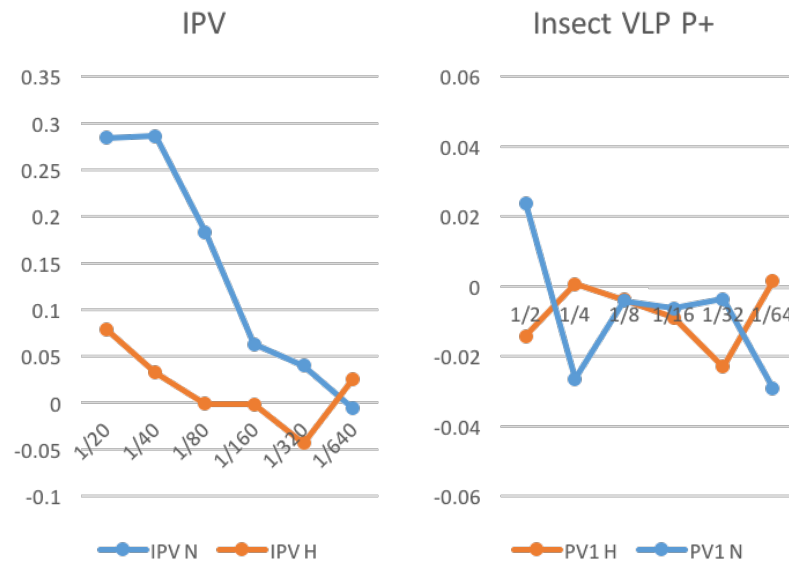


Figure 6.8. N/H ELISA analysis for 10-30 % nycodenz gradient peak fraction (Figure 6.7) for Mahoney wt VLPs from High Five cells infection by Bac-PV1P1-3C purified with Pleconaril at Reading

(Left) ELISA assay for IPV standard as assay control. It shows the constant N specific reading decline with dilution while H specific readings remained not significantly changed. (Right) VLPs from High Five cells infection by Bac-PV1P1-3C showed no major difference between N- and H- specific OD readings.

Pleconaril in yeast cells expression system

RAY3A-D-PV3SC8-3C was chosen to study whether Pleconaril increases the N conformation VLPs by converting H conformation VLPs. Although PV3 Skt SC8 had the enhanced capsid stability for PV (Fox *et al.*, 2017) and plant originated VLPs (Marsian *et al.*, 2017), in the work described here VLPs from RAY3A-D-PV3SC8-3C were always H conformation dominant (Figure 6.3). For this experiment, 500ml RAY3A-D-PV3SC8-3C culture with and without Pleconaril was prepared and purified side by side following the method in 2.4.2. For the yeast cell culture grown with Pleconaril, 10 µg/ml was added and was kept for the purification steps. The harvested cells were lysed by zymolyase and N₂ cavitation method as described in 5.2.3 and VLP separation was carried out by a 30 % sucrose cushion by ultracentrifugation (2.5.2). The clarified 30 % sucrose cushion pellet resuspension was examined by N/H ELISA for the conformation as described in 2.8. The data in Figure 6.9 confirmed the assay format with the EU standard by showing the N specific OD readings are higher than H readings throughout the dilution and the readings declined as the sample are further diluted (left panel). However the result for Pleconaril supplemented (+) and non-supplemented (-) culture origin VLPs were

almost identical and as with the insect VLPs the level of VLP was low as indicated by the overall OD values. It is unclear whether the PV1 pocket is filled with any other molecule or simply that Pleconaril is not able to bind to the pocket in our culture condition.

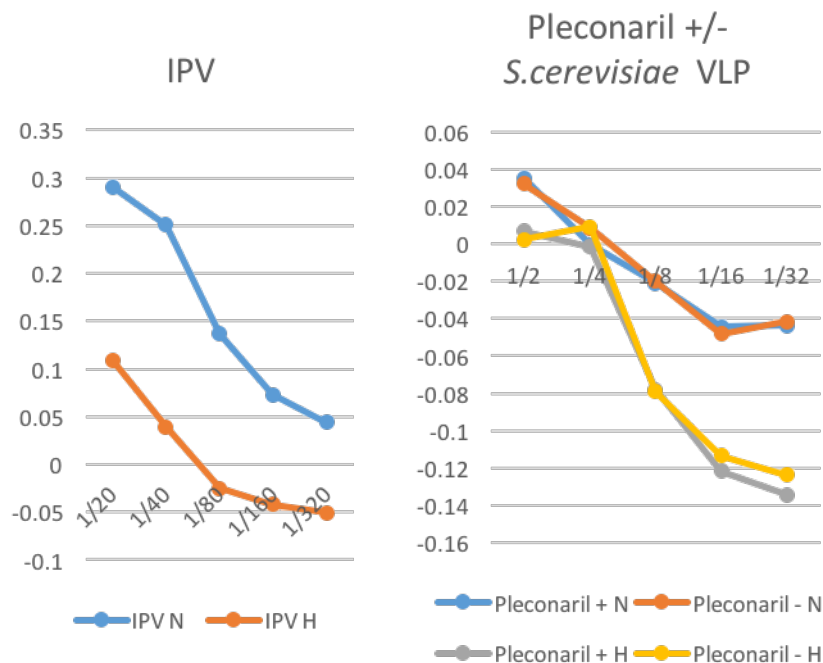


Figure 6.9. N/H ELISA for VLPs conformation from RAY3A-D-PV3SC8-3C +/- Pleconaril at Reading.

VLPs from RAY3A-D-PV3SC8-3C were prepared following zymolyase and N₂ cavitation method and 30% sucrose cushion. 10 µg/ml Pleconaril was maintained through the purification for Pleconaril + sample.

(Left) PV standard (IPV reference) serving as assay control. IPV was diluted into 1/20 at the beginning of a 2-fold serial dilution to 1/320. N specific reading (indicated in blue) showed decline pattern with dilution while H specific (orange) showed lower reading than N readings generally but also a decreasing pattern. (Right) PV VLPs produced from *S. cerevisiae* either with Pleconaril supplemented (+) / non-supplemented (-) culture and purification. Pleconaril +, N specific readings (blue) and Pleconaril -, N specific readings (orange) showed almost identical readings while Pleconaril +, H specific readings (grey) and Pleconaril -, H specific readings (yellow) showed similar reading pattern. N readings were above H readings.

6.4 VLP stabilising mutations for PV1 at VP4 and VP1

During the course of this work to stabilise the VLPs by VP1 pocket factor mimicking, Wang *et al.* (2018) produced EV71 VLPs wholly lacking in VP4, using the baculovirus expression system, which proved to be highly immunogenic and gave protection against EV71 challenge in mice. As discussed in chapter 1, the mature capsid changes to the 135S particle by the

externalisation of VP4 during uncoating (Butan *et al.*, 2014) which is followed by loss of VP4 and RNA to form the 80S empty capsid (Bergelson & Coyne, 2013) and the authors thought to produce 80S-like empty capsids, suggesting that a VLP_{ΔVP4} might improve EV71 vaccine stability by minimising the autocleavage of VP0 into VP4 and VP2 which occurs in VLPs with time (Li *et al.*, 2013; Zhang *et al.*, 2015). Expression of VLP_{ΔVP4} lead to cryo-EM and immunisation. The vaccine potency results for immunogenicity and virus challenge test showed that the VLP_{ΔVP4} was superior to VLP_{full} suggesting it as an EV71 vaccine candidate but more generally the study challenges a number of traditional views in the picornavirus field. The assembly of VLP_{ΔVP4} was myristoylation independent, previously supposed to be essential for pentamer formation, and further suggests that VP4 has no essential role in assembly. These findings are intriguing and point towards further areas of manipulation for PV VLP assembly.

PV1 Mahoney SC6b

As mentioned in chapter 1, an improved PV thermostable mutant, Mahoney SC6b, was isolated from the study of Fox *et al.* (2017). As the various introduction of pocket lining mutations and the addition of pocket binding drugs had not significantly improved expression or thermostability in PV1 VLP produced in insect cells, the Mahoney SC6b P1 sequence was assessed a source of improved VLPs. The P1 sequence was codon optimised for *Sf9* cells and was introduced by switching the P1 region of pOPINE Mahoney P1_2A_FS_3C_{EV71} (WT) at the *BstEII* and *NotI* sites that flank the P1 coding region to produce pOPINE Mahoney SC6b P1_2A_FS_3C_{EV71} as described in 2.2.1. Following sequence confirmation, it was transfected as per 2.3.1 to produce a recombinant baculovirus, Bac-PV1SC6bP1-3C. The high titre virus was used for small scale *Tnao38* 3 day infections to compare VP1 expression with WT recombinant baculovirus expression as explained in 2.3.2. WB analysis with an anti-VP1 antibody as described in 2.6. Figure 6.12 showed higher VP1 reactivity for SC6b indicating that the use of the mutant sequence had improved VLP protein expression. Following WB analysis, a 100 ml *Tnao38* cells infection with Bac-PV1SC6bP1-3C was set as per 2.3.2 and at 3 d.p.i. the cells were harvested and lysed by NP40 and loaded to a 30 % sucrose cushion followed by removal of cell debris as explained in 2.5. The pellet was resuspended and the

clarified supernatant was observed under TEM following the method in section 2.7.2 (Figure 6.10A). The image revealed baculoviruses and PV VLPs characterised by the negative staining. Helen Fox at NIBSC analysed the same sample by N/H ELISA to determine conformation status. Figure 6.10B indicated that PV SC6b VLPs are still dominantly the H antigenic form but notably the OD readings were much higher than previous N/H ELISA results (Figure 6.2, Figure 6.3, Figure 6.8 and Figure 6.9).

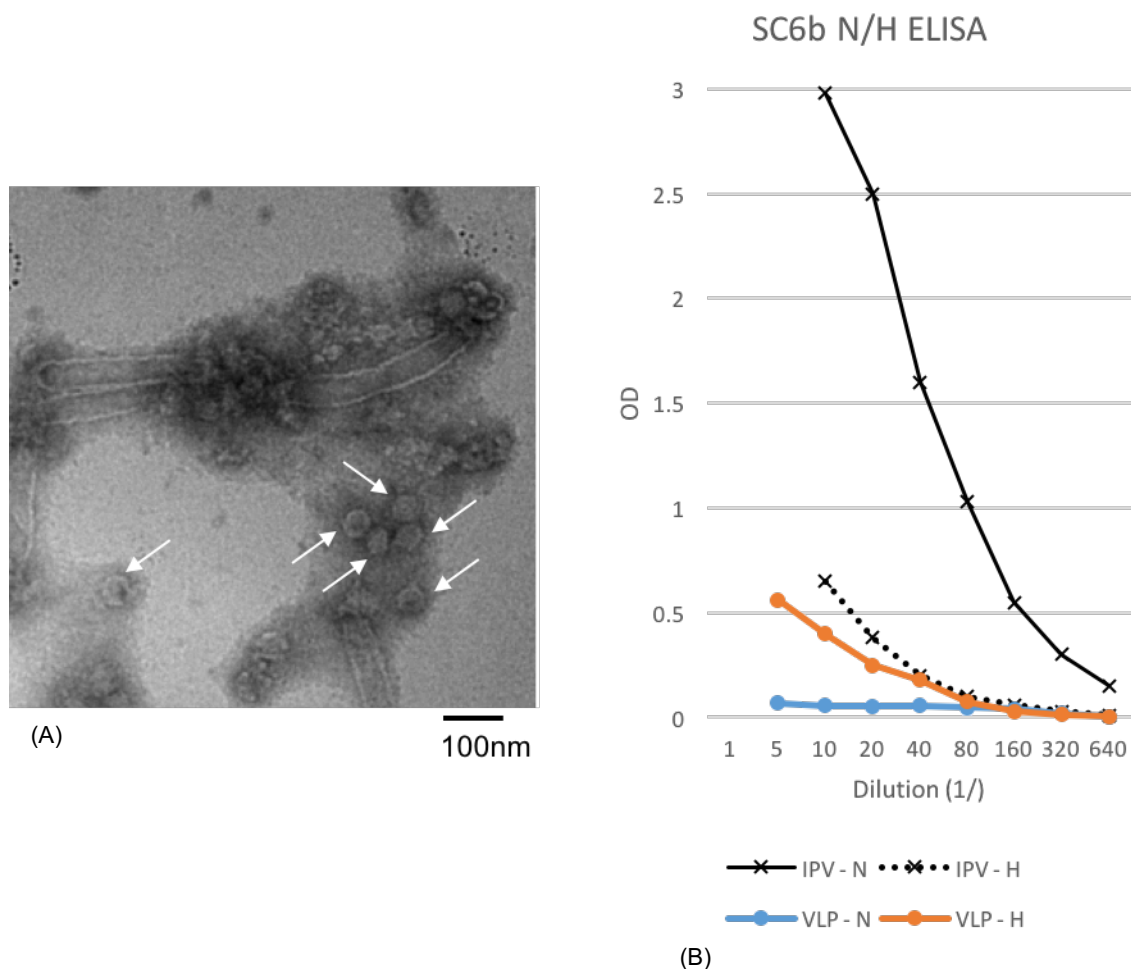


Figure 6.10. PV Mahoney SC6b VLP TEM image by negative staining (A) and N/H ELISA result (B)

3 d.p.i Bac-PV1SC6bP1-3C infection of *Tnao38* was lysed with NP40 and ultracentrifuged at 30% sucrose cushion to obtain VLPs. (A) 2% uranyl acetate was used for grid staining. PV VLPs (indicated by white arrows. Average size of 44.3 nm) as well as baculovirus were visible in the sample. 2 % uranyl acetate was used as stain on a copper grid with carbon coated formvar film (Agar scientific).. (B) SC6b VLP readings are indicated by orange for H specific reading and blue for N specific. The sample were applied as 1/5 dilution and 2-fold dilution is made to 1/640. H readings showed the decline as the dilution went further whereas the N reading remained almost unchanged. IPV (PV standard) readings served as control, starting the dilution from 1/10 to 1/640 by 2-fold dilution, showing N dominant characteristic and confirming the assay format.

6.4.1 Modification of the VP4 N-terminus

The assembly of EV71 VLP_{ΔVP4} has questioned the VP4 involvement in capsid assembly. VP4 is known for its conformation flexibility and myristoylation in many picornaviruses. During the PV capsid uncoating, VP4 is extruded from the inner surface of the virion (De Sena & Mandel, 1977) and the N-terminus of VP4 is myristoylated and has been previously considered as essential for virion assembly (Chow *et al.*, 1987) as 5S protomer association to form 14S pentamers is promoted by myristoylation (Ansardi *et al.*, 1992) for the infectious and naturally occurring empty capsid assembly. For PV, the first 3 amino acids of VP4, which includes the Gly at position 2 where myristic acid is added (Moscufo *et al.*, 1991). To study the N terminus of PV VP4 in VLP assembly, a conservative strategy was adopted in which residues were changed but the signal for myristoylation was maintained. Accordingly, the first 10, 15 and 20 amino acids were exchanged for the sequence of another myristoylated protein, the HIV matrix protein (p17) which is part of the HIV-1 gag polyprotein which also forms virus capsids and VLPs (Wu *et al.*, 2004). Figure 6.11 summarises the detail of the amino acid exchange.

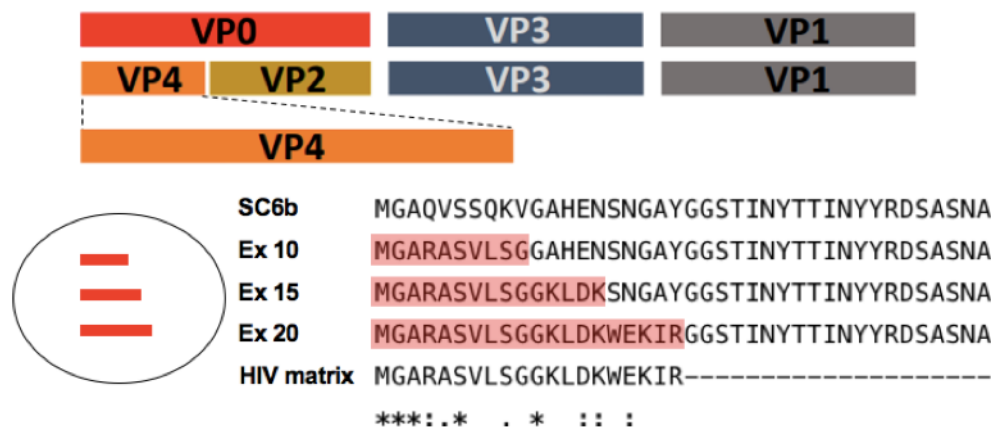


Figure 6.11. Schematic representation of VP4 N-terminus mutant sequences exchanged with N-terminus of HIV matrix protein, p17

N-terminus of VP4 amino acid sequences are shown indicating the p17 sequence insertion. Ex10 mutant contains first 10 amino acids from p17. For Ex15, 15 amino acids are contained and 20 amino acids for Ex20.

In order to exchange the first 10, 15 or 20 amino acids of VP4 with HIV matrix protein p17, Geneblock for Ex10, Ex15 and Ex20 were designed as shown in Figure 6.11. The detail of cloning is described in 2.2.1. Using unique sites *Bst*EII and *Eco*RI in pOPINE Mahoney SC6b P1_2A_FS_3C_{EV71}, VP4 mutations were introduced to produce pOPINE Mahoney SC6b P1

Ex10, Ex15 and Ex20_2A_FS_3C_{EV71} using a Quick-Fusion Kit. Once the exchange was confirmed by sequencing, transfection of Sf9 cells was carried out to produce recombinant baculoviruses, Bac-PV1SC6bP1Ex10, Ex15 and Ex20 as before. Once virus had been produced, small scale infections with *Tnao38* cells were set and, at 3 d.p.i. the cells were harvested and prepared for the WB analysis using anti-VP1 antibody (Figure 6.12). The image showed VP1 reactivity for all the mutants with the VP1 expression level being Ex10>Ex15≥Ex20>Sc6b>WT. The result showed that VP1 reactivity for all mutants was improved compared to Mah SC6b and Mah WT but especially for Ex10. In order to investigate the effect of the mutation on capsid assembly, mutant Ex10 was prepared for VLP purification by a 15-45 % sucrose gradient. A 100 ml *Tnao38* cells infection with Bac-PV1SC6bP1Ex10 was set, harvested at 3 d.p.i., the cells lysis and cell debris were removed by centrifugation followed by VLP enrichment through a 30 % sucrose cushion. The pellet formed at the bottom of the tube was then resuspended and clarified before banding on a 15-45 % sucrose gradient. 1 ml fractions were made from the top of the tube as described in 2.5.2. and WB analysis by anti-VP1 antibody (as per section 2.6) for all fractions was carried out. Figure 6.13 showed the VP1 reactivity from fraction 3 to fraction 13 as well as pellet resuspension. The reactivity was highest in fractions 5 to 9 peaking in fraction 7, a sucrose concentration of 25-35 % which is where PV empty capsids sediment. The additional reactivities at higher molecular weight than VP1 may indicate partially processed P1 and some partial VP1 cleavage or capsid degradation for lower molecular weight reactivity. After fraction concentration, the sample was visualised under TEM as before. Figure 6.14 showed numerous VLPs with average size of 34.6 nm with +/- SEM of 2.28, n = 10 and the number of VLP was greater than the equivalent culture volume of SC6b although the VLP appeared filled rather than having the typical "hollow" VLP appearance with uranyl acetate penetration. The VLPs also appeared somewhat distorted although this could be an artefact of the grid preparation. Overall the Ex10 mutant clearly stimulated PV antigen expression levels without compromising VLP assembly, adding to the emerging data on the role of VP4 in VLP assembly.

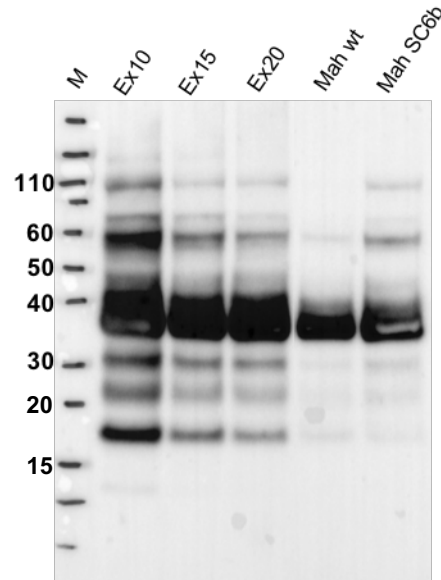


Figure 6.12. WB analysis using anti-VP1 antibody (MAB8566, Millipore) for small scale 3 d.p.i. of Bac-PV1P1-3C (shown as Mah wt), Bac-PV1SC6bP1-3C (Mah SC6b), Bac-PV1SC6bP1Ex10, Ex15 and Ex20

~37 kDa reactivity which agrees with MW of VP1 was seen in all samples. The reactivity level was highest for Ex10, slightly lower for Ex15, further lower for Ex20 and Sc6b is slightly higher than WT which is the lowest. Additional reactivities were seen at higher molecular weight (~60 kDa and ~100 kDa) and at lower molecular weight (~32 kDa, ~23 kDa and ~18 kDa). Those reactivity reflected the intensity of VP1 reactivity. Protein molecular markers are shown to the left of the gel (M) and are in kilodaltons. Bolt™4-12% Bis-Tris Plus Gels (ThermoFisher) and Novex™ sharp pre-stained protein standard (ThermoFisher) were used.

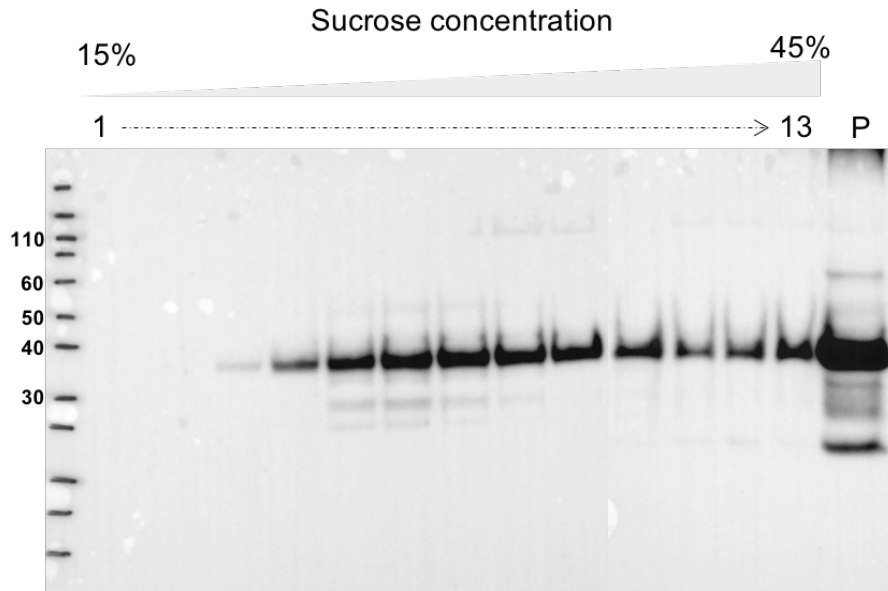


Figure 6.13. WB analysis with anti-VP1 antibody (MAB8566, Millipore) for 3 d.p.i. of Bac-PV1SC6bP1Ex10 for *Tnao38* cells following NP40 lysis, 30 % sucrose cushion and 15-45 % sucrose gradient 1ml fractions were taken from top of the tube to the bottom and analysed over 2 gels which were processed for WB. The image is the composite of the two WB membranes. A ~37 kDa VP1 reactive band is seen in fractions 3 - 13 peaking around fractions 7 - 9 and declining to fraction 12. There is also signal in the pellet and preceding fraction. Fraction 7 (as indicated) was used for TEM. Protein molecular markers are show to the left of the gel (M) and are in kilodaltons. Bolt™4-12% Bis-Tris Plus Gels (ThermoFisher) and Novex™ sharp pre-stained protein standard (ThermoFisher) were used.

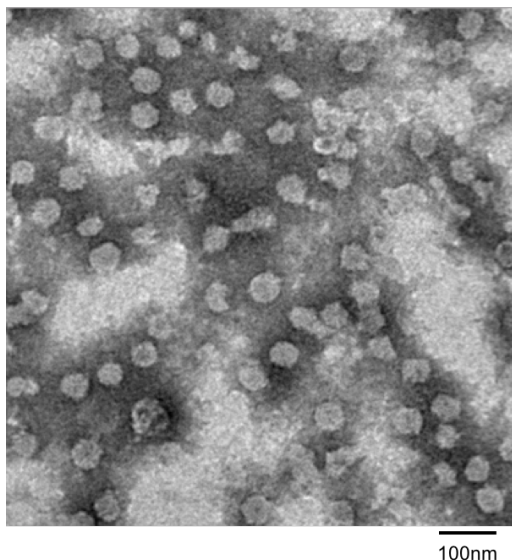


Figure 6.14. TEM image for negatively stained of VLPs of Mahoney SC6b Ex10 from Figure 6.13 concentrated fraction 7 (3 d.p.i. of Bac-PV1SC6bP1Ex10 for *Tnao38* cells)

2 % uranyl acetate was used for grid staining. A grid full of VLPs was observed although they appear filled rather than having typical stain penetration. The average sizes of VLP is 34.6 nm with +/- SEM of 2.28, n = 10 which is expanded for PV VLPs. The number of VLPs were greater than Figure 6.10A. 2 % uranyl acetate was used as stain on a copper grid with carbon coated formvar film (Agar scientific).

6.4.2 Modification of the VP1 N-terminus

A conclusion from Wang *et al.* (2018) described above was that in the EV71 VLP $_{\Delta VP4}$ particles the VP1 N-terminus was externalised. During PV virion uncoating, the externalisation of the VP1 N-terminus has been suggested to involve a number of different steps including anchoring to a susceptible cell surface which leads to the association with the tip of the VP2 propeller feature. The association is also associated with a rearranged GH loop in VP3 and some rearranged GH loop in the neighbouring protomer both of which suggest that the VP1 N-terminus could be involved in capsid assembly (Butan *et al.*, 2014). It follows that the movement of the VP1 N-terminus could be part of instability seen in PV VLPs. As the movement must have some basis in the sequence of this region alterations of the N-terminus of VP1 could modify stability although it has to be accepted these could all be detrimental changes, much as were the pocket lining residues.

In order to investigate the contribution of the VP1 externalisation for our PV VLP assembly, a flexible GS linker (GGGGSGGGGS) was substituted for the resident sequence in three separate positions in the VP1 N-terminus with each insertion shifted by 4 or 5 amino acids from the last. GS linkers are commonly used when flexibility is required, for example in the assembly of single chain antibodies (van Rosmalen *et al.*, 2017). The insertions began after the 4th amino acid as it was considered that a minimum number of amino acids may be required for accurate 3C proteolytic processing at the VP3/VP1 junction. The detail of the GS linker insertions, which were all made in the PV1 SC6b background, is indicated in Figure 6.15.

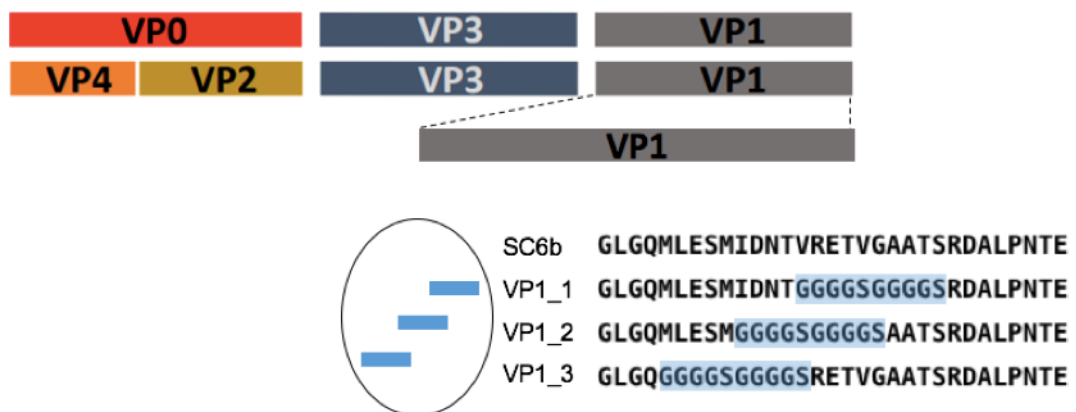


Figure 6.15. Schematic representation for N-terminus VP1 mutations designed to contain GS linkers consisting of GGGGSGGGGS in 4 or 5 amino acid shifted positions.

VP1_1 contains GS linker at V14 replacing the resident 10 amino acids. For VP1_2, the GS linker was inserted at I10 and at M5 for VP1_3.

Geneblock fragments was designed to contain the mutations, and an extra 15 nucleotides upstream and downstream for each mutant and used in an infusion reaction with pOPINE Mahoney SC6b P1_2A_FS_3C_{EV71} using unique sites, *Bse*JI and *Not*I, both which flank the region to be changed. The newly constructed transfer vectors, pOPINE Mahoney SC6b P1 VP1_1, VP1_2 and VP1_3, _2A_FS_3C_{EV71} were transformed into *E. coli* competent cells for plasmid preparation and sent for sequencing (section 2.2.1). Positive plasmids were used for Sf9 cell transfection to generate recombinant baculoviruses, Bac-PV1SC6bP1VP1_1, VP1_2 and VP1_3 as described in 2.3. Once high titre viruses were produced, a small scale infection of *Tnao38* cells was set and the cells harvested at 3 d.p.i. as before and analysed for VP1 expression by WB (section 2.6). Figure 6.16 shows VP1 reactivity in VP1_2 and Ex10 (as control), indicating the reactivity being VP1_2<Ex10 and no reactivity for VP1_1 and VP1_3

lanes. This result confirms this area of VP1 as highly sensitive to change as, in two of the tests expression was abolished undoubtedly as assembly fails and the protomers are degraded. However insertion 2 indicates that some positions are tolerate to the insertion. To confirm that this mutant is still VLP competent a 100 ml *Tnao38* cell infection was prepared as described before. At 3 d.p.i. the infected cells were harvested and lysed followed by a 30 % sucrose cushion, and a 15-45 % sucrose gradient. 1 ml fractions were collected and analysed by WB using an anti-VP1 antibody. The procedure followed was the same as the method in 6.5.1. Figure 6.17 showed VP1 reactivity in fraction 4 to fraction 9 which peaked in fraction 5 and gradually declined to fraction 9. These fractions are in sucrose concentration of 20 % to 30 % which corresponds the sedimentation position in sucrose for PV empty capsid. Fractions 6 and 8 were concentrated separately and visualised under TEM. Fraction 6 did not show any VLPs and very few baculovirus. Fraction 8 (Figure 6.18) showed VLPs which were at a slightly lower level to Ex10 VLPs (*cf.* Figure 6.14) but the VLPs appeared as typical empty capsids characterised by the penetration of uranyl acetate with average size of 48.2 nm with +/- SEM of 3.65, n = 9. These results indicate that the VP1_2 mutant is self-assembly competent although the yield is less than Ex10.

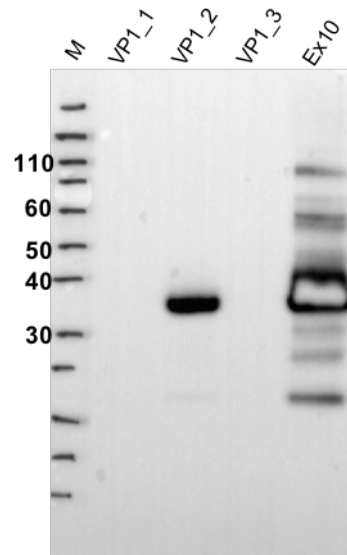


Figure 6.16. WB analysis by anti-VP1 antibody (MAB8566, Millipore) for small scale 3 d.p.i. of Bac-PV1SC6bP1VP1_1, VP1_2, VP1_3 and Bac-PV1SC6bP1Ex10 for *Tnao38* cells

Amongst the VP1 mutants, only VP1_2 showed ~37kDa VP1 reactivity. The level was much lower than Ex10 which showed additional reactivities at higher and lower molecular weight as seen in Figure 6.12. Protein molecular markers are show to the left of the gel (M) and are in kilodaltons. Bolt™4-12% Bis-Tris Plus Gels (ThermoFisher) and Novex™ sharp pre-stained protein standard (ThermoFisher) were used.

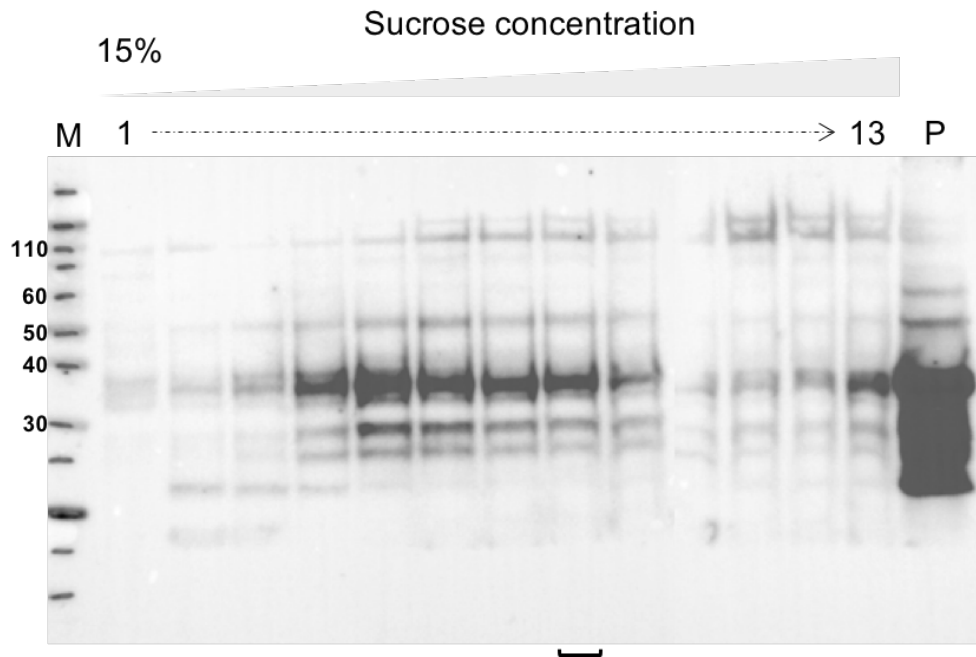


Figure 6.17. WB analysis using anti-VP1 antibody (MAB8566, Millipore) for 15-45 % sucrose gradient fractions of 3 d.p.i. of *Tnao38* cells Bac-PV1SC6bP1VP1_2

100ml *Tnao38* culture infected with Bac-PV1SC6bP1VP1_2-3C was harvested at 3 d.p.i. and lysed with NP40 and ultracentrifuged at 30 % sucrose cushion and 15-45 % sucrose gradient. The blot image is the composite of 2 WBs. ~37 kDa VP1 reactivity was found throughout the gradient, but more prominent in fractions 4 to 8 and fraction 13. The peak of the reactivity occurred in fraction 5. Protein molecular markers are show to the left of the gel (M) and are in kilodaltons. Bolt™4-12% Bis-Tris Plus Gels (ThermoFisher) and Novex™ sharp pre-stained protein standard (ThermoFisher) were used.

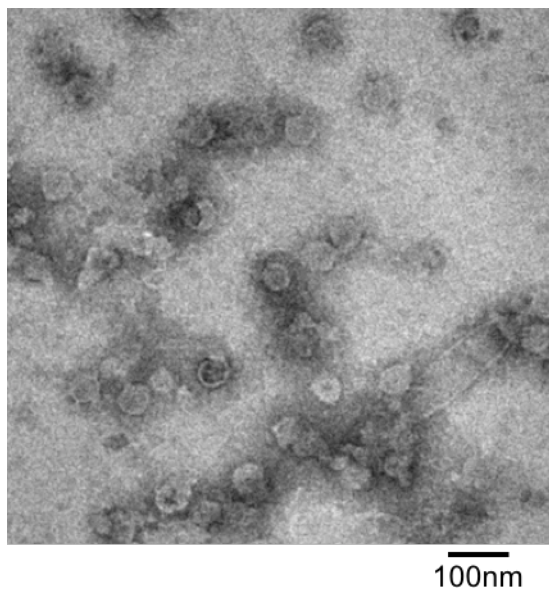


Figure 6.18. TEM image for negative staining of VLPs of Mahoney SC6b VP1_2 from concentrated fraction 8 indicated in Figure 6.17 (Bac-PV1SC6bP1VP1_2 infection of 100 mL *Tnao38* cells)

2 % uranyl acetate was used for the grid staining. Well scattered VLPs and a baculovirus were found. There were two types of particles; empty capsids which are characterised by the penetration of uranyl acetate (majority) and capsids which appeared white and filled as seen for Ex10 VLPs (Figure 6.14). The average size is 48.2 nm with +/- SEM of 3.65, n = 9. 2 % uranyl acetate was used as stain on a copper grid with carbon coated formvar film (Agar scientific).

The results from section 6.5 showed that the VLP assembly for Ex10 and VP1_2 and a higher yield of VLP from all previous constructs. These VLPs are analysed by N/H ELISA for their conformation status. For this analysis, VLPs were directly coated to the ELISA plate rather than capturing the VLPs with the capture Ab. The sample used for TEM imaging was diluted 1/2 with bicarbonate coating buffer, pH 7 and 2-fold dilutions made to 1/64. Following overnight incubation at 4°C, the plate was washed 3 times with PBST and the primary mAbs were added. After this step, the same method as that described in 2.8 was followed.

Figure 6.19 shows that both H readings for Ex10 and VP1_2 VLPs declined as the sample was diluted while the N readings remained almost unchanged indicated that both VLPs are of the H specific conformation. The H readings difference (Ex10 readings being higher than VP1_2) reflects the VLPs concentration difference. It has to be noted that this assay did not contain the IPV standard and that VLPs were directly coated to the plate which could have induced the H conformation in any N antigenic form VLPs present. Thus, the result cannot be compared directly with the other N/H ELISA results. Although the mutation was considered for

improvement in the antigenicity, the data obtained suggest the VLPs are still an H specific conformation.

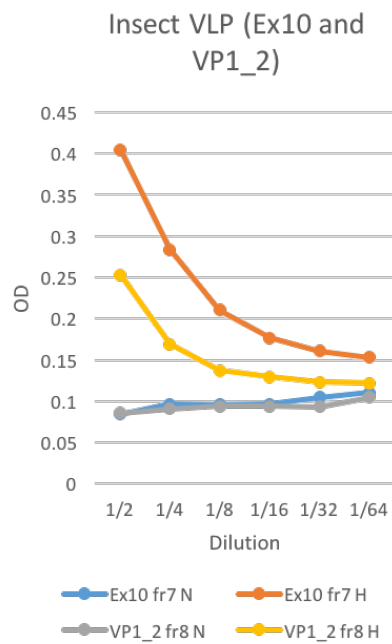


Figure 6.19. N/H ELISA analysis for concentrated peak fractions from 15-45 % sucrose gradient for PV Mahoney SC6b Ex10 (fraction 7) as seen under TEM in Figure 6.14 and VP1_2 (fraction 8) of Figure 6.18 at Reading VLPs were directly coated onto the ELISA plate surface and probed with N- and H- specific antibodies. H specific readings of Ex10 and VP1_2 showed a decline with dilution while N specific readings remained unchanged. H specific reading of Ex10 was generally higher than VP1_2 throughout the dilutions.

6.5 Discussion

Improvements in capsid thermostability is one of the criteria for a new PV vaccine as current vaccines are less than ideal (Milstien *et al.*, 1997). PV particles undergo conformational change during prolonged storage and/or storage temperature (Breindl, 1971) and assume a Heated conformation which cannot induce protective immunity, whereas Native conformation particles can (Hummeler & Hamparian, 1958). For any PV vaccine replacing the current two types, it is essential that the N conformation of capsid is maintained, and this includes VLP candidate vaccines. The conformation of expressed VLPs was examined by ELISA assay using antibodies specific for the H or N conformation and VLPs extracted from insect cells were found to be in the H conformation. VLPs from yeast cells also contained H type antigenicity but showed some N reactivity dependent on the purification method. VLPs derived from PV infection themselves can exhibit the H conformation (Fox *et al.*, 2017). Similarly recent high yielding sources of VLP such as expression in plants, have also observed a variable level of the H/N types (Marsian *et al.*, 2017). While improved therefore, a system providing universal N reactivity remains to be found. The VP1 pocket is a structural feature among enteroviruses and is located in the VP1 interior and normally filled with a pocket factor (Filman *et al.*, 1989). When PV undergoes uncoating upon receptor binding, the pocket factor is dislodged from the pocket to trigger capsid disassembly and lead to RNA release into the host cell (Plevka *et al.*, 2013). Thus the VP1 pocket could be turned to an advantage to maintain capsid structure via molecular engineering of the pocket to mimic pocket occupation. If successful, the capsid should remain in the N conformation and possibly present the PV receptor binding cleft for a longer period which might result in enhanced immunity. Accordingly, residues lining the VP1 pocket were altered and, separately, pocket binding compounds were introduced. For VP1 lining residues, mutations to provide higher hydrophobicity and some structure reinforcement were introduced. The synthetic compounds were expected to bind to the VP1 pocket with higher affinity than any natural pocket factor. The expression assay of VP1 mutants in insect cells demonstrated that none of the mutants improved the VLP yield and some of amino acid changes lead to the cessation of VLP synthesis. There was no significant expression difference among the other mutants. The small-scale expression assay for insect cells infection carried

out with GPV13 showed that the drug is tolerated in the system and that it influenced the expression level. Bac-PV1P1-3C and Bac-Y205W infection showed that the expression level was enhanced by GPV13. On the other hand, analysis of Bac-Y159W indicated an adverse effect on expression. Depending on the side chains that line the pocket, the drug might further stabilise or destabilise the cavity, with associated gain or loss of expression level. Following the enhanced expression observed with GPV13 for Bac-PV1P1-3C, Pleconaril was added to the insect cell culture and a full purification carried out but overall yields were low and a conclusion on N or H predominance was not reached. The same result was obtained for the addition of Pleconaril in yeast cells despite the use of PV3 Skt SC8 which is supposed to have higher initial capsid stability. Further titration of drug level and its effect on overall synthesis are clearly needed.

Overall, the addition of pocket binding drugs or mutation of VP1 residues lining the pocket did not bring about to capsid stability improvements in either system. However, the difference in VP1 levels by WB for each mutant confirmed a contribution of the VP1 pocket to the expression of viral proteins which then affects capsid assembly and stability. The reactivity level difference for the M132 mutants is particularly interesting. VP1 expression was observed for M132L whereas no VP1 was detected for M132W. This indicates that the degree of the VP1 pocket filling by amino acids alters protein expression and suggests a much wider range of amino acid replacements may need to be tested. Similarly, the combination of mutations showed different VP1 reactivity levels, M132W-H207W-F237W \gg M132W-F237W > H207W-F237W (no expression) whereas the F237W showed VP1 reactivity among the single amino acid mutations. Therefore the context of each mutant must also be taken into account and mutations are not additive. M132W and H207W appear to be notably destabilising and even when some expression was seen, such as in M132W-F237W, it was at a lower reactivity compared to WT Bac-PV1P1-3C. On the other hand, the triple mutation M132W-H207W-F237W showed expression as high as Bac-PV1P1-3C. These findings suggest a consideration of the overall shape of the cavity is important and that the WT PV capsid has possibly the default VP1 cavity shape or hydrophobicity. Only a narrow margin of variation within this envelope may be accepted.

Whilst the VP1 pocket was being targeted for stability improvement in this work, further research from Fox *et al.* (2017) isolated the PV Mohoney SC6b mutation which improves thermostability. The P1 sequence of this mutant was inserted into the standard transfer vector and the expression level of VP1 compared to the wildtype sequence. This showed an increased reactivity on a cell for cell basis and TEM imaging confirmed abundant VLP assembly. However, when antigenicity was analysed the N/H ELISA result showed it retained the H antigenic conformation as least when purified as described. In addition, Wang *et al.* (2018) produced a high potency empty 80S-like VLP for EV71 by deleting VP4 sequence from full P1 sequence entirely raising the question of whether VP4 is needed at all for VLP assembly. The density mapping of the VLP by cryo-EM showed the lack of VP4 but also that the N-terminus of VP1 was externalised. During PV virion assembly, VP4 is characterised by flexibility N-terminal myristoylation which is believed to be required for assembly of the protomer into pentamers (Ansardi *et al.*, 1992). The N-terminus of VP4 has various functions during the capsid uncoating such as reversible capsid anchoring to susceptible cells and formation of a finger-like structure together with reorganised GH loop of VP3 (Butan *et al.*, 2014). In order to assess if either of these areas had an effect on PV VLP assembly and stability, mutations were introduced separately. It is worth noting that structure based approaches here are impossible as the flexibility of these regions means they are poorly mapped in either cryo-EM or crystal structures. At the VP4 N-terminus, the N terminal sequence from another myristoylated protein, HIV matrix protein p17, was exchanged with first 10(Ex10), 15(Ex15) and 20(Ex20) amino acids of VP4. Expression level notably increased for all mutants with Ex10 being the most stimulatory when compared to SC6b. It should be noted that, because of the conservation of residues necessary for myristoylation, the amino acid sequence difference between Ex10 and HIV matrix protein, p17 is only 6 amino acids (Figure 6.11). Among these residues are some which are obviously inhibitory for PV VLP assembly in the WT form. For the N-terminus of VP1, a GS linker at 4 or 5 amino acid shifted positions (VP1_1, VP1_2 and VP1_3) was introduced. Of 3 mutants tested, VP1_2 showed protein expression and assembly but this was lower than that observed for Ex10. The difference in the expression among the mutants confirms that the N-terminus of VP1 is an essential part of virus particle assembly and indicates an area for more analysis.

Disappointingly the H antigenicity observed for both Ex10 and VP1_2 VLPs indicated that the neutralising site conformation is not maintained, although noting the difference observed by many groups in VLP preparation, these assays need to be repeated.

The results from the VP4 and VP1 mutational analysis suggests that VLP assembly maybe more flexible than previously thought, also supported by the myristoylation independent mechanism of VLP assembly shown for EV71 VLP $_{\Delta VP4}$ (Wang *et al.*, 2018). Although Wang *et al.* (2018) showed that the EX71 VLP $_{\Delta VP4}$ is an EV71 80S-like particle having an externalised VP1 N-terminus without VP4, the detailed 135S and 80S (Levy *et al.*, 2010) capsid cryo-EM structures for PV indicated that loss of VP4 occurs later than the externalisation of the N-terminus of VP1 but before RNA loss (Butan *et al.*, 2014). The virion uncoating process is therefore in flux and various types of intermediate capsids exist. Some of these intermediates could be, or tend towards, the H antigenic form but as the mechanisms involved must depend on the sequence, mutants able to cement the N conformation could be realistically expected. However, attempts to produce N conformational VLPs from our insect and yeast cell expression systems has not been achieved to date. However, the amino acid substitution to aliphatic and aromatic amino acids at VP1 pocket interior residues and the pocket binding drug addition to one of the mutants have demonstrated that there is strict preference of hydrophobicity or overall shape for the VP1 pocket, for the assembly of VLPs. This area may therefore be a relatively poor target for further mutational analysis. The modification of VP4 or the N-terminus of VP1 and the maintenance of VLPs is entirely new and somewhat unexpected. It may indicate areas for further manipulation in pursuit of a VLP form that is 100 % N type irrespective of the expression system or purification protocol.

Chapter 7 General Discussion

The aim of this project was to produce PV VLPs from insect and/or yeast cells and to investigate their stability and conformational status to assess if empty PV capsids could lead to be a future PV vaccine. Throughout the research, attempts to optimise purification methods for higher VLP yield were also explored. VLP vaccines for picornaviruses have been developed since around 1990. PV VLP was produced originally in insect cells using baculovirus and yeast expression system. Insertion of the complete PV1 genome into a baculovirus transfer vector led to the synthesis of structural proteins and assembly of PV empty capsids which showed weak neutralising responses (Urakawa *et al.*, 1989). Co-expression of PV structural protein, P1 and its protease, 3CD^{pro} in yeast resulted in viral protein expression and VLPs which were non-immunogenic unless a capsid stabilising drug was added (Rombaut & Jore, 1997). Both VLP produced in foreign expression systems did not meet the criteria necessary for a viable vaccine candidate and they were not pursued further. More recently however, VLP vaccine development for some other members of the *picornaviridae* such as FMDV and EV71 has attracted renewed research interest. FMDV VLP production in insect cells defined the minimal requirements for empty capsid synthesis. In the system described, the structural protein (P1-2A) was processed by a modified protease 3C^{pro} (Sweeney *et al.*, 2007) combined with a HIV-1 ribosomal frameshift (Dinman *et al.*, 2002) which together lowered protease activity to a point where cellular toxicity was reduced. This modification produces P1 as majority product and P1-2A-3C^{pro} as a minor product. The expression cassette (P1-2A-FS-3C*) improved yields substantially and demonstrated potential for not only FMDV but also for other picornavirus empty capsid production in insect cells (Porta *et al.*, 2013). Research within the host group at Reading first adapted the cassette for EV71 empty capsid synthesis (Cone, 2015). In the process, EV71 3C^{pro} with a S128A mutation, which reduces the protease activity in an equivalent way to the 142 mutation in FMDV 3C, was produced (Cui *et al.*, 2011). As EV71 and polio 3C proteases share 55 % homology and are structurally very similar (Cui *et al.*, 2011; Zhang *et al.*, 2010) PV VLP synthesis was attempted using the EV71 3C sequence to cleave PV P1. That is, for PV VLP production for this project the P1 region of the EV71 cassette was

adapted by just replacing with PVP1. This resulted in the expression cassette consisting of (PVP1-PV2A-FS-EV713C*).

This chimeric expression cassette, in a single expression vector, was shown to synthesis cleaved viral proteins and that they self-assembled into VLPs in both the baculovirus and yeast expression systems. The result revealed that PV structural protein P1 can be proteolytically processed into viral proteins efficiently by modified 3C_{EV71}. PV structural protein cleavage has been widely accepted to be most efficiently achieved by PV 3CD^{pro} (Harris *et al.*, 1992; Kitamura *et al.*, 1981; Kräusslich *et al.*, 1988; Lawson & Semler, 1990; Pallansch *et al.*, 1984; Parsley *et al.*, 1999). However, PV 3CD^{pro} activity was not efficient in the baculovirus expression system describe here and only poor protein processing was observed. The findings support of control of protease activity more than the origin of protease, assuming their cleavage recognition sites are the same. A detailed examination of 3CD levels may have allowed an efficient cassette to be constructed but this was not done. To reconcile this finding with the originally published data, translation of much larger 3CD^{pro} will require a longer time compared to that of 3C^{pro} and, as a consequence, less 3CD^{pro} than 3C^{pro} will be produced. The lower level of 3CD in the original papers may have suited the *in vitro* translation experiments done but maybe too low in the expression cassette assembled here. Indeed, abundant P1 was observed on the gels when all constructs using 3CD were analysed, consistent with poor levels of processing. In the insect cells and *S. cerevisiae* expression systems used in this project however, an efficient ratio of P1 to 3C was met by use of the HIV-1 ribosomal frameshift and lowered activity 3C_{EV71} and this was the basis of all further constructs.

Purifying VLPs following expression of the capsid proteins in insect cell and yeast systems proved difficult and changes to the purification method were adopted throughout the course of the work. A combination of PV sequence changes and improvements in capsid extraction, in part suggested by collaborators based on their experience in other systems, led to substantial yield enhancements over the course of the study. Enhanced capsid stability, which is part of the improvements, should benefit during not only the purification of VLPs but also their storage and transport if and when they became a vaccine. The instability of PV VLPs are known from previous studies (Rombaut & Jore, 1997; Urakawa *et al.*, 1989), particularly heat sensitivity (Filman *et al.*, 1989; Macadam *et al.*, 1989). All purification procedures were therefore carried

out at 4°C or below whenever possible but VLP loss was nevertheless encountered. Physical homogenization, mechanical pressurising and bead-beating was able to lyse cells efficiently in a short period of time but appeared to damage the VLPs. A simple non-ionic detergent (NP40) seemed suitable for insect cells but could not remove the yeast membrane after cell wall removal. N₂ cavitation seemed to show more promising VLP recovery. For heat sensitive products such as PV VLPs, a low temperature purification method is required so mechanical methods that generate heat were generally not compatible. For yeast cells, zymolyase digest of the yeast cell wall was essential as it decreased the robustness of the cell prior to mechanical breaking. However this could become a cost sensitive step for very large cultures. Overall, some PV VLP yield improvement by using N₂ cavitation and NP40 method for insect cell derived PV VLPs and N₂ cavitation and zymolyase method for yeast origin VLPs was demonstrated during the study.

Capsid stability is also intimately related to VLPs antigenicity. The “H” antigenic form is defined as heated and is a known sensitivity for current vaccines where improvements are made. A characteristic of the PV capsid structure is the hydrophobic cavity, the “pocket” which is located at the bottom of canyon within the body of VP1. Stable mature PV particles have long molecules, pocket factors, bound and pocket factor removal is observed during capsid conformational change after the PV particle has attached to the receptor and prior to RNA release (Plevka *et al.*, 2013). This feature has been targeted for anti-viral drug development to stop PV infection. Those compounds replace the natural pocket factor and bind so tightly to the capsid that conformational change is prevented. VLPs do not need to uncoat for virus replication and so modifications aimed at locking the pocket, in the manner analogous to a bound drug, which would be lethal for the virus, are permitted and could provide a level of stability. This strategy was attempted as part of these studies by the introduction of hydrophobic and bulky amino acids such as leucine and tryptophan in place of the residues that naturally line the pocket. In addition the addition of pocket binding drugs, pleconaril and GPV13 was investigated. PV viral protein expression levels varied depending on the mutation made but universally to lower levels, almost to the point of losing expression completely. Combination of mutations performed similarly. These findings confirm that maintenance of the pocket structure contributes to the conformation of the capsid in the content of VLPs but no

significant increases in expression (stability) were seen. It seems that even variation in the pocket area is poorly acceptable for VLP assembly and that disassembled material degrades, lowering the levels observed. Similarly supplementing with pleconaril or GPV13 failed to improve stability significantly although when combined with one mutation a positive trend was observed and further work in this area could be productive. Katpally and Smith (2007) have shown for HRV16 an inability to uncoat due to increased stability achieved through pocket filling mutations in the pocket area so the strategy has a clear precedent. Although stable VLP were not obtained in these tests, it was clear that pocket shape was important for VLP assembly and it seems likely a much greater range of mutations will need to be assessed, as those predicted failed to achieve the desired outcome (also since confirmed following vaccinia expression by Oxford collaborators). In addition to pocket region manipulations for enhanced thermostability, mutations discovered from a novel virus thermostability screen (Fox *et al.*, 2017) were used in the VLP expression cassette. Empty capsid with these novel mutations were shown to be thermostable while remaining immunogenic in animal models. A PV3 construct, termed SC8, and SC6 for PV1 that contained these mutations did increase yield somewhat in the expression systems tested here and equivalent mutations in PV2 would be worth investigating.

Results from section 6.4 also suggested that novel mutations, not based on any previous selection criteria, could also benefit VLP yield. In particular modification of the N-terminus of the VP4 sequence was shown to enhance expression levels and retain VLP assembly. The rationale for these mutations was that the N terminus of VP4 moves during capsid breathing and that if this was prevented the capsid could become more rigid. However, neither the structure of the N-terminus of VP4 within the VLP, nor its precise track to the exterior is clear from current PV structures so the requirement for any mutation to prevent such movement is impossible to design. In the event, as myristoylation of VP4 has been reported to be essential for PV assembly (Chow *et al.*, 1987) a sequence from another myristoylated protein, the HIV matrix protein was exchanged for the resident VP4 N-terminus. VLP synthesis was abundant for the new Ex10 mutant but the reasons why it should be so are not clear and further analysis of the mutant is required, not least for its N/H ratio following careful purification. Nevertheless,

the data indicate that many more mutants within the ~900 residues of PVP1 could have an effect on capsid stability, especially in the context of VLPs with a non-cleaved VP0 protein. How such a wide ranging set of mutations could be screened is difficult to see but it is clear that “wild” mutations could have a role to play.

Whatever the ideally stable VLP is, if it was achieved it could obviously deliver a vaccine for the polio free world but could also act as the platform technology for the development of recombinant PV capsids as carrier for other cargoes. One approach may be to improve the breadth of the immune response to provide a single vaccine for all three serotypes. A study carried out with a related picornavirus, FMDV, has shown that mutations in dominant epitopes can result in immune refocusing which improves neutralising activity (Tobin *et al.*, 2008). Capsids of PV could perhaps be similarly engineered to introduce the defocusing mutation into the major epitopes. Another approach to the use VLPs as a generic vaccine platform is the icosahedral capsid itself, which offers abundant copies of a unit which is available for the presentation of diverse epitopes (Burke *et al.*, 1991; Evans & Almond, 1991). Indeed once sufficient amounts of native antigenic PV VLPs are obtained and the immunogenicity of the vaccine is confirmed, the PV vaccine could become a platform with a future that is not only polio free but also free of many other diseases where current vaccination strategies are limited.

Chapter 8 References

- Abe, T., Hemmi, H., Miyamoto, H., Moriishi, K., Tamura, S., Takaku, H., Akira, S. & Matsuura, Y. (2005). Involvement of the toll-like receptor 9 signaling pathway in the induction of innate immunity by baculovirus. *Journal of Virology* **79**, 2847-2858.
- Adeyemi, O. O., Nicol, C., Stonehouse, N. J. & Rowlands, D. J. (2017). Increasing Type 1 Poliovirus Capsid Stability by Thermal Selection. *Journal of Virology* **91**, e01586-01516.
- Adu, F., Iber, J., Bukbuk, D., Gumede, N., Yang, S. J., Jorba, J., Campagnoli, R., Sule, W. F., Yang, C. F., Burns, C., Pallansch, M., Harry, T. & Kew, O. (2007). Isolation of recombinant type 2 vaccine-derived poliovirus (VDPV) from a Nigerian child. *Virus Res* **127**, 17-25.
- Agirre, A., Barco, A., Carrasco, L. & Nieva, J. L. (2002). Viroporin-mediated membrane permeabilization - Pore formation by nonstructural poliovirus 2B protein. *Journal of Biological Chemistry* **277**, 40434-40441.
- Ailor, E. & Betenbaugh, M. J. (1999). Modifying secretion and post-translational processing in insect cells. *Current Opinion in Biotechnology* **10**, 142-145.
- Aldabe, R., Barco, A. & Carrasco, L. (1996). Membrane permeabilization by poliovirus proteins 2B and 2BC. *Journal of Biological Chemistry* **271**, 23134-23137.
- Aldabe, R. & Carrasco, L. (1995). Induction of Membrane Proliferation by Poliovirus Proteins 2C and 2BC. *Biochemical and Biophysical Research Communications* **206**, 64-76.
- Altmann, F., Staudacher, E., Wilson, I. B. H. & März, L. (1999). Insect cells as hosts for the expression of recombinant glycoproteins. *Glycoconjugate Journal* **16**, 109-123.
- Ambros, V. & Baltimore, D. (1980). Purification and properties of a HeLa cell enzyme able to remove the 5'-terminal protein from poliovirus RNA. *Journal of Biological Chemistry* **255**, 6739-6744.
- Andino, R., Rieckhof, G. E., Achacoso, P. L. & Baltimore, D. (1993). Poliovirus RNA synthesis utilizes an RNP complex formed around the 5'-end of viral RNA. *Embo J* **12**, 3587-3598.
- Andino, R., Rieckhof, G. E. & Baltimore, D. (1990). A functional ribonucleoprotein complex forms around the 5' end of poliovirus RNA. *Cell* **63**, 369-380.
- Andries, K., Dewindt, B., Snoeks, J., Willebrords, R., van Eemeren, K., Stokbroekx, R. & Janssen, P. A. (1992). In vitro activity of pirodavir (R 77975), a substituted phenoxy-pyridazinamine with broad-spectrum antipicornaviral activity. *Antimicrob Agents Chemother* **36**, 100-107.
- Ansardi, D. C., Porter, D. C. & Morrow, C. D. (1991). Coinfection with recombinant vaccinia viruses expressing poliovirus P1 and P3 proteins results in polyprotein processing and formation of empty capsid structures. *J Virol* **65**, 2088-2092.
- Ansardi, D. C., Porter, D. C. & Morrow, C. D. (1992). Myristylation of poliovirus capsid precursor P1 is required for assembly of subviral particles. *Journal of virology* **66**, 4556-4563.
- Arita, M., Shimizu, H. & Miyamura, T. (2004). Characterization of in vitro and in vivo phenotypes of poliovirus type 1 mutants with reduced viral protein synthesis activity. *J Gen Virol* **85**, 1933-1944.
- Barton, D. J. & Flanagan, J. B. (1997). Synchronous replication of poliovirus RNA: initiation of negative-strand RNA synthesis requires the guanidine-inhibited activity of protein 2C. *Journal of Virology* **71**, 8482-8489.
- Basavappa, R., Gómez-Yafal, A. & Hogle, J. M. (1998). The Poliovirus Empty Capsid Specifically Recognizes the Poliovirus Receptor and Undergoes Some, but Not All, of the Transitions Associated with Cell Entry. *Journal of Virology* **72**, 7551-7556.
- Basavappa, R., Syed, R., Flore, O., Icenogle, J. P., Filman, D. J. & Hogle, J. M. (1994). Role and mechanism of the maturation cleavage of VP0 in poliovirus assembly: structure of the empty capsid assembly intermediate at 2.9 Å resolution. *Protein science : a publication of the Protein Society* **3**, 1651-1669.
- Belnap, D. M., McDermott, B. M., Filman, D. J., Cheng, N. Q., Trus, B. L., Zuccola, H. J., Racaniello, V. R., Hogle, J. M. & Steven, A. C. (2000). Three-dimensional structure

- of poliovirus receptor bound to poliovirus. *Proceedings of the National Academy of Sciences of the United States of America* **97**, 73-78.
- Bergelson, J. M. & Coyne, C. B. (2013).** Picornavirus Entry. In *Viral Entry into Host Cells*, pp. 24-41. Edited by S. Pöhlmann & G. Simmons. New York, NY: Springer New York.
- Berlec, A. & Strukelj, B. (2013).** Current state and recent advances in biopharmaceutical production in *Escherichia coli*, yeasts and mammalian cells. *Journal of Industrial Microbiology & Biotechnology* **40**, 257-274.
- Berrow, N. S., Alderton, D., Sainsbury, S., Nettleship, J., Assenberg, R., Rahman, N., Stuart, D. I. & Owens, R. J. (2007).** A versatile ligation-independent cloning method suitable for high-throughput expression screening applications. *Nucleic Acids Res* **35**, e45.
- Beske, O., Reichelt, M., Taylor, M. P., Kirkegaard, K. & Andino, R. (2007).** Poliovirus infection blocks ERGIC-to-Golgi trafficking and induces microtubule-dependent disruption of the Golgi complex. *J Cell Sci* **120**, 3207-3218.
- Bienz, K., Egger, D., Pfister, T. & Troxler, M. (1992).** Structural and functional characterization of the poliovirus replication complex. *Journal of Virology* **66**, 2740-2747.
- Bill, R. M. (2015).** Recombinant protein subunit vaccine synthesis in microbes: a role for yeast? *J Pharm Pharmacol* **67**, 319-328.
- Binford, S. L., Maldonado, F., Brothers, M. A., Weady, P. T., Zalman, L. S., Meador, J. W., Matthews, D. A. & Patick, A. K. (2005).** Conservation of amino acids in human rhinovirus 3C protease correlates with broad-spectrum antiviral activity of rupintrivir, a novel human rhinovirus 3C protease inhibitor. *Antimicrobial Agents and Chemotherapy* **49**, 619-626.
- Binford, S. L., Weady, P. T., Maldonado, F., Brothers, M. A., Matthews, D. A. & Patick, A. K. (2007).** In Vitro Resistance Study of Rupintrivir, a Novel Inhibitor of Human Rhinovirus 3C Protease. *Antimicrobial Agents and Chemotherapy* **51**, 4366-4373.
- Blomqvist, S., Savolainen, C., Laine, P., Hirttio, P., Lamminsalo, E., Penttila, E., Joks, S., Roivainen, M. & Hovi, T. (2004).** Characterization of a highly evolved vaccine-derived poliovirus type 3 isolated from sewage in Estonia. *J Virol* **78**, 4876-4883.
- Blondel, B., Colbere-Garapin, F., Couderc, T., Wirotius, A. & Guivel-Benhassine, F. (2005).** Poliovirus, pathogenesis of poliomyelitis, and apoptosis. *Curr Top Microbiol Immunol* **289**, 25-56.
- Bodian, D. (1949).** Differentiation of types of poliomyelitis viruses; reinfection experiments in monkeys (second attacks). *American journal of hygiene* **49**, 200-223.
- Bodian, D. (1951).** Immunologic classification of poliomyelitis viruses. I. A cooperative program for the typing of one hundred strains. *American journal of hygiene* **54**, 191-204.
- Bodian, D. (1955).** Emerging Concept of Poliomyelitis Infection. *Science* **122**, 105-108.
- Bodian, D. & Horstmann, D. H. (1965).** Polioviruses. In *Viral and Rickettsial Infections of Man*, pp. 430-473. Edited by L. F. Horsfall. & T. I. Philadelphia: Lippincott.
- Bodian, D., Morgan, I. M. & Howe, H. A. (1949).** DIFFERENTIATION OF TYPES OF POLIOMYELITIS VIRUSES: III. THE GROUPING OF FOURTEEN STRAINS INTO THREE BASIC IMMUNOLOGICAL TYPES. *American Journal of Epidemiology* **49**, 234-247.
- Bostina, M., Levy, H., Filman, D. J. & Hogle, J. M. (2011).** Poliovirus RNA is released from the capsid near a twofold symmetry axis. *J Virol* **85**, 776-783.
- Brandenburg, B., Lee, L. Y., Lakadamyali, M., Rust, M. J., Zhuang, X. W. & Hogle, J. M. (2007).** Imaging poliovirus entry in live cells. *PLoS Biol* **5**, 1543-1555.
- Breindl, M. (1971).** The Structure of Heated Poliovirus Particles. *Journal of General Virology* **11**, 147-156.
- Brown, A. J. P., Brown, G. D., Netea, M. G. & Gow, N. A. R. (2014).** Metabolism impacts upon *Candida* immunogenicity and pathogenicity at multiple levels. *Trends in Microbiology* **22**, 614-622.
- Burgess, S. (1977).** Molecular Weights of Lepidopteran Baculovirus DNAs: Derivation by Electron Microscopy. *Journal of General Virology* **37**, 501-510.
- Burke, K. L., Almond, J. W. & Evans, D. J. (1991).** Antigen chimeras of poliovirus. *Prog Med Virol* **38**, 56-68.

- Butan, C., Filman, D. J. & Hogle, J. M. (2014).** Cryo-electron microscopy reconstruction shows poliovirus 135S particles poised for membrane interaction and RNA release. *J Virol* **88**, 1758-1770.
- Cammack, N., Phillips, A., Dunn, G., Patel, V. & Minor, P. D. (1988).** Intertypic genomic rearrangements of poliovirus strains in vaccinees. *Virology* **167**, 507-514.
- CDC (2007).** Update on vaccine-derived polioviruses--worldwide, January 2006-August 2007. *MMWR Morb Mortal Wkly Rep* **56**, 996-1001.
- CDC (2017).** For Healthcare Professionals. Atlanta: Centers for Disease Control and Prevention.
- Centers for Disease Control and Prevention (2012).** *Epidemiology and Prevention of Vaccine-Preventable Diseases*. Washington DC: Public Health Foundation.
- Chackerian, B. (2007).** Virus-like particles: flexible platforms for vaccine development. *Expert Rev Vaccines* **6**, 381-390.
- Charlton, C. A. & Volkman, L. E. (1991).** Sequential rearrangement and nuclear polymerization of actin in baculovirus-infected *Spodoptera frugiperda* cells. *Journal of Virology* **65**, 1219-1227.
- Chen, S.-A., Lee, T.-Y. & Ou, Y.-Y. (2010).** Incorporating significant amino acid pairs to identify O-linked glycosylation sites on transmembrane proteins and non-transmembrane proteins. *BMC Bioinformatics* **11**, 536-536.
- Cherkasova, E. A., Yakovenko, M. L., Rezapkin, G. V., Korotkova, E. A., Ivanova, O. E., Eremeeva, T. P., Krasnoproshina, L. I., Romanenkova, N. I., Rozaeva, N. R., Sirota, L., Agol, V. I. & Chumakov, K. M. (2005).** Spread of vaccine-derived poliovirus from a paralytic case in an immunodeficient child: an insight into the natural evolution of oral polio vaccine. *Journal of Virology* **79**, 1062-1070.
- Chisholm, G. E. & Henner, D. J. (1988).** Multiple early transcripts and splicing of the *Autographa californica* nuclear polyhedrosis virus IE-1 gene. *Journal of Virology* **62**, 3193-3200.
- Cho, M. W., Teterina, N., Egger, D., Bienz, K. & Ehrenfeld, E. (1994).** Membrane Rearrangement and Vesicle Induction by Recombinant Poliovirus 2C and 2BC in Human Cells. *Virology* **202**, 129-145.
- Chow, M., Newman, J. F. E., Filman, D., Hogle, J. M., Rowlands, D. J. & Brown, F. (1987).** Myristylation of picornavirus capsid protein VP4 and its structural significance. *Nature* **327**, 482-486.
- Chumakov, K. & Ehrenfeld, E. (2008).** New generation of inactivated poliovirus vaccines for universal immunization after eradication of poliomyelitis. *Clin Infect Dis* **47**, 1587-1592.
- Chung, Y. C., Huang, J. H., Lai, C. W., Sheng, H. C., Shih, S. R., Ho, M. S. & Hu, Y. C. (2006).** Expression, purification and characterization of enterovirus-71 virus-like particles. *World Journal of Gastroenterology* **12**, 921-927.
- Cifuentes, J. O., Lee, H., Yoder, J. D., Shingler, K. L., Carnegie, M. S., Yoder, J. L., Ashley, R. E., Makhov, A. M., Conway, J. F. & Hafenstein, S. (2013).** Structures of the Procapsid and Mature Virion of Enterovirus 71 Strain 1095. *Journal of Virology* **87**, 7637-7645.
- Collett, M. S., Neyts, J. & Modlin, J. F. (2008).** A case for developing antiviral drugs against polio. *Antiviral Research* **79**, 179-187.
- Cone, A. (2015).** Assembly of Foot and Mouth Disease Virus and Enterovirus 71 Virus-Like Particles. In *PhD thesis*: University of Reading.
- Cox, S., Buontempo, P. J., Wright-Minogue, J., DeMartino, J. L., Skelton, A. M., Ferrari, E., Schwartz, J., Rozhon, E. J., Linn, C.-C., Girijavallabhan, V. & O'Connell, J. F. (1996).** Antipicornavirus activity of SCH 47802 and analogs: in vitro and in vivo studies. *Antiviral Research* **32**, 71-79.
- Cui, S., Wang, J., Fan, T., Qin, B., Guo, L., Lei, X., Wang, J., Wang, M. & Jin, Q. (2011).** Crystal Structure of Human Enterovirus 71 3C Protease. *Journal of Molecular Biology* **408**, 449-461.
- Curran, B. P. G. & Bugeja, V. C. (2000).** Yeast Cloning and Biotechnology. In *Molecular Biology and Biotechnology*. Edited by J. M. Walker, E. Green & E. J. Murray. Cambridge, GB: Royal Society of Chemistry.
- Curry, S., Chow, M. & Hogle, J. M. (1996).** The poliovirus 135S particle is infectious. *J Virol* **70**, 7125-7131.

- Dales, S., Eggers, H. J., Tamm, I. & Palade, G. E. (1965).** Electron microscopic study of the formation of poliovirus. *Virology* **26**, 379-389.
- Danthi, P., Tosteson, M., Li, Q.-h. & Chow, M. (2003).** Genome Delivery and Ion Channel Properties Are Altered in VP4 Mutants of Poliovirus. *Journal of Virology* **77**, 5266-5274.
- De Colibus, L., Wang, X., Spyrou, J. A. B., Kelly, J., Ren, J., Grimes, J., Puerstinger, G., Stonehouse, N., Walter, T. S., Hu, Z., Wang, J., Li, X., Peng, W., Rowlands, D. J., Fry, E. E., Rao, Z. & Stuart, D. I. (2014).** More-powerful virus inhibitors from structure-based analysis of HEV71 capsid-binding molecules. *Nat Struct Mol Biol*, advance online publication.
- De Jesus, N. H. (2007).** Epidemics to eradication: the modern history of poliomyelitis. *Viol J* **4**, 70.
- De Palma, A. M., Pürstinger, G., Wimmer, E., Patick, A. K., Andries, K., Rombaut, B., De Clercq, E. & Neyts, J. (2008a).** Potential Use of Antiviral Agents in Polio Eradication. *Emerging Infectious Diseases* **14**, 545-551.
- De Palma, A. M., Vliegen, I., De Clercq, E. & Neyts, J. (2008b).** Selective inhibitors of picornavirus replication. *Medicinal Research Reviews* **28**, 823-884.
- De Sena, J. & Mandel, B. (1977).** Studies on the in vitro uncoating of poliovirus. II. Characteristics of the membrane-modified particle. *Virology* **78**, 554-566.
- Dijkstra, J. & Jager, C. P. (1998).** Density-Gradient Centrifugation. In *Practical Plant Virology: Protocols and Exercises*, pp. 232-237. Berlin: Springer Berlin Heidelberg.
- Dinman, J. D., Richter, S., Plant, E. P., Taylor, R. C., Hammell, A. B. & Rana, T. M. (2002).** The frameshift signal of HIV-1 involves a potential intramolecular triplex RNA structure. *Proceedings of the National Academy of Sciences of the United States of America* **99**, 5331-5336.
- Dorschhasler, K., Yogo, Y. & Wimmer, E. (1975).** Replication of picornaviruses. I. Evidence from in vitro RNA synthesis that poly(A) of the poliovirus genome is genetically coded. *Journal of Virology* **16**, 1512-1527.
- Dowdle, W. R., De Gourville, E., Kew, O. M., Pallansch, M. A. & Wood, D. J. (2003).** Polio eradication: the OPV paradox. *Reviews in Medical Virology* **13**, 277-291.
- Dragovich, P. S., Webber, S. E., Babine, R. E., Fuhrman, S. A., Patick, A. K., Matthews, D. A., Lee, C. A., Reich, S. H., Prins, T. J., Marakovits, J. T., Littlefield, E. S., Zhou, R., Tikhe, J., Ford, C. E., Wallace, M. B., Meador, J. W., Ferre, R. A., Brown, E. L., Binford, S. L., Harr, J. E. V., DeLisle, D. M. & Worland, S. T. (1998).** Structure-based design, synthesis, and biological evaluation of irreversible human rhinovirus 3C protease inhibitors. 1. Michael acceptor structure-activity studies. *J Med Chem* **41**, 2806-2818.
- Egger, D., Teterina, N., Ehrenfeld, E. & Bienz, K. (2000).** Formation of the Poliovirus Replication Complex Requires Coupled Viral Translation, Vesicle Production, and Viral RNA Synthesis. *Journal of Virology* **74**, 6570-6580.
- Ehrenfeld, E., Modlin, J. & Chumakov, K. (2009).** Future of polio vaccines. *Expert Rev Vaccines* **8**, 899-905.
- EMD Chemicals Inc (2011).** *TB250 pTriEx™ System Manual*. Darmstadt, Germany.
- Enders, J. F., Weller, T. H. & Robbins, F. C. (1949).** Cultivation of the Lansing Strain of Poliomyelitis Virus in Cultures of Various Human Embryonic Tissues. *Science* **109**, 85-87.
- Evans, D. J. & Almond, J. W. (1991).** Design, construction, and characterization of poliovirus antigen chimeras. *Methods Enzymol* **203**, 386-400.
- Felgner, J. H., Kumar, R., Sridhar, C. N., Wheeler, C. J., Tsai, Y. J., Border, R., Ramsey, P., Martin, M. & Felgner, P. L. (1994).** Enhanced gene delivery and mechanism studies with a novel series of cationic lipid formulations. *Journal of Biological Chemistry* **269**, 2550-2561.
- Feng, Z., Hensley, L., McKnight, K. L., Hu, F., Madden, V., Ping, L., Jeong, S.-H., Walker, C., Lanford, R. E. & Lemon, S. M. (2013).** A pathogenic picornavirus acquires an envelope by hijacking cellular membranes. *Nature* **496**, 367-371.
- Fenwick, M. L. & Cooper, P. D. (1962).** Early interactions between poliovirus and ERK cells: some observations on the nature and significance of the rejected particles. *Virology* **18**, 212-223.

- Filman, D. J., Syed, R., Chow, M., Macadam, A. J., Minor, P. D. & Hogle, J. M. (1989).** Structural factors that control conformational transitions and serotype specificity in type 3 poliovirus. *EMBO J* **8**, 1567-1579.
- Flint, J., Racaniello, V. R., Rall, G. F., Skalka, A. & Enquist, L. W. (2015a).** Picornavirus. In *Principles of Virology*, 4th edn, pp. 522-523. Edited by AMS Press. Washington, DC: AMS Press.
- Flint, J., Racaniello, V. R., Rall, G. F., Skalka, A. & Enquist, L. W. (2015b).** Structure. In *Principles of Virology*, 4th edn, pp. 80-120. Edited by AMS Press. Washington, DC: AMS Press.
- Flint, J., Racaniello, V. R., Rall, G. F., Skalka, A. & Enquist, L. W. (2015c).** Vaccines. In *Principles of Virology*, 4th edn, pp. 254-280. Edited by AMS Press. Washington, DC: AMS Press.
- Florea, N. R., Maglio, D. & Nicolau, D. P. (2003).** Pleconaril, a novel antipicornaviral agent. *Pharmacotherapy* **23**, 339-348.
- Fox, H., Knowlson, S., Minor, P. D. & Macadam, A. J. (2017).** Genetically Thermo-Stabilised, Immunogenic Poliovirus Empty Capsids; a Strategy for Non-replicating Vaccines. *PLoS Pathog* **13**, e1006117.
- Fraser, M. J. (1986).** Ultrastructural observations of virion maturation in *Autographa californica* nuclear polyhedrosis virus infected *Spodoptera frugiperda* cell cultures. *Journal of Ultrastructure and Molecular Structure Research* **95**, 189-195.
- Fricks, C. E. & Hogle, J. M. (1990).** Cell-induced conformational change in poliovirus: externalization of the amino terminus of VP1 is responsible for liposome binding. *J Virol* **64**, 1934-1945.
- Galassi, F. M., Habicht, M. E. & Rühli, F. J. (2017).** Poliomyelitis in Ancient Egypt? *Neurological Sciences* **38**, 375-375.
- Garriga, D., Pickl-Herk, A., Luque, D., Wruss, J., Castón, J. R., Blaas, D. & Verdaguer, N. (2012).** Insights into Minor Group Rhinovirus Uncoating: The X-ray Structure of the HRV2 Empty Capsid. *PLoS Pathog* **8**, e1002473.
- Gary, H. E., Jr., Freeman, C., Penaranda, S., Maher, K., Anderson, L. & Pallansch, M. A. (1997).** Comparison of a monoclonal antibody-based IgM capture ELISA with a neutralization assay for assessing response to trivalent oral poliovirus vaccine. *J Infect Dis* **175 Suppl 1**, S264-267.
- Ghendon, Y. & Robertson, S. E. (1994).** Interrupting the transmission of wild polioviruses with vaccines: immunological considerations. *Bulletin of the World Health Organization* **72**, 973-983.
- Goffeau, A., Barrell, B. G., Bussey, H., Davis, R. W., Dujon, B., Feldmann, H., Galibert, F., Hoheisel, J. D., Jacq, C., Johnston, M., Louis, E. J., Mewes, H. W., Murakami, Y., Philippsen, P., Tettelin, H. & Oliver, S. G. (1996).** Life with 6000 Genes. *Science* **274**, 546-567.
- Goodwin, S., Tuthill, T. J., Arias, A., Killington, R. A. & Rowlands, D. J. (2009).** Foot-and-mouth disease virus assembly: processing of recombinant capsid precursor by exogenous protease induces self-assembly of pentamers in vitro in a myristoylation-dependent manner. *J Virol* **83**, 11275-11282.
- GPEI (2016).** HISTORY OF POLIO. Geneva: Global Polio Eradication Initiative.
- Granados, R. R., Guoxun, L., Derksen, A. C. G. & McKenna, K. A. (1994).** A new insect cell line from *Trichoplusia ni* (BTI-Tn-5B1-4) susceptible to *Trichoplusia ni* single enveloped nuclear polyhedrosis virus. *Journal of Invertebrate Pathology* **64**, 260-266.
- Grant, R. A., Hiremath, C. N., Filman, D. J., Syed, R., Andries, K. & Hogle, J. M. (1994).** Structures of poliovirus complexes with anti-viral drugs: implications for viral stability and drug design. *Current biology : CB* **4**, 784-797.
- Guskey, L. E., Smith, P. C. & Wolff, D. A. (1970).** Patterns of Cytopathology and Lysosomal Enzyme Release in Poliovirus-infected HEp-2 Cells Treated With Either 2-(α -Hydroxybenzyl)-Benzimidazole or Guanidine HCl. *Journal of General Virology* **6**, 151-161.
- Guttman, N. & Baltimore, D. (1977).** Morphogenesis of poliovirus. IV. existence of particles sedimenting at 150S and having the properties of provirion. *Journal of Virology* **23**, 363-367.

- Hambidge, S. J. & Sarnow, P. (1992).** Translational Enhancement of the Poliovirus 5' Noncoding Region Mediated by Virus-Encoded Polypeptide 2A. *Proceedings of the National Academy of Sciences of the United States of America* **89**, 10272-10276.
- Hanecak, R., Semler, B. L., Anderson, C. W. & Wimmer, E. (1982).** Proteolytic processing of poliovirus polypeptides: antibodies to polypeptide P3-7c inhibit cleavage at glutamine-glycine pairs. *Proceedings of the National Academy of Sciences* **79**, 3973-3977.
- Harber, J. J., Bradley, J., Anderson, C. W. & Wimmer, E. (1991).** Catalysis of poliovirus VP0 maturation cleavage is not mediated by serine 10 of VP2. *Journal of Virology* **65**, 326-334.
- Harris, K. S., Reddigari, S. R., Nicklin, M. J., Hämmerle, T. & Wimmer, E. (1992).** Purification and characterization of poliovirus polypeptide 3CD, a proteinase and a precursor for RNA polymerase. *Journal of Virology* **66**, 7481-7489.
- Harris, K. S., Xiang, W. K., Alexander, L., Lane, W. S., Paul, A. V. & Wimmer, E. (1994).** Interaction of poliovirus polypeptide 3CDpro with the 5'-termini and 3'-termini of the poliovirus genome. Identification of viral and cellular cofactors needed for efficient binding. *Journal of Biological Chemistry* **269**, 27004-27014.
- Hashimoto, Y., Zhang, S. & Blissard, G. W. (2010).** Ao38, a new cell line from eggs of the black witch moth, *Ascalapha odorata* (Lepidoptera: Noctuidae), is permissive for AcMNPV infection and produces high levels of recombinant proteins. *BMC Biotechnology* **10**, 50.
- Hashimoto, Y., Zhang, S., Zhang, S., Chen, Y.-R. & Blissard, G. W. (2012).** Erratum to: BTI-Tnao38, a new cell line derived from *Trichoplusia ni*, is permissive for AcMNPV infection and produces high levels of recombinant proteins. *BMC Biotechnology* **12**, 12.
- He, Y. N., Bowman, V. D., Mueller, S., Bator, C. M., Bella, J., Peng, X. H., Baker, T. S., Wimmer, E., Kuhn, R. J. & Rossmann, M. G. (2000).** Interaction of the poliovirus receptor with poliovirus. *Proceedings of the National Academy of Sciences of the United States of America* **97**, 79-84.
- Heimpel, A. M., Thomas, E. D., Adams, J. R. & Smith, L. J. (1973).** The Presence of Nuclear Polyhedrosis Viruses of *Trichoplusia ni* on Cabbage from the Market Shelf. *Environmental Entomology* **2**, 72-75.
- Henry, J. L., Jaikaran, E. S., Davies, J. R., Tomlinson, A. J., Mason, P. J., Barnes, J. M. & Beale, A. J. (1966).** A study of poliovaccination in infancy: excretion following challenge with live virus by children given killed or living poliovaccine. *The Journal of Hygiene* **64**, 105-120.
- Hershey, J. W. B. & Marrick, W. C. (2000).** The pathway and mechanism of initiation of protein synthesis. In *Translational control of gene expression*, pp. 33-88. Edited by N. Sonenberg, J. W. B. Hershey & M. Mathews. NY: Cold Spring Harbor Laboratory Press.
- Herskowitz (2012).** Protocols: Yeast Transformation, 2012 edn.
- Hewlett, M. J., Rose, J. K. & Baltimore, D. (1976).** 5'-Terminal Structure of Poliovirus Polyribosomal RNA is pUp. *Proceedings of the National Academy of Sciences of the United States of America* **73**, 327-330.
- Hird, T. R. & Grassly, N. C. (2012).** Systematic Review of Mucosal Immunity Induced by Oral and Inactivated Poliovirus Vaccines against Virus Shedding following Oral Poliovirus Challenge. *PLoS Pathog* **8**, e1002599.
- Hitchman, R. B., Locanto, E., Possee, R. D. & King, L. A. (2011).** Optimizing the baculovirus expression vector system. *Methods* **55**, 52-57.
- Ho, S. N., Hunt, H. D., Horton, R. M., Pullen, J. K. & Pease, L. R. (1989).** Site-directed mutagenesis by overlap extension using the polymerase chain reaction. *Gene* **77**, 51-59.
- Hogle, J. M., Chow, M. & Filman, D. J. (1985).** Three-dimensional structure of poliovirus at 2.9 Å resolution. *Science* **229**, 1358-1365.
- Holland, J. J. & Kiehn, E. D. (1968).** Specific cleavage of viral proteins as steps in the synthesis and maturation of enteroviruses. *Proceedings of the National Academy of Sciences of the United States of America* **60**, 1015-1022.
- Hsiung, G.-D., Black, F. & JR, H. (1964).** Susceptibility of primates to viruses in relation to taxonomic classification. In *Evolutionary and genetic biology of primates vol II*, pp. 1-23. Edited by Buettener-Janusch. New York: Academic Press.

- Huhti, L., Blazevic, V., Nurminen, K., Koho, T., Hytönen, V. P. & Vesikari, T. (2010). A comparison of methods for purification and concentration of norovirus GII-4 capsid virus-like particles. *Arch Virol* **155**, 1855-1858.
- Hummeler, K. & Hamparian, V. V. (1958). Studies on the Complement Fixing Antigens of Poliomyelitis: I. Demonstration of Type and Group Specific Antigens in Native and Heated Viral Preparations. *The Journal of Immunology* **81**, 499-505.
- Ida-Hosonuma, M., Iwasaki, T., Yoshikawa, T., Nagata, N., Sato, Y., Sata, T., Yoneyama, M., Fujita, T., Taya, C., Yonekawa, H. & Koike, S. (2005). The alpha/beta interferon response controls tissue tropism and pathogenicity of poliovirus. *Journal of Virology* **79**, 4460-4469.
- Ida-Hosonuma, M., Sasaki, Y., Toyoda, H., Nomoto, A., Gotoh, O., Yonekawa, H. & Koike, S. (2003). Host range of poliovirus is restricted to simians because of a rapid sequence change of the poliovirus receptor gene during evolution. *Arch Virol* **148**, 29-44.
- Jackson, W. T., Giddings, T. H., Taylor, M. P., Mulinyawe, S., Rabinovitch, M., Kopito, R. R. & Kirkegaard, K. (2005). Subversion of cellular autophagosomal machinery by RNA viruses. *PLoS Biol* **3**, 861-871.
- Jacobson, M. F. & Baltimore, D. (1968a). Morphogenesis of poliovirus. I. Association of the viral RNA with coat protein. *Journal of Molecular Biology* **33**, 369-378.
- Jacobson, M. F. & Baltimore, D. (1968b). Polypeptide cleavages in the formation of poliovirus proteins. *Proceedings of the National Academy of Sciences of the United States of America* **61**, 77-84.
- Jacobson, S. J., Konings, D. A. M. & Sarnow, P. (1993). BIOCHEMICAL AND GENETIC-EVIDENCE FOR A PSEUDOKNOT STRUCTURE AT THE 3' TERMINUS OF THE POLIOVIRUS RNA GENOME AND ITS ROLE IN VIRAL-RNA AMPLIFICATION. *Journal of Virology* **67**, 2961-2971.
- Jarvis, D. L. (2003). Developing baculovirus-insect cell expression systems for humanized recombinant glycoprotein production. *Virology* **310**, 1-7.
- Jia, K.-T., Wu, Y.-Y., Liu, Z.-Y., Mi, S., Zheng, Y.-W., He, J., Weng, S.-P., Li, S. C., He, J.-G. & Guo, C.-J. (2013). Mandarin Fish Caveolin 1 Interaction with Major Capsid Protein of Infectious Spleen and Kidney Necrosis Virus and Its Role in Early Stages of Infection. *Journal of Virology* **87**, 3027-3038.
- Jiang, P., Liu, Y., Ma, H. C., Paul, A. V. & Wimmer, E. (2014). Picornavirus morphogenesis. *Microbiology and molecular biology reviews : MMBR* **78**, 418-437.
- Johnson, K. L. & Sarnow, P. (1991). Three poliovirus 2B mutants exhibit noncomplementable defects in viral RNA amplification and display dosage-dependent dominance over wild-type poliovirus. *Journal of Virology* **65**, 4341-4349.
- Jones, M. E. (1992). Orotidylate decarboxylase of yeast and man. *Current topics in cellular regulation* **33**, 331-342.
- Jore, J., Degeus, B., Jackson, R. J., Pouwels, P. H. & Engervalk, B. E. (1988). Poliovirus protein 3CD is the active protease for processing of the precursor protein P1 in vitro. *Journal of general virology* **69**, 1627-1636.
- Jore, J. P. M., Veldhuisen, G., Kottenhagen, M., Pouwels, P. H., Foriers, A., Rombaut, B. & Boeyé, A. (1994). Formation of poliomyelitis subviral particles in the yeast *Saccharomyces cerevisiae*. *Yeast (Chichester, England)* **10**, 907-922.
- Jurgens, C. K., Barton, D. J., Sharma, N., Morasco, B. J., Ogram, S. A. & Flanagan, J. B. (2006). 2A(pro) is a multifunctional protein that regulates the stability, translation and replication of poliovirus RNA. *Virology* **345**, 346-357.
- Katpally, U. & Smith, T. J. (2007). Pocket Factors Are Unlikely To Play a Major Role in the Life Cycle of Human Rhinovirus. *Journal of Virology* **81**, 6307-6315.
- Kawai, S., Hashimoto, W. & Murata, K. (2010). Transformation of *Saccharomyces cerevisiae* and other fungi: Methods and possible underlying mechanism. *Bioengineered Bugs* **1**, 395-403.
- Kew, O., Morris-Glasgow, V., Landaverde, M., Burns, C., Shaw, J., Garib, Z. I. a., Andr  , J., Blackman, E., Freeman, C. J., Jorba, J., Sutter, R., Tambini, G., Venczel, L., Pedreira, C., Laender, F., Shimizu, H., Yoneyama, T., Miyamura, T., van der Avoort, H., Oberste, M. S., Kilpatrick, D., Cochi, S., Pallansch, M. & de Quadros, C. (2002). Outbreak of Poliomyelitis in Hispaniola Associated with Circulating Type 1 Vaccine-Derived Poliovirus. *Science* **296**, 356-359.

- Kim, H. J. & Kim, H. J. (2017).** Yeast as an expression system for producing virus-like particles: what factors do we need to consider? *Letters in Applied Microbiology* **64**, 111-123.
- Kim, H. J., Kim, S. Y., Lim, S. J., Kim, J. Y., Lee, S. J. & Kim, H. J. (2010).** One-step chromatographic purification of human papillomavirus type 16 L1 protein from *Saccharomyces cerevisiae*. *Protein Expression and Purification* **70**, 68-74.
- King, L. A., Hitchman, R. & Possee, R. D. (2007).** Recombinant baculovirus isolation. *Methods in molecular biology (Clifton, NJ)* **388**, 77-94.
- Kitamura, K. & Yamamoto, Y. (1972).** Purification and properties of an enzyme, zymolyase, which lyses viable yeast cells. *Archives of Biochemistry and Biophysics* **153**, 403-406.
- Kitamura, N., Semler, B. L., Rothberg, P. G., Larsen, G. R., Adler, C. J., Dorner, A. J., Emini, E. A., Hanecak, R., Lee, J. J., Vanderwerf, S., Anderson, C. W. & Wimmer, E. (1981).** Primary structure, gene organization and polypeptide expression of poliovirus RNA. *Nature* **291**, 547-553.
- Kitts, P. A., Ayres, M. D. & Possee, R. D. (1990).** Linearization of baculovirus DNA enhances the recovery of recombinant virus expression vectors. *Nucleic Acids Res* **18**, 5667-5672.
- Kitts, P. A. & Possee, R. D. (1993).** A method for producing recombinant baculovirus expression vectors at high frequency. *Biotechniques* **14**, 810-817.
- Klionsky, D. J. (2005).** The molecular machinery of autophagy: unanswered questions. *Journal of Cell Science* **118**, 7-18.
- Knudson, D. L. & Harrap, K. A. (1976).** Replication of a Nuclear Polyhedrosis Virus in a Continuous Cell Culture of *Spodoptera frugiperda*: Microscopy Study of the Sequence of Events of the Virus Infection. *Journal of Virology* **17**, 254-268.
- Koho, T., Mäntylä, T., Laurinmäki, P., Huhti, L., Butcher, S. J., Vesikari, T., Kulomaa, M. S. & Hytönen, V. P. (2012).** Purification of norovirus-like particles (VLPs) by ion exchange chromatography. *Journal of Virological Methods* **181**, 6-11.
- Koike, S., Ise, I. & Nomoto, A. (1991).** Functional domains of the poliovirus receptor. *Proc Natl Acad Sci U S A* **88**, 4104-4108.
- Kozak, M. (1986).** Point mutations define a sequence flanking the AUG initiator codon that modulates translation by eukaryotic ribosomes. *Cell* **44**, 283-292.
- Kozak, M. (1989).** The scanning model for translation: an update. *The Journal of Cell Biology* **108**, 229-241.
- Kräusslich, H.-G., Nicklin, M. J. H., Lee, C.-K. & Wimmer, E. (1988).** Polyprotein processing in picornavirus replication. *Biochimie* **70**, 119-130.
- Kuge, S., Kawamura, N. & Nomoto, A. (1989).** Genetic variation occurring on the genome of an in vitro insertion mutant of poliovirus type 1. *Journal of Virology* **63**, 1069-1075.
- Kuo, C.-J., Shie, J.-J., Fang, J.-M., Yen, G.-R., Hsu, J. T. A., Liu, H.-G., Tseng, S.-N., Chang, S.-C., Lee, C.-Y., Shih, S.-R. & Liang, P.-H. (2008).** Design, synthesis, and evaluation of 3C protease inhibitors as anti-enterovirus 71 agents. *Bioorganic & Medicinal Chemistry* **16**, 7388-7398.
- Kushnirov, V. V. (2000).** Rapid and reliable protein extraction from yeast. *Yeast (Chichester, England)* **16**, 857-860.
- Lama, J., Paul, A. V., Harris, K. S. & Wimmer, E. (1994).** Properties of purified recombinant poliovirus protein 3aB as substrate for viral proteinases and as co-factor for RNA polymerase 3Dpol. *Journal of Biological Chemistry* **269**, 66-70.
- Landry, C. R., Townsend, J. P., Hartl, D. L. & Cavalieri, D. (2006).** Ecological and evolutionary genomics of *Saccharomyces cerevisiae*. *Molecular Ecology* **15**, 575-591.
- Landsteiner, K. & Popper, E. (1908).** Mikroskopische präparate von einem menschlichen und zwei affentückermarker. *Wien Klin Wochenschr* **21**, 1930.
- Lawson, M. A. & Semler, B. L. (1990).** Picornavirus protein processing--enzymes, substrates, and genetic regulation. *Curr Top Microbiol Immunol* **161**, 49-87.
- Lee, C.-K. & Wimmer, E. (1988).** Proteolytic processing of poliovirus polyprotein: Elimination of 2Apro-mediated, alternative cleavage of polypeptide 3CD by in Vitro mutagenesis. *Virology* **166**, 405-414.
- Lee, H. H. & Miller, L. K. (1979).** Isolation, Complementation, and Initial Characterization of Temperature-Sensitive Mutants of the Baculovirus *Autographa californica* Nuclear Polyhedrosis Virus. *Journal of Virology* **31**, 240-252.

- Lee, J.-C., Shih, S.-R., Chang, T.-Y., Tseng, H.-Y., Shih, Y.-F., Yen, K.-J., Chen, W.-C., Shie, J.-J., Fang, J.-M., Liang, P.-H., Chao, Y.-S. & Hsu, J. T. A. (2008). A mammalian cell-based reverse two-hybrid system for functional analysis of 3C viral protease of human enterovirus 71. *Analytical Biochemistry* **375**, 115-123.
- Lee, Y. F., Nomoto, A., Detjen, B. M. & Wimmer, E. (1977). A protein covalently linked to poliovirus genome RNA. *Proc Natl Acad Sci U S A* **74**, 59-63.
- Lentz, K. N., Smith, A. D., Geisler, S. C., Cox, S., Buontempo, P., Skelton, A., DeMartino, J., Rozhon, E., Schwartz, J., Girijavallabhan, V., O'Connell, J. & Arnold, E. (1997). Structure of poliovirus type 2 Lansing complexed with antiviral agent SCH48973: comparison of the structural and biological properties of three poliovirus serotypes. *Structure* **5**, 961-978.
- Levy, H. C., Bostina, M., Filman, D. J. & Hogle, J. M. (2010). Catching a Virus in the Act of RNA Release: a Novel Poliovirus Uncoating Intermediate Characterized by Cryo-Electron Microscopy. *Journal of Virology* **84**, 4426-4441.
- Lewis, S. A., Morgan, D. O. & Grubman, M. J. (1991). Expression, processing, and assembly of foot-and-mouth disease virus capsid structures in heterologous systems: induction of a neutralizing antibody response in guinea pigs. *Journal of Virology* **65**, 6572-6580.
- Li, H.-Y., Han, J.-F., Qin, C.-F. & Chen, R. (2013). Virus-like particles for enterovirus 71 produced from *Saccharomyces cerevisiae* potently elicits protective immune responses in mice. *Vaccine* **31**, 3281-3287.
- Lin, J., Cheng, N., Chow, M., Filman, D. J., Steven, A. C., Hogle, J. M. & Belnap, D. M. (2011). An externalized polypeptide partitions between two distinct sites on genome-released poliovirus particles. *J Virol* **85**, 9974-9983.
- Lin, S.-Y., Chiu, H.-Y., Chiang, B.-L. & Hu, Y.-C. (2015). Development of EV71 virus-like particle purification processes. *Vaccine* **33**, 5966-5973.
- Lipke, P. N. & Ovalle, R. (1998). Cell Wall Architecture in Yeast: New Structure and New Challenges. *Journal of Bacteriology* **180**, 3735-3740.
- Liu, F., Wu, X., Li, L., Liu, Z. & Wang, Z. (2013). Use of baculovirus expression system for generation of virus-like particles: Successes and challenges. *Protein Expression and Purification* **90**, 104-116.
- Liu, Y., Wang, C. L., Mueller, S., Paul, A. V., Wimmer, E. & Jiang, P. (2010). Direct Interaction between Two Viral Proteins, the Nonstructural Protein 2C(ATPase) and the Capsid Protein VP3, Is Required for Enterovirus Morphogenesis. *PLoS Pathog* **6**, 14.
- Lloyd, R. E. & Bovee, M. (1993). Persistent Infection of Human Erythroblastoid Cells by Poliovirus. *Virology* **194**, 200-209.
- Lu, W., Chapple, S. D., Lissini, O. & Jones, I. M. (2002). Characterization of a truncated soluble form of the baculovirus (AcMNPV) major envelope protein Gp64. *Protein Expr Purif* **24**, 196-201.
- Luckow, V. A., Lee, S. C., Barry, G. F. & Olins, P. O. (1993). Efficient generation of infectious recombinant baculoviruses by site-specific transposon-mediated insertion of foreign genes into a baculovirus genome propagated in *Escherichia coli*. *Journal of Virology* **67**, 4566-4579.
- Luckow, V. A. & Summers, M. D. (1988). Trends in the Development of Baculovirus Expression Vectors. *Nat Biotech* **6**, 47-55.
- Lulla, V., Dinan, A. M., Hosmillo, M., Chaudhry, Y., Sherry, L., Irigoyen, N., Nayak, K. M., Stonehouse, N. J., Zilbauer, M., Goodfellow, I. & Firth, A. E. (2019). An upstream protein-coding region in enteroviruses modulates virus infection in gut epithelial cells. *Nature Microbiology* **4**, 280-292.
- Lyu, K., He, Y. L., Li, H. Y. & Chen, R. (2015). Crystal Structures of Yeast-Produced Enterovirus 71 and Enterovirus 71/Coxsackievirus A16 Chimeric Virus-Like Particles Provide the Structural Basis for Novel Vaccine Design against Hand-Foot-and-Mouth Disease. *Journal of Virology* **89**, 6196-6208.
- Macadam, A. J., Arnold, C., Howlett, J., John, A., Marsden, S., Taffs, F., Reeve, P., Hamada, N., Wareham, K., Almond, J. & et al. (1989). Reversion of the attenuated and temperature-sensitive phenotypes of the Sabin type 3 strain of poliovirus in vaccinees. *Virology* **172**, 408-414.
- Macadam, A. J., Ferguson, G., Arnold, C. & Minor, P. D. (1991). An assembly defect as a result of an attenuating mutation in the capsid proteins of the poliovirus type 3 vaccine strain. *Journal of Virology* **65**, 5225-5231.

- Macauley-Patrick, S., Fazenda, M. L., McNeil, B. & Harvey, L. M. (2005).** Heterologous protein production using the *Pichia pastoris* expression system. *Yeast (Chichester, England)* **22**, 249-270.
- Macejak, D. G. & Sarnow, P. (1991).** Internal initiation of translation mediated by the 5' leader of a cellular mRNA. *Nature* **353**, 90-94.
- Maloy, S. (2004).** Plasmids in eukaryotic microbes: an example: San Diego State University.
- Maranga, L., Rueda, P., Antonis, A., Vela, C., Langeveld, J., Casal, J. & Carrondo, M. (2002).** Large scale production and downstream processing of a recombinant porcine parvovirus vaccine. *Applied microbiology and biotechnology* **59**, 45-50.
- Marc, D., Masson, G., Girard, M. & van der Werf, S. (1990).** Lack of myristoylation of poliovirus capsid polypeptide VP0 prevents the formation of virions or results in the assembly of noninfectious virus particles. *Journal of Virology* **64**, 4099-4107.
- Marek, M., van Oers, M. M., Devaraj, F. F., Vlak, J. M. & Merten, O.-W. (2011).** Engineering of baculovirus vectors for the manufacture of virion-free biopharmaceuticals. *Biotechnology and bioengineering* **108**, 1056-1067.
- Marsian, J., Fox, H., Bahar, M. W., Kotecha, A., Fry, E. E., Stuart, D. I., Macadam, A. J., Rowlands, D. J. & Lomonosoff, G. P. (2017).** Plant-made polio type 3 stabilized VLPs-a candidate synthetic polio vaccine. *Nature communications* **8**, 245.
- Mayer, M. M., Rapp, H. J., Roizman, B., Klein, S. W., Cowan, K. M. & Lukens, D. (1957).** The purification of poliomyelitis virus as studied by complement fixation. *Journal of immunology (Baltimore, Md : 1950)* **78**, 435-455.
- Mazzone, H. M. (1998).** *CRC handbook of viruses : mass-molecular weight values and related properties*. Boca Raton: CRC Press LLC.
- McKinney, R. E., Jr., Katz, S. L. & Wilfert, C. M. (1987).** Chronic enteroviral meningoencephalitis in agammaglobulinemic patients. *Reviews of infectious diseases* **9**, 334-356.
- McSharry, J. J., Caliguiri, L. A. & Eggers, H. J. (1979).** Inhibition of uncoating of poliovirus by arildone, a new antiviral drug. *Virology* **97**, 307-315.
- Mendelsohn, C. L., Wimmer, E. & Racaniello, V. R. (1989).** Cellular receptor for poliovirus: Molecular cloning, nucleotide sequence, and expression of a new member of the immunoglobulin superfamily. *Cell* **56**, 855-865.
- Miller, L. K. (1988).** Baculoviruses as gene expression vectors. *Annual review of microbiology* **42**, 177-199.
- Milstien, J. B., Lemon, S. M. & Wright, P. F. (1997).** Development of a more thermostable poliovirus vaccine. *Journal of Infectious Diseases* **175**, S247-S253.
- Minor, P. D. (2012).** The polio-eradication programme and issues of the end game. *J Gen Virol* **93**, 457-474.
- Minor, P. D., Ferguson, M., Evans, D. M., Almond, J. W. & Icenogle, J. P. (1986).** Antigenic structure of polioviruses of serotypes 1, 2 and 3. *J Gen Virol* **67 (Pt 7)**, 1283-1291.
- Mizushima, N., Ohsumi, Y. & Yoshimori, T. (2002).** Autophagosome formation in mammalian cells. *Cell Struct Funct* **27**, 421-429.
- Mohsen, M. O., Zha, L., Cabral-Miranda, G. & Bachmann, M. F. (2017).** Major findings and recent advances in virus-like particle (VLP)-based vaccines. *Seminars in immunology* **34**, 123-132.
- Morikawa, Y., Goto, T., Yasuoka, D., Momose, F. & Matano, T. (2007).** Defect of human immunodeficiency virus type 2 Gag assembly in *Saccharomyces cerevisiae*. *Journal of Virology* **81**, 9911-9921.
- Moscufo, N., Simons, J. & Chow, M. (1991).** Myristoylation is important at multiple stages in poliovirus assembly. *Journal of Virology* **65**, 2372-2380.
- Mosimann, S. C., Cherney, M. M., Sia, S., Plotch, S. & James, M. N. G. (1997).** Refined x-ray crystallographic structure of the poliovirus 3C gene product. *Journal of Molecular Biology* **273**, 1032-1047.
- Mosser, A. G. & Rueckert, R. R. (1993).** WIN 51711-dependent mutants of poliovirus type 3: evidence that virions decay after release from cells unless drug is present. *J Virol* **67**, 1246-1254.
- Muckelbauer, J. K., Kremer, M., Minor, I., Diana, G., Dutko, F. J., Groarke, J., Pevear, D. C. & Rossmann, M. G. (1995).** The structure of coxsackievirus B3 at 3.5 Å resolution. *Structure* **3**, 653-667.

- Nathanson, N. & Kew, O. M. (2010).** From emergence to eradication: the epidemiology of poliomyelitis deconstructed. *Am J Epidemiol* **172**, 1213-1229.
- Nicholson, R., Pelletier, J., Le, S. Y. & Sonenberg, N. (1991).** STRUCTURAL AND FUNCTIONAL-ANALYSIS OF THE RIBOSOME LANDING PAD OF POLIOVIRUS TYPE-2 - INVIVO TRANSLATION STUDIES. *Journal of Virology* **65**, 5886-5894.
- Nicklin, M. J., Kräusslich, H. G., Toyoda, H., Dunn, J. J. & Wimmer, E. (1987).** Poliovirus polypeptide precursors: expression in vitro and processing by exogenous 3C and 2A proteinases. *Proceedings of the National Academy of Sciences of the United States of America* **84**, 4002-4006.
- Nomoto, A. & Arita, I. (2002).** Eradication of Poliomyelitis. *Nature Immunology* **3**, 205.
- Nomoto, A., Detjen, B., Pozzatti, R. & Wimmer, E. (1977a).** The location of the polio genome protein in viral RNAs and its implication for RNA synthesis. *Nature* **268**, 208-213.
- Nomoto, A., Kitamura, N., Golini, F. & Wimmer, E. (1977b).** The 5'-terminal Structures of Poliovirion RNA and Poliovirus mRNA Differ Only in the Genome-Linked Protein VPg. *Proceedings of the National Academy of Sciences of the United States of America* **74**, 5345-5349.
- Novak, J. E. & Kirkegaard, K. (1991).** Improved method for detecting poliovirus negative strands used to demonstrate specificity of positive-strand encapsidation and the ratio of positive to negative strands in infected cells. *Journal of Virology* **65**, 3384-3387.
- O'Reilly, D. R., Miller, L. K. & Luknow, V. A. (1992).** BACULOVIRUS EXPRESSION VECTORS A Laboratory Manual, pp. 3-10. New York: W.H.Freeman and Company.
- Odorizzi, G. (2003).** Preparation of Yeast Spheroplasts.
- OET (2019).** baculoCOMPLETE. Oxford: Oxford Expression Technologies;.
- Ogra, P. L., Karzon, D. T., Righthand, F. & MacGillivray, M. (1968).** Immunoglobulin Response in Serum and Secretions after Immunization with Live and Inactivated Poliovaccine and Natural Infection. *New England Journal of Medicine* **279**, 893-900.
- Oliveira, M. A., Zhao, R., Lee, W. M., Kremer, M. J., Minor, I., Rueckert, R. R., Diana, G. D., Pevear, D. C., Dutko, F. J., McKinlay, M. A. & et al. (1993).** The structure of human rhinovirus 16. *Structure* **1**, 51-68.
- Pallansch, M., Oberste, M. S. & Whitton, J. L. (2013).** Enterovirus: Polioviruses, Coxsackieviruses, Echoviruses and Newer Enteroviruses. In *Fields Virology*, 6th edn, pp. 490-530. Edited by D. M. Knipe & P. M. Howley. Philadelphia, PA: Lippincott Williams & Wilkins,.,.
- Pallansch, M. A., Kew, O. M., Semler, B. L., Omilianowski, D. R., Anderson, C. W., Wimmer, E. & Rueckert, R. R. (1984).** Protein processing map of poliovirus. *Journal of Virology* **49**, 873-880.
- Parr Instrument Company (2015).** Cell Disruption Vessels. Illinois.
- Parsley, T. B., Cornell, C. T. & Semler, B. L. (1999).** Modulation of the RNA binding and protein processing activities of poliovirus polypeptide 3CD by the viral RNA polymerase domain. *Journal of Biological Chemistry* **274**, 12867-12876.
- Patrick, M. (2014).** Plasmids 101: Yeast Vectors: addgene.
- Paul, A. V., van Boom, J. H., Filippov, D. & Wimmer, E. (1998).** Protein-primed RNA synthesis by purified poliovirus RNA polymerase. *Nature* **393**, 280-284.
- Peixoto, C., Sousa, M. F. Q., Silva, A. C., Carrondo, M. J. T. & Alves, P. M. (2007).** Downstream processing of triple layered rotavirus like particles. *Journal of Biotechnology* **127**, 452-461.
- Pelletier, I., Duncan, G. & Colbere-Garapin, F. (1998).** One amino acid change on the capsid surface of poliovirus Sabin 1 allows the establishment of persistent infections in HEp-2c cell cultures. *Virology* **241**, 1-13.
- Pelletier, J. & Sonenberg, N. (1988).** Internal initiation of translation of eukaryotic mRNA directed by a sequence derived from poliovirus RNA. *Nature* **334**, 320-325.
- Pevear, D. C., Fancher, M. J., Felock, P. J., Rossmann, M. G., Miller, M. S., Diana, G., Treasurywala, A. M., McKinlay, M. A. & Dutko, F. J. (1989).** Conformational change in the floor of the human rhinovirus canyon blocks adsorption to HeLa cell receptors. *Journal of Virology* **63**, 2002-2007.
- Pevear, D. C., Tull, T. M., Seipel, M. E. & Groarke, J. M. (1999).** Activity of Pleconaril against Enteroviruses. *Antimicrobial Agents and Chemotherapy* **43**, 2109-2115.

- Pfister, T. & Wimmer, E. (1999).** Characterization of the nucleoside triphosphatase activity of poliovirus protein 2C reveals a mechanism by which guanidine inhibits poliovirus replication. *Journal of Biological Chemistry* **274**, 6992-7001.
- Phillips, B. A. & Fennell, R. (1973).** Polypeptide Composition of Poliovirions, Naturally Occurring Empty Capsids, and 14S Precursor Particles. *Journal of Virology* **12**, 291-299.
- Piirainen, L., Airaksinen, A., Hovi, T. & Roivainen, M. (1996).** Selective cleavage by trypsin of the capsid protein VP1 of type 3 poliovirus results in improved sorting of cell bound virions. *Arch Virol* **141**, 1011-1020.
- Pincus, S. E., Diamond, D. C., Emini, E. A. & Wimmer, E. (1986).** Guanidine-selected mutants of poliovirus: mapping of point mutations to polypeptide 2C. *Journal of Virology* **57**, 638-646.
- Pipkin, P. A. & Minor, P. D. (1998).** Studies on the loss of infectivity of live type 3 poliovaccine on storage. *Biologicals* **26**, 17-23.
- Plevka, P., Perera, R., Yap, M. L., Cardoso, J., Kuhn, R. J. & Rossmann, M. G. (2013).** Structure of human enterovirus 71 in complex with a capsid-binding inhibitor. *Proceedings of the National Academy of Sciences* **110**, 5463-5467.
- Plotkin, S. A. (1991).** Current issues in evaluating the efficacy of oral poliovirus vaccine and inactivated poliovirus vaccine immunization. *Pediatr Infect Dis J* **10**, 979-981.
- Plotkin, S. A. (1997).** Polio vaccine production. *Science* **278**, 19.
- Plotkin, S. A., Murdin, A. & Vidor, E. (1999).** Inactivated Polio Vaccines. In *Vaccines*, pp. 345-363. Edited by O. W. Plotkin S., Philadelphia, PA.: WB Saunders Company.
- Porro, D., Gasser, B., Fossati, T., Maurer, M., Branduardi, P., Sauer, M. & Mattanovich, D. (2011).** Production of recombinant proteins and metabolites in yeasts. *Applied microbiology and biotechnology* **89**, 939-948.
- Porro, D., Sauer, M., Branduardi, P. & Mattanovich, D. (2005).** Recombinant protein production in yeasts. *Molecular biotechnology* **31**, 245-259.
- Porta, C., Xu, X. D., Loureiro, S., Paramasivam, S., Ren, J. Y., Al-Khalil, T., Burman, A., Jackson, T., Belsham, G. J., Curry, S., Lomonosoff, G. P., Parida, S., Paton, D., Li, Y. M., Wilsden, G., Ferris, N., Owens, R., Kotecha, A., Fry, E., Stuart, D. I., Charleston, B. & Jones, I. M. (2013).** Efficient production of foot-and-mouth disease virus empty capsids in insect cells following down regulation of 3C protease activity. *Journal of Virological Methods* **187**, 406-412.
- Possee, R. D., Thomas, C. J. & King, L. A. (1999).** The use of baculovirus vectors for the production of membrane proteins in insect cells. *Biochemical Society transactions* **27**, 928-932.
- Pronk, J. T. (2002).** Auxotrophic Yeast Strains in Fundamental and Applied Research. *Appl Environ Microbiol* **68**, 2095-2100.
- Puckette, M., Clark, B. A., Smith, J. D., Turecek, T., Martel, E., Gabbert, L., Pisano, M., Hurtle, W., Pacheco, J. M., Barrera, J., Neilan, J. G. & Rasmussen, M. (2017).** Foot-and-Mouth Disease (FMD) Virus 3C Protease Mutant L127P: Implications for FMD Vaccine Development. *J Virol* **91**.
- Racaniello, V. R. (2013).** Picornaviridae: the viruses and their replication. In *Fields Virology*, 6th edn, pp. 795-838. Edited by D. M. Knipe & P. M. Howley. Philadelphia, PA: Lippincott Williams & Wilkins,.
- Racaniello, V. R. & Baltimore, D. (1981).** Cloned Poliovirus Complementary DNA is Infectious in Mammalian Cells. *Science* **214**, 916-919.
- Ren, R. & Racaniello, V. R. (1992).** Human poliovirus receptor gene expression and poliovirus tissue tropism in transgenic mice. *Journal of Virology* **66**, 296-304.
- Reynisdóttir, I., O'Reilly, D. R., Miller, L. K. & Prives, C. (1990).** Thermally inactivated simian virus 40 tsA58 mutant T antigen cannot initiate viral DNA replication in vitro. *Journal of Virology* **64**, 6234-6245.
- Rodríguez, P. L. & Carrasco, L. (1995).** Poliovirus Protein 2C Contains Two Regions Involved in RNA Binding Activity. *Journal of Biological Chemistry* **270**, 10105-10112.
- Rodríguez, P. L. & Carrasco, L. (1993).** Poliovirus protein 2C has ATPase and GTPase activities. *Journal of Biological Chemistry* **268**, 8105-8110.
- Romanos, M. A., Scorer, C. A. & Clare, J. J. (1992).** Foreign gene expression in yeast: a review. *Yeast (Chichester, England)* **8**, 423-488.

- Romanova, L. I., Tolskaya, E. A., Kolesnikova, M. S. & Agol, V. I. (1980).** Biochemical evidence for intertypic genetic recombination of polioviruses. *FEBS Letters* **118**, 109-112.
- Rombaut, B., Jore, J. & Boeyé, A. (1994).** A competition immunoprecipitation assay of unlabeled poliovirus antigens. *Journal of Virological Methods* **48**, 73-79.
- Rombaut, B. & Jore, J. P. (1997).** Immunogenic, non-infectious polio subviral particles synthesized in *Saccharomyces cerevisiae*. *Journal of general virology* **78**, 1829-1832.
- Roosien, J., Belsham, G. J., Ryan, King, A. M. Q. & Vlak, J. M. (1990).** Synthesis of foot-and-mouth disease virus capsid proteins in insect cells using baculovirus expression vectors. *Journal of general virology* **71 (Pt 8)**, 1703-1711.
- Rossmann, M. G. (1994).** Viral Cell Recognition and Entry. *Protein Sci* **3**, 1712-1725.
- Ruggieri, R., Tanaka, K., Nakafuku, M., Kaziro, Y., Akio Toh, E. & Matsumoto, K. (1989).** MS11, a Negative Regulator of the RAS-cAMP Pathway in *Saccharomyces cerevisiae*. *Proceedings of the National Academy of Sciences of the United States of America* **86**, 8778-8782.
- Sabin, A. B. (1956).** Pathogenesis of poliomyelitis; reappraisal in the light of new data. *Science (New York, NY)* **123**, 1151-1157.
- Sabin, A. B. (1985).** Oral Poliovirus Vaccine: History of Its Development and Use and Current Challenge to Eliminate Poliomyelitis from the World. *Journal of Infectious Diseases* **151**, 420-436.
- Saccharomyces Genome Database (2016).** URA3 / YEL021W Overview.
- Sakuragi, S., Goto, T., Sano, K. & Morikawa, Y. (2002).** HIV type 1 Gag virus-like particle budding from spheroplasts of *Saccharomyces cerevisiae*. *Proceedings of the National Academy of Sciences of the United States of America* **99**, 7956-7961.
- Salk, J. (1960).** PERSISTENCE OF IMMUNITY AFTER ADMINISTRATION OF FORMALIN-TREATED POLIOVIRUS VACCINE. *The Lancet* **276**, 715-723.
- Schlegel, A., Giddings, T. H., Ladinsky, M. S. & Kirkegaard, K. (1996).** Cellular origin and ultrastructure of membranes induced during poliovirus infection. *Journal of Virology* **70**, 6576-6588.
- Selinka, H. C., Zibert, A. & Wimmer, E. (1991).** Poliovirus can enter and infect mammalian cells by way of an intercellular adhesion molecule 1 pathway. *Proc Natl Acad Sci U S A* **88**, 3598-3602.
- Semler, B. L., Anderson, C. W., Hanecak, R., Dorner, L. F. & Wimmer, E. (1982).** A membrane-associated precursor to poliovirus VPg identified by immunoprecipitation with antibodies directed against a synthetic heptapeptide. *Cell* **28**, 405-412.
- Shulman, L. M., Manor, Y., Sofer, D., Handsher, R., Swartz, T., Delpeyroux, F. & Mendelson, E. (2006).** Neurovirulent vaccine-derived polioviruses in sewage from highly immune populations. *PLoS One* **1**, e69.
- Singh, K. K. & Heinemann, J. A. (1997).** Yeast Plasmids. In *Recombinant Gene Expression Protocols*, pp. 113-130. Edited by R. S. Tuan. Totowa, NJ: Humana Press.
- Skinner, M. A., Racaniello, V. R., Dunn, G., Cooper, J., Minor, P. D. & Almond, J. W. (1989).** New model for the secondary structure of the 5' non-coding RNA of poliovirus is supported by biochemical and genetic data that also show that RNA secondary structure is important in neurovirulence. *Journal of Molecular Biology* **207**, 379-392.
- Smith, G. E., Summers, M. D. & Fraser, M. J. (1983).** Production of human beta interferon in insect cells infected with a baculovirus expression vector. *Molecular and Cellular Biology* **3**, 2156-2165.
- Smith, T. J., Kremer, M. J., Luo, M., Vriend, G., Arnold, E., Kamer, G., Rossmann, M. G., McKinlay, M. A., Diana, G. D. & Otto, M. J. (1986).** The Site of Attachment in Human Rhinovirus 14 for Antiviral Agents that Inhibit Uncoating. *Science* **233**, 1286-1293.
- Smyth, M., Pettitt, T., Symonds, A. & Martin, J. (2003).** Identification of the pocket factors in a picornavirus. *Arch Virol* **148**, 1225-1233.
- Sokolenko, S., George, S., Wagner, A., Tuladhar, A., Andrich, J. M. S. & Aucoin, M. G. (2012).** Co-expression vs. co-infection using baculovirus expression vectors in insect cell culture: Benefits and drawbacks. *Biotechnology Advances* **30**, 766-781.
- Sorensen, H. P. (2010).** Towards universal systems for recombinant gene expression. *Microbial cell factories* **9**, 27.

- Spector, D. H. & Baltimore, D. (1974).** Requirement of 3'-terminal poly(adenylic acid) for the infectivity of poliovirus RNA. *Proceedings of the National Academy of Sciences of the United States of America* **71**, 2983-2987.
- Stern, L. J. & Wiley, D. C. (1992).** The human class II MHC protein HLA-DR1 assembles as empty alpha beta heterodimers in the absence of antigenic peptide. *Cell* **68**, 465-477.
- Summers, D. F. & Maizel, J. V., Jr. (1968).** Evidence for large precursor proteins in poliovirus synthesis. *Proceedings of the National Academy of Sciences of the United States of America* **59**, 966-971.
- Sweeney, T. R., Roque-Rosell, N., Birtley, J. R., Leatherbarrow, R. J. & Curry, S. (2007).** Structural and mutagenic analysis of foot-and-mouth disease virus 3C protease reveals the role of the beta-ribbon in proteolysis. *Journal of Virology* **81**, 115-124.
- Tanaka, K., Nakafuku, M., Tamanoi, F., Kaziro, Y., Matsumoto, K. & Toh-e, A. (1990).** IRA2, a second gene of *Saccharomyces cerevisiae* that encodes a protein with a domain homologous to mammalian ras GTPase-activating protein. *Molecular and Cellular Biology* **10**, 4303-4313.
- Taylor, M. P., Burgon, T. B., Kirkegaard, K. & Jackson, W. T. (2009).** Role of Microtubules in Extracellular Release of Poliovirus. *Journal of Virology* **83**, 6599-6609.
- The Global Polio Eradication Initiative (2015).** Global eradication of wild poliovirus type 2 declared.
- Thomas, C. J., Brown, H. L., Hawes, C. R., Lee, B. Y., Min, M.-K., King, L. A. & Possee, R. D. (1998).** Localization of a Baculovirus-Induced Chitinase in the Insect Cell Endoplasmic Reticulum. *Journal of Virology* **72**, 10207-10212.
- Thompson, K. M., Tebbens, R. J. D., Pallansch, M. A., Kew, O. M., Sutter, R. W., Aylward, R. B., Watkins, M., Gary, H. E., Alexander, J., Jafari, H. & Cochi, S. L. (2008).** The risks, costs, and benefits of possible future global policies for managing polioviruses. *American Journal of Public Health* **98**, 1322-1330.
- Tobin, G. J., Trujillo, J. D., Bushnell, R. V., Lin, G., Chaudhuri, A. R., Long, J., Barrera, J., Pena, L., Grubman, M. J. & Nara, P. L. (2008).** Deceptive imprinting and immune refocusing in vaccine design. *Vaccine* **26**, 6189-6199.
- Tolskaya, E. A., Romanova, L. A., Kolesnikova, M. S. & Agol, V. I. (1983).** Intertypic recombination in poliovirus: genetic and biochemical studies. *Virology* **124**, 121-132.
- Tosteson, M. T., Wang, H., Naumov, A. & Chow, M. (2004).** Poliovirus binding to its receptor in lipid bilayers results in particle-specific, temperature-sensitive channels. *Journal of General Virology* **85**, 1581-1589.
- Toyoda, H., Franco, D., Fujita, K., Paul, A. V. & Wimmer, E. (2007).** Replication of Poliovirus Requires Binding of the Poly(rC) Binding Protein to the Cloverleaf as Well as to the Adjacent C-Rich Spacer Sequence between the Cloverleaf and the Internal Ribosomal Entry Site. *Journal of Virology* **81**, 10017-10028.
- Toyoda, H., Kohara, M., Kataoka, Y., Suganuma, T., Omata, T., Imura, N. & Nomoto, A. (1984).** Complete nucleotide sequences of all three poliovirus serotype genomes: Implication for genetic relationship, gene function and antigenic determinants. *Journal of Molecular Biology* **174**, 561-585.
- Toyoda, H., Nicklin, M. J. H., Murray, M. G., Anderson, C. W., Dunn, J. J., Studier, F. W. & Wimmer, E. (1986).** A second virus-encoded proteinase involved in proteolytic processing of poliovirus polyprotein. *Cell* **45**, 761-770.
- Tropp, B. E. (2012).** Genetec Analysis in Molecular Biology. In *Principles of Molecular Biology*. Burlington, MA: Jones and Bartlett Publishers, Inc.
- Tsang, S. K., McDermott, B. M., Racaniello, V. R. & Hogle, J. M. (2001).** Kinetic Analysis of the Effect of Poliovirus Receptor on Viral Uncoating: the Receptor as a Catalyst. *Journal of Virology* **75**, 4984-4989.
- Tuthill, T. J., Bubeck, D., Rowlands, D. J. & Hogle, J. M. (2006).** Characterization of Early Steps in the Poliovirus Infection Process: Receptor-Decorated Liposomes Induce Conversion of the Virus to Membrane-Anchored Entry-Intermediate Particles. *Journal of Virology* **80**, 172-180.
- Tuthill, T. J., Groppe, E., Hogle, J. M. & Rowlands, D. J. (2010).** Picornaviruses. In *Cell Entry by Non-Enveloped Viruses*, pp. 43-89. Berlin: Springer-Verlag Berlin.
- Umez, K., Amaya, T., Yoshimoto, A. & Tomita, K. (1971).** Purification and Properties of Orotidine-5'-Phosphate Pyrophosphorylase and Orotidine-5'-Phosphate Decarboxylase from Bakers' Yeast. *Journal of Biochemistry* **70**, 249-262.

- Urakawa, T., Ferguson, M., Minor, P. D., Cooper, J., Sullivan, M., Almond, J. W. & Bishop, D. H. (1989).** Synthesis of immunogenic, but non-infectious, poliovirus particles in insect cells by a baculovirus expression vector. *J Gen Virol* **70 (Pt 6)**, 1453-1463.
- Valtanen, S., Roivainen, M., Piirainen, L., Stenvik, M. & Hovi, T. (2000).** Poliovirus-Specific Intestinal Antibody Responses Coincide with Decline of Poliovirus Excretion. *The Journal of Infectious Diseases* **182**, 1-5.
- Van der Beek, C. P., Saaier-Riep, J. D. & Vlak, J. M. (1980).** On the origin of the polyhedral protein of *Autographa californica* nuclear polyhedrosis virus Isolation, characterization, and translation of viral messenger RNA. *Virology* **100**, 326-333.
- van Kuppeveld, F. J. M., Hoenderop, J. G. J., Smeets, R. L. L., Willems, P., Dijkman, H., Galama, J. M. D. & Melchers, W. J. G. (1997a).** Coxsackievirus protein 2B modifies endoplasmic reticulum membrane and plasma membrane permeability and facilitates virus release. *Embo J* **16**, 3519-3532.
- van Kuppeveld, F. J. M., Melchers, W. J. G., Kirkegaard, K. & Doedens, J. R. (1997b).** Structure-function analysis of coxsackie B3 virus protein 2B. *Virology* **227**, 111-118.
- van Oers, M. M., Pijlman, G. P. & Vlak, J. M. (2015).** Thirty years of baculovirus–insect cell protein expression: from dark horse to mainstream technology. *Journal of General Virology* **96**, 6-23.
- van Rosmalen, M., Krom, M. & Merckx, M. (2017).** Tuning the Flexibility of Glycine-Serine Linkers To Allow Rational Design of Multidomain Proteins. *Biochemistry* **56**, 6565-6574.
- Vaughn, J. L., Goodwin, R. H., Tompkins, G. J. & McCawley, P. (1977).** The establishment of two cell lines from the insectspodoptera frugiperda (lepidoptera; noctuidae). *In Vitro* **13**, 213-217.
- Vega, C. (2014).** 3D STED (Stimulated Emission Depletion) Microscopy How it works with the Leica TCS SP8 STED 3X: Leica Microsystems.
- Vicente, T., Roldão, A., Peixoto, C., Carrondo, M. J. T. & Alves, P. M. (2011).** Large-scale production and purification of VLP-based vaccines. *Journal of Invertebrate Pathology* **107**, S42-S48.
- Volkman, L. E. & Goldsmith, P. A. (1983).** In Vitro Survey of *Autographa californica* Nuclear Polyhedrosis Virus Interaction with Nontarget Vertebrate Host Cells. *Appl Environ Microbiol* **45**, 1085-1093.
- Wagner, E., K., Hewlett, M., J., Bloom, D., C. & Camerini, D. (2008).** *Basic virology*. Oxford: Blackwell Publishing.
- Wang, C., Jiang, P., Sand, C., Paul, A. V. & Wimmer, E. (2012a).** Alanine Scanning of Poliovirus 2CATPase Reveals New Genetic Evidence that Capsid Protein/2CATPase Interactions Are Essential for Morphogenesis. *Journal of Virology* **86**, 9964-9975.
- Wang, X., Ku, Z., Zhang, X., Ye, X., Chen, J., Liu, Q., Zhang, W., Zhang, C., Fu, Z., Jin, X., Cong, Y. & Huang, Z. (2018).** Structure, Immunogenicity, and Protective Mechanism of an Engineered Enterovirus 71-Like Particle Vaccine Mimicking 80S Empty Capsid. *J Virol* **92**.
- Wang, X., Peng, W., Ren, J., Hu, Z., Xu, J., Lou, Z., Li, X., Yin, W., Shen, X., Porta, C., Walter, T. S., Evans, G., Axford, D., Owen, R., Rowlands, D. J., Wang, J., Stuart, D. I., Fry, E. E. & Rao, Z. (2012b).** A sensor-adaptor mechanism for enterovirus uncoating from structures of EV71. *Nature Structural & Molecular Biology* **19**, 424.
- Wang, Y., Lilley, K. S. & Oliver, S. G. (2014).** A protocol for the subcellular fractionation of *Saccharomyces cerevisiae* using nitrogen cavitation and density gradient centrifugation. *Yeast (Chichester, England)* **31**, 127-135.
- Watanabe, Y., Watanabe, K., Katagiri, S. & Hinuma, Y. (1965).** Virus-specific proteins produced in HeLa cells infected with poliovirus: characterization of subunit-like protein. *Journal of biochemistry* **57**, 733-741.
- Wenner, H. A. & Kamitsuka, P. (1957).** Primary sites of virus multiplication following intramuscular inoculation of poliomyelitis virus in cynomolgus monkeys. *Virology* **3**, 429-443.
- WHO (2006).** Temperature Sensitivity of Vaccines. Geneva: WHO.
- WHO (2017).** WILD POLIOVIRUS LIST. Geneva: GLOBAL POLIO ERADICATION INITIATIVE.

- Wickham, T. J. & Nemerow, G. R. (1993).** Optimization of Growth Methods and Recombinant Protein Production in BTI-Tn-5B1-4 Insect Cells Using the Baculovirus Expression System. *Biotechnology Progress* **9**, 25-30.
- Wilson, W., Braddock, M., Adams, S. E., Rathjen, P. D., Kingsman, S. M. & Kingsman, A. J. (1988).** HIV expression strategies: ribosomal frameshifting is directed by a short sequence in both mammalian and yeast systems. *Cell* **55**, 1159-1169.
- Wimmer, E. (1982).** Genome-linked proteins of viruses. *Cell* **28**, 199-201.
- Wu, Z., Alexandratos, J., Ericksen, B., Lubkowski, J., Gallo, R. C. & Lu, W. (2004).** Total chemical synthesis of N-myristoylated HIV-1 matrix protein p17: structural and mechanistic implications of p17 myristoylation. *Proceedings of the National Academy of Sciences of the United States of America* **101**, 11587-11592.
- Xing, L., Tjarnlund, K., Lindqvist, B., Kaplan, G. G., Feigelstock, D., Cheng, R. H. & Casasnovas, J. M. (2000).** Distinct cellular receptor interactions in poliovirus and rhinoviruses. *Embo J* **19**, 1207-1216.
- Xu, Y., Ma, S., Huang, Y., Chen, F., Chen, L., Ding, D., Zheng, Y., Li, H., Xiao, J., Feng, J. & Peng, T. (2019).** Virus-like particle vaccines for poliovirus types 1, 2, and 3 with enhanced thermostability expressed in insect cells. *Vaccine* **37**, 2340-2347.
- Yamazaki, S. (1988).** Method of purifying recombinant pres-1/S-2/S hepatitis B antigen from yeast. Germany.
- Ypmawong, M. F., Dewalt, P. G., Johnson, V. H., Lamb, J. G. & Semler, B. L. (1988a).** Protein 3CD is the major poliovirus proteinase responsible for cleavage of the P1 capsid precursor. *Virology* **166**, 265-270.
- Ypmawong, M. F., Filman, D. J., Hogle, J. M. & Semler, B. L. (1988b).** Structural domains of the poliovirus polyprotein are major determinants for proteolytic cleavage at Gln-Gly pairs. *Journal of Biological Chemistry* **263**, 17846-17856.
- Zell, R., Delwart, E., Gorbalenya, A. E., Hovi, T., King, A. M. Q., Knowles, N. J., Lindberg, A. M., Pallansch, M. A., Palmenberg, A. C., Reuter, G., Simmonds, P., Skern, T., Stanway, G., Yamashita, T. & Consortium, I. R. (2017).** ICTV Virus Taxonomy Profile: Picornaviridae. *Journal of General Virology* **98**, 2421-2422.
- Zhang, C., Ku, Z., Liu, Q., Wang, X., Chen, T., Ye, X., Li, D., Jin, X. & Huang, Z. (2015).** High-yield production of recombinant virus-like particles of enterovirus 71 in *Pichia pastoris* and their protective efficacy against oral viral challenge in mice. *Vaccine* **33**, 2335-2341.
- Zhang, X.-N., Song, Z.-G., Jiang, T., Shi, B.-S., Hu, Y.-W. & Yuan, Z.-H. (2010).** Rupintrivir is a promising candidate for treating severe cases of Enterovirus-71 infection. *World journal of gastroenterology* **16**, 201-209.
- Zhao, H., Li, H.-Y., Han, J.-F., Deng, Y.-Q., Li, Y.-X., Zhu, S.-Y., He, Y.-L., Qin, E. D., Chen, R. & Qin, C.-F. (2013).** Virus-like particles produced in *Saccharomyces cerevisiae* elicit protective immunity against Coxsackievirus A16 in mice. *Applied microbiology and biotechnology* **97**, 10445-10452.
- Zhao, Y., Chapman, D. A. G. & Jones, I. M. (2003).** Improving baculovirus recombination. *Nucleic Acids Research* **31**, e6-e6.
- Zhou, Y., Shen, C., Zhang, C., Zhang, W., Wang, L., Lan, K., Liu, Q. & Huang, Z. (2016).** Yeast-produced recombinant virus-like particles of coxsackievirus A6 elicited protective antibodies in mice. *Antiviral Research* **132**, 165-169.